Expanding the Scope of Boronic Acid Catalysis: New and Improved Reactivity, Asymmetric Transformation

by

Hwee Ting Ang

A thesis submitted in partial fulfillment of the requirements for the degree of

Doctor of Philosophy

Department of Chemistry
University of Alberta

Abstract

Catalysis is one of the 12 principles of green chemistry and is the key to sustainable chemical processes, providing numerous advantages over the conventional stoichiometric chemical procedures, such as reduction of waste, better atom economy, and lower energy consumption. Furthermore, the ability to lower the activation energy allows direct transformations of previously non-reactive and inert compounds. In this context, boronic acid catalysis (BAC) has become an emerging area in catalysis, offering a general and mild strategy for electrophilic or nucleophilic activation of hydroxy and carbonyl functional groups to promote further transformations into useful products. An overview of the recent advances, advantages, modes of activation, as well as challenges and current limitations of BAC, is covered in Chapter 1. Efforts toward expanding the potential of BAC and addressing some of the limitations are presented in this thesis.

Chapter 2 summarizes the development of a mild boronic acid catalyzed Beckmann rearrangement of oximes for the preparation of various functionalized amide products. A unique class of arylboronic acids bearing an ortho-carboxyester group was identified as efficient catalysts for the direct activation of oxime N–OH bonds. Furthermore, perfluoropinacol also was identified as an effective co-catalyst to improve the reactivity of boronic acid catalysts. Further mechanistic studies revealed that the reaction proceeds via a two-step mechanism, which involves a novel boron-induced oxime transesterification and a fully catalytic self-sufficient Beckmann rearrangement.

Several boronic acids were identified previously as general and efficient catalysts for the direct activation of benzylic alcohols for Friedel–Crafts benzylation of arenes to prepare unsymmetrical diarylmethane products. Highly electron-deficient benzylic alcohols, however, were found to be ineffective substrates in these systems because of the increased difficulty to promote the C–O bond ionization. Chapter 3 describes the discovery of perfluoropinacol as an efficient co-catalyst to enhance the catalytic activity of boronic acids in the challenging Friedel–Crafts benzylation with deactivated benzylic alcohols. Mechanistic investigations strongly suggest that the activation of the hydroxy group likely occurs through an indirect Brønsted acid mechanism, where a mild hydronium Brønsted acid forms *in situ* via condensation of boronic acid catalyst with perfluoropinacol.

Chapter 4 presents the discovery and optimization of a novel chiral hemiboronic acid derived from BINOL for the catalytic enantioselective desymmetrization of 2-aryl-1,3-propanediols via *O*-benzylation. Systematic studies provide insights toward further structural optimization of the catalyst to improve the enantioselectivity. To this end, an optimal catalyst was discovered affording monoalkylated products in enantiomeric ratios equal to or over 95:5 for a wide range of 2-aryl-1,3-propanediols. The optimal chiral catalyst features a large trityl ether moiety as a "steric shield" for the differentiation of the enantiotopic hydroxy units and an ortho-methyl substituent on the boroxarophenanthrene as an "ortho-blocker" to minimize the deleterious effect of an undesired competing conformer.

Preface

Chapter 2 of this thesis has been published as Mo, X.; Morgan, T. D. R.; Ang, H. T.; Hall, D. G. "Scope and Mechanism of a True Organocatalytic Beckmann Rearrangement with a Boronic Acid/Perfluoropinacol System under Ambient Conditions", *J. Am. Chem. Soc.* **2018**, *140*, 5264–5271. I was involved partly in the examination of the substrate scope. I was responsible for mechanistic investigations to support the true organocatalytic mechanism of the Beckmann rearrangement and rule out the possibility of Brønsted acid-promoted rearrangement in this BAC protocol, which included ^{18}O-labeling experiments and reaction progress monitoring.

Chapter 3 of this thesis has been published as Ang, H. T.; Rygus, J. P. G.; Hall, D. G. "Two-Component Boronic Acid Catalysis for Increased Reactivity in Challenging Friedel–Crafts Alkylations with Deactivated Benzylic Alcohols", *Org. Biomol. Chem.* **2019**, *17*, 6007–6014. I was responsible for the experimental studies involving primary benzylic alcohol and 2-aryl ethanol substrates, which included the co-catalyst screening, optimization of reaction conditions, examination of substrate scope and mechanistic studies. I was responsible for data collection and analysis, as well as the preparation of supporting information. I wrote the manuscript with assistance from Prof. D. G. Hall, who was the supervisory author and was involved with concept formation, and J. P. G. Rygus, who was the co-author of this publication and was involved in the experimental studies with diarylmethanol substrates.

Chapter 4 of this thesis has been published as Estrada, C. D.; Ang, H. T.; Vetter, K. M.; Ponich, A. A.; Hall, D. G. "Enantioselective Desymmetrization of 2-Aryl-1,3-propanediols by Direct *O*-Alkylation with a Rationally Designed Chiral Hemiboronic Acid Catalyst That Mitigates Substrate Conformational Poisoning", *J. Am. Chem. Soc.* **2021**, *143*, 4162–4167. I was responsible for experimental works involving the optimal catalyst with a "methyl-blocker", which included the mechanistic investigations, synthesis of the catalyst, and the examination of the substrate scope. Prof. D. G. Hall was responsible for the molecular modeling, and Dr. M. J. Ferguson was responsible for the X-ray crystallographic analyses. I was

responsible for data collection and analysis, as well as the preparation of supporting information. I assisted in the preparation of the manuscript, written mostly by Prof. D. G. Hall, who was the supervisory author and was involved with concept development.

Acknowledgement

First and foremost, I wish to express my sincere appreciation to my supervisor, Prof. Dennis Hall, for his constant guidance and support during my PhD study. His invaluable training and suggestions have aided in preparing me for my future aspirations as a successful chemist. I am exceedingly grateful for all the opportunities he has provided me, through conference participation and supporting my applications for several scholarships and awards. The meticulous edits and recommendations he provided during the preparation of this dissertation are appreciated deeply.

I would like to extend my sincere thanks to my Supervisory Committee and PhD Examination Committee members: Professor Ratmir Derda, Professor Frederick West, Professor Florence Williams, Professor Eric Rivard, Professor Lingzi Sang, and Professor Rebecca Davis, for their insightful comments, advice, and encouragement.

I gratefully recognize the excellent administrative and research services at the University of Alberta. Many thanks to Anita Weiler and Laura Pham for their administrative assistance. I am thankful to the scientific services staff for their expertise in providing suggestion and assistance to my research, especially Ed Fu (HPLC), Mark Miskolzie (NMR), Dr. Michael Ferguson (X-ray crystallography), Wayne Moffat and Jennifer Jonnes (analytical services), as well as Jing Zheng and Bela Reiz (mass spectrometry). I am grateful to other staff members from the machine shop, the chemical storeroom, and the glass shop. I am deeply indebted to Dr. Anna D. Jordan for her assistance in editing my thesis. I must also thank Dr. Hayley Wan for the opportunity to teach in the Organic Chemistry Laboratories, as well as for her support and friendship.

I also would like to extend my deepest gratitude to all the wonderful Hall Group members, past and present. I had the pleasure of working with and learning from these talented people. I am extremely grateful to the following group members that I worked with in the research described in this thesis: Dr. Xiaobin Mo, Dr. Timothy Morgan, Jason Rygus, Carl Estrada, Kim-Marie Vetter, and Ashley Ponich. Many thanks to Dr. Burcin Akgun, Dr. Helen Clement, Dr. Xiangyu Li, and Dr.

Table of Contents

List of Figures

List of Tables

List of Schemes

List of Abbreviations

Ac	Acetyl
ACS	American Chemical Society
app	Apparent
aq	Aqueous
Ar	Aryl group
BA	Boronic acid
BAC	Boronic acid catalysis
BINOL	1,1'-Bi-2-naphthol
Bn	Benzyl
Boc	*tert*-Butyloxycarbonyl
BOP-Cl	Bis(2-oxo-3-oxazolidinyl)phosphinic chloride
br	Broad
brsm	Based on recovered starting material
n-Bu	*n*-Butyl
t-Bu	*tert*-Butyl
Bz	Benzoyl
calcd	Calculated
Cbz	Benzyl chloroformate
CNC	Cyanuric chloride
comp m	Complex multiplet
conc.	Concentrated
CPI-Cl	Dichloridecyclopropene
CSA	Camphorsulfonic acid
Cy	Cyclohexyl
d	Doublet
DBI	Dibromoisocyanuric acid
DCC	*N,N'*-Dichlorohexylcarbodiimide
DCE	1,2-Dichloroethane

DCID	Dichloroimidazolidinedione
DCM	Dichloromethane
dd	Doublet of doublets
ddd	Doublet of doublet of doublets
dddd	Doublet of doublet of doublet of doublets
DFT	Density functional theory
DIAD	Diisopropyl azodicarboxylate
DIC	*N,N'*-Diisopropylcarbodiimide
DIPEA	*N,N*-Diisopropylethylamine
DMAP	4-Dimethylaminopyridine
DMAPO	4-Dimethylaminopyridine *N*-oxide
DMF	*N,N*-Dimethylformamide
DMSO	Dimethylsulfoxide
dppf	1,1′-Ferrocenediyl-bis(diphenylphosphine)
dr	Diastereomeric ratio
E	Electrophile
EDC	*N*-(3-Dimethylaminopropyl)-*N'*-ethylcarbodiimide
EDG	Electron-donating group
ee	Enantiomeric excess
EI	Electron impact
equiv	Equivalents
er	Enantiomeric ratio
ESI	Electrospray ionization
Et	Ethyl
EtOAc	Ethyl acetate
EWG	Electron-withdrawing group
FDA	Food and Drug Administration
FG	Functional group
Fmoc	Fluorenylmethyloxycarbonyl
GP	General procedure

h	Hour
HAT	Hydrogen atom transfer
HDMS	Hexamethyldisilazane
HE	Hantzsch ester
Hex	Hexanes
HFIP	Hexafluoro-2-propanol
HPLC	High performance liquid chromatography
HRMS	High resolution mass spectroscopy
IR	Infrared spectroscopy
LC-MS	Liquid chromatography–mass spectrometry
LED	Light-emitting diode
LUMO	Lowest unoccupied molecular orbital
m	Multiplet
[M]	Molar concentration
Me	Methyl
min	Minutes
mont	Montmorillonite
Mp	Melting point
MS	Molecular sieves
MTBE	Methyl *tert*-butyl ether
m/z	Mass-to-charge
NBS	*N*-Bromosuccinimide
NHC	*N*-Heterocyclic carbene
NMI	*N*-Methylimidazole
NMR	Nuclear magnetic resonance
Nu	Nucleophile
PG	Protecting Group
Ph	Phenyl
PhD	Doctor of Philosophy
pin	Pinacolato

PMA	Phosphomolybdic acid
PMB	*para*-Methoxybenzyl
i-Pr	Isopropyl
PTLC	Preparative thin layer chromatography
q	Quartet
R_f	Retention factor
rds	Rate determining step
rt	Room temperature
s	Singlet
Ser	Serine
SIM	Selective ion monitoring
t	Triplet
T	Time
TAPC	1,3,5-Triazo-2,4,6-triphosphorine-2,2,4,4,6,6-chloride
TBS	*tert*-Butyldimethylsilyl
td	Triplet of doublets
temp	Temperature
TEPO	Triethylphosphine oxide
Tf	Triflyl
TFA	Trifluoroacetic acid
THF	Tetrahydrofuran
Thr	Threonine
TLC	Thin layer chromatography
TMEDA	Tetramethylethylenediamine
TMS	Trimethylsilyl
TOF	Time-of-flight
T3P	Propylphosphonic anhydride
Ts	*para*-Toluenesulfonyl
TS	Transition state
tt	Triplet of triplets

UV   Ultraviolet

XPhos   2-Dicyclohexylphosphino-2′,4′,6′-triisopropylbiphenyl

XPhos Pd G2   X-Phos aminobiphenyl palladium chloride precatalyst

CHAPTER 1

An Emerging Area of Catalysis: Boronic Acid Catalysis

1.1 Brief Introduction of Boronic Acids

1.1.1 Background and Applications of Boronic Acids

Over the past few decades, boronic acids have emerged as a popular and important class of compounds used in a variety of chemistry research fields, despite the fact that they have no natural source and can be obtained only synthetically.[1] The growing popularity of boronic acids in research can be attributed to their use in the renowned Suzuki–Miyaura cross-coupling reaction, in addition to their unique properties and reactivity.

In 1860, Frankland and Duppa reported the preparation and isolation of the very first boronic acid, ethylboronic acid, from the reaction of diethyl zinc and triethyl borate.[2] Ethylboronic acid was obtained after two subsequent oxidations of a highly reactive triethylborane intermediate in ambient air. Following this initial discovery, the synthesis and isolation of the first arylboronic acid, phenylboronic acid, was reported in 1880 by Michaelis and Becker using diphenylmercury ($HgPh_2$) with boron trichloride through a reactive dichlorophenylborane intermediate.[3] A century after these discoveries, boronic acids started to gain more attention from chemists with the revolutionary palladium catalyzed C–C cross-coupling reaction reported by Suzuki and Miyaura in 1979.[4] In recognition of the great significance that the Suzuki–Miyaura cross-coupling reaction holds in different fields of chemistry, especially medicinal and materials chemistry, Professor Akira Suzuki was awarded the Nobel Prize in 2010.[5] Since the initial report of the Suzuki–Miyaura reaction, the synthetic utilities of boronic acids have expanded vastly to other well-known reactions, such as Matteson homologation,[6] carbonyl allylboration,[7] the Petasis reaction,[8] Chan–Lam coupling,[9] and Liebeskind–Srogl coupling,[10] and continue to grow and prosper. The wide recognition of boronic acids as versatile building blocks has led to major

advances in the preparation of boronic acids and their derivatives, which also led to an increase of their commercial availability.

With many well-established borylation protocols,[11–15] the applications of boronic acids have grown beyond organic synthesis and are expanding swiftly in various scientific research fields (Figure 1-1). Recently, boronic acids have emerged as useful components in medicinal chemistry as therapeutic agents[16] and bioconjugates.[17,18] In this regard, the most notable example is the approval of bortezomib, the first boronic acid containing drug, by the FDA in 2003. Since then, the number of bioactive boronic acids disclosed has increased exponentially. Additionally, the use of boronic acids is well-appreciated in materials and analytical chemistry. Boronic acids have been used extensively in the construction of covalent organic frameworks, hydrogels, polymers, and nanomaterials for various applications including drug delivery.[19–21] Boronic acid-based fluorescent sensors[22,23] and chromatography supports[24] also have become a valuable tool for analytical scientists for the detection and separation of carbohydrates, diols, and some ionic compounds.

More interestingly, boronic acids recently have found new applications in the field of organic chemistry besides their use as synthetic building blocks. The utility of boronic acids in catalysis is an emerging research area, and it will be described in more detail in Section 1.2.[25,26]
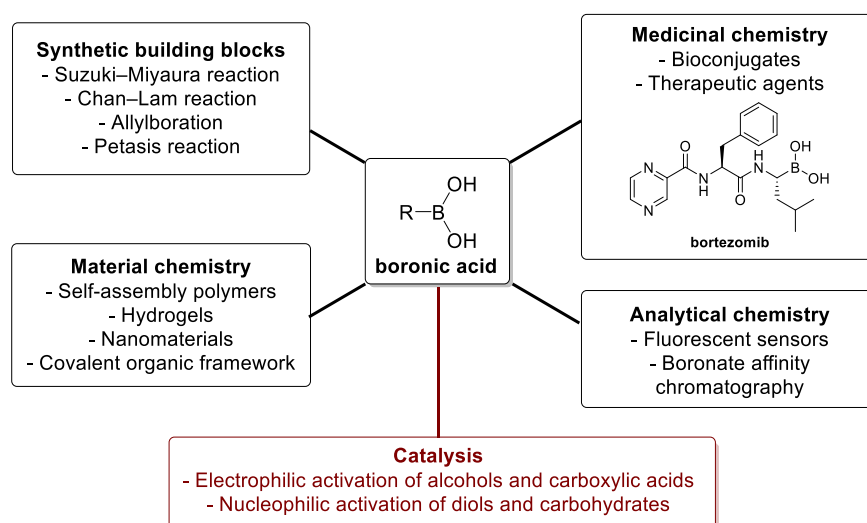
Figure 1-1 The applications of boronic acids in various research fields.

1.1.2 Physicochemical Properties

Structurally, boronic acids are trivalent organoboron compounds bearing one carbon substituent and two hydroxy groups on the central boron atom. With a deficiency of two valence electrons, the boron atom possesses a vacant p-orbital and is sp^2 hybridized (Figure 1-2A). Most boronic acids, especially arylboronic acids, exist as air stable crystalline solids with extended shelf-stability and can be handled without special precaution. Moreover, boronic acids generally possess low toxicity, and are deemed as environmentally friendly compounds since they ultimately degrade into benign boric acid.[1]
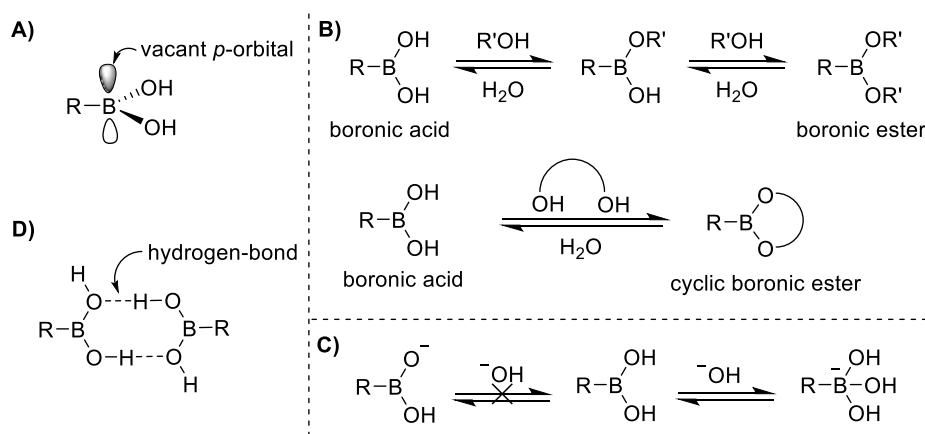
Figure 1-2 Boronic acids: A) structure; B) reversible B–O bond exchange; C) in basic conditions; D) hydrogen-bonded dimer in solid state.

With the vacant p-orbital on the boron center, boronic acids are regarded as a mild class of organic Lewis acids that are capable of establishing reversible covalent bonds with basic compounds and nucleophiles. The pK_a of boronic acids displays a range of 5–9 and can be tuned by manipulating the nearby substituents. This distinctive nature of boronic acids also enables facile exchange of the B–OH groups with the hydroxy group of alcohols and carboxylic acids, generating boronic esters, and with vicinal nucleophiles, such as polyol, carbohydrates, and amino alcohols, forming cyclic boronic esters (Figure 1-2B). This dynamic exchange occurs at a higher rate with boronic acids with a lower pK_a due to the increase in electrophilicity of the boron center. Furthermore, under basic conditions of pH greater than the pK_a of a boronic acid, Lewis acid–base interaction results in a tetrahedral anionic boronate

3

species. Despite having two hydroxy groups, boronic acids hardly ever act as Brønsted acids in aqueous or basic conditions by losing a proton from one of the hydroxy groups (Figure 1-2C). Boronic acids also can behave as hydrogen bond donors and acceptors, as evidenced by X-ray crystallographic structures of boronic acids, where they generally exist as hydrogen-bonded dimers (Figure 1-2D).[27] All the aforementioned distinctive physicochemical properties of boronic acids are highly beneficial for various applications and led to a renaissance of research surrounding the chemistry of boronic acids.

1.2 Boronic Acid Catalysis (BAC)

Recently, boronic acid catalysis (BAC) has emerged as an attractive strategy for the activation of hydroxy-containing compounds in a mild and selective fashion by taking advantage of the reversible interaction of boronic acids and hydroxy groups. A comprehensive tutorial review on the development of BAC in the past decades was published by Professor Dennis Hall in 2019, highlighting a diversity of reactions and mechanisms amenable to BAC.[26] Hence, in this section, the boronic acid catalysts highlighted in the review will be summarized, and the development of BAC after the publication of the tutorial review will be emphasized.

Historically, the first boronic acid catalyzed reaction was reported in 1963 by Letsinger and co-workers.[28] The authors disclosed the use of 8-quinolineboronic acid (**BA-1**) to facilitate the hydrolysis of 2-chloroethanol in the presence of collidine (Scheme 1-1A). In this reaction, **BA-1** acts as a bifunctional catalyst, where the boronic acid unit brings the alcohol substrate and water together by formation of boronic ester **1-1**, and the nitrogen atom of the quinoline assists in the nucleophilic substitution of the chloride, presumably via hydrogen bonding and a cooperative base effect. Another early example of BAC with phenylboronic acid (**BA-2**) was disclosed by Philipp and Rao in 1991 for the hydrolysis of salicylaldehyde imine (Scheme 1-1B).[29] The coordination of the ortho-phenoxy group to **BA-2** generates the anionic boronate **1-2**, which not only holds and properly orients the substrates but also increases the nucleophilicity of the hydroxy group on the boron center for the subsequent nucleophilic attack onto the imine moiety. Despite having little

practicality, these BAC studies emphasized the ability of boronic acids to form covalent interactions with hydroxy groups that can be used to bring the reactants together and provide additional cooperative effects to accelerate the reactions.
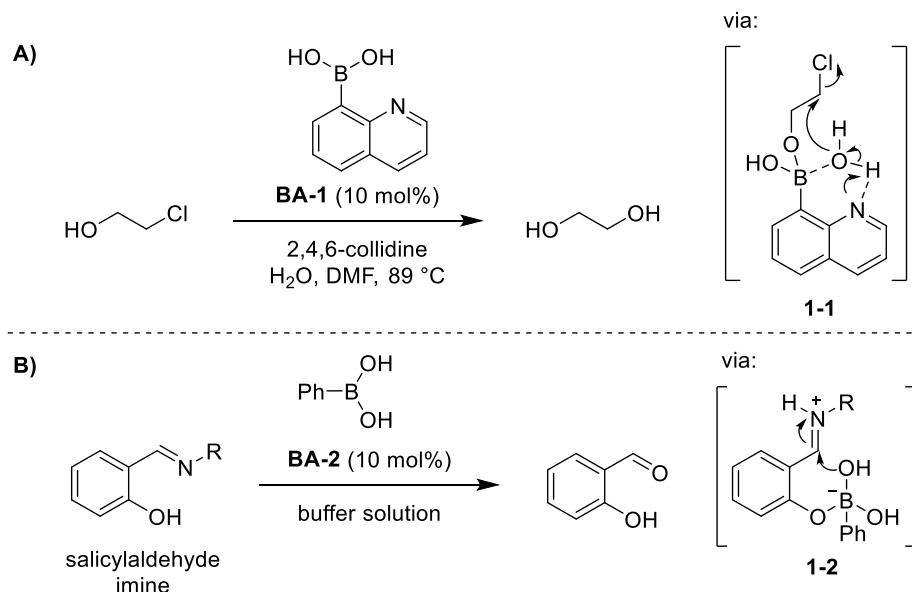
Scheme 1-1 Boronic acid catalyzed hydrolysis of A) 2-chloroethanol and B) salicylaldehyde imine.

To this end, boronic acids have been utilized to effect both electrophilic and nucleophilic activation of hydroxy-containing compounds in a series of organic reactions. One of the most studied areas is the electrophilic activation of carboxylic acid using BAC for direct amide formation with amines (Figure 1-3). In 1996, Yamamoto and co-workers disclosed the use of 3,4,5-trifluorophenylboronic acid (**BA-3**) as an efficient catalyst for direct amidations in non-polar solvent under azeotropic reflux conditions.[30] Since then, several boronic acid catalysts (**BA-4**–**BA-10**) have been reported for direct amidations.[31–37] Generally, the activation of carboxylic acids by a boronic acid catalyst is proposed to originate from the formation of hydrogen-bonded intermediate **1-3**. However, in a recent work with extensive experimental and computational studies, Whiting and co-workers claimed that a dimeric intermediate, **1-4**, which is bridged by two carboxylates, is more likely to be the reactive intermediate.[38] Aside from amines, the use of other nucleophiles, such as sodium azide, sodium borohydride, and urea, were also reported. In 2005,

Yamamoto and co-workers also identified *N*-methylpyridiniumboronic acid (**BA-11**) as a suitable catalyst for the direct esterification of α-hydroxycarboxylic acids using alcohols as the solvent.[39] A bifunctional boronic acid catalyst, **BA-12**, bearing two ortho-aminomethyl substituents, was introduced by Ishihara and co-workers in 2011 for the intramolecular dehydration of dicarboxylic acids to yield cyclic anhydrides.[40]
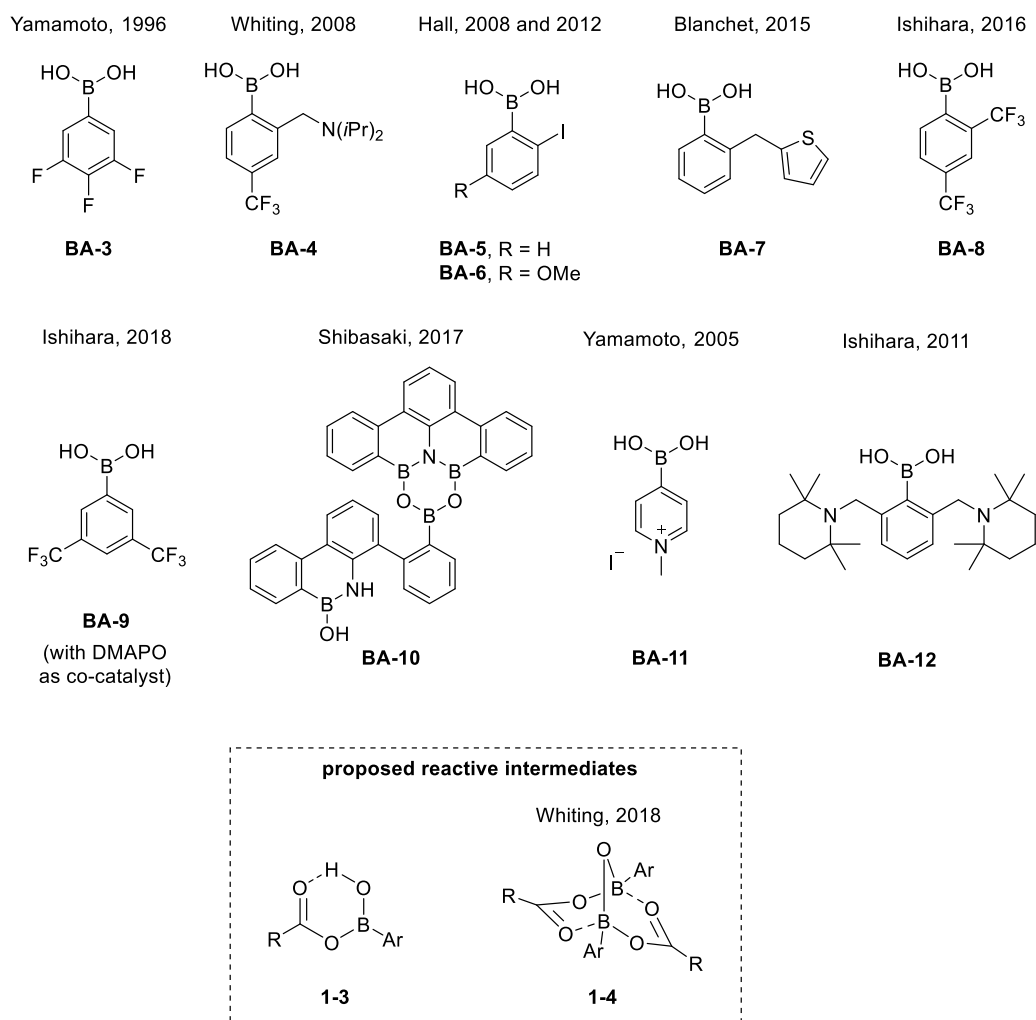
Figure 1-3 Examples of boronic acid catalysts for electrophilic activation of carboxylic acids and proposed reactive intermediate.

The concept of BAC was extended also to the electrophilic activation of α,β-unsaturated carboxylic acids towards cycloadditions and conjugate additions (Figure 1-4). 2-Bromophenyl-boronic acid (**BA-13**) and 2-nitrophenylboronic acid (**BA-14**) were reported by Hall and co-workers to be suitable catalysts for the Diels–

Alder cycloaddition[41] and Huisgen cycloaddition[42] of α,β-unsaturated carboxylic acids. As evidenced by NMR spectroscopic studies, the hydrogen-bonded acylboronate intermediate **1-5** provides activation by lowering the LUMO energy of the unsaturated carboxylic acids.[42] In 2014, a dual catalytic system using **BA-9** and a chiral aminothiourea, **1-6**, for the asymmetric intramolecular conjugate additions of unsaturated carboxylic acid was disclosed by Takemoto and co-workers.[43] Inspired by this work, the same group then designed a new boronic acid catalyst, **BA-15**, by integrating the chiral aminothiourea scaffold onto the boronic acid. In the presence of benzoic acid as an additive, **BA-15** can catalyze intermolecular conjugate additions using O-benzylhydroxylamine (BnONH$_2$) as the nucleophile.[44]

Figure 1-4 Examples of boronic acid catalysts for the electrophilic activation of α,β-unsaturated carboxylic acids.

The application of BAC also has been expanded to the electrophilic activation of alcohols through the dynamic interaction of alcohols and boronic acids, which facilitates the complete or partial ionization of the C–O bond (Figure 1-5). The first example of such activation was discovered by McCubbin and co-workers in 2010 using a highly Lewis acidic boronic acid, pentafluoroboronic acid (**BA-16**), for the direct use of allylic alcohols for Friedel–Crafts allylation with electron rich arenes.[45] Soon after, Hall and co-workers reported the use of 2,3,4,5-tetrafluorophenylboronic acid (**BA-17**) and hexafluoronaphthalene boronic acid (**BA-18**) to catalyze the 1,3-transposition of allylic and propargylic alcohols.[46] In 2012, *N*-methyl-difluoro-pyridinium boronic acid (**BA-19**), along with **BA-17** and **BA-18,** also were identified as effective catalysts for the intramolecular cyclization of allylic alcohols with pendent nucleophiles.[47] In 2015, Hall and co-workers discovered improved conditions

for the Friedel–Crafts allylation and alkylation of benzylic alcohols with less activated arenes using catalyst **BA-17** and ferroceniumboronic acid (**BA-20**) in a solvent mixture containing hexafluoroisopropanol (HFIP).[48,49] Hall and co-workers then developed a dual catalytic system using **BA-20** and a chiral enamine, **1-7**, to effect enantioselective α-allylation of aldehydes, where the activated allylic alcohols were trapped with transient enamines generated from aldehydes.[50] In 2013, Moran and co-workers reported an example of the use of oxalic acid as a co-catalyst to enhance the reactivity of **BA-16** in the Friedel–Crafts alkylation.[51] This boronic acid/oxalic acid co-catalytic system was exploited by Hall and co-workers for the direct sulfonamidation of benzylic alcohols using catalyst **BA-17**[52] and by Taylor and co-workers for the dehydrative etherification of benzylic alcohols using **BA-16**.[53] Additionally, catalyst **BA-17** was employed also in the activation of pentadienols for a Nazarov-type cyclization[54] and furanyl alcohols for an aza-Piancatelli reaction,[55] whereas **BA-9** was used to activate indolyl alcohols for a [4+3] cycloaddition with 1,3-butadienes.[56]
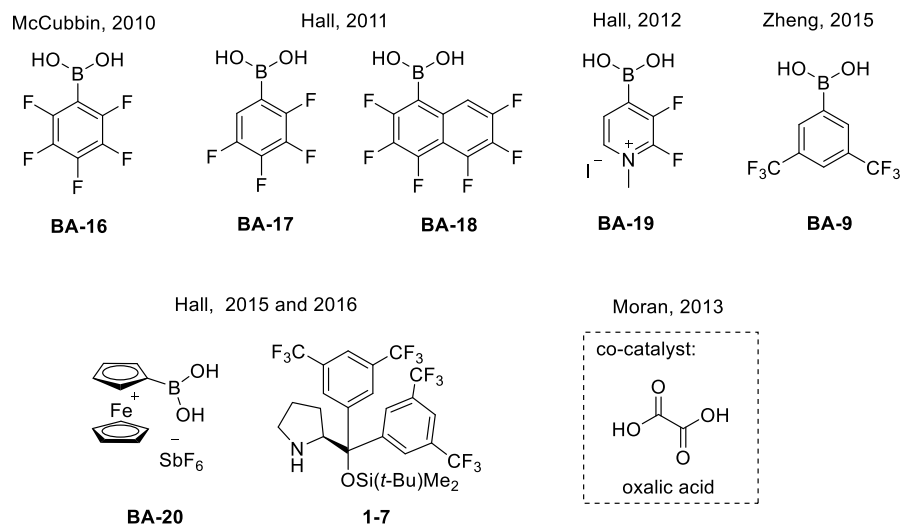
Figure 1-5 Examples of boronic acid catalysts for the electrophilic activation of allylic and benzylic alcohols.

Apart from electrophilic activation, BAC also can trigger nucleophilic activation of carbonyl compounds and polyols under basic conditions. The activation of a carbonyl group with a boronic acid occurs via the formation of enolates **1-8**,

which promote the nucleophilicity on the α-carbon for downstream transformations (Figure 1-6). In 2006, Carboni and co-workers reported the use of catalytic phenylboronic acid (**BA-2**) to accelerate the three-component Biginelli reaction involving ethyl acetoacetate, aryl aldehyde, and urea.[57] Later, an anionic boronate, **BA-21,** was disclosed by Whiting and co-workers as an excellent catalyst for the cross-aldol reaction of α-hydroxyketones and aldehydes in water.[58] Whiting and co-workers also identified an asymmetric variant of boronic acid-catalyzed aldol reaction between 4-nitrobenzaldehyde and acetone using a proline-based boronic acid, **BA-22**, and co-catalytic (*R,R*)-hydrobenzoin **1-9**.[59] Dixon and co-workers introduced the use of 3-nitrophenylboronic acid (**BA-23**) to catalyze the intramolecular ene-carbocyclization of acetylenic1,3-dicarbonyl compounds.[60]
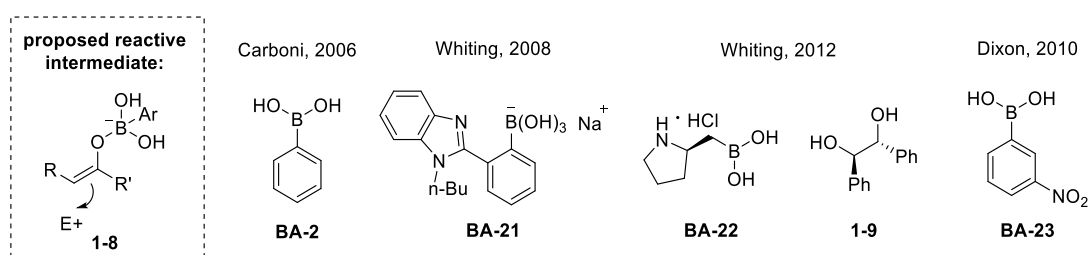
Figure 1-6 Examples of boronic acid catalysts for the nucleophilic activation of carbonyl compounds.

On the other hand, the activation of polyols such as diols and carbohydrates proceeds via the formation of anionic tetrahedral boronate adducts **1-10**, which enhances the nucleophilicity of the oxygen atoms, as the negative charge formally drawn on the boron center is actually distributed onto the heteroatoms (Figure 1-7A). In 2013, a co-catalytic system of 3,5-trifluoromethylphenylboronic acid **BA-9** and tributylphosphine oxide was introduced by Taylor and co-workers for the regioselective silylation of unprotected monosaccharides.[61] Toshima and co-workers also identified 4-methoxyphenyl boronic acid (**BA-24**) and 4-nitrophenylboronic acid (**BA-25**) as efficient catalysts for the regio- and 1,2-cis-selective glycosylation of carbohydrate derivatives.[62] The activation of 1,2-diols through the anionic intermediate **1-10** also was exploited by Onomura and co-workers for the selective

mono-oxidation of diols into the corresponding α-hydroxyketone using methylboronic acid (**BA-26**) and dibromoisocyanuric acid (DBI) as the oxidant.[63]
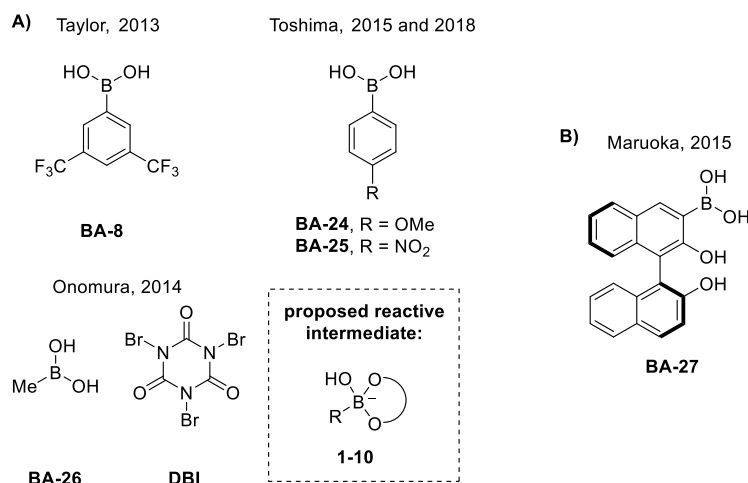
Figure 1-7 Examples of boronic acid catalysts for the nucleophilic activation of A) polyols and B) hydroxamic acids.

Lastly, an unusual example of boronic acid-catalyzed enantioselective aza-Michael addition of hydroxamic acid was reported by Maruoka and co-workers by using a BINOL-based boronic acid **BA-27** and a sub-stoichiometric amount of 2-nitrobenzoic acid (Figure 1-7B).[64]

1.2.1 Recent Advances in BAC since Hall's Review

Over the past two years, several advances have been made in the field of BAC, which often consist of (a) new reactions amenable to BAC using previously reported boronic acid catalysts and of (b) new boronic acid catalysts for established and new reactions adapted to BAC.

1.2.1.1 New Reactions using Previously Reported Boronic Acid Catalysts

In two recent publications, Wang and co-workers reported the use of catalysts **BA-3** and **BA-23** in C3 selective ring opening of epoxy homoallylic alcohols **1-11** with amines and thiols as nucleophiles (Scheme 1-2).[65,66] In general, complete regio- and diastereoselectivies (C3:C4 >99:1 and >99:1 dr) were achieved with this BAC protocol. The high selectivity of this system likely originated from the formation of a chair-like six-membered transition state, **1-12**, via coordination of both the hydroxy

groups of **1-11** and the nucleophile to the boron center, which facilitates the intramolecular nucleophilic attack on the epoxide at the C3 position. Apart from acting as a template, it is proposed that the boronic acid also provides nucleophilic activation to the nucleophiles through the formation of the anionic boronate **1-12**.
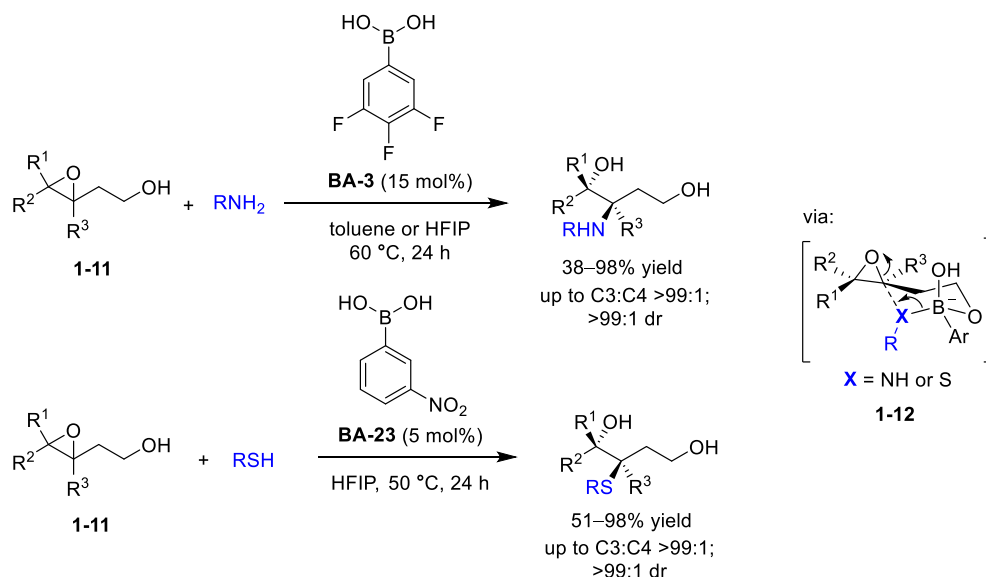
Scheme 1-2 Boronic acid catalyzed diastereoselective and C3 selective ring opening of epoxy homoallylic alcohols **1-11** with amines and thiols.

In 2019, Judeh and co-workers described a boronic acid catalyzed direct α-stereoselective addition of alcohols to deactivated peracetylated D-galatal **1-13** to yield a series of 2-deoxygalactosides, **1-14**, in moderate to good yields (Scheme 1-3).[67] To investigate the reaction mechanism, ^{1}H NMR studies of the reaction mixtures in CD_3NO_2 were performed, however, no obvious changes in chemical shift of the olefinic proton of **1-13** was observed, which rules out any activation of substrates by **BA-16** via a Lewis acid–base interaction. Based on these observations, the authors proposed that **BA-16** likely acts as an indirect Brønsted acid source through the generation of alkyloxonium ions **1-15** by a Lewis acid-mediated ionization equilibrium of **BA-16** and two moles of alcohols. Hydronium ions also can be formed in a similar fashion with adventitious water in the reaction. To this end, it is proposed that the reaction proceeds through the formation of oxonium intermediate **1-16** induced by a Brønsted acid.
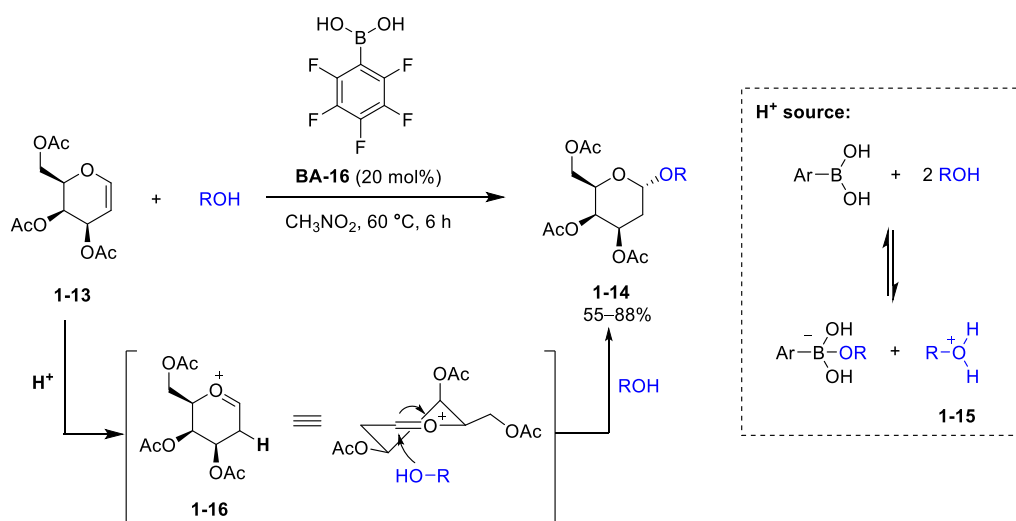
Scheme 1-3 Direct α-stereoselective synthesis of 2-deoxygalactosides **1-14** from acetylated D-galactal **1-13** and alcohols catalyzed by **BA-16**.

In 2020, Taylor and co-workers extended the application of their **BA-16**/oxalic acid co-catalytic protocol to enable the construction of new C–C bonds with secondary benzylic alcohols as the electrophiles and 1,3-dicarbonyl compounds or allyltrimethylsilane as the nucleophiles (Scheme 1-4).[68] Similar to their previous work on dehydrative etherification of benzylic alcohols, a Brønsted acid-promoted electrophilic activation of alcohols involving the hydronium boronate ester **1-17**, which is formed by the condensation of **BA-16** and oxalic acid, was proposed. The formation of the hydronium species **1-17** was supported by X-ray crystallographic analysis and NMR spectroscopy from their previous report.[53]
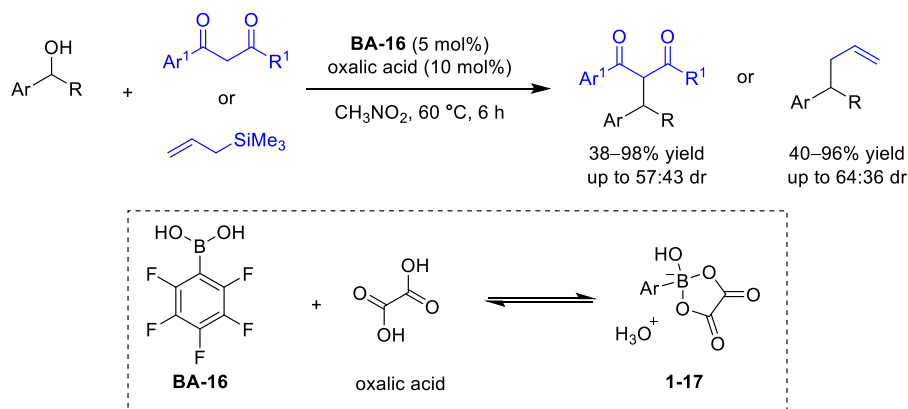
Scheme 1-4 Boronic acid/oxalic acid catalyzed C–C bond formation of secondary benzylic alcohols with 1,3-dicarbonyl or allyltrimethylsilane.

Inspired by the pioneering work of MacMillan and co-workers on the selective functionalization of alcohol α-hydroxy C−H bonds in the presence of a zinc Lewis acid via photoredox-mediated hydrogen atom transfer (HAT) catalysis,[69] Taylor and co-workers reported a similar protocol for the stereo- and site-selective C–H alkylation of carbohydrates using diphenylborinic acid as a co-catalyst to activate selectively the cis-1,2-diol moiety.[70] Later, in 2020, they disclosed the use of **BA-16** as a co-catalyst for the site-selective redox isomerization of furanosides **1-18** to 2-keto-3-deoxyfuranosides **1-19** via photoredox-mediated HAT catalysis (Scheme 1-5).[71] Interestingly, diphenylborinic acid, the optimal co-catalyst in their previous work, was found to be ineffective in this transformation. Based on experimental and computational studies, this transformation is believed to take place via hydrogen atom abstraction from the 2-position of the boronate ester intermediate **1-20** and subsequent C3–O bond cleavage to deliver the product **1-19**. In this case, quinuclidine, a common hydrogen atom transfer mediator, also acts as a Lewis base and coordinates to the boron center in **1-20**, leading to an increase in hydridic character of the α-C–H bonds toward hydrogen atom abstraction. This example demonstrated elegantly the potential of boronic acid catalysts in promoting the formation of radicals with polyols.
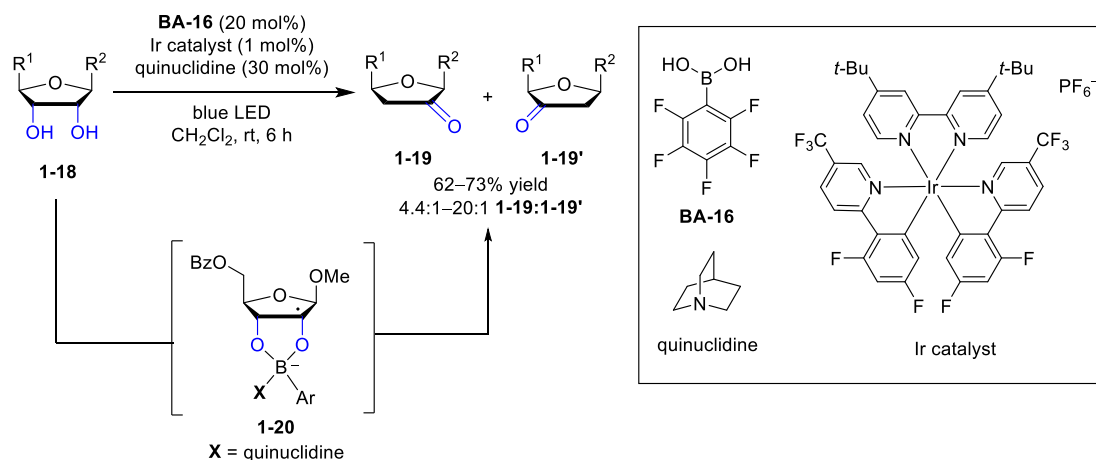
Scheme 1-5 Site-selective redox isomerization of furanosides **1-18** to 2-keto-3-deoxyfuranosides **1-19** via arylboronic acid/photoredox/HAT catalysis.

In 2020, Reddy and co-workers described an unprecedented boronic acid catalyzed tandem formation of C–S and S–S bonds for the preparation of benzyl disulfanylsulfone derivatives **1-22** from easily accessible *S*-benzyl thiosulfonates **1-21** using **BA-2** (Scheme 1-6).[72] While the mechanistic details of this reaction are being investigated currently by the authors, a plausible mechanism was proposed, based on control experiments and knowledge garnered from the literature. They envisioned that **BA-2** behaves as a Lewis acid in this transformation and coordinates with the divalent sulfur atom in **1-21** to form an anionic boronate complex, **1-23**, which triggers the deprotonation of the benzylic proton under basic conditions and ruptures the S–SO$_2$ bond, generating sulfinic acid and boron-sulfonium species **1-24**. Recombination of sulfinic acid and boron species **1-24** via nucleophilic attack results in intermediate **1-25**, which then reacts with another molecule of thiosulfonate **1-21** that is brought to proximity by a hydrogen-bonding interaction with the boronate moiety, yielding the product **1-22**.
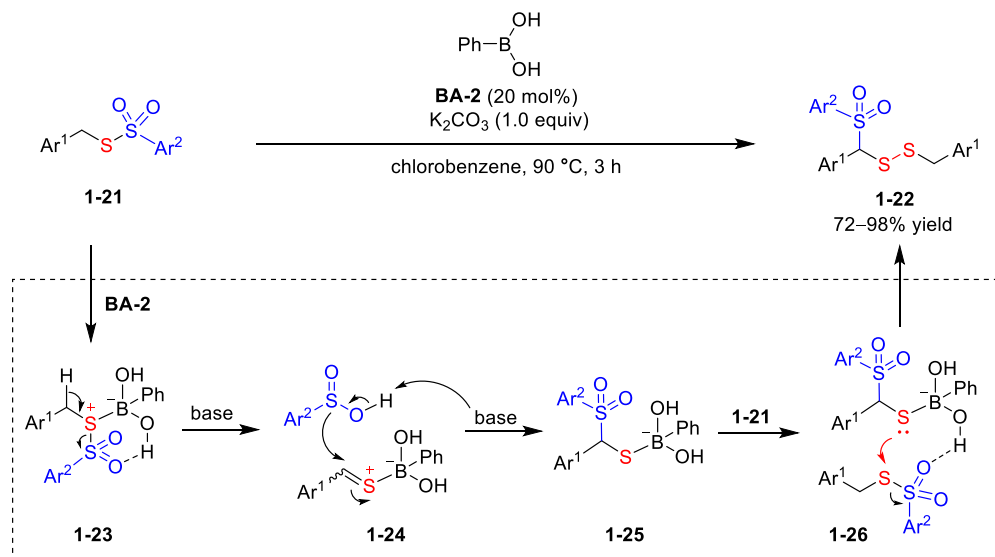
Scheme 1-6 Postulated mechanism for boronic acid catalyzed tandem formation of C–S and S–S bonds from *S*-benzylthiosulfonates **1-21**.

1.2.1.2 Discovery of New Boronic Acid Catalysts

Given the importance of amides, research on efficient, sustainable, and green amidation methodologies remains active. Specifically, the recent finding by Whiting and co-workers of the dimeric reactive intermediate **1-4** that is bridged by a B–O–B

moiety and two carboxylate groups, has encouraged the design of new generation boronic acid catalysts with a pre-organized B–X–B motif.

In 2019, Shimada and co-workers identified the diboronic acid anhydride **BA-28** as a highly efficient catalyst, with a low loading (0.5 mol%), for the hydroxy-directed amidation of β-hydroxy-carboxylic acids (Scheme 1-7A).[73] Unlike previously reported amidation protocols, dehydrative conditions, such as use of molecular sieves or azeotropic reflux, were not required; however, high temperatures still were needed for effective transformation. The **BA-28** catalytic system was found to remain active when the reaction was conducted in a mixture of 19:1 toluene/H_2O. The formation of reactive intermediate **1-27**, which is consistent with Whiting's dimeric intermediate **1-4**, was detected by ESI mass spectrometry. In 2020, Shimada and co-workers successfully expanded the scope of this BAC protocol to direct peptide bond formation with β-hydroxy-α-amino acids, affording the peptide products in high to excellent yields with minimal epimerization (Scheme 1-7B).[74]
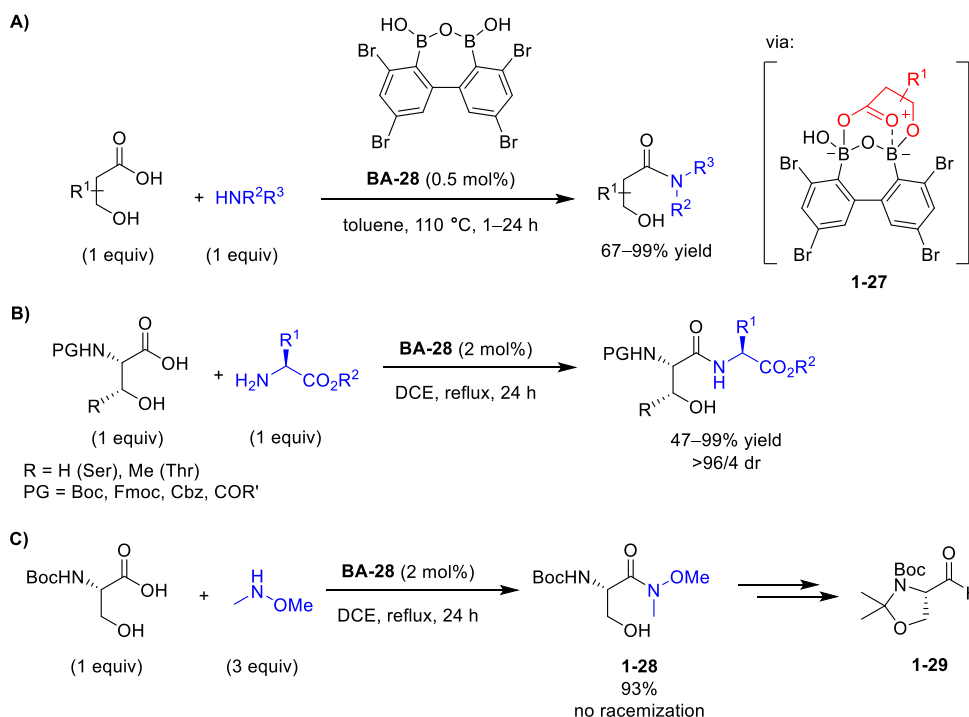
Scheme 1-7 Diboronic acid anhydride **BA-28** catalyzed direct functionalization of β-hydroxy carboxylic acid with A) amines; B) amino acids; and C) *N,O*-dimethylhydroxylamine.

15

While the scope is limited to β-hydroxy-α-amino acids, this discovery can be considered as a breakthrough, as direct peptide bond formation via BAC is known to be difficult due to catalyst inhibition by the amino acids via formation of a stable five-membered chelate.[36,37,75] Furthermore, the authors also utilized this system to prepare *N*-protected serine-derived Weinreb amide **1-28** with high optical purity for the concise synthesis of Garner's aldehyde **1-29**, a widely used chiral intermediate in total synthesis (Scheme 1-7C).[76]

In 2020, Takemoto and co-workers also reported the use of a novel gem-diboronic acid, **BA-29**, bearing a B–C–B motif, for catalytic direct dehydrative peptide synthesis with minimal epimerization of the electrophiles (Scheme 1-8).[77] Various α-amino acids protected with common carbamates (Boc, Cbz, and Fmoc) were found to be compatible in this protocol. Preliminary mechanistic investigations indicate a bidentate carboxylate activation by **BA-29**, presumably via intermediate **1-30**.
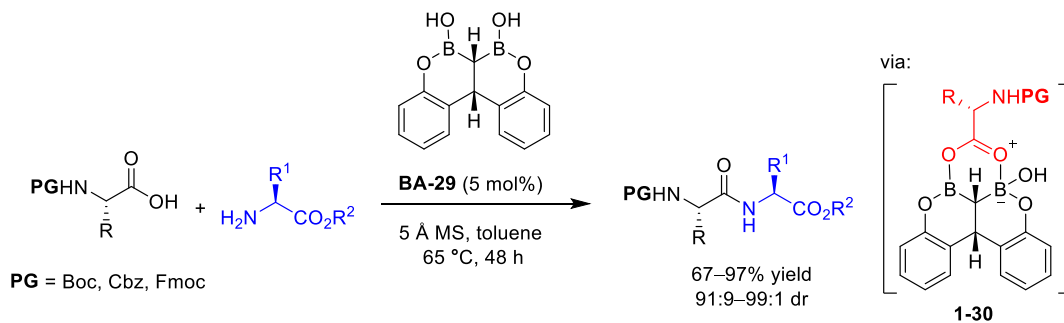
Scheme 1-8 gem-Diboronic acid **BA-29** catalyzed direct peptide formation.

Encouraged by the boronic acid/chiral amine dual catalyzed enantioselective allylation of branched aldehydes by Hall and co-workers, Ishihara and co-workers developed a similar dual catalytic system for the enantioselective conjugate addition using **BA-30** and (*R*)-BINOL derived chiral amine **1-31** (Scheme 1-9).[78] In general, the corresponding products, **1-32**, were obtained in good yield with high enantioselectivity but moderate diastereoselectivity. The authors attributed the moderate diastereoselectivity of this protocol to the ease of self-epimerization of the products. Similar to the previous report by Hall and co-workers, it is proposed that the

carboxylic acids and cycloalkanones are activated by boronic acid and chiral amine, respectively, as illustrated in the transition state **1-33.**
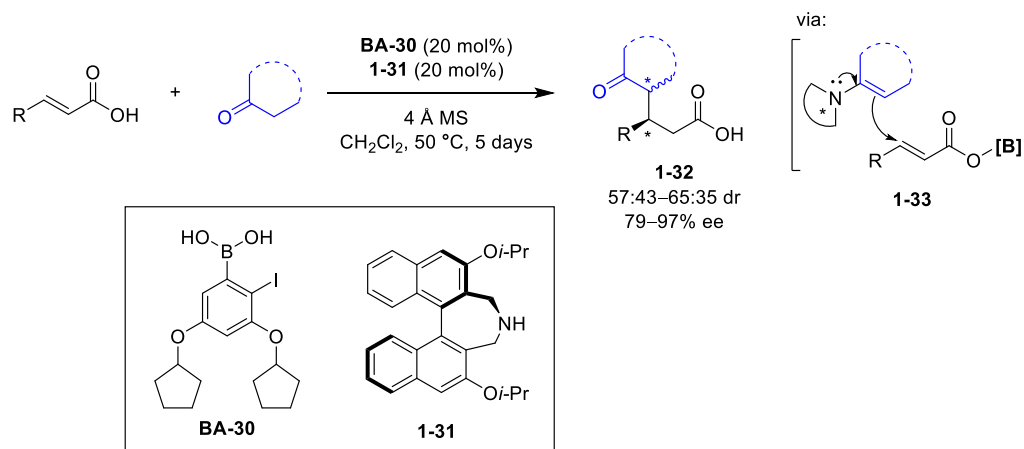
Scheme 1-9 Enantioselective conjugate addition of α,β-unsaturated carboxylic acids with cycloalkanones via boronic acid/chiral amine dual catalysis.

New advances also have been made in the field of nucleophilic activation of polyols via BAC. In 2019, Shimada and co-workers introduced a new bifunctional boronic acid, **BA-31**, with an ortho-imidazole moiety for the site-selective acylation of unprotected carbohydrates at the equatorial position of cis-vicinal diols (Scheme 1-10A).[79]
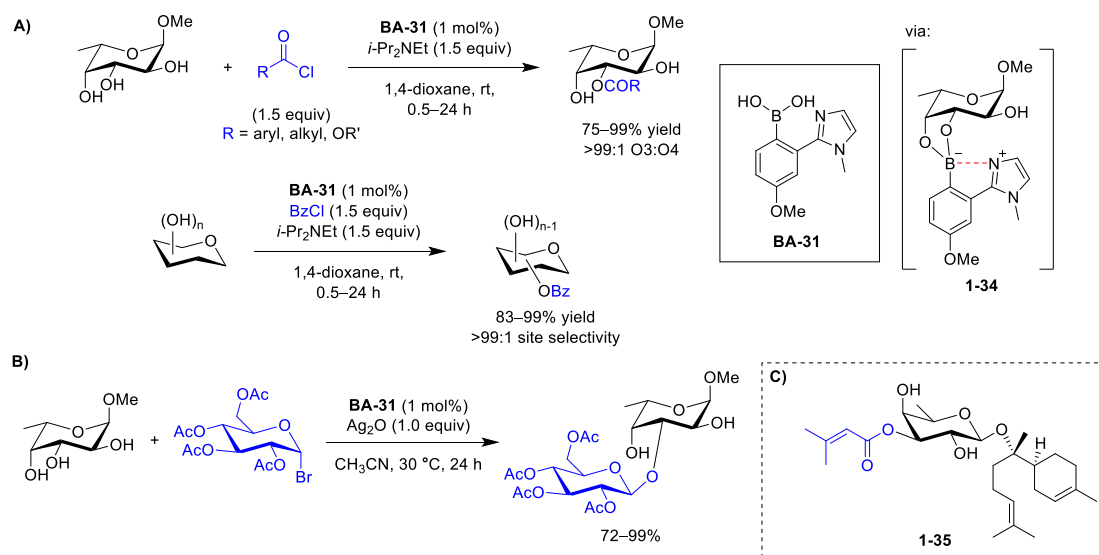
Scheme 1-10 Boronic acid catalyzed A) site-selective acylation of unprotected carbohydrates; and B) regioselective Koenigs–Knorr-type glycosylation; C) structure of O-3'-senecioyl α-bisabolol β-ᴅ-fucopyranoside **1-45.**

17

In this case, the ortho-imidazole moiety is thought to serve as a Lewis base in the reaction to increase the nucleophilicity of the hydroxy group via intramolecular coordination of imidazole nitrogen atom and boron in the intermediate **1-34**. Later, they expanded the scope of the **BA-31** catalytic system to the highly regioselective Koenigs–Knorr–type glycosylation of unprotected or partly protected carbohydrates (Scheme 1-10B)[80] and late-stage site-selective acylation in the total synthesis of O3' senecioyl α-bisabolol β-D-fucopyranoside **1-35** (Scheme 1-10C).[81]

Furthermore, two hemiboronic acids were identified also as suitable catalysts for selective mono-functionalization of cis-1,2-diols. In 2019, Arai and co-workers introduced a novel chiral benzazaborole **BA-32** derived from cinchonine for the catalytic enantioselective sulfonylation of cis-1,2-diols with *N*-methylimidazole (NMI) as a co-catalyst (Scheme 1-11A).[82] However, this asymmetric system is limited to *cis*-1,2-cyclohexanediol as a suitable diol substrate to fashion the corresponding products **1-36** in high yield and good enantioselectivity. Mechanistically, like other boronic acid catalysts, benzazaborole **BA-32** activates the diols through a tetrahedral boronate intermediate **1-37** in basic conditions, and the enantioselectivity is believed to arise from the chiral cinchonine moiety in **BA-32**. On the other hand, the co-catalyst NMI acts as a Lewis base and activates sulfonyl chlorides via the formation of the imidazolium salt **1-38**. Following this work, in 2020, Hayashida and co-workers reported the use of a novel benzoxaborole derivative, **BA-33**, for a more general catalytic site-selective functionalization of polyols containing a cis-1,2-diol moiety, including unprotected carbohydrates (Scheme 1-11B).[83] A diverse functionalization of polyols, such as acylation, sulfonylation, alkylation, and glycosylation, was possible with this catalytic system. Similarly, the reaction also proceeds through a tetrahedral boronate **1-39**.
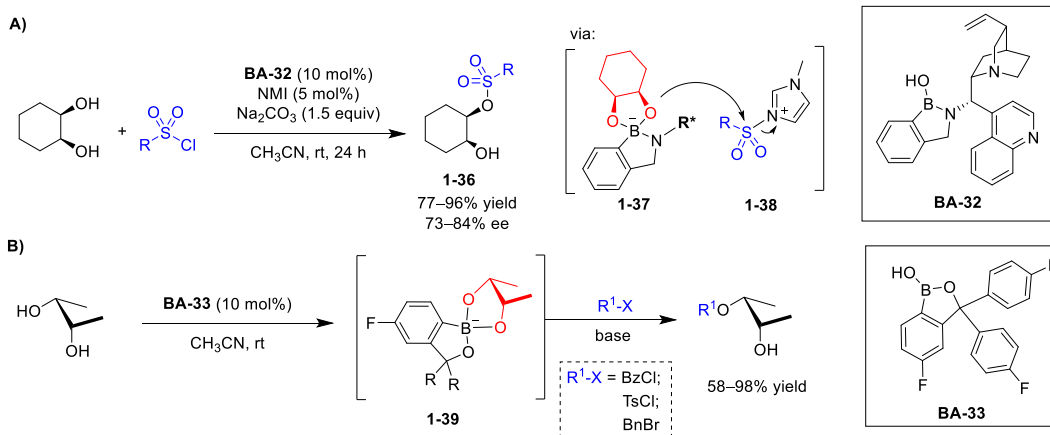
Scheme 1-11 Hemiboronic acids as catalysts for selective mono-functionalization of cis-1,2-diols.

Along the same lines, a very specific diastereoselective desymmetrization of meso-diols by 1,2-cis-glycosylation catalyzed by 4-nitrophenylboronic acid (**BA-34**) was developed by Toshima and co-workers in 2020 (Scheme 1-12).[84] This desymmetrization protocol is restricted to the *meso-myo*-inositol 1,3,5-orthoester substrates **1-40** and optically active 1,2-anhydro glycosyl donors. Based on computational studies, the differentiation of the enantiotopic hydroxy groups of substrates **1-40** was controlled by the stereochemistry of the glycosyl donors at the C2 position, as shown in the boronate intermediates **1-41** and **1-42,** where the glycosyl donors approach the boron atom differently.
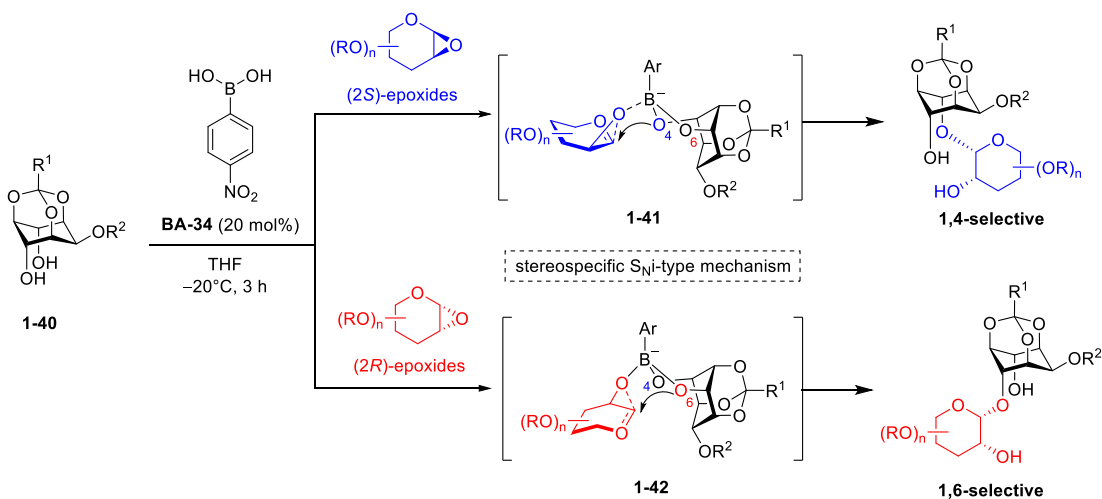
Scheme 1-12 Boronic acid catalyzed diastereoselective desymmetrization of *meso-myo*-inositol 1,3,5-orthoester substrates **1-40** by 1,2-cis-glycosylation.

Recently, the concept of BAC was expanded further to two new transformations. In 2020, Kürti and co-workers demonstrated the use of 3,5-difluorophenylboronic acid (**BA-35**) in promoting the *C*-allylation of oximes with allyl diisopropyl boronate **1-43** (Scheme 1-13A).[85] The use of **BA-35** was found to be crucial in the transformation, as only a trace amount of product was obtained in the absence of **BA-35**. While the role of **BA-35** is still under investigation, the authors postulated that **BA-35** facilitates the reaction by activating the allylic boronate **1-43** via transesterification to generate a more reactive boronic acid intermediate. To showcase the utility of this reaction, they employed this BAC protocol in a concise total synthesis of *N*-Me-euphococcine **1-44**.
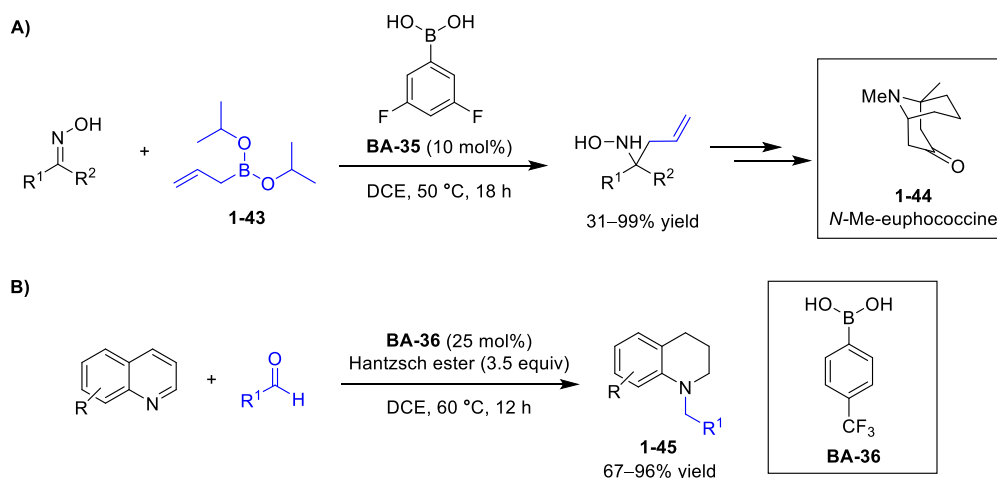
Scheme 1-13 Boronic acid-catalyzed A) *C*-allylation of oximes; B) reductive alkylation of quinolines to *N*-alkyl tetrahydroquinolines.

In 2021, a reductive alkylation of quinolines to *N*-alkyl tetrahydroquinolines catalyzed by 4-trifluoromethyl-phenylboronic acid (**BA-36**) was reported by Das and co-workers (Scheme 1-13B).[86] This protocol features a mild and step-economical synthesis of tetrahydroquinoline from readily available quinolines and aldehydes using Hantzsch ester (HE) as the reductant. Based on extensive NMR studies, a dual-role of **BA-36** was proposed in this transformation, where **BA-36** activates quinoline, aldehyde, as well as HE via hydrogen bonding interactions. **BA-36** also assists in the condensation of aldehydes with the tetrahydroquinoline intermediate as a Lewis acid. The proposed hydrogen bonding activation manifold agrees with the findings of

Franz and co-workers in their study of NMR quantification of hydrogen bonding activation by organocatalysts, including boronic acids, where they showed that **BA-36** exhibits strong hydrogen bond interactions with triethylphosphine oxide.[87]

In addition, an interesting application of boronic acids as a co-catalyst to improve the enantioselectivity of a chiral *N*-heterocyclic carbene (NHC, **1-46**) catalyzed benzoin condensation of electron-deficient benzaldehydes using **BA-36** was disclosed by Milo and co-workers in 2019 (Scheme 1-14).[88] The improvement in reactivity and enantioselectivity with **BA-36** was attributed to the formation of boronate species **1-47** through dynamic covalent interactions between **1-46**, **BA-36** and aldehydes, where **BA-36** creates a secondary coordination sphere to enhance the enantioselectivity further.
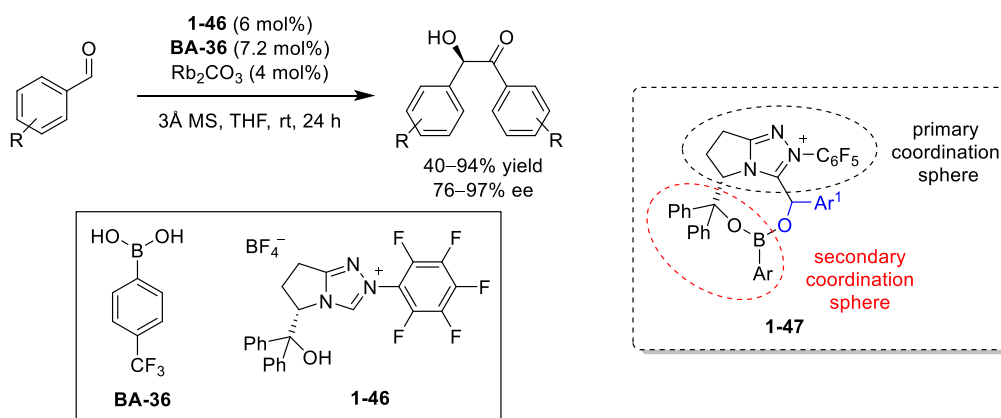
Scheme 1-14 Boronic acid as a co-catalyst for the NHC catalyzed enantioselective benzoin condensation.

1.3 Practicality and Versatility of BAC

As illustrated in Section 1.2, a diversity of reactions has been adapted successfully to BAC. The main factors that contributed to such remarkable advancements are the practicality and versatility offered by BAC.

1.3.1 Practicality of BAC

As mentioned above, the physicochemical properties of arylboronic acids make them good candidates as catalysts with high practicality. Due to their high stability, boronic acid catalysts can be recovered easily by column chromatography or acid–base extraction. Although arylboronic acids are generally inexpensive, the ability to

recover them after a reaction would be highly advantageous in industrial settings, specifically, in terms of improving atom-economy and reducing the cost of manufacturing, where the reactions are conducted in large scale. This recoverability of boronic acids has been demonstrated by Hall and co-workers in their work on the direct amidation of carboxylic acid and intramolecular cyclization of allylic alcohols bearing a pendent nucleophile.[32,47]

Furthermore, the mildness of BAC protocols offers higher efficiency and tolerance of sensitive functional groups compared to the conventional protic acid systems. For example, in the boronic acid catalyzed [4+3] cycloaddition with indolyl alcohols by Zheng and co-workers, while BAC protocols afforded the desired products in moderate to high yields, strong protic acids, such as *p*-toluenesulfonic acid (TsOH) or camphorsulfonic acid (CSA), failed to deliver the desired products and resulted in undesired self-condensation (Scheme 1-15A).[56] The superiority of boronic acid over protic acids was testified also by Hall and co-workers in the intramolecular cyclization of allylic alcohols, where compared to the use of TsOH, **BA-17** resulted in higher product yields and cleaner reactions (Scheme 1-15B).[47] Moreover, the mildness of BAC systems is demonstrated also by the minimal extent of epimerization observed in the boronic acid catalyzed direct dehydrative peptide synthesis by Shimada and co-workers (Scheme 1-7B), as well as by Takemoto and co-workers (Scheme 1-8).

A) Zheng, 2015
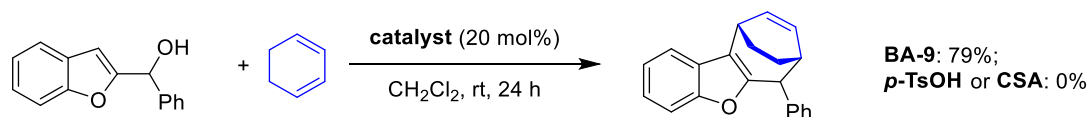
B) Hall, 2012
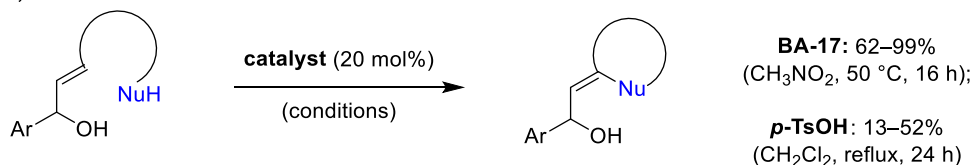
Scheme 1-15 Examples illustrating the mildness of BAC system.

BAC also imparts better atom- and step-economy compared to conventional methods, which is beneficial in the concept of green chemistry. For example, the direct electrophilic activation of hydroxy group via BAC not only circumvents the need of pre-activation of the hydroxy group into more reactive intermediates using excess reagents, it also generates water as the only by-product. Moreover, as shown by Shimada and co-workers (Scheme 1-10), due to the selective recognition of boronic acids toward cis-1,2-diols, the need for protection of other nucleophilic moieties can be avoided in the site-selective functionalization of polyols, especially carbohydrate substrates. Lastly, the operational simplicity of BAC, which does not require special precautions, is also an attractive aspect regarding practicality.

1.3.2 Multiple Catalytic Activation Mechanisms

The versatility of BAC arises from the ability of boronic acid to activate different substrates via different mechanisms. Conventionally, boronic acids are believed to act as a mild Lewis acid and provide electrophilic and nucleophilic activations through temporary covalent interactions between the substrates and the boron center (Figure 1-8A). More recently, other activation mechanisms, such as indirect Brønsted acid and hydrogen-bonding, have been proposed, based on preliminary mechanistic experiments (Figure 1-8B and C). For example, an indirect Brønsted acid mechanism was suggested by Taylor and co-workers in their **BA-16**/oxalic acid co-catalytic system for direct electrophilic activation of secondary benzylic alcohols via the formation of the hydronium species **1-17** (Scheme 1-4), and by Judeh and co-workers in their publication on the boronic acid catalyzed direct addition of deactivated peracetylated D-galatal (Scheme 1-3). The ability of boronic acids to act as hydrogen-bond donors to facilitate reactions has been proposed in the past, where secondary interactions are provided via hydrogen-bonding to bind and hold reagents in close proximity. However, the direct activation of nitrogen- and oxygen-containing compounds via a hydrogen-bonding mechanism was proposed recently, based on NMR studies by Das and co-workers in the boronic acid catalyzed reductive alkylation of quinolines to *N*-alkyl tetrahydroquinolines (Scheme 1-13B).
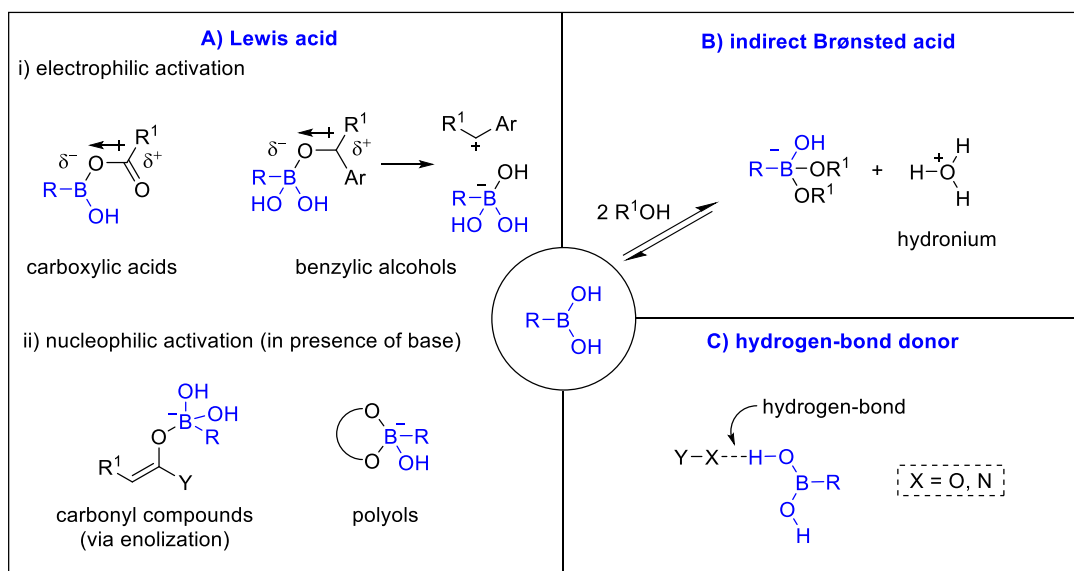
Figure 1-8 Putative activation modes via BAC.

More interestingly, boronic acids often play multiple roles in the mechanism by providing a different type of activation. For example, in the boronic acid catalyzed Biginelli synthesis of 3,4-hydropyrimidone reported by Carboni and co-workers, the boronic acid catalyst **BA-2** was proposed to play a dual role (Scheme 1-16A).[57] It was envisioned that **BA-2** not only provides nucleophilic activation to ethyl acetoacetate via the formation of enolate intermediate **1-48** but also provides electrophilic activation to the acylimine intermediate **1-49**, which was generated from the condensation between aldehyde and urea via a boron–nitrogen covalent interaction. Toshima and co-workers also proposed multiple roles of boronic acid **BA-24** in their regioselective and 1,2-cis-α-stereoselective glycosylation BAC protocol.[62] As depicted in Scheme 1-16B, **BA-24** not only serves as a template to bring both the glycosyl donor and acceptor together, it also provides electrophilic activation to the 1,2-anhydro glycosyl donor via complex **1-50**, which triggers the epoxide ring opening, generating the anionic boronate intermediate **1-51**. The formation of intermediate **1-51** then enhances the nucleophilicity of the glycosyl acceptor and facilitates the glycosylation through the addition of the more accessible 6-alkoxy group to the bottom face of the oxonium cation.
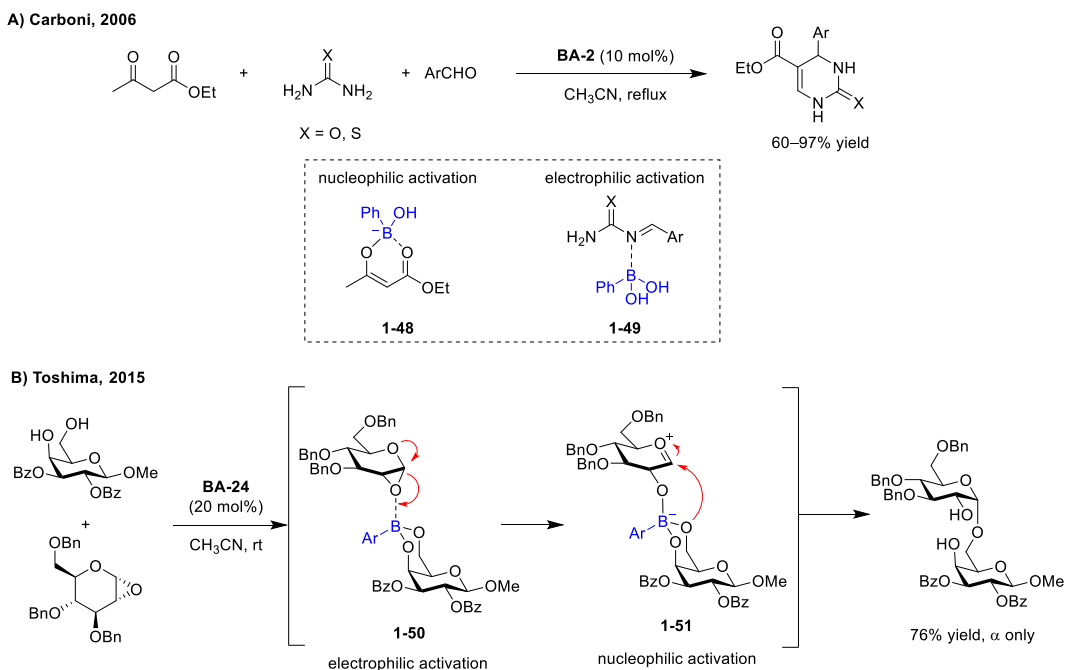
Scheme 1-16 Examples of dual role of boronic acid in BAC.

Additionally, as manifested by 36 different boronic acid catalysts shown above, it is clear that not all boronic acids catalyze the same reactions; there is often a specific boronic acid required for most transformations. This aspect of BAC was employed by Hall and co-workers in a sequential multicatalytic tandem reaction in one-pot using three different boronic acid catalysts for three classic BAC transformations: 1,3-transposition and elimination of allylic alcohol, Diels–Alder cycloaddition of α,β-unsaturated carboxylic acid, and the direct amidation of carboxylic acid (Scheme 1-17).[46]
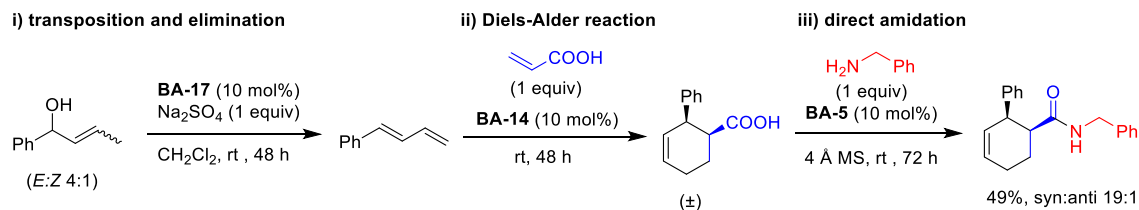
Scheme 1-17 Multi-catalytic tandem BAC sequence.

In addition, owing to their high stability and selectivity towards oxygen- and nitrogen-containing moieties, boronic acids have been shown to be compatible in dual catalysis expanding the scope of reactions amenable to BAC.

25

1.3.3 Ease of Catalyst Modification

The well-established methods to prepare boronic acids, especially arylboronic acids, allow easy fine-tuning of boronic acid catalysts for better performance (Figure 1-9A). The electrophilicity of the boron center can be modulated readily by installing electron-donating or electron-withdrawing substituents on the arene core. Moreover, the installation of ortho-substituents can be beneficial, as ortho-substituted arylboronic acids are viewed often as bifunctional catalysts. As demonstrated by catalysts **BA-1** and **BA-31** in the above sections, ortho-substituents can act as a template to direct reagents or provide further activation to the substrate via cooperative effects (Figure 1-9B).
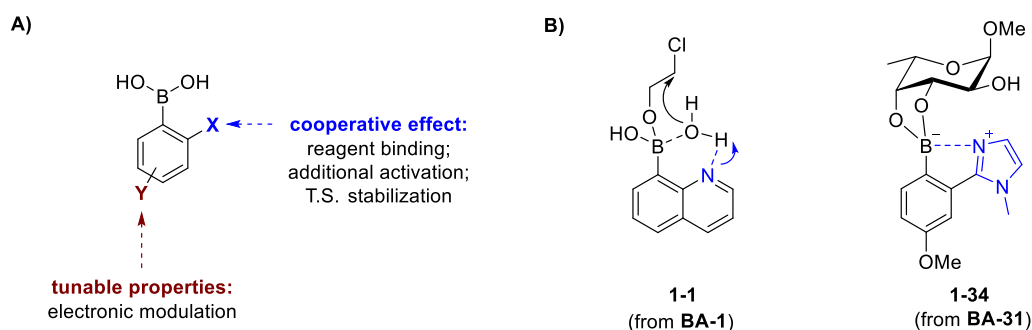
Figure 1-9 A) Modulation of boronic acid; B) examples of bifunctional boronic acid catalysts.

This advantage of BAC enables the identification of optimal or second-generation catalysts by tuning the electronic properties and allows rational design of boronic acid catalysts, based on postulated mechanisms or knowledge garnered from the literature. In their work on the direct amidation in ambient conditions, Hall and co-workers exploited this feature and identified 5-methoxy-2-iodophenylboronic acid (**BA-6**) as a more efficient catalyst by optimizing the electronic properties of the arene core of *ortho*-iodophenylboronic acid (**BA-5**), the first-generation catalyst (Scheme 1-18A).[33] Based on their previous findings of a dual catalytic asymmetric intramolecular hetero-Michael reaction using **BA-14** and chiral thiourea **1-6,** this attribute also enabled Takemoto and co-workers to develop the chiral thiourea-aminoboronic acid catalyst **BA-15** for the asymmetric intermolecular hetero-Michael reaction (Scheme 1-18B).[44] More recently, based on the knowledge

that the formation of an anionic tetrahedral boronate in the presence of a base is required to provide nucleophilic activation to polyols, Shimada and co-workers rationally designed a boronic acid catalyst bearing a Lewis base motif at the ortho-position for the site-selective functionalization of unprotected carbohydrates (Scheme 1-10). In this study, several ortho-Lewis basic motifs were screened, and the imidazole moiety was identified to be the optimal substituent. Further tuning of electronic properties of the arene core led to the identification of the optimal catalyst **BA-31** (Scheme 1-18C).[79]
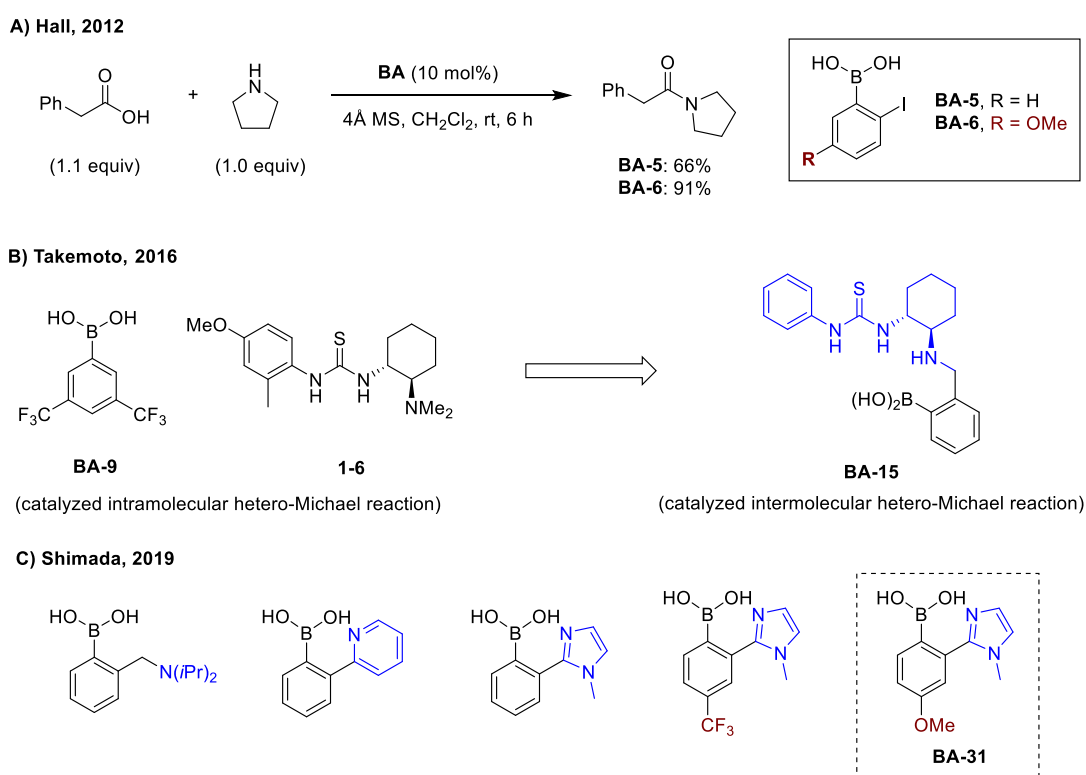
Scheme 1-18 Representative examples highlighting the ease of catalyst modification in BAC.

1.4 Challenges and Current Limitations of BAC

1.4.1 High Catalyst Loading

Compared to transition-metal catalysis, BAC generally requires a higher catalyst loading (5–20 mol%). However, this disadvantage of BAC is offset easily by the price and recoverability of boronic acids.

1.4.2 Scarcity of Asymmetric Transformations

Despite the impressive breakthroughs achieved in BAC, only a handful of asymmetric transformations have been reported. This limitation is likely due to the achiral and planar nature of arylboronic acids. Chemists have overcome this problem partially by incorporating BAC in dual catalysis with a chiral catalyst and appending an ortho-chiral substituent onto the arylboronic acid catalysts (Figure 1-10). However, the reactions often display a very limited substrate scope and moderate selectivity. Therefore, there is an ample opportunity for the development of more general and selective asymmetric BAC in the future.
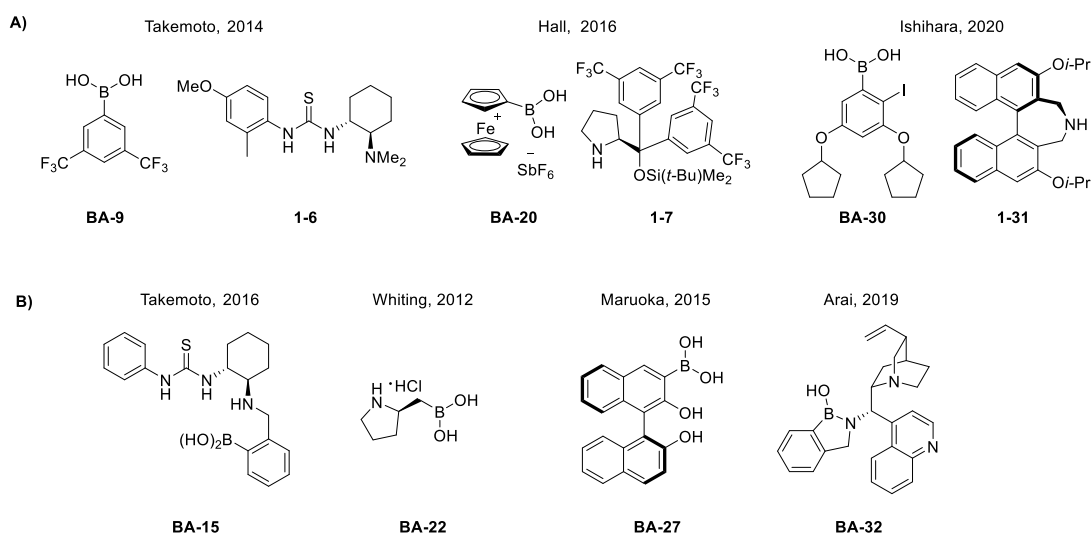
Figure 1-10 Examples of BAC systems for asymmetric transformations: A) with a chiral co-catalyst; and B) with a chiral boronic acid.

1.4.3 Limitation in the Direct Activation of Non-π-activated Alcohols

Despite the fact that several BAC protocols have been established for the direct dehydrative functionalization of alcohols and offer great advantages in terms of green chemistry, these procedures still face significant limitations. These protocols are restricted to the activation of π-activated alcohols, and expansion beyond π-activated alcohols has proved to be challenging. In addition to this significant substrate constraint, these protocols proceed via an S_N1 mechanism. Thus, the functionalization of unsymmetrical secondary alcohols results in racemic products; this is less desirable, given the importance of enantioenriched compounds in medicinal chemistry.

1.4.4 Mechanistic Ambiguities

As mentioned in Section 1.3.2, boronic acid catalysts confer multiple modes of activations, which can operate concurrently in a reaction. Accordingly, it also creates mechanistic ambiguities at the same time, as exemplified by recent debates regarding the mode of catalysis for electrophilic activation of hydroxy groups. Conventionally, it has been proposed that activation of hydroxy groups involves covalent bonding with a boron atom. However, a recent study by Moran and co-workers implies that the activation involves either Brønsted acid or hydrogen-bond mediated catalysis.[89] Furthermore, it was found that strong Brønsted acids are generated when HFIP was used as the solvent, indicating the existence of solvent-dependent activation modes, which has been overlooked. Thus, due to the unique properties of boronic acids, the activation mechanism can be very complicated, and a broad range of mechanistic studies and control experiments are required to determine the mode of activation. In this context, Franz and co-workers developed a quantification method to study the strength of hydrogen bonding activation of boronic acids, using triethylphosphine oxide (TEPO) as a probe for $\Delta\delta$ ^{31}P NMR measurements.[87] The $\Delta\delta$ ^{31}P NMR shifts were used as the parameters to define the hydrogen bonding strength and proved to correlate strongly with the catalytic activity via hydrogen bonding interactions. Extensive control experiments were conducted to rule out the possibility of Lewis acid binding to TEPO, hence, the $\Delta\delta$ ^{31}P NMR shifts are solely due to hydrogen bonding interactions. While these mechanistic ambiguities remain as a challenge, BAC undoubtedly offers mild reaction conditions with great functional group tolerability.

1.5 Thesis Objectives

As a promising emerging area of catalysis, it is believed strongly that the potential of BAC has not been realized fully yet, as several limitations remain to be addressed. Therefore, the goals of this thesis are: (1) to expand the scope of reactions amenable to BAC, including asymmetric transformations; (2) to improve the efficiency of the existing BAC protocols; and (3) to learn more about the role of the boronic acid

functionality in the BAC. It can be anticipated that achievement of these goals will provide important insights enabling future advances of BAC.

As delineated above, BAC has emerged as a promising strategy for the activation of various hydroxy-containing compounds, such as carboxylic acids, alcohols, and polyols. It is envisioned that oximes, which contain an N–hydroxy group (N–OH), can be activated by boronic acid and undergo subsequent transformation. In this regard, a unique class of boronic acid was discovered as a suitable catalyst for the Beckmann rearrangement under mild conditions. Chapter 2 will describe efforts made in the mechanistic investigations of this catalytic system to understand the role of the boronic acid catalyst. These mechanistic studies revealed a novel and unique role of the boronyl group of the catalyst. These findings may provide inspirations toward a new activation mode and design of boronic acid catalysts for hydroxy group activation.

The direct electrophilic activation of benzylic alcohols is one of the most studied areas in BAC, and several boronic acid catalytic systems were identified in the past decade. However, highly electron-deficient benzylic alcohols were found to be poor substrates in these systems. Chapter 3 will describe studies towards improving the efficiency of BAC in challenging Friedel–Crafts alkylation reactions with highly deactivated benzylic alcohols by using a diol co-catalyst. Mechanistic studies were conducted to gain insights toward the role of the co-catalyst in improving the reactivity of BAC. These studies may encourage the use of a diol co-catalyst in other BAC protocols for enhancing the reactivity.

Finally, the site-selective functionalization of polyols is another popular research area in BAC. However, due to their natural abundancy, especially in carbohydrates, most of the studies focus more on cis-1,2-diols; while 1,3-diols, another important class of polyols, often are neglected. Therefore, it would be of interest to fill the gap by developing a BAC system for the direct monofunctionalization of 1,3-diols and, more importantly, a system that can enable enantioselective desymmetrization of symmetrical, prochiral 1,3-diols to produce optically enriched monofunctionalized products. As such, Chapter 4 will introduce

the discovery of a rationally designed chiral hemiboronic acid catalyst derived from BINOL for the enantioselective desymmetrization of prochiral 1,3-diols by direct O-alkylation. It can be envisioned that this discovery will lead to further accomplishments in BAC for other enantioselective transformations.

1.6 References

(1) Hall, D. G., Ed. *Boronic Acids: Preparation and Applications in Organic Synthesis*, 2nd edn.; Wiley-VCH: Weinheim, 2011.

(2) Frankland, E.; Duppa, B. F. *Liebigs Ann.* **1860**, *115*, 319–322.

(3) Michaelis, A.; Becker, P. *Ber. Dtsch. Chem. Ges.* **1880**, *13*, 58–61.

(4) Miyaura, N.; Yamada, K.; Suzuki, A. *Tetrahedron Lett.* **1979**, *20*, 3437–3440.

(5) The Nobel Prize in Chemistry 2010 https://www.nobelprize.org/prizes/chemistry/2010/summary/ (accessed Jun 28, 2021).

(6) Matteson, D. S.; Collins, B. S. L.; Aggarwal, V. K.; Ciganek, E. The Matteson Reaction. In *Organic Reactions*; American Cancer Society, 2021; pp 427–860.

(7) Lachance, H.; Hall, D. G. Allylboration of Carbonyl Compounds. In *Organic Reactions*, **2009**, 1–574.

(8) Pyne, S. G.; Tang, M. The Boronic Acid Mannich Reaction. In *Organic Reactions*, **2014**, 211–498.

(9) Chen, J.-Q.; Li, J.-H.; Dong, Z.-B. *Adv. Synth. Catal.* **2020**, *362*, 3311–3331.

(10) Cheng, H.-G.; Chen, H.; Liu, Y.; Zhou, Q. *Asian J. Org. Chem.* **2018**, *7*, 490–508.

(11) Tian, Y.-M.; Guo, X.-N.; Braunschweig, H.; Radius, U.; Marder, T. B. *Chem. Rev.* **2021**, *121*, 3561–3597.

(12) Wang, M.; Shi, Z. *Chem. Rev.* **2020**, *120*, 7348–7398.

(13) Hartwig, J. F. *Chem. Soc. Rev.* **2011**, *40*, 1992–2002.

(14) Iqbal, S. A.; Pahl, J.; Yuan, K.; Ingleson, M. J. *Chem. Soc. Rev.* **2020**, *49*, 4564–4591.

(15) Chow, W. K.; Yuen, O. Y.; Choy, P. Y.; So, C. M.; Lau, C. P.; Wong, W. T.; Kwong, F. Y. *RSC Adv.* **2013**, *3*, 12518–12539.

(16) Plescia, J.; Moitessier, N. *Eur. J. Med. Chem.* **2020**, *195*, 112270.

(17) António, J. P. M.; Russo, R.; Carvalho, C. P.; Cal, P. M. S. D.; Gois, P. M. P. *Chem. Soc. Rev.* **2019**, *48*, 3513–3536.

(18) Akgun, B.; Hall, D. G. *Angew. Chem. Int. Ed.* **2018**, *57*, 13028–13044.

(19) Nishiyabu, R.; Kubo, Y.; D. James, T.; S. Fossey, J. *Chem. Commun.* **2011**, *47*, 1124–1150.

(20) Brooks, W. L. A.; Sumerlin, B. S. *Chem. Rev.* **2016**, *116*, 1375–1397.

(21) Kubo, Y.; Nishiyabu, R.; D. James, T. *Chem. Commun.* **2015**, *51*, 2005–2020.

(22) Wang, R.; Bian, Z.; Zhan, D.; Wu, Z.; Yao, Q.; Zhang, G. *Dyes Pigm.* **2021**, *185*, 108885.

(23) Fang, G.; Wang, H.; Bian, Z.; Sun, J.; Liu, A.; Fang, H.; Liu, B.; Yao, Q.; Wu, Z. *RSC Adv.* **2018**, *8*, 29400–29427.

(24) Espina-Benitez, M. B.; Randon, J.; Demesmay, C.; Dugas, V. *Sep. Purif. Rev.* **2018**, *47*, 214–228.

(25) Zheng, H.; Hall, D. G. *Aldrichimica Acta* **2014**, *47*, 41–51.

(26) Hall, D. G. *Chem. Soc. Rev.* **2019**, *48*, 3475–3496.

(27) Martínez-Aguirre, M. A.; Yatsimirsky, A. K. *J. Org. Chem.* **2015**, *80*, 4985–4993.

(28) Letsinger, R. L.; Dandegaonker, S.; Vullo, W. J.; Morrison, J. D. *J. Am. Chem. Soc.* **1963**, *85*, 2223–2227.

(29) Rao, G.; Philipp, M. *J. Org. Chem.* **1991**, *56*, 1505–1512.

(30) Ishihara, K.; Ohara, S.; Yamamoto, H. *J. Org. Chem.* **1996**, *61*, 4196–4197.

(31) Arnold, K.; Batsanov, A. S.; Davies, B.; Whiting, A. *Green Chem.* **2008**, *10*, 124–134.

(32) Al-Zoubi, R. M.; Marion, O.; Hall, D. G. *Angew. Chem. Int. Ed.* **2008**, *47*, 2876–2879.

(33) Gernigon, N.; Al-Zoubi, R. M.; Hall, D. G. *J. Org. Chem.* **2012**, *77*, 8386–8400.

(34) Mohy El Dine, T.; Erb, W.; Berhault, Y.; Rouden, J.; Blanchet, J. *J. Org. Chem.* **2015**, *80*, 4532–4544.

(35) Ishihara, K.; Lu, Y. *Chem. Sci.* **2016**, *7*, 1276–1280.

(36) Wang, K.; Lu, Y.; Ishihara, K. *Chem. Commun.* **2018**, *54*, 5410–5413.

(37) Noda, H.; Furutachi, M.; Asada, Y.; Shibasaki, M.; Kumagai, N. *Nat. Chem.* **2017**, *9*, 571–577.

(38) Arkhipenko, S.; Sabatini, M. T.; Batsanov, A. S.; Karaluka, V.; Sheppard, T. D.; Rzepa, H. S.; Whiting, A. *Chem. Sci.* **2018**, *9*, 1058–1072.

(39) Maki, T.; Ishihara, K.; Yamamoto, H. *Org. Lett.* **2005**, *7*, 5047–5050.

(40) Sakakura, A.; Ohkubo, T.; Yamashita, R.; Akakura, M.; Ishihara, K. *Org. Lett.* **2011**, *13*, 892–895.

(41) Zheng, H.; Hall, D. G. *Tetrahedron Lett.* **2010**, *51*, 3561–3564.

(42) Zheng, H.; McDonald, R.; Hall, D. G. *Chem. Eur. J.* **2010**, *16*, 5454–5460.

(43) Azuma, T.; Murata, A.; Kobayashi, Y.; Inokuma, T.; Takemoto, Y. *Org. Lett.* **2014**, *16*, 4256–4259.

(44) Hayama, N.; Azuma, T.; Kobayashi, Y.; Takemoto, Y. *Chem. Pharm. Bull.* **2016**, *64*, 704–717.

(45) McCubbin, J. A.; Hosseini, H.; Krokhin, O. V. *J. Org. Chem.* **2010**, *75*, 959–962.

(46) Zheng, H.; Lejkowski, M.; Hall, D. G. *Chem. Sci.* **2011**, *2*, 1305–1310.

(47) Zheng, H.; Ghanbari, S.; Nakamura, S.; Hall, D. G. *Angew. Chem. Int. Ed.* **2012**, *51*, 6187–6190.

(48) Ricardo, C. L.; Mo, X.; McCubbin, J. A.; Hall, D. G. *Chem. Eur. J.* **2015**, *21*, 4218–4223.

(49) Mo, X.; Yakiwchuk, J.; Dansereau, J.; McCubbin, J. A.; Hall, D. G. *J. Am. Chem. Soc.* **2015**, *137*, 9694–9703.

(50) Mo, X.; Hall, D. G. *J. Am. Chem. Soc.* **2016**, *138*, 10762–10765.

(51) Wolf, E.; Richmond, E.; Moran, J. *Chem. Sci.* **2015**, *6*, 2501–2505.

(52) Verdelet, T.; Ward, R. M.; Hall, D. G. *Eur. J. Org. Chem.* **2017**, 5729–5738.

(53) Estopiñá-Durán, S.; Donnelly, L. J.; Mclean, E. B.; Hockin, B. M.; Slawin, A. M.; Taylor, J. *Chem. Eur. J.* **2019**, *25*, 3950–3956.

(54) Zheng, H.; Lejkowski, M.; Hall, D. G. *Tetrahedron Lett.* **2013**, *54*, 91–94.

(55) Tang, W.-B.; Cao, K.-S.; Meng, S.-S.; Zheng, W.-H. *Synthesis* **2017**, *49*, 3670–3675.

(56) Cao, K.-S.; Bian, H.-X.; Zheng, W.-H. *Org. Biomol. Chem.* **2015**, *13*, 6449–6452.

(57) Debache, A.; Boumoud, B.; Amimour, M.; Belfaitah, A.; Rhouati, S.; Carboni, B. *Tetrahedron Lett.* **2006**, *47*, 5697–5699.

(58) Aelvoet, K.; Batsanov, A. S.; Blatch, A. J.; Grosjean, C.; Patrick, L. G.; Smethurst, C. A.; Whiting, A. *Angew. Chem. Int. Ed.* **2008**, *47*, 768–770.

(59) Georgiou, I.; Whiting, A. *Org. Biomol. Chem.* **2012**, *10*, 2422–2430.

(60) Li, M.; Yang, T.; Dixon, D. J. *Chem. Commun.* **2010**, *46*, 2191–2193.

(61) Lee, D.; Taylor, M. S. *Org. Biomol. Chem.* **2013**, *11*, 5409–5412.

(62) Tanaka, M.; Nakagawa, A.; Nishi, N.; Iijima, K.; Sawa, R.; Takahashi, D.; Toshima, K. *J. Am. Chem. Soc* **2018**, *140*, 3644–3651.

(63) William, J. M.; Kuriyama, M.; Onomura, O. *Adv. Synth. Catal.* **2014**, *356*, 934–940.

(64)	Hashimoto, T.; Galvez, A. O.; Maruoka, K. *J. Am. Chem. Soc.* **2015**, *137*, 16016–16019.

(65)	Liu, J.; Yao, H.; Wang, C. *ACS Catal.* **2018**, *8*, 9376–9381.

(66)	Yao, H.; Liu, J.; Wang, C. *Org. Biomol. Chem.* **2019**, *17*, 1901–1905.

(67)	Tatina, M. B.; Moussa, Z.; Xia, M.; Judeh, Z. M. A. *Chem. Commun.* **2019**, *55*, 12204–12207.

(68)	Estopina-Duran, S.; Mclean, E. B.; Donnelly, L. J.; Hockin, B. M.; Taylor, J. E. *Org. Lett.* **2020**, *22*, 7547–7551.

(69)	Twilton, J.; Christensen, M.; DiRocco, D. A.; Ruck, R. T.; Davies, I. W.; MacMillan, D. W. C. *Angew. Chem. Int. Ed.* **2018**, *57*, 5369–5373.

(70)	Dimakos, V.; Su, H. Y.; Garrett, G. E.; Taylor, M. S. *J. Am. Chem. Soc.* **2019**, *141*, 5149–5153.

(71)	Dimakos, V.; Gorelik, D.; Su, H. Y.; Garrett, G. E.; Hughes, G.; Shibayama, H.; Taylor, M. S. *Chem. Sci.* **2020**, *11*, 1531–1537.

(72)	Reddy, R. J.; Waheed, M.; Krishna, G. R. *Org. Biomol. Chem.* **2020**, *18*, 3243–3248.

(73)	Shimada, N.; Hirata, M.; Koshizuka, M.; Ohse, N.; Kaito, R.; Makino, K. *Org. Lett.* **2019**, *21*, 4303–4308.

(74)	Koshizuka, M.; Makino, K.; Shimada, N. *Org. Lett.* **2020**, *22*, 8658–8664.

(75)	Fatemi, S.; Gernigon, N.; Hall, D. G. *Green Chem.* **2015**, *17*, 4016–4028.

(76)	Shimada, N.; Ohse, N.; Takahashi, N.; Urata, S.; Koshizuka, M.; Makino, K. *Synlett* **2021**, *32*, 1024–1028.

(77)	Michigami, K.; Sakaguchi, T.; Takemoto, Y. *ACS Catal.* **2020**, *10*, 683–688.

(78)	Horibe, T.; Hazeyama, T.; Nakata, Y.; Takeda, K.; Ishihara, K. *Angew. Chem. Int. Ed.* **2020**, *59*, 17256–17260.

(79)	Shimada, N.; Nakamura, Y.; Ochiai, T.; Makino, K. *Org. Lett.* **2019**, *21*, 3789–3794.

(80)	Shimada, N.; Sugimoto, T.; Noguchi, M.; Ohira, C.; Kuwashima, Y.; Takahashi, N.; Sato, N.; Makino, K. *J. Org. Chem.* **2021**, *86*, 5973–5982.

(81)	Nakamura, Y.; Ochiai, T.; Makino, K.; Shimada, N. *Chem. Pharm. Bull.* **2021**, *69*, 281–285.

(82)	Kuwano, S.; Hosaka, Y.; Arai, T. *Org. Biomol. Chem.* **2019**, *17*, 4475–4482.

(83)	Kusano, S.; Miyamoto, S.; Matsuoka, A.; Yamada, Y.; Ishikawa, R.; Hayashida, O. *Eur. J. Org. Chem.* **2020**, 1598–1602.

(84)	Tanaka, M.; Sato, K.; Yoshida, R.; Nishi, N.; Oyamada, R.; Inaba, K.; Takahashi, D.; Toshima, K. *Nat. Commun.* **2020**, *11*, 2431.

(85)	Siitonen, J. H.; Kattamuri, P. V.; Yousufuddin, M.; Kürti, L. *Org. Lett.* **2020**, *22*, 2486–2489.

(86)	Adhikari, P.; Bhattacharyya, D.; Nandi, S.; Kancharla, P. K.; Das, A. *Org. Lett.* **2021**, *23*, 2437–2442.

(87)	Diemoz, K. M.; Franz, A. K. *J. Org. Chem.* **2019**, *84*, 1126–1138.

(88)	Dhayalan, V.; Gadekar, S. C.; Alassad, Z.; Milo, A. *Nat. Chem.* **2019**, *11*, 543–551.

(89)	Zhang, S.; Lebœuf, D.; Moran, J. *Chem. Eur. J.* **2020**, *26*, 9883–9888.

CHAPTER 2

Study of True Organocatalytic Beckmann Rearrangement using Boronic Acid/Perfluoropinacol Co-catalytic System[†]

2.1 Introduction

Amides are one of the most essential functional groups in the living world, as it is the key bond linkage found in peptide bonds, which are crucial for protein formation. Amides also can be found in major marketed pharmaceuticals (Figure 2-1), ranging from the household medication, paracetamol, to lifesaving medication, such as penicillin. Other examples include lidocaine,[1] an amino amide type local anesthetic, sulpiride,[2] an atypical antipsychotic medication, and benazepril,[3] a medication for hypertension. Furthermore, amides are also prevalent in the polymer industry to produce important plastics, such as Nylons[4] and Kevlar[5]. Given the importance of amides, the development of a more efficient and sustainable methodology for amide synthesis remains a high-priority research area.

Paracetamol
(painkiller and treats fever)

Lidocaine
(local anesthetic)

Benazepril
(treats high blood pressure, heart failure and diabetic kidney disease)

Penicillin G
(antibiotic; treats infectious diseases)

Sulpiride
(antipsychotic, antidepressant)
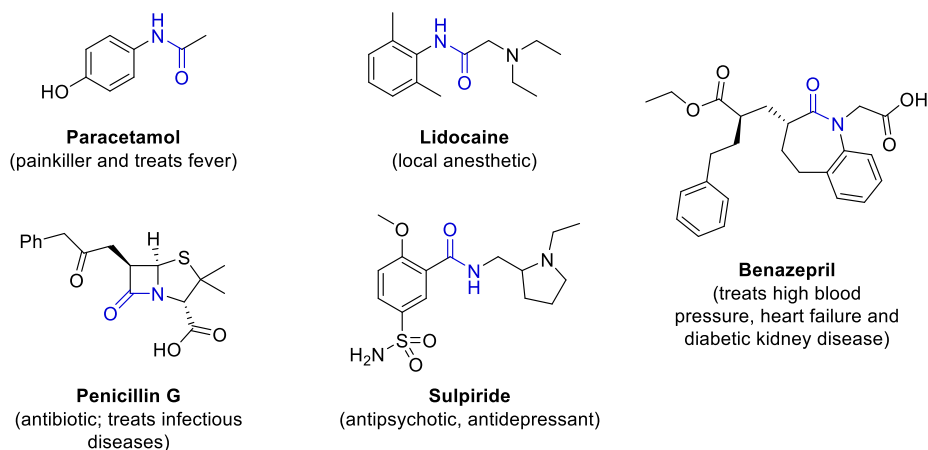
Figure 2-1 Selected examples of amide containing pharmaceuticals.

[†] A version of this chapter has been published as Mo, X.; Morgan, T. D. R.; Ang, H. T.; Hall, D. G. *J. Am. Chem. Soc.* **2018**, *140*, 5264−5271.

Other than the conventional coupling of carboxylic acids with amines,[6] the Beckmann rearrangement is another common practical method for amide synthesis. The Beckmann rearrangement, an acid-promoted rearrangement of oximes to amides (Scheme 2-1A), was discovered in 1886 by Ernst Otto Beckmann, a German chemist, and has received great attention since its discovery.[7] One reason is that oximes are synthesized easily via condensation of hydroxylamine (NH_2OH), which is a widely available functional group, with ketones. Therefore, this methodology enables facile transformation of ketones into amides in two operations. For instance, this strategy has been used in the industrial synthesis of caprolactam from cyclohexanone, which is a feedstock for Nylon-6 production (Scheme 2-1B).[4] This transformation also has been used in the final step towards the synthesis of paracetamol to transform a methyl ketone into an acetamide (Scheme 2-1C).[8] The general proposed reaction mechanism proceeds by activation of the oxime hydroxy group with strong acid, followed by anti-periplanar migration of the R-group (aryl or alkyl) and simultaneous expulsion of the activated hydroxy group to form a nitrilium ion; then, subsequent hydrolysis and tautomerization generates the amide product (Scheme 2-1D).[9]
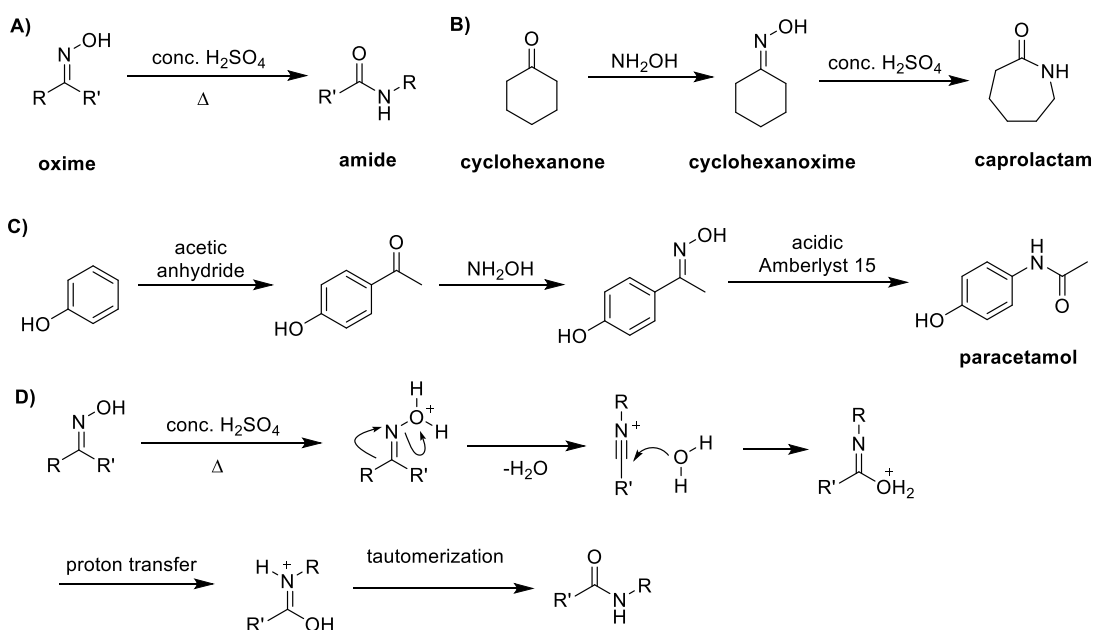
Scheme 2-1 A) The Beckmann rearrangement, its industrial applications: B) synthesis of caprolactam and C) synthesis of paracetamol, and D) proposed reaction mechanism.

As shown in the examples above, the traditional Beckmann rearrangement often is promoted stoichiometrically using strong Brønsted or Lewis acids, such as concentrated sulfuric acid, phosphorus pentachloride, polyphosphoric acid, and thionyl chloride, at elevated temperature.[10] However, due to a lack of functional group compatibility and poor atom-economy, the use of such harsh conditions hampers the utility of this significant transformation. Moreover, bases also are needed to neutralize the reaction, thus generating large amounts of salt by-products. Considering the significance of this reaction in industry, the development of a mild and greener catalytic system for the Beckmann rearrangement is highly desired. In fact, a vast number of catalytic methods in a different medium, such as liquid phase, vapor phase, ionic liquids, and supercritical water, have been developed in the past 20 years and were summarized in a comprehensive review written by Kaur and Srivastava in 2020.[11]

Particularly, organocatalytic Beckmann rearrangements in the liquid phase attract more interest due to their high efficiency, broader functional group tolerability, and operational simplicity (Scheme 2-2). The first organocatalytic system was reported by Yamamoto and co-workers in 2005 using cyanuric chloride (CNC) with zinc chloride as the co-catalyst in refluxing acetonitrile; however, this catalytic system was not effective for six to eight membered cyclic oximes.[12] Later, Deng and co-workers also discovered that bis(2-oxo-3-oxazolidinyl)phosphinic chloride (BOP-Cl)[13] and *p*-toluenesulfonyl chloride (TsCl)[14], a common dehydrating reagent, were efficient catalysts for the Beckmann rearrangement using co-catalytic zinc chloride in refluxing acetonitrile. In 2007, Hashimoto and co-workers reported an efficient catalytic system with the use of 1,3,5-triazo-2,4,6-triphosphorine-2,2,4,4,6,6-chloride (TAPC), without the need of any co-catalytic Lewis acid in HFIP or acetonitrile, at elevated temperature (70 °C); this system was found to be more efficient than CNC when using cyclohexanone as a substrate.[15] In 2010, Lambert and co-workers reported the use of 1,1-dichloro-2,3-diphenylcyclopropenone (CPI-Cl), which is generated *in situ* from 2,3-cyclopropenone and oxalyl chloride, as a stand-alone catalyst in acetonitrile at room temperature.[16] In the same year, Augustine and

co-workers also disclosed the use of propanephosphonic acid anhydride (T3P) as a stand-alone catalyst in refluxing THF.[17] Lastly, in 2018, Gao and co-workers reported that readily available geminal dichloroimidazolidinediones (DCIDs) also were viable catalysts in acetonitrile at 80 °C.[18]

	organocatalyst	co-catalyst	solvent, temp
Yamamoto, 2005 CNC system	**CNC**	$ZnCl_2$	CH_3CN, reflux
Deng, 2006 BOP-Cl system	**BOP-Cl**	$ZnCl_2$	CH_3CN, reflux
Hashimoto, 2007 TAPC system	**TAPC**	—	HFIP or CH_3CN, 70 °C
Deng, 2009 TsCl system	**TsCl**	$ZnCl_2$	CH_3CN, reflux
Lambert, 2010 CPI-Cl system	**CPI-Cl** (formed *in-situ*)		CH_3CN, rt
Augustine, 2010 T3P system	**T3P**	—	THF, 70 °C
Gao, 2018 DCID system	**DCID**	—	CH_3CN, 70 °C
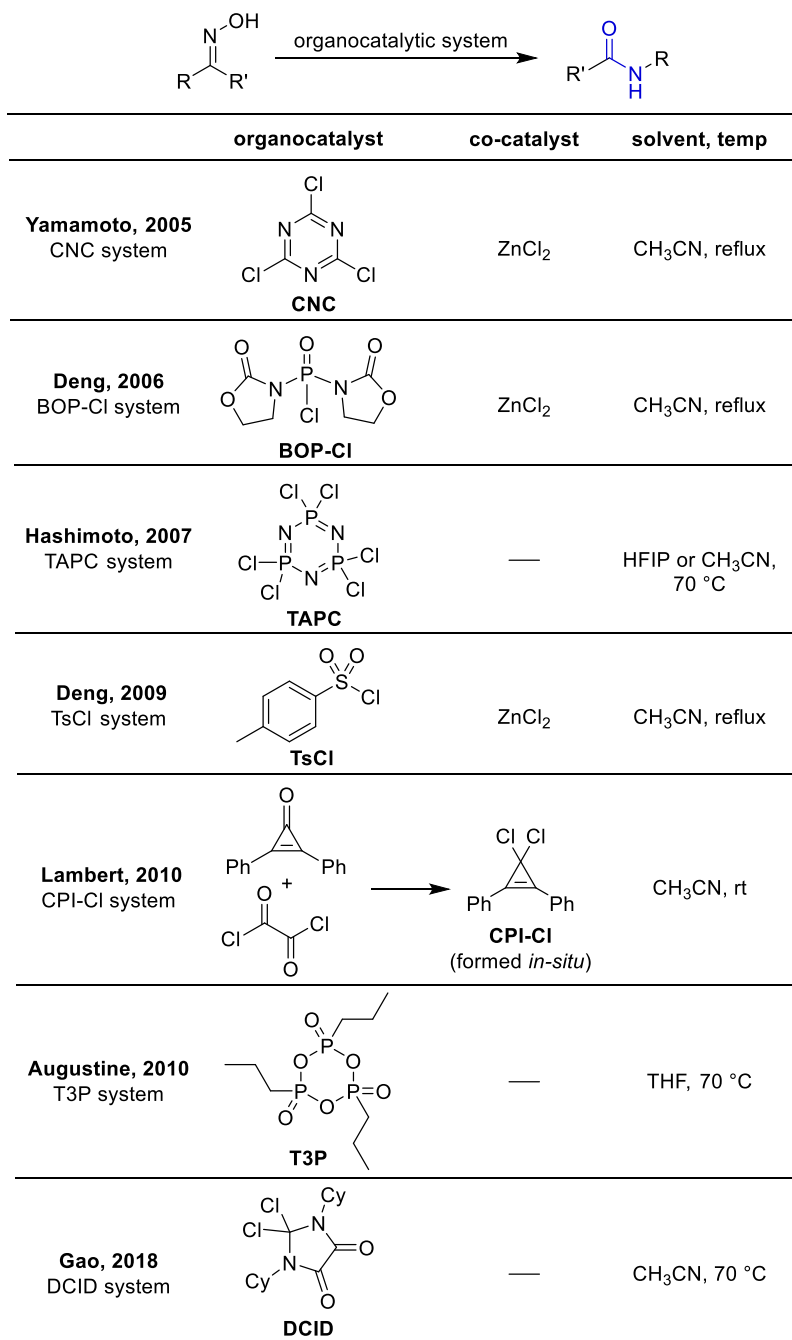
Scheme 2-2 List of reported organocatalytic systems for the Beckmann rearrangement in liquid phase.

Regardless of their efficiency, these organocatalytic systems still require a Lewis acid co-catalyst or elevated temperature (60−100 °C). Furthermore, the toxic and corrosive nature of these chlorine or phosphorus-based catalysts limit their application in industry. Moreover, in their report in 2010, Lambert and co-workers proposed that CPI-Cl in their system may not be a catalyst but merely an initiator or promoter for a self-propagating Beckmann rearrangement mechanism.[16] The self-propagating mechanism was proposed first by Chapman in 1935,[19] but it was not until recently that it had been studied in detail. In the proposed self-propagating mechanistic cycle (Scheme 2-3), the organocatalyst acts as an initiator for the self-propagating cycle by forming the nitrilium cation intermediate, which can activate another molecule of oxime for the rearrangement. Furthermore, a dimerized side product, formed by the nucleophilic attack of the amide product to the nitrilium intermediate, has been reported previously in this self-propagating mechanism.[12,20] Following the proposed self-propagating mechanism by Lambert and co-workers, in 2013 Eriksson and co-workers investigated the organocatalytic mechanism of the Beckmann rearrangement by using density-functional theory (DFT) calculations and found that most of the previously reported catalysts including CNC, BOP-Cl, TsCl, BOP-Cl, and TAPC likely act as initiators for the self-propagating mechanism instead of behaving as true and recycled catalysts.[20,21] Hence, a true organocatalytic Beckmann rearrangement, which is milder, more efficient, and less toxic, has remained unsolved.
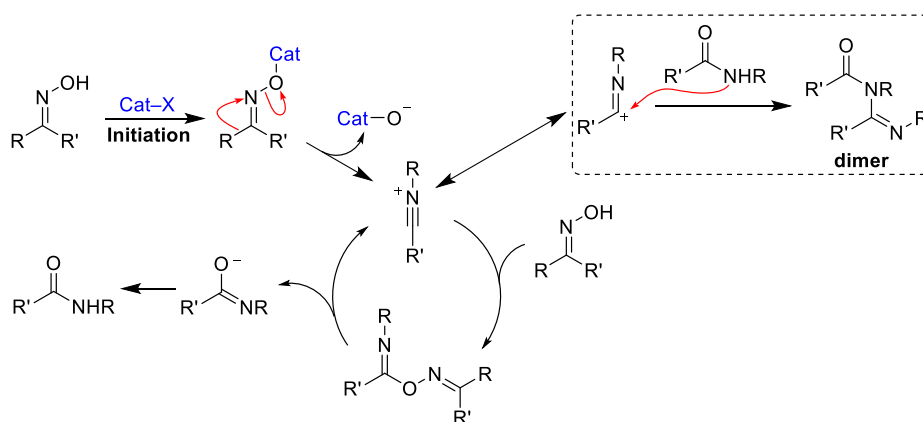
Scheme 2-3 The proposed self-propagating mechanism for the Beckmann rearrangement with an organo-initiator.

In this context, boronic acid catalysis (BAC), which was already established as a mild and direct strategy for the activation of hydroxy group (Chapter 1), was envisioned to provide a potential solution to this problem. It was hypothesised that oximes could be activated through the dynamic interaction of the boron center with the oxime hydroxy group (N–OH). In support of the feasibility of the proposed BAC system, a boron compound, metaboric acid, which forms from boric acid at 100 °C/0.1 Torr, was reported to promote the Beckmann rearrangement in a solvent-free condition at high temperature.[22]

2.2 Initial Development of Boronic Acid Catalyzed Beckmann Rearrangement by Previous Group Members

The development of a BAC system for the Beckmann rearrangement was initiated by two previous group members, Xiaobin Mo, a PhD student, and Dr. Timothy D. R. Morgan, a postdoctoral researcher. This section will summarize their key findings in the reaction development. Hence, all results described in this section were obtained by these two colleagues.

2.2.1 Screening of Boronic Acids and Reaction Optimizations

An extensive catalyst screening was performed using acetophenone oxime (**2-1a**) as a representative substrate for the Beckmann rearrangement. A panel consisting of 20 functionalized aryl boronic acids, specifically, the previously reported boronic acid catalysts mentioned in Chapter 1 and many commercially available ortho-substituted aryl boronic acids, were screened in 14 different solvents at 80 °C for 72 h. Unfortunately, some of the previously reported boronic acid catalysts for electrophilic activations, **BA-5**, **BA-9**, **BA-14**, **BA-16,** and **BA-17**, were not effective in any solvents screened. Out of all boronic acid and solvent combinations evaluated, only five different *ortho*-carbonyl phenylboronic acid (**BA-37**–**41**) showed noticeable product formation in HFIP/CH_3NO_2 (4:1), which was the previously optimized solvent mixture for direct Friedel–Crafts alkylation (Scheme 2-4).[23,24] Notably, 2-methoxycarbonylphenylboronic acid (**BA-41**) furnished the amide product (**2-2a**) in quantitative yield.
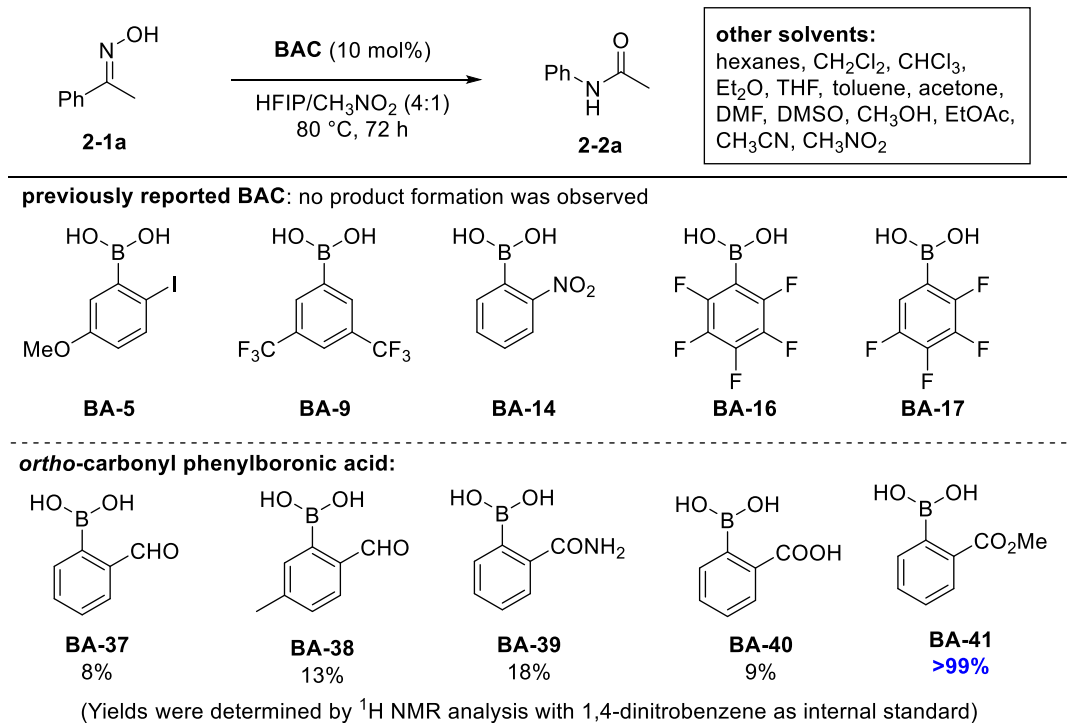
Scheme 2-4 Selected examples of boronic acids screened for the prototypic Beckmann rearrangement of oxime **2-1a**.

After identifying boronic acid **BA-41** as an effective catalyst for the Beckmann rearrangement of **2-1a**, further optimization of other reaction parameters was performed to enhance the practicality of this transformation (Table 2-1). In short, it was found that in the presence of co-catalytic perfluoropinacol (**A-1**), the reaction proceeded efficiently using only 5 mol% of **BA-41** in a 1.0 M solvent mixture of 4:1 HFIP/CH$_3$NO$_2$ at room temperature for 24 h (entry 8). The use of perfluoropinacol as a co-catalyst was prompted by the importance of HFIP in this transformation, where it was shown that the reactivity decreases as the amount of HFIP decreases (entries 2–4). It was envisioned that, on top of providing a polar reaction medium and stabilization of cationic intermediate,[25] HFIP could interact with the boronic acid to form a more electrophilic boronic ester, thus modulating the Lewis acidity of the boron center. Hence, perfluoropinacol (**A-1**) was employed as a co-catalyst to imitate and even accentuate the proposed effect of HFIP by forming a more favorable cyclic boronic ester.

Table 2-1 Reaction Optimization of **BA-41** Catalyzed Beckmann Rearrangement[a]
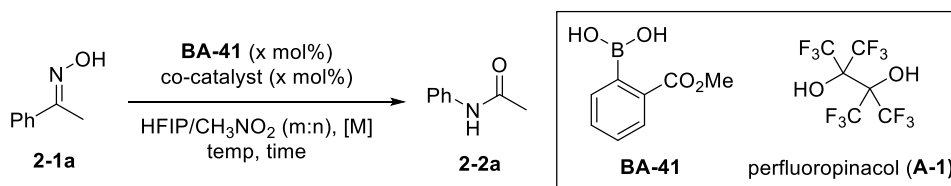
entry	x mol%	co-catalyst	m:n	[M]	temp (°C)	time (h)	NMR yield (%)[b]
1	10	–	4:1	0.5	50	72	100
2	10	–	2:1	0.5	50	72	93
3	10	–	1:1	0.5	50	72	79
4	10	–	1:4	0.5	50	72	60
5	10	–	4:1	1.0	50	72	87
6	10	–	4:1	1.0	rt	24	72
7	10	**A-1**	4:1	1.0	rt	24	94
8	5	**A-1**	4:1	1.0	rt	24	93[c]
9	5	**A-1**	4:1	1.0	rt	6	37[c]

[a]Reaction conditions: **2-1a** (0.5 mmol) in the indicated conditions. [b]NMR yield was determined by ^{1}H NMR analysis of reaction crude using 1,4-dinitrobenzene as internal standard. [c]Isolated yield.

A final round of optimization was conducted with a small library of diols and ortho-carboxyester aryl boronic acids. The effect of other commercially available electron-poor diols was investigated with catalyst **BA-41**, and all of them resulted in lower conversion as compared to perfluoropinacol (Scheme 2-5A). Furthermore, structural modifications of boronic acid **BA-41** were conducted, hoping to enhance the catalytic reactivity further (Scheme 2-5B). Tuning of the electronic characteristics of the aryl ring with electron donating or withdrawing substituents did not result in any improvements. Gratifyingly, an improvement of reactivity was observed with boronic acid **BA-42,** where methyl ester of **BA-41** is replaced with a phenoxy group. The use of phenoxy **BA-42** considerably shortened the reaction time, yielding amide **2-2a** in excellent yield after 6 h at room temperature.
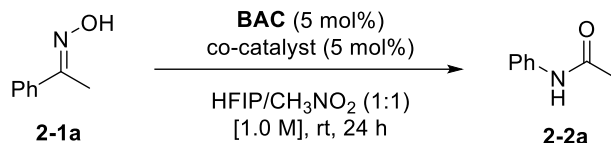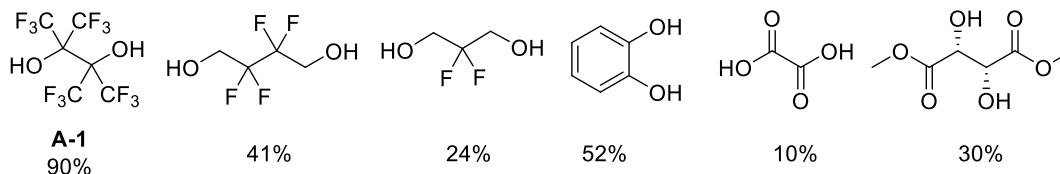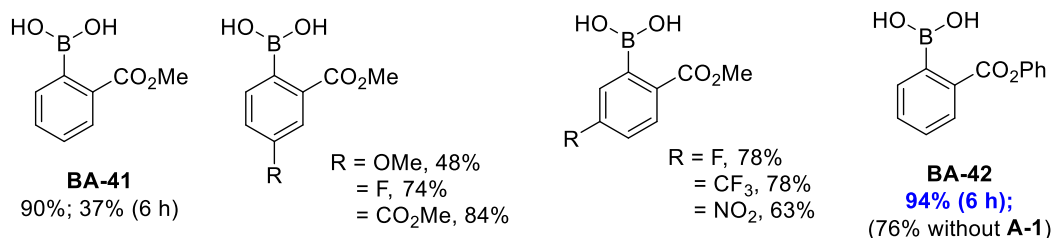
Scheme 2-5 Further optimization of A) diol co-catalysts and B) boronic acids with *ortho*-carboxyester substituents.

In summary, two effective boronic acid catalysts (**BA-41** and **BA-42**) were identified for the Beckmann rearrangement of oxime **2-1a** at ambient temperature. Although catalyst **BA-42** was more efficient, catalyst **BA-41** is preferred owing to its commercial availability.

2.2.2 Substrate Scope

With the optimal reaction conditions in hand, the substrate scope of the boronic acid catalyzed Beckmann rearrangement was examined with a variety of aromatic and alkyl substituted oximes first with catalyst **BA-41**, whereas the more effective catalyst **BA-42** was employed only for more challenging substrates. As illustrated in Scheme 2-6, for most substrates the reaction proceeded efficiently at room temperature using **BA-41**.

The practicality of this BAC system was demonstrated by a gram-scale synthesis of amide **2-2a**, where a good isolated yield was obtained with a longer reaction time (30 h). A series of substituted acetophenone oximes, especially electron rich oximes, underwent the Beckmann rearrangement at ambient temperature,

affording the amide **2-2b** to **2-2j** in high isolated yield. Electron poor oximes **2-1j** to **2-1k** were not successful, presumably due to the poor migratory aptitude of these aryl groups. Fortunately, brominated oxime **2-1j** underwent the rearrangement in 85% yield when the more reactive catalyst **BA-42** was employed. However, oximes **2-1l** and **2-2k** bearing a highly deactivating group ($-NO_2$ and $-CF_3$) did not afford any amide product, even when using catalyst **BA-42**. Pharmaceutically important heteroaromatic oximes, such as **2-1m** to **2-1r**, also underwent the rearrangement efficiently at ambient conditions or at slightly elevated temperature, except for oxime **2-1p**. The failure with oxime **2-1p** is **likely** due to catalyst inhibition from chelation of the ortho-amine and oxime moieties with the boronic acid. Of note, a range of functional groups, including phenol (**2-2h**), halides (**2-2i** and **2-2j**), acid-sensitive Boc (**2-2g**), and tosyl (**2-2r**) protecting groups, were tolerated under these reaction conditions.

The rearrangement of aryl-alkyl and alkyl-alkyl oximes **2-1s** to **2-1aa** also proceeded smoothly under this BAC procedure. The temperature sensitive enamide product **2-2y** was obtained in good yield at room temperature using catalyst **BA-42**. Moreover, the biologically active pregnenolone oxime **2-1aa** was transformed smoothly into the amide product, with quantitative yield without protection of the free alcohol. Lastly, cyclic oximes **2-1ab** to **2-1ad** were also suitable substrates in this BAC system. Even cyclohexanone oxime **2-1ab**, a notoriously difficult substrate,[12,13,15] delivered the product in 65% yield upon using more forcing conditions with 30 mol% **BA-42** at 80 °C.

Notably, the superiority of catalyst **BA-42** over **BA-41** is shown clearly by several oxime substrates, especially **2-2j**, **2-2n**, **2-2x**, **2-2y** and **2-2ab**. Additionally, while a number of oximes examined in this study were formed as a mixture of E/Z isomers, the mixture was resolved mostly to a single major product, with good selectivity, in accordance with the expected migratory aptitude of R and R' groups. This non-stereospecific nature of this rearrangement presumably arose from the fast E/Z interconversion of oximes in the presence of the Lewis acidic boronic acid in a protic solvent prior to the rearrangement.[26]
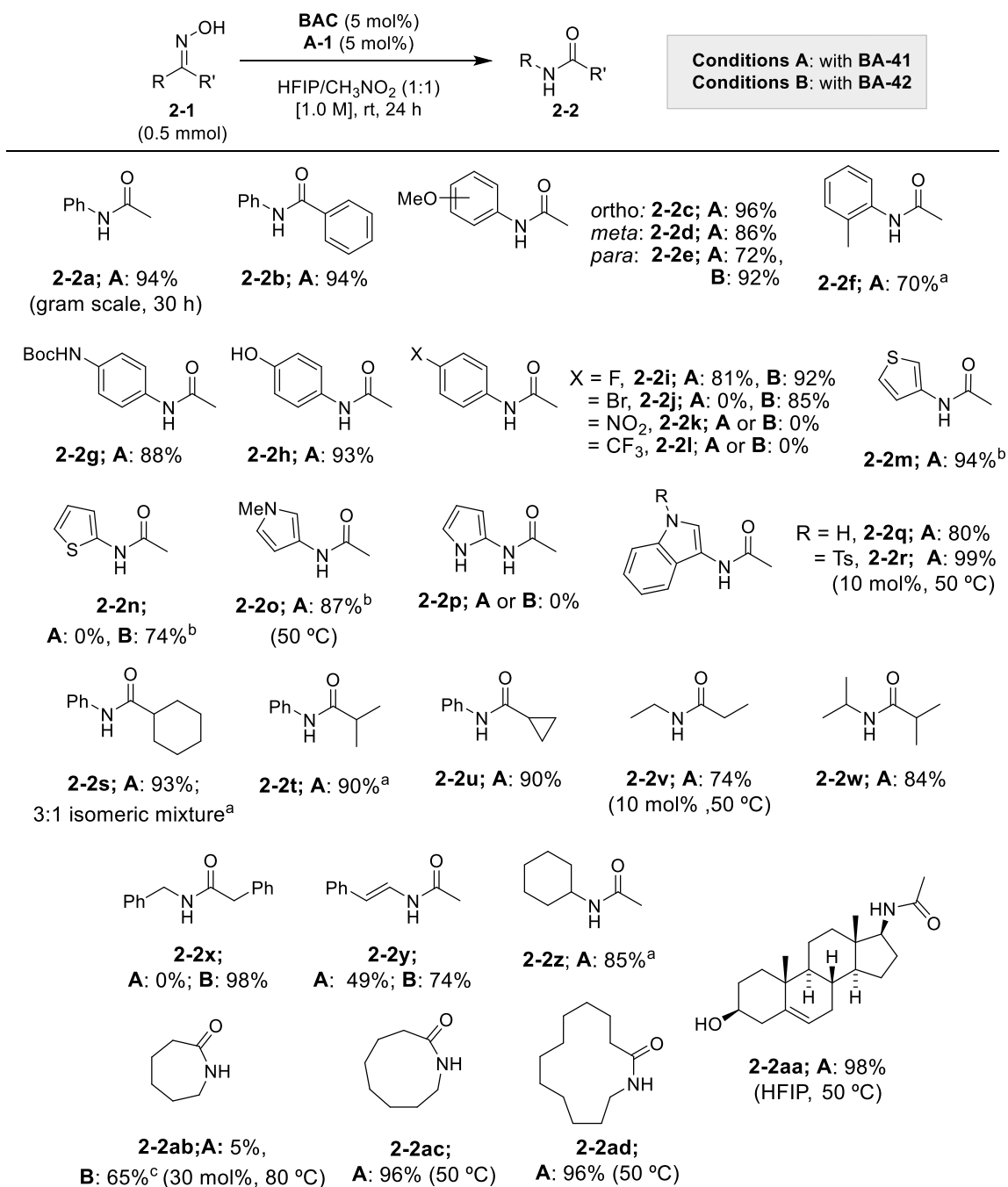
Scheme 2-6 Substrate scope of boronic acid catalyzed Beckmann rearrangement.

2.2.3 Mechanistic Studies

Preliminary studies were conducted to understand the mechanism of the boronic acid catalyzed Beckmann rearrangement, specifically, the mode of activation by the boronic acid catalysts and the role of HFIP and the perfluoropinacol co-catalyst. More

importantly, the nature of the boronic acid catalyst as a true organocatalyst or organo-initiator in the Beckmann rearrangement was evaluated.

2.2.3.1 Comparison Studies of BAC with Other Organocatalysts

First, to demonstrate that the superior activity of catalyst **BA-41** and **BA-42** in this BAC system is not merely because of the use of HFIP, which is known to facilitate many ionic reactions,[25,27] the BAC conditions were compared to other reported Beckmann rearrangement organocatalysts. Gratifyingly, when T3P was utilized for a subset of oxime substrates, poorer conversion was observed in all cases compared to the BAC system (Scheme 2-7). Furthermore, the rearrangement of the prototypic oxime substrate **2-1a** was unsuccessful with the use of catalytic or stoichiometric amounts of trifluoroacetic acid (TFA), showing that the efficacy of this BAC system is also not due to the presence of adventitious acid.
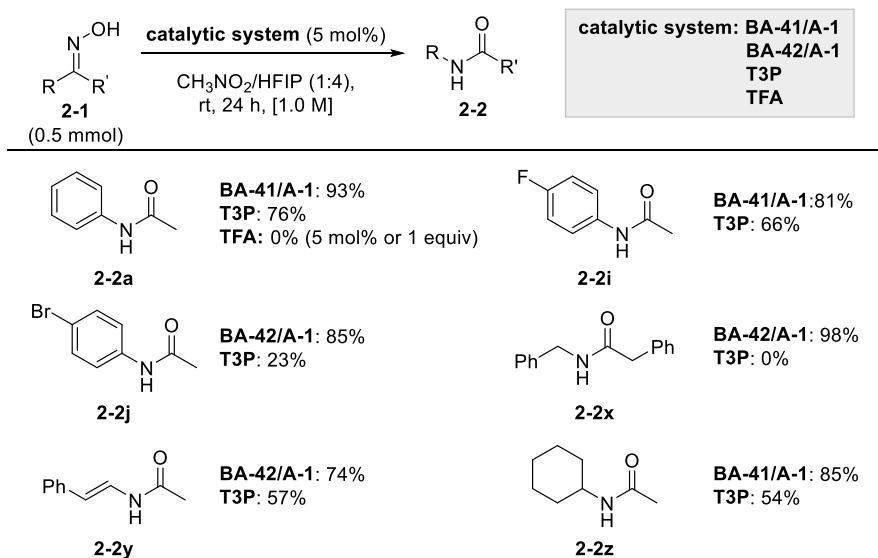
Scheme 2-7 Comparison of organocatalysts for the Beckmann rearrangement in HFIP/CH$_3$NO$_2$.

2.2.3.2 Mode of Activation by the Boronic Acid Catalysts

As opposed to the initial proposal, the distinctive catalytic reactivity in the Beckmann rearrangement seen in boronic acids **BA-41** and **BA-42** bearing ortho-carboxyester substituents hinted that the oxime may interact with the ortho-carboxyester moiety via transesterification to form *o*-boronyl oxime ester (**2-3**) as the reactive intermediate (Scheme 2-8). The results from the structural modifications of **BA-41**, where no

improvement was observed by tuning the electronics of the aryl ring, while great improvement was detected by replacing the methoxy ester with a more reactive phenoxy ester, also agree with the proposed intermediacy of *ortho*-boronyl oxime ester **2-3**. Moreover, the documentation of oxime esters as suitable precursors for the Beckmann rearrangement in the presence of strong acid by Kuhara in 1906 further reinforces the hypothesis.[28,29] Thus, to support the existence of oxime ester **2-3** and elucidate the role of *ortho*-boronic acid in this reaction, several mechanistic experiments were conducted.
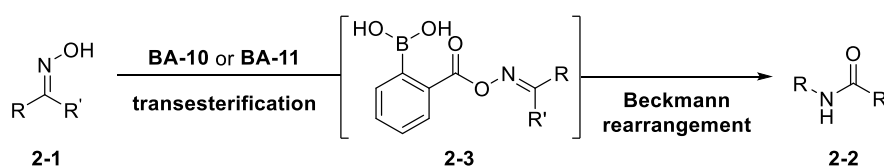
Scheme 2-8 Proposed mode of activation by boronic acids **BA-41** and **BA-42** for the Beckmann rearrangement.

Contrary to catalyst **BA-41** and **BA-42**, 2-carboxyphenylboronic acid (**BA-40**) is not an effective catalyst for the Beckmann rearrangement under the BAC reaction conditions (Scheme 2-9A). However, when an esterification reagent, 1-ethyl-3-(3-dimethylaminopropyl)carbodiimide (EDC), was used as a co-catalyst with boronic acid **BA-40** in the reaction, amide product **2-2a** was obtained in a moderate yield (Scheme 2-9B). Furthermore, removal and replacement of the ortho-boronyl group of **BA-40** with electron-withdrawing substituents ($-NO_2$ and $-CF_3$) resulted in no product formation, hence, suggesting that the boronyl group also plays an important role in activation of oximes for the Beckmann rearrangement (Scheme 2-9C). To support the intermediacy of oxime ester **2-3** further, compound **2-3a** was synthesized independently and it was found to be an efficient catalyst for the Beckmann rearrangement providing the amide product **2-2a** quantitatively (Scheme 2-9D).
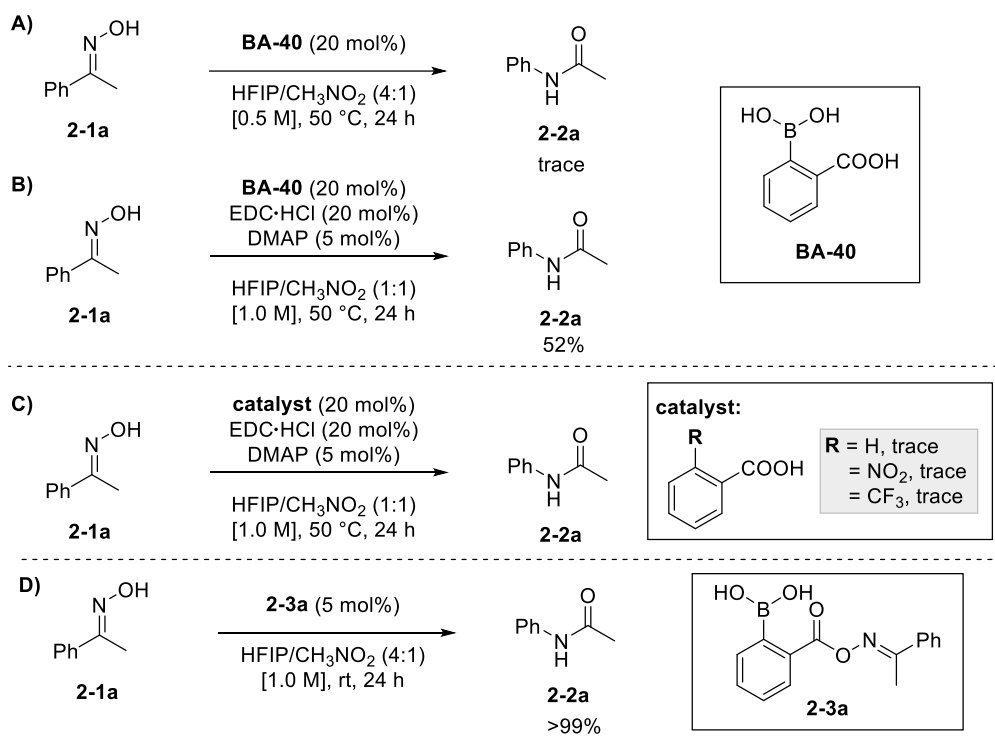
Scheme 2-9 Control experiments to support the intermediacy of oxime ester **2-3**. Yields were determined by ^{1}H NMR analysis with 1,4-dinitrobenzene as internal standard.

To gain more insight on the exact role of the ortho-boronic acid moiety in both the oxime transesterification and Beckmann rearrangement, more control experiments were conducted. When the pinacol protected catalyst **BA-41** was employed in the reaction, only a trace amount of product **2-2a** was obtained (Scheme 2-10A). However, pinacol protection of intermediate **2-3a** did not inhibit the reaction, yielding amide **2-2a** in good yield, while removal of the boronic acid of intermediate **2-3a** led to no product formation (Scheme 2-10B). These results suggest that the Beckmann rearrangement can be facilitated by the less Lewis acidic boronate, but a free boronic acid is required for triggering the initial transesterification step. In addition, when exposed to the reaction solvent, oxime ester **2-3a** underwent the rearrangement spontaneously, generating amide **2-2a** and a mixture of **BA-40** and the HFIP ester of the catalyst **2-4**, which was detected by LC-MS and ^{1}H NMR spectroscopy (Scheme 2-10C). This result indicates that the transesterification of oximes is likely the rate determining step of this BAC system, and the Beckmann

rearrangement does not proceed through a self-propagating "nitrilium" mechanism as a second molecule of oxime was not required in the reaction.
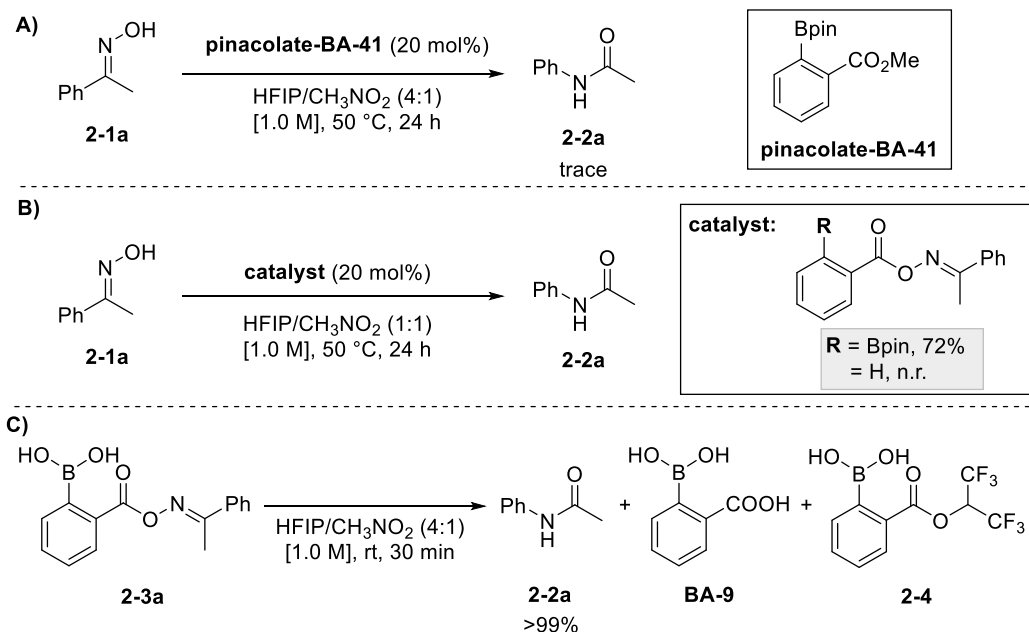
Scheme 2-10 Control experiments to understand the role of the ortho-boronyl group in the Beckmann rearrangement. Yields were determined by ^{1}H NMR analysis with 1,4-dinitrobenzene as internal standard.

2.2.3.3 Role of Perfluoropinacol

As alluded before, aside from being a polar solvent, HFIP is suspected to engage in reversible formation of a highly electrophilic boronic ester with the boronic acid catalyst. This hypothesis led to the use of perfluoropinacol as a co-catalyst, which potentially forms a more stable five-membered boronic ester. Moreover, the need of a free boronic acid moiety in the catalyst to trigger the oxime transesterification (Scheme 2-10A) also suggests that the formation of such electrophilic boronic ester is crucial to initiate the boronic acid catalyzed Beckmann rearrangement.

The formation of the reactive perfluoropinacol boronic ester **2-5** is corroborated by NMR spectroscopic studies. A mixture of equimolar boronic acid **BA-41** and perfluoropinacol was stirred in CD$_3$CN for 18 h, then subjected to NMR spectroscopy analysis. A new set of NMR signals was observed in ^{1}H, ^{13}C, ^{11}B, and ^{19}F NMR spectra, indicating the partial formation of compound **2-5** (Scheme 2-11A). Along with the ^{11}B NMR signal of **BA-41** at 30 ppm, a new signal was observed at 15

ppm, which strongly indicates the presence of a neutral tetrahedral boron center arising from the internal coordination of the carbonyl to the boron atom. Likewise, a new ^{19}F NMR signal observed at –69.9 ppm, along with the signal of perfluoropinacol at –71.0 ppm, also was evident for the partial formation of **2-5**. Furthermore, downfield shifts also were observed in the ^{1}H and ^{13}C NMR signals for the methoxy group (3.9 to 4.5 ppm) and carbonyl group (170 to 183 ppm), which suggested an increase in the electrophilicity of the carboxyl ester group, presumably through the internal coordination of the carbonyl group to the electrophilic boron atom. This interaction likely accounts for the enhancement in reactivity when perfluoropinacol is used as a co-catalyst, by accelerating the oxime transesterification and promoting the subsequent Beckmann rearrangement.

To validate that the new observed signals corresponded to boronic ester **2-5**, compound **2-5** was synthesized independently and subjected to NMR analysis (Scheme 2-11B). Gratifyingly, the ^{1}H and ^{11}B NMR characterization of boronic ester **2-5** agreed with the new signals observed above. Moreover, when boronic ester **2-5** was used as the catalyst in the prototypic Beckmann rearrangement of oxime **2-1a**, the amide product **2-2a** was obtained in a similar yield (93%) as the optimal conditions where co-catalytic perfluoropinacol was used (Table 2-1, entry 8, 93% yield), thus confirming the catalytic reactivity of boronic ester **2-5** (Scheme 2-11C).
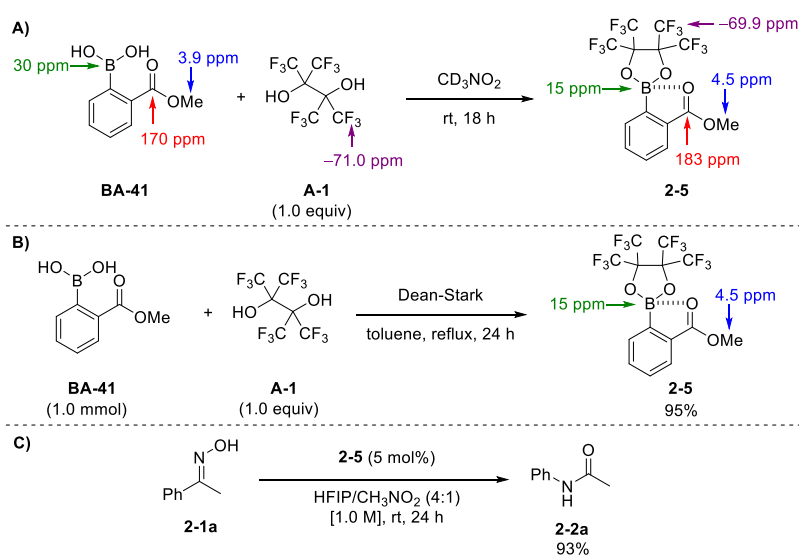
Scheme 2-11 Control experiments to support the formation of the electrophilic boronic ester **2-5**.

2.2.3.4 Catalytic versus Self-Propagating Mechanism

As mentioned earlier, most of the previously reported organocatalysts for the Beckmann rearrangement were found to be acting merely as an initiator for the self propagating mechanism (Scheme 2-3). Therefore, it is important to determine the exact role of catalysts **BA-41** and **BA-42** in the Beckmann rearrangement. According to the preliminary results, where oxime ester **2-3a** was found to undergo rearrangement spontaneously and quantitively without a need for another molecule of oxime (Scheme 2-10C), this boronic acid catalyzed Beckmann rearrangement is believed to proceed through a fully catalytic and unimolecular mechanism. To support the claim further, a control experiment was conducted based on an experimental observation by Ericksson and co-workers.

Other than the in-depth computational studies by Ericksson and co-workers, experimental investigations also were conducted with the TsCl catalytic system and confirmed the self-propagating mechanism.[20] In their efforts to understand why cyclohexanone oxime **2-1ab** is a difficult substrate for most of the organocatalytic systems, it was found that a stable dimerized product **2-6** was formed from nucleophilic attack of the amide product **2-2ab** to the nitrilium intermediate, and it severely suppressed the turnover in the self-propagating mechanism (Scheme 2-12A). This dimer **2-6** can be hydrolyzed to the desired caprolactam **2-2ab** using strong acid with reflux conditions. A similar outcome also was observed by Hashimoto and co-workers in the TAPC system.[15] When catalytic TsCl and **BA-41** were employed for the Beckmann rearrangement of cyclohexanone oxime **2-1ab** using the BAC conditions, the formation of dimer **2-6** was observed by ^{1}H NMR and HRMS spectroscopies for the TsCl system but not for the BAC system (Scheme 2-12B). The absence of the dimer **2-6** further supports that catalysts **BA-41** and **BA-42** likely act as a true catalyst instead of an initiator in the Beckmann rearrangement.

A)

B)

Distinctive ^{1}**H NMR** signal for **2-6** in CDCl$_3$: 4.08-4.06 (m, 2 H), 3.84-3.82 (m, 2 H), 3.01-2.99 (m, 2H), 2.86-2.84 (m, 2 H).

ESI-HRMS for C$_{12}$H$_{20}$N$_2$O [M+H]$^+$: cald. 209.1648; found 209.1641
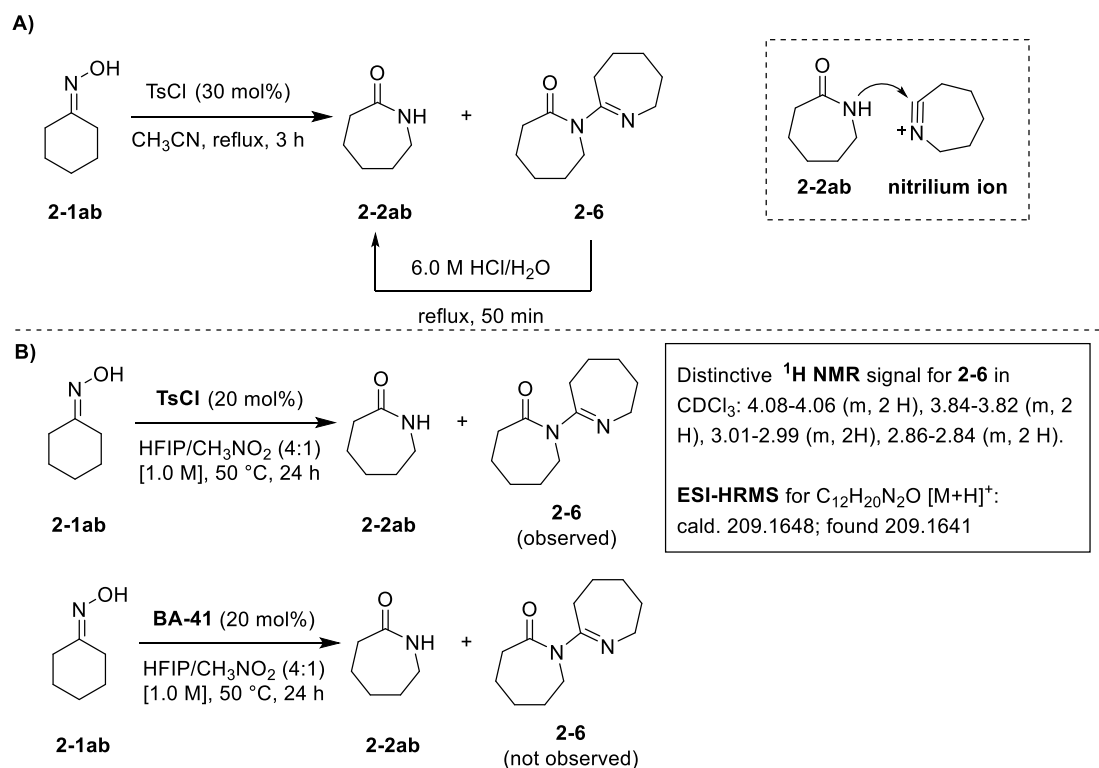
Scheme 2-12 A) Experimental investigation to address the low reactivity of cyclohexanone oxime **2-1ab** in the TsCl-catalyzed system by Eriksson and co-workers[20] and B) control experiments using cyclohexanone oxime **2-1ab** to determine the role of boronic acid catalyst **BA-41** in the Beckmann rearrangement.

2.2.4 Proposed Catalytic Cycle

In accordance with the above mechanistic studies, a catalytic cycle for the Beckmann rearrangement using the boronic acid/perfluoropinacol system is illustrated in Scheme 2-13 with **BA-41** and oxime **2-1a**. The proposed mechanism is divided into two major steps: the boron-assisted oxime transesterification, followed by a self-sufficient Beckmann rearrangement.

As illustrated in Scheme 2-13, the catalyst **BA-41** first reacts with perfluoropinacol to form a highly electrophilic boronic ester **2-5**, which facilitates the oxime transesterification through the electrophilic activation of the carboxyester group, generating the oxime ester intermediate **2-3a**. This boron-assisted transesterification is believed to be the rate determining step, which is supported by the superiority of catalyst **BA-42** bearing a phenoxy group as a better leaving group. Owing to the high reactivity and self-sufficiency of intermediate **2-3a**, a concerted unimolecular mechanism is proposed for the Beckmann rearrangement to form the

acyl imidate intermediate **2-7**. However, the actual mechanism of the rearrangement of oxime ester **2-3a** to acyl imidate **2-7** and the role of the boron group in this step remain unclear (see **TS** in Scheme 2-13). The acyl imidate **2-7**, which is expected to be more active than **BA-41/BA-42** and **2-3a**, undergoes rapid transesterification with another molecule of oxime, releasing the amide product **2-2a**. At the end of the cycle, when no more oxime is present, transesterification of intermediate **2-7** with HFIP results in the formation of by-product **2-4**. Therefore, in this proposed catalytic cycle, oxime ester **2-3a** is believed to be the active catalytic species for the Beckmann rearrangement, while **BA-41** and **BA-42** act as a pre-catalyst that become activated through the oxime transesterification.
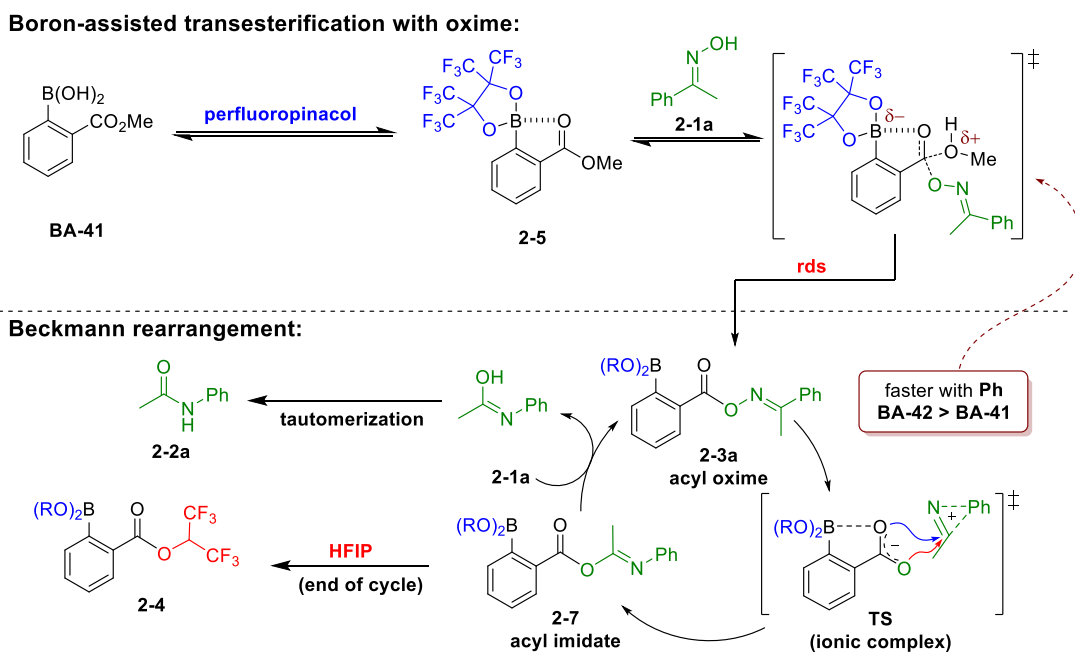
Scheme 2-13 Proposed catalytic cycle for the Beckmann rearrangement using the boronic acid/perfluoropinacol system.

2.3 Objective

In summary, a powerful yet mild boronic acid/perfluoropinacol co-catalytic system was developed for the Beckmann rearrangement. This BAC protocol is operationally simple, without the need for inert atmosphere or exhaustive pre-drying of solvents, and it displays a broad substrate scope with good functional group tolerability. Although the initial mechanistic investigations shed light onto the plausible mechanism of the catalytic cycle, there are some questions that remain unresolved,

particularly on the self-sufficient Beckmann rearrangement step. The main objective of this chapter is to conduct more in-depth mechanistic studies to address the unanswered mechanistic questions of the Beckmann rearrangement. In addition, my efforts toward refining aspects of this BAC system, such as expanding the substrate scope and improving the synthesis of boronic acid **BA-42,** also will be disclosed in this chapter.

2.4 Additional Substrate Scope in the Boronic Acid Catalyzed Beckmann Rearrangement

As shown above in Scheme 2-6, this BAC protocol demonstrates good utility with a broad substrate scope and good tolerance of functional groups, such as halides, phenol, and acid sensitive protecting groups. To reinforce the functional group tolerance of this method, additional substrates were evaluated. As it is determined that electron deficient aryl oximes are poor substrates in this BAC system, a small library of para-substituted acetophenone oximes **2-9** bearing different functional groups at the terminal position of the alkyl chain was judiciously selected for the additional substrate scope.

A total of four oxime substrates **2-9** bearing a hydroxy, amide, carboxyester, or a nitrile group were synthesized from the corresponding arenes **2-8** via Friedel–Crafts acylation at the para-position, followed by condensation with hydroxylamine (Scheme 2-14A). When these oxime substrates were subjected to the Beckmann rearrangement under the optimal reaction conditions, the corresponding amide products **2-10** were obtained in high yields (Scheme 2-14B). These results clearly indicate that hydroxy, amide, ester, and nitrile groups also are compatible and tolerated in this mild protocol. Furthermore, catalyst **BA-42** also displays its superiority here with substrates **2-9a**, **2-9b** and **2-9c**, where a higher yield was obtained when it was employed as a catalyst compared to **BA-41**.
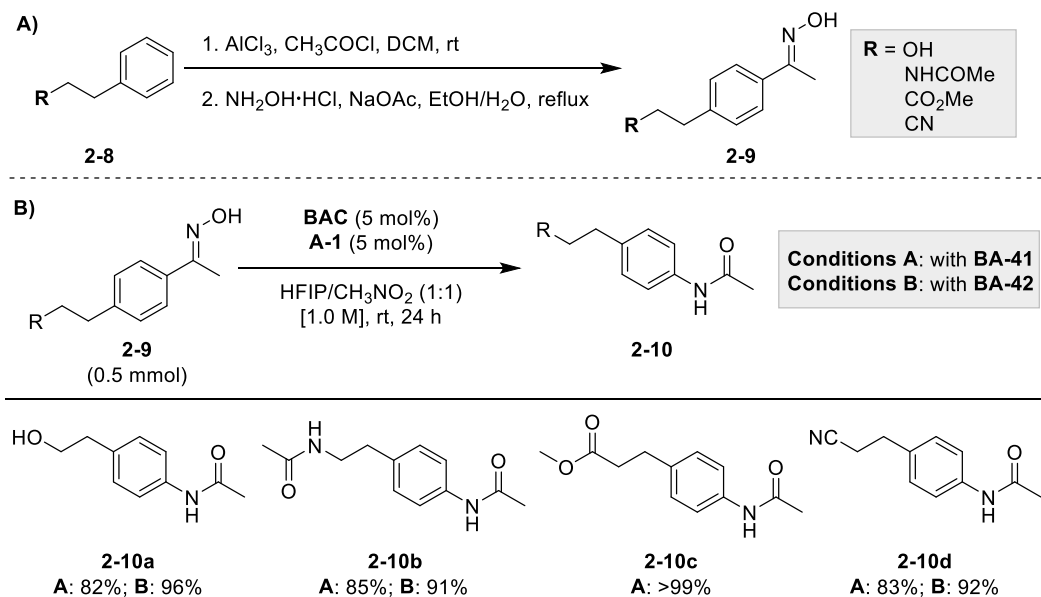
Scheme 2-14 A) General synthetic route for the preparation of oxime substrate **2-9**; B) Additional substrate scope in the boronic acid catalyzed Beckmann rearrangement.

2.5 Further Mechanistic Investigations

To address some of the unresolved questions on the mechanism of the Beckmann rearrangement via the BAC system, several studies were performed, including some reaction progress monitoring, ^{18}O-labelling experiments, and additional control experiments.

2.5.1 Reaction Profile Monitoring

In the previous mechanistic studies, oxime ester intermediate **2-3a** was found to be highly reactive and to undergo the Beckmann rearrangement spontaneously to yield the amide product and a mixture of **BA-40** and HFIP ester **2-4** (Scheme 2-10A). Moreover, it also was revealed to be an efficient catalyst and is proposed to be the active catalytic species in this BAC protocol for Beckmann rearrangement (Scheme 2-9D). Therefore, to support the proposed mechanism depicted in Scheme 2-13 further, qualitative reaction progress analyses were conducted.

2.5.1.1 Synthesis of Oxime Ester 2-3a

To begin with, a new batch of oxime ester **2-3a** was synthesized from 2-bromo-benzoic acid **2-11,** according to the synthetic route developed by Xiaobin Mo, starting with esterification of arene **2-11** with oxime **2-1a**, followed by Miyaura borylation

with neopentyl diboron and subsequent deprotection (Scheme 2-15A). It is important to note that due to the difficulty in removing pinacol from the Bpin group, the neopentyl diboron was employed instead of the more common B_2pin_2 reagent for the Miyaura borylation. Given the low yield in the last step of the synthesis, another approach for the deprotection of intermediate **2-13** was attempted using the procedure reported by Hutton and co-workers[30] (Scheme 2-15B). Although intermediate **2-13** was transformed smoothly into the trifluoroborate **2-14**, the hydrolysis of trifluoroborate to boronic acid resulted in boronic acid **BA-40** instead of the desired oxime ester **2-3a**, presumably due to the highly reactive oxime ester moiety, which is hydrolyzed easily in the reaction conditions. Nonetheless, the oxime ester **2-3a** obtained from the synthetic routes in Scheme 2-15A was isolated in sufficient amount for the intended purpose.
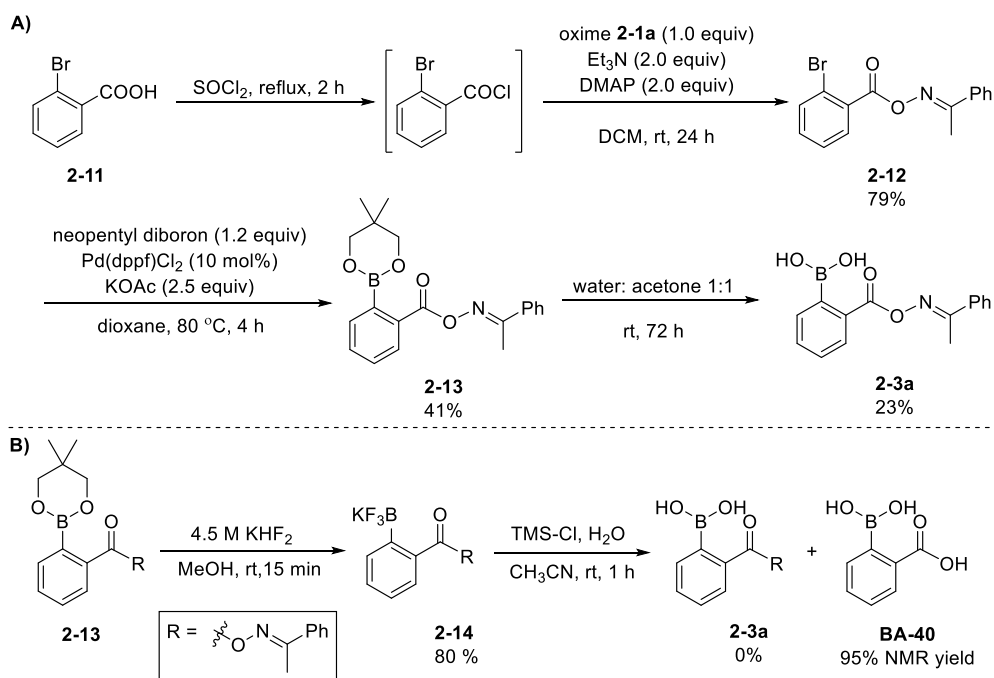
Scheme 2-15 A) Preparation of oxime ester **2-3a** according to synthetic route developed by Xiaobin Mo and B) approach for the deprotection of intermediate **2-13**.

2.5.1.2 Self-Sufficient Rearrangement of Oxime Ester 2-3

With oxime ester **2-3a** in hand, the reaction progress of the rearrangement of oxime ester **2-3a** into product **2-2a** and **2-4** was monitored by LC-MS with UV detection. A 0.1 M solution of oxime ester **2-3a** in HFIP was prepared and stirred at room temperature. An aliquot of 5 μL was collected from the solution and stopped with 1 mL of acetonitrile every minute for about 20 min, The aliquots were subjected to LC-MS for analysis. The amount of each compound was determined, by the peak area of their absorption peak at 254 nm at their corresponding elution time, and a graph of peak area over time for each compound was plotted (Figure 2-2).
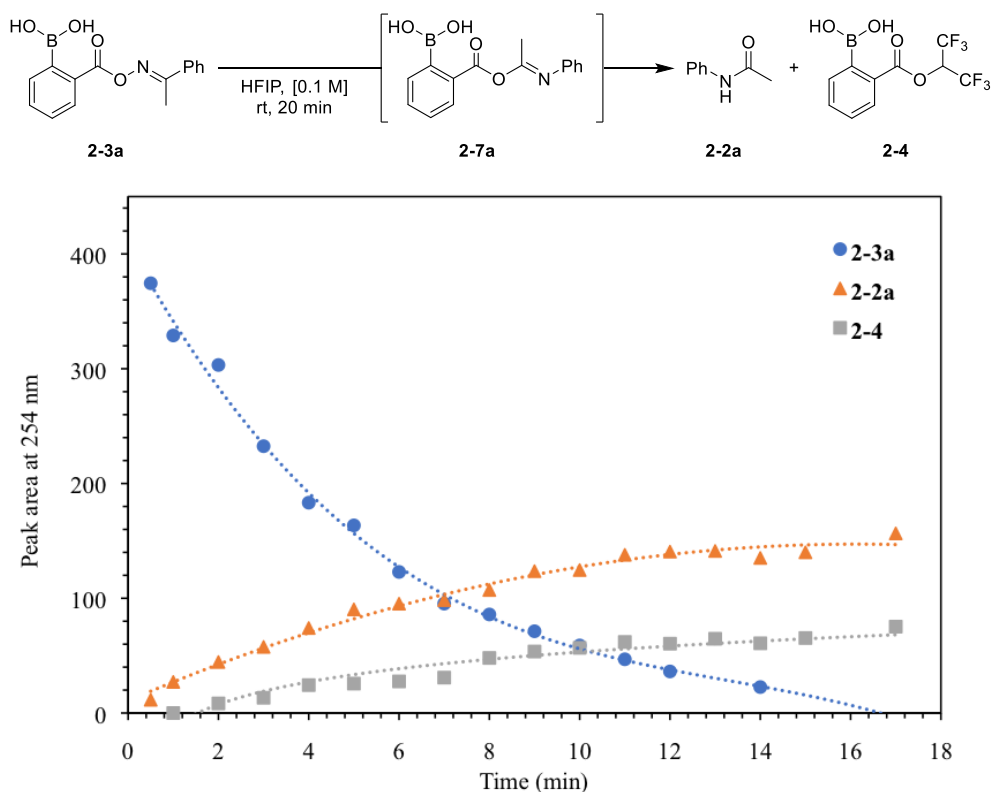
Figure 2-2 Reaction progress analysis of the Beckmann rearrangement of oxime ester **2-3a**. Relative peak areas are not normalized.

The full conversion of oxime ester **2-3a** within a short period of time (20 min) reaffirmed the rapid and smooth self-sufficient rearrangement of oxime ester into the desired amide product and HFIP ester **2-4** side product when exposed to the reaction solvent at ambient temperature. According to the plot shown in Figure 2-2, the breakdown of oxime ester **2-3a** does not seem to display a linear relationship, as

expected for a zero-order rearrangement. This non-linear relationship is most likely due to the participation of HFIP in the transesterification of the acyl imidate intermediate **2-7** to release the amide product and HFIP ester **2-4**. The poor nucleophilicity of HFIP potentially results in a slower transesterification, causing the observed pseudo-first order situation shown in the plot. It is worth mentioning that only a negligible amount of *ortho*-boronyl benzoic acid **BA-40** was observed in all aliquots.

To validate the above observations, a similar experiment was conducted using the fluorinated oxime ester **2-3i**, which was synthesized by Dr. Timothy Morgan. Unsurprisingly, a similar non-linear relationship also was observed for the decay of oxime ester **2-3i** (Figure 2-3). Furthermore, a slightly longer reaction time was required for the full conversion of oxime ester **2-3i** (25 min) as compared to **2-3a** (20 min). This result is expected because the rate of the rearrangement depends on the migration power of the *N*-bound aryl groups.
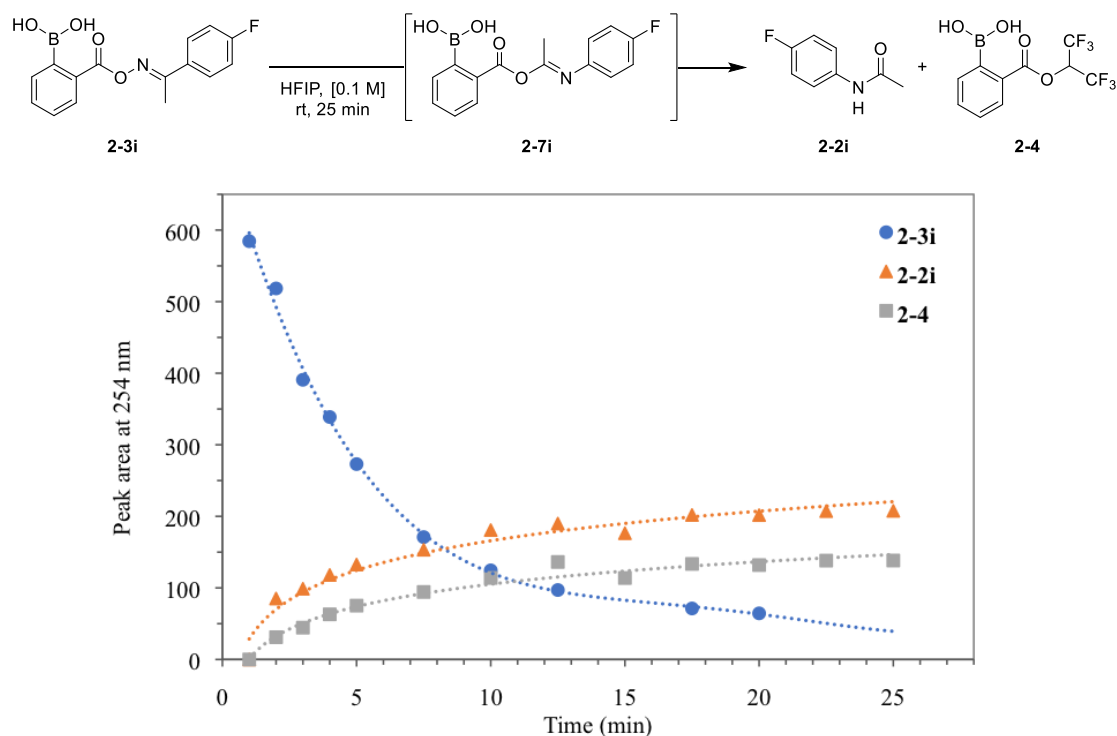
Figure 2-3 Reaction progress analysis of the Beckmann rearrangement of oxime ester **2-3i**. Relative peak areas are not normalized.

2.5.1.3 Rearrangement of Oxime Ester 2-3 in the Presence of Oxime

As oxime ester **2-3** is proposed to be the actual catalyst for the Beckmann rearrangement, the reaction progress analysis of the rearrangement of oxime ester **2-3i** in the presence of one equivalent of oxime was conducted. Oxime ester **2-3i** was chosen for this study simply due to the lower reaction rate and ease of monitoring as compared to **2-3a**.

Using the same procedure as before, the reaction with addition of oxime **2-1i** was monitored over 30 min, and the reaction progress over time was plotted (Figure 2-4).
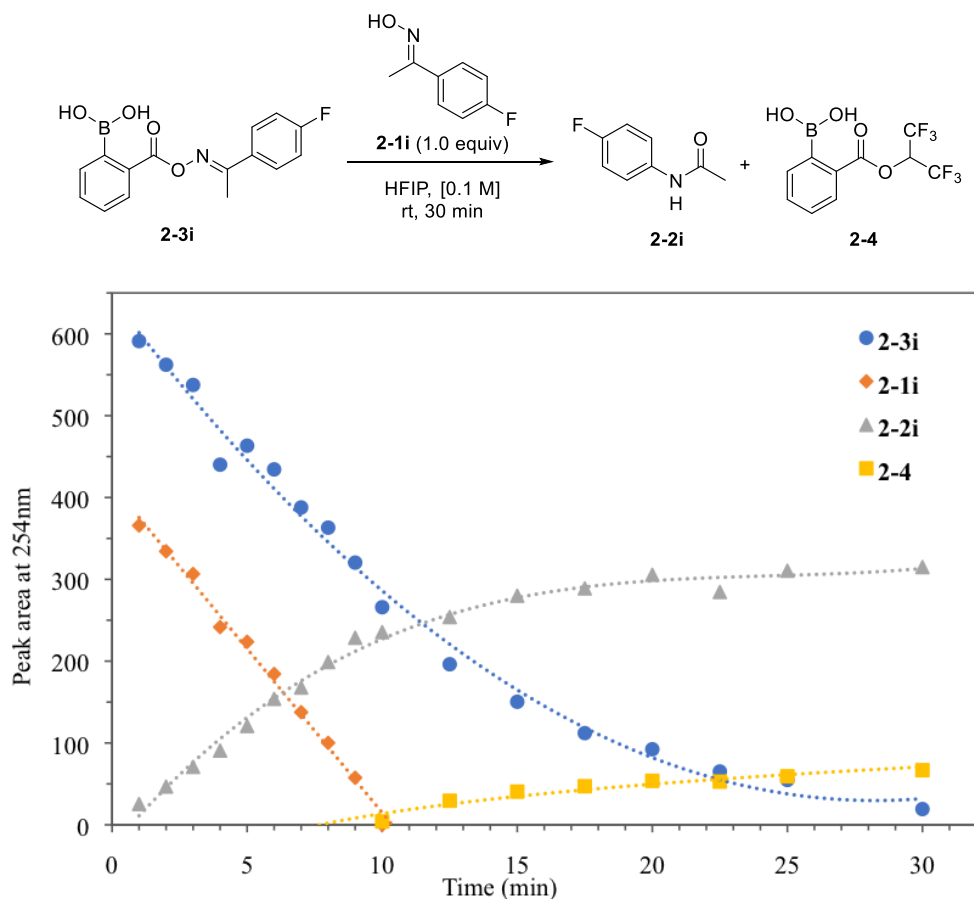
Figure 2-4 Reaction progress analysis of the Beckmann rearrangement of oxime ester **2-3i** in the presence of oxime **2-1i**. Relative peak areas are not normalized.

As shown in the graph, the oxime **2-1i** was consumed fully within 10 min, yielding the amide product **2-2i**. The HFIP ester **2-4**, the end-product of the catalytic

cycle, was formed only after all oxime was consumed. Furthermore, the consumption of oxime **2-1i** displayed a linear relationship, suggesting that the oxime is zeroth order in the rearrangement. An overall non-linear relationship was observed for the decomposition of oxime ester **2-3i** and formation of amide product **2-2i**, however, there seems to be a subtle change in the relationship at the transition point when the oxime was fully consumed.

To analyze the subtle change in the relationship further, the plot of the reaction progress was divided into two parts, before and after the full consumption of oxime **2-1i** at the 10 min point (Figure 2-5).
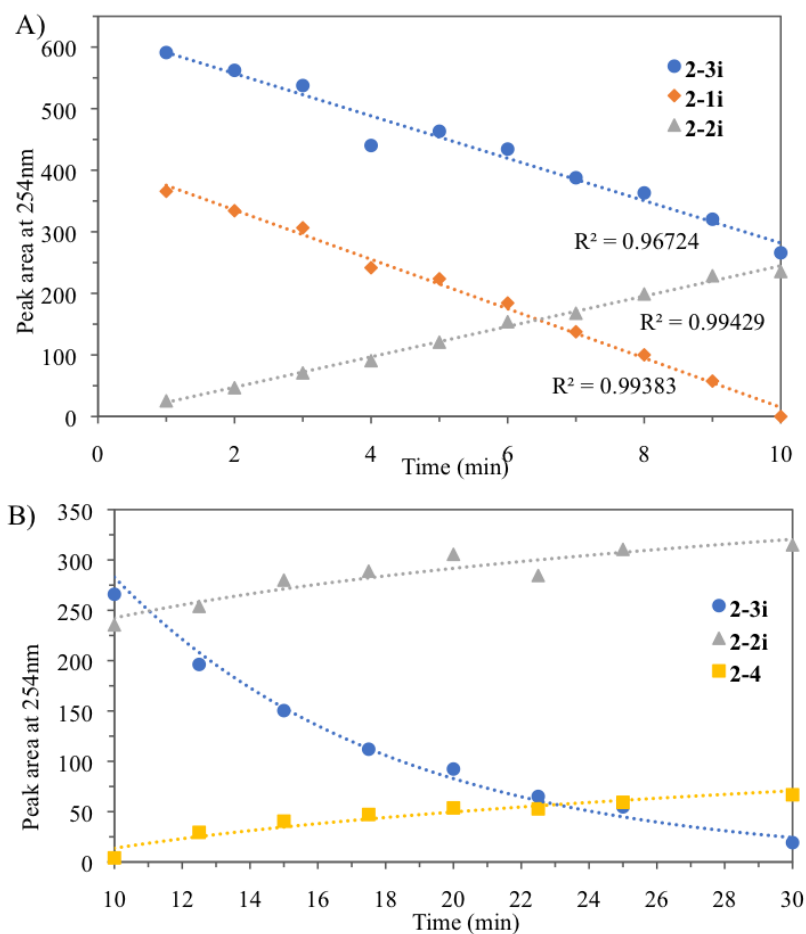
Figure 2-5 Reaction progress analysis of the Beckmann rearrangement of oxime ester **2-3i** in the presence of oxime **2-1i**; A) 0 to 10 min, and B) 10 to 30 min. Relative peak areas are not normalized.

In the presence of oxime **2-1i**, a linear relationship was observed for all compounds **2-1i–3i** (Figure 2-5A). This observation corroborates with the expected zeroth order dependence on aryl group migration. After the full consumption of oxime **2-1i**, the decomposition of oxime ester **2-3i** showed a non-linear relationship that mirrored the above plot without oxime (Figure 2-5B); this strengthens the postulated pseudo-first-order-reaction due to the slow transesterification of acyl imidate **2-7** with HFIP, a weaker nucleophile as compared to the free oxime (e.g., **2-1i**).

All of these observations agree with the proposed true organocatalytic mechanism in Scheme 2-13, where **BA-41** and **BA-42** serve as pre-catalysts in this protocol and the rate determining boron-assisted transesterification with oxime results in the actual active catalytic species **2-3** leading to a highly efficient Beckmann rearrangement catalytic cycle.

2.5.1.4 Control Experiment with HFIP Ester 2-4

Because HFIP ester **2-4** was formed as the by-product of the catalyst, to rule out the possibility of HFIP ester **2-4** as the active catalytic species, a control experiment was conducted and analyzed by LC-MS. After the quantitative decay of oxime ester **2-3a** into HFIP ester **2-4**, 10 equivalents of *para*-bromoacetophenone oxime **2-1j** were added to the reaction mixture, and the conversion to the corresponding amide **2-2j** was monitored by LC-MS analysis at different reaction times over the reaction (Scheme 2-16).
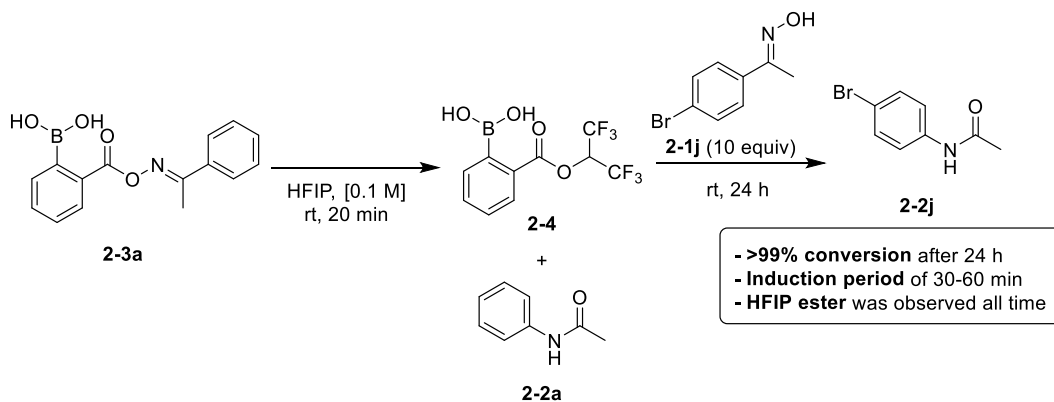
Scheme 2-16 Control experiment of catalytic activity of HFIP ester **2-4**.

In the event, full conversion of oxime **2-1j** into the amide product was observed after 24 h, indicating that HFIP ester **2-4** is also effective in promoting the Beckmann rearrangement. However, HFIP ester **2-4** was observed all the time, suggesting that not all HFIP ester was consumed and only a fraction of HFIP ester **2-4** was transformed into the reactive oxime ester **2-3j**. Furthermore, an induction period of about 1 h was observed, where amide **2-2j** was not detected in the first hour. This induction period is likely due to the slower boron-assisted transesterification of HFIP ester **2-4** with oxime to form the oxime ester **2-3j**. Once a small fraction of the oxime ester **2-3j** was generated in the reaction, the Beckmann rearrangement of oxime can proceed smoothly through the proposed catalytic cycle with the active catalytic species, oxime ester **2-3j**; thus, some HFIP ester **2-4** remained unreacted over the course of the reaction. These results indicate that HFIP ester **2-4** is not the actual catalytically active species but is an effective pre-catalyst for the Beckmann rearrangement.

2.5.2 ^{18}O-Labeling Studies

To support the proposed mechanism further and to understand the nature of the rearrangement step, an isotope labeling study using ^{18}O-labeled oxime ester **2-3a*** was designed (Scheme 2-17). It was envisioned that if the rearrangement proceeds through a unimolecular ionic pathway, the ^{18}O-label should distribute equally into the amide product **2-2a*** and HFIP ester **2-4***. If the rearrangement proceeds with a concerted pathway, the ^{18}O-label should be observed exclusively in either the amide product **2-2a*** or HFIP ester **2-4***, depending on which oxygen atom of the carboxylate unit is involved in the migration. Finally, if the rearrangement proceeds via a self-propagating pathway, the ^{18}O-label would incorporate solely into the 2-carboxyphenylboronic acid **BA-40***.
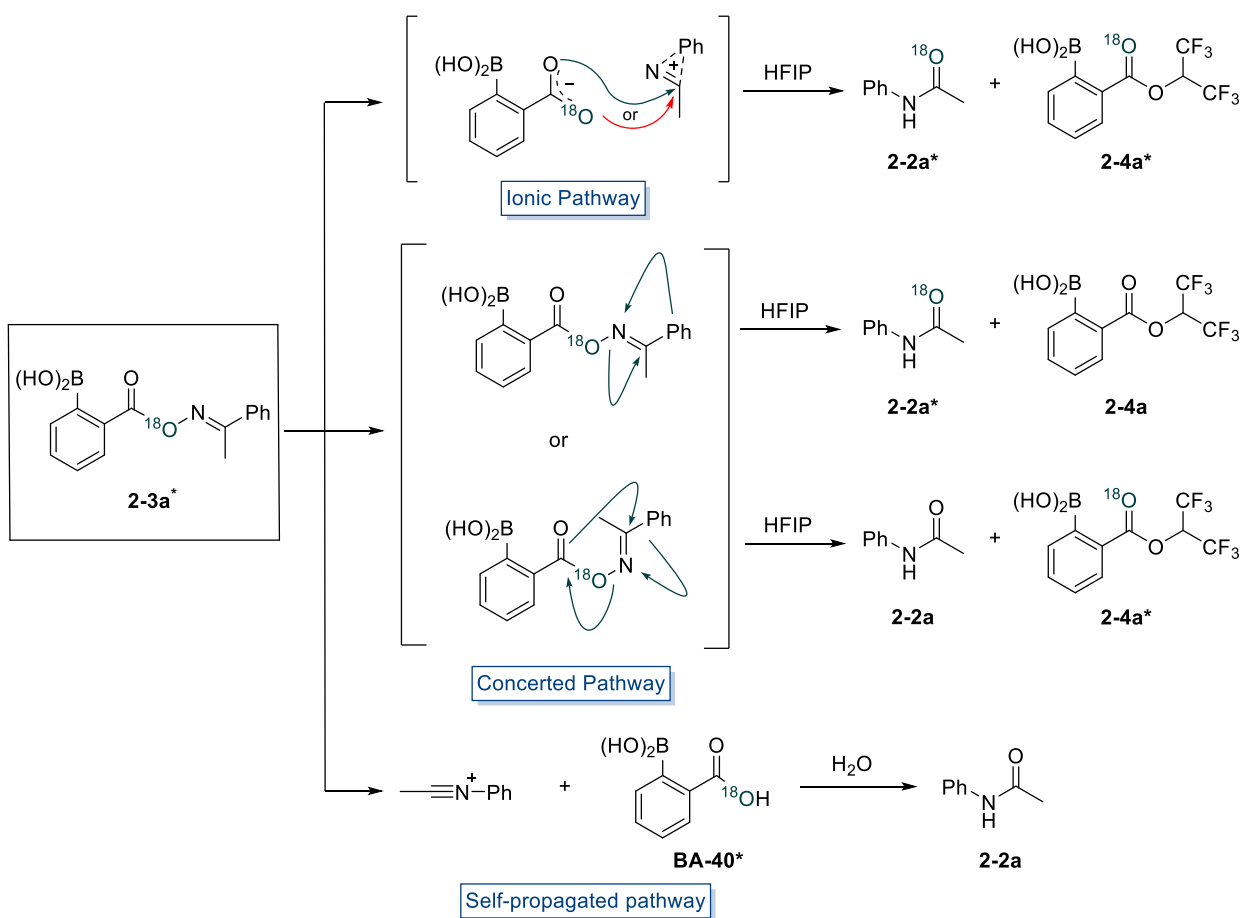
Scheme 2-17 Proposed ^{18}O-labeling experiment with oxime ester **2-3a*** and its potential outcomes.

2.5.2.1 Synthesis of the ^{18}O-Labeled Oxime Ester 2-13*

The ^{18}O-enriched acetophenone oxime **2-1i** was synthesized according to a literature procedure using ^{18}O-enriched water and used in the synthesis of ^{18}O-enriched oxime ester **2-13***.[31] Utilizing the same procedure developed by Xiaobin Mo, the oxime ester **2-13*** was synthesized successfully with 51% ^{18}O incorporation (Scheme 2-18). The percent ^{18}O incorporation was determined using the selective ion monitoring (SIM) mode in LC-MS. Given the difficulty of deprotection of neopentyl glycol of oxime ester **2-13**, the scarce amount of oxime ester **2-13*** in hand, and the high cost of ^{18}O-enriched water, the deprotection of oxime ester **2-13*** to the free boronic acid **2-3a*** was not attempted. Thus, instead of boronic acid **2-3a***, the labile boronic ester **2-13*** was used for the ^{18}O-labeling study.
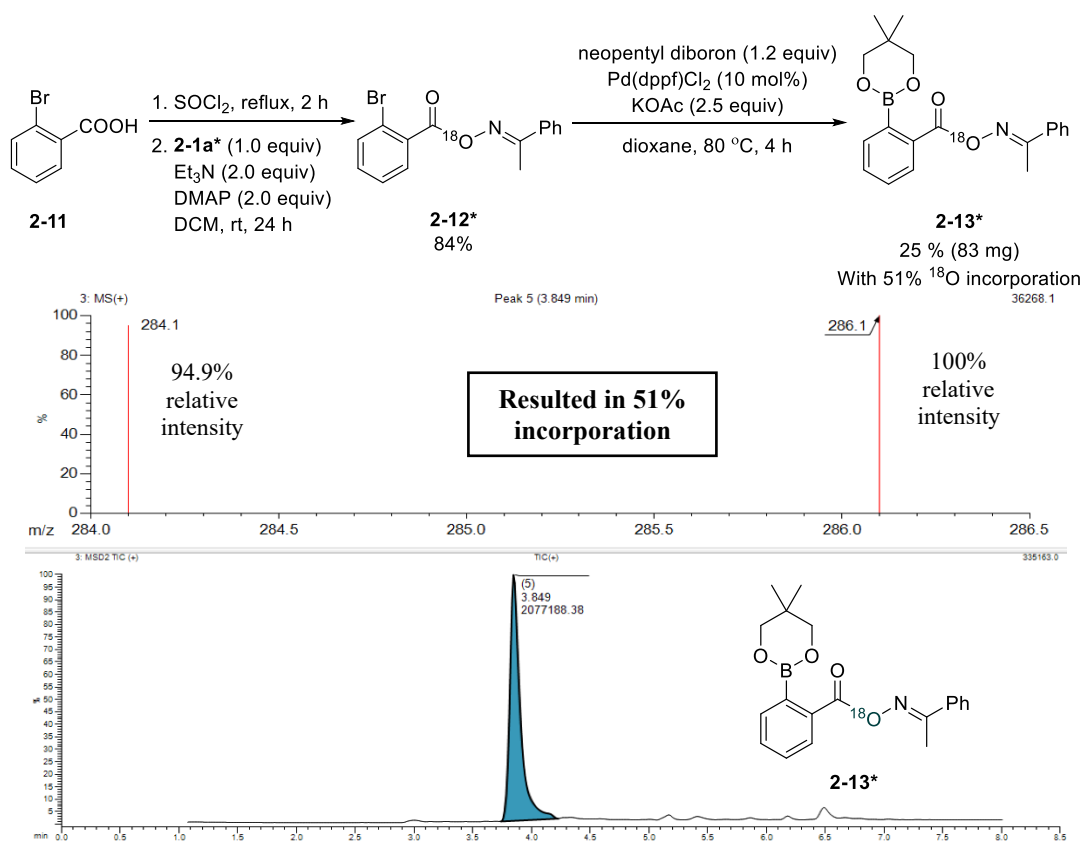
Scheme 2-18 Synthesis of ^{18}O-enriched oxime ester **2-13*** and LC-MS (SIM mode) analysis for the percent ^{18}O incorporation

2.5.2.2 Evaluation of Reaction Conditions for the Rearrangement with Oxime Ester 2-13

Before conducting the ^{18}O-labeling study, the reaction conditions were investigated using the non-labeled oxime ester **2-13**. The self-rearrangement of the boronic ester **2-13** at ambient temperature was found to be very slow, as unreacted boronic ester **2-13** still was observed by LC-MS analysis after 24 h. It is noteworthily that, this observation further illustrates the importance of the free ortho-boronyl group in the Beckmann rearrangement.

To speed up the reaction, water was added to the reaction to induce in-situ boronate hydrolysis to the more reactive boronic acid. Gratifyingly, when the rearrangement of boronic ester **2-13** was performed with 10 equivalents of water at 50 °C, full conversion to the amide product and HFIP ester **2-4** was observed after 6 h (Scheme 2-19A). To ensure that the addition of water does not affect the Beckmann rearrangement, a control experiment with addition of 50 mol% water in the optimized

63

Beckmann rearrangement reaction conditions with pre-catalyst **BA-41** was performed using oxime **2-1a** (Scheme 2-19B). The reaction proceeded smoothly to yield the amide product **2-2a** in a slightly decreased yield (86%) as compared to the optimized reaction conditions (93%). This result shows that the presence of water has no significant effect on the Beckmann rearrangement and validates the addition of water in the rearrangement of oxime ester **2-13** for the ^{18}O-labeling investigation. Moreover, with the presence of water in the isotope labeling study, the potential role of adventitious water as the origin of the oxygen atom in the amide product could be investigated or ruled out.
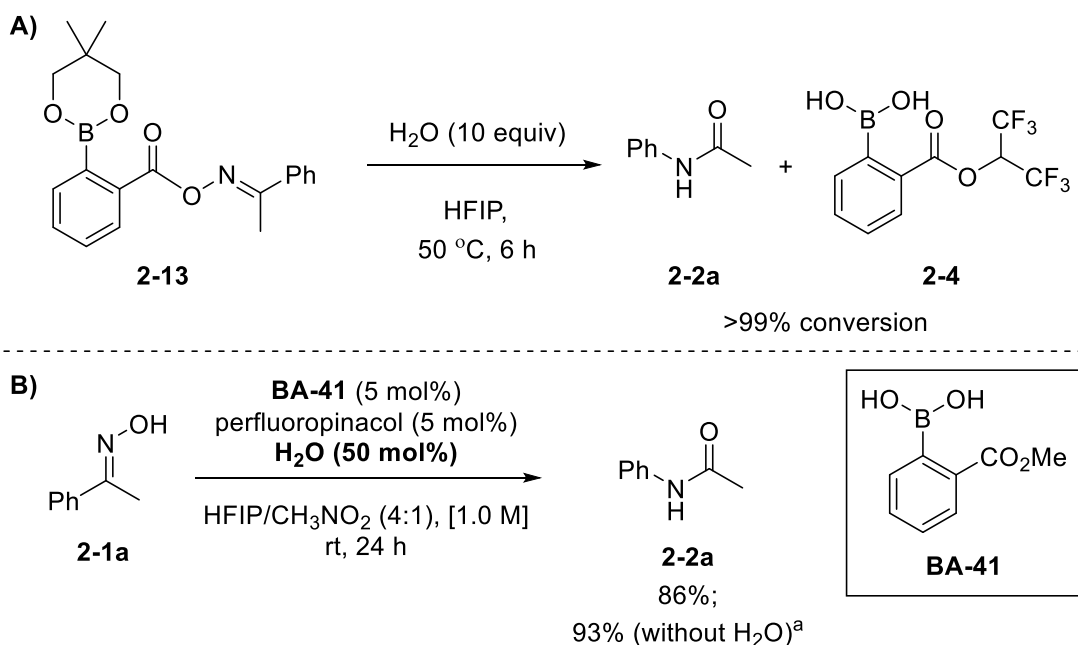
Scheme 2-19 A) Reaction conditions for the rearrangement of boronic ester **2-13**; B) Effect of water in the BAC protocol for the Beckmann rearrangement. [a]Result was obtained by Xiaobin Mo.

2.5.2.3 ^{18}O-Labeling Study with Boronic Ester 2-13*

With boronic ester **2-13*** and the rearrangement reaction conditions in hand, the ^{18}O-labeling study was conducted. A 0.1 M solution of boronic ester **2-13*** in HFIP was prepared, 10 equivalents of water were added, and the reaction mixture was stirred at 50 °C for 6 h before subjecting a sample to LC-MS analysis (Scheme 2-20). It was found that the ^{18}O-label was incorporated in both the amide **2-2a** and HFIP ester **2-4**. Only a negligible amount of 2-carboxylphenylboronic acid **BA-40** was observed.
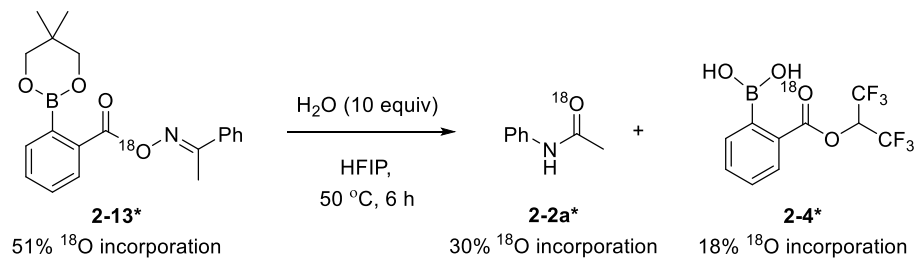
Scheme 2-20 The rearrangement of ^{18}O-labeled boronic ester **2-13***.

Using the SIM mode in LC-MS analysis, the percent ^{18}O-incorporation in the amide product **2-2a*** and HFIP ester **2-4*** was determined to be 30% and 18% respectively (Figure 2-6).
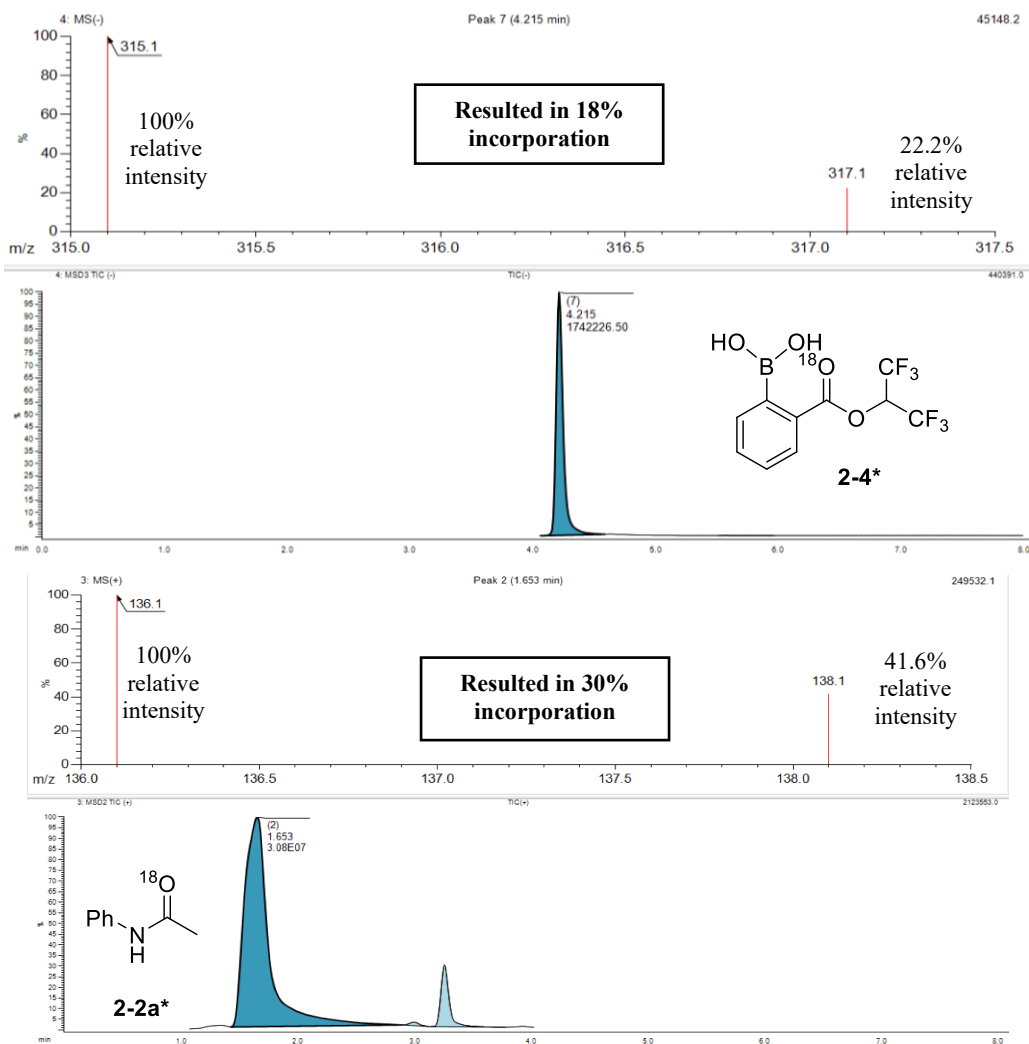
Figure 2-6 LCMS SIM mode quantification of percent ^{18}O incorporation of amide **2-2a*** and HFIP ester **2-4*** after 6 h.

With % ^{18}O incorporation of boronic ester **2-13*** normalized as 100%, about 6% loss of the ^{18}O-label was observed, and the ^{18}O-label ended up distributed unevenly into the amide **2-2a*** (59%) and HFIP ester **2-4*** (35%). These results rule out both the role of adventitious water as the origin of the oxygen atom in the amide product and the self-propagating pathway for the rearrangement. Furthermore, the ^{18}O-incorporation in both the amide product **2-2a*** and HFIP ester **2-4*** suggests that the Beckmann rearrangement likely occurs via an ionic pathway.

It is worth mentioning that a consistent % ^{18}O-label incorporation was observed in both amide **2-2a*** and HFIP ester **2-4*** as the reaction progressed (Table 2-2). This observation rules out any potential background oxygen exchange reactions and confirms the validity of this ^{18}O labeling experiment.

Table 2-2 The % ^{18}O-Label Incorporation in Amide **2-2a*** and HFIP Ester **2-4*** over Time

time (h)		2	3	4	5	6
% ^{18}O-incorporation[a]	**2-2a***	29	30	30	30	30
	2-4*	17.5	18	18.5	18	18

[a]The % ^{18}O-incorporation was quantified using LC-MS via SIM mode

2.5.2.4 Control Experiment of Boronic Acid BA-40

As mentioned above, the non-formation of boronic acid **BA-40** in the ^{18}O-labeling study implies that the rearrangement does not proceed via the self-propagated pathway. Therefore, in order to rule out confidently the possibility of the self-propagated pathway, it is essential to show that **BA-40** is unable to transform into HFIP ester **2-4** under the reaction conditions. Indeed, when 2-carboxyphenylboronic acid **BA-40** was subjected to the reaction solvents with and without oxime **2-1a**, the formation of the HFIP ester **2-4** was not observed using LC-MS analysis (Scheme 2-21).
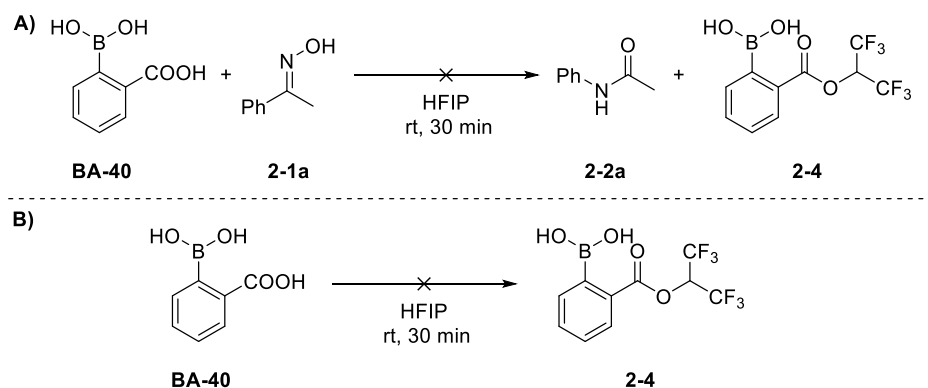
Scheme 2-21 Control experiments for the non-formation of HFIP ester **2-4** from **BA-40** A) with oxime **2-1a** and B) without oxime **2-1a**.

2.5.2.5 Plausible Explanation for Uneven ^{18}O-Label Distribution

The results of the ^{18}O-labeling experiment, where the ^{18}O-label was partitioned into both amide product **2-2a*** and HFIP ester **2-4***, is in closer agreement with the ionic pathway. However, as opposed to the expected equal distribution of ^{18}O label, a slightly uneven distribution of the label (59:37) was obtained. With the use of the highly polar HFIP as solvent, it is reasonable to envision that the rearrangement could happen asynchronously through a short-lived ion pair **2-14** containing the carboxylate and a π-complex.

The non-equal distribution of the label can be rationalized with two plausible explanations (Scheme 2-22). First, as the ^{16}O oxygen is coordinated internally to the boron atom, the ^{18}O-label is more available to react with the π-complex in the ion pair **2-14***, forming the acyl imidate **2-7***, hence resulting in the higher proportion of ^{18}O-label incorporation in the amide **2-2a*** (Scheme 2-22A). Alternately, given that the formation of the acyl imidate is reversible through a tight ion pair of the carboxylate and nitrilium ion, complex kinetic and/or equilibrium isotopic effects could play a role and lead to a small bias in favor of amide **2-2a*** (Scheme 2-22B). Nonetheless, according to the ^{18}O-labeling investigation, the rearrangement mechanism proceeds most likely through the ionic pathway.
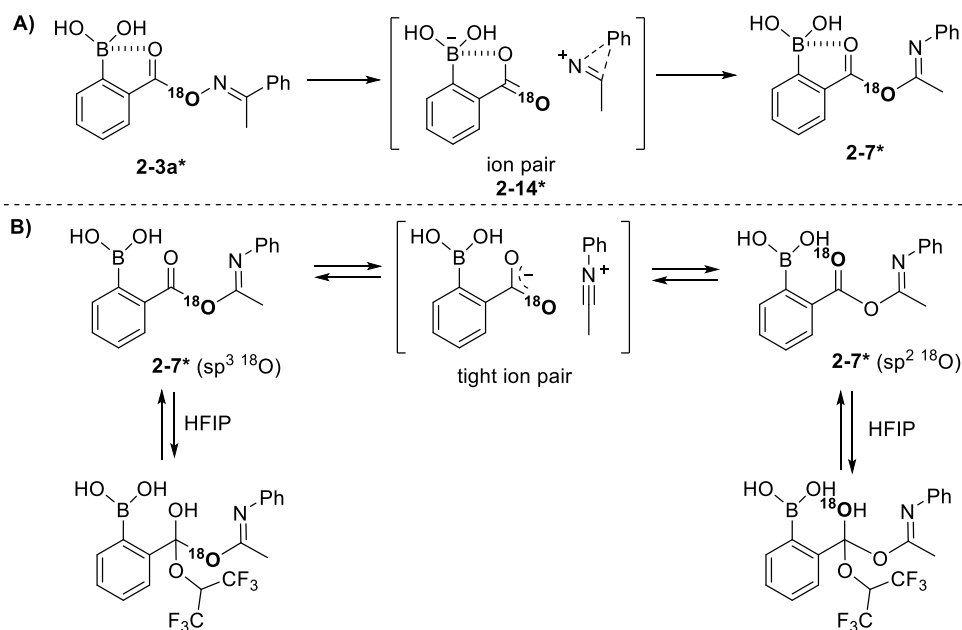
Scheme 2-22 Plausible explanations for the uneven **2-2a*** and **2-4*** proportions.

2.5.3 Investigation of the Possibility of a Brønsted Acid Catalyzed Mechanism

Recently, based on experimental evidence, Moran and co-workers proposed alternative Brønsted acid catalyzed mechanisms in the Beckmann rearrangement for some oxime substrates.[32] The ability of our co-catalytic BAC system (**BA-41/A-1**) to catalyze the ring-opening hydroarylation of phenylcyclopropane, delivering the desired product in high yield (96%), which is comparable to the yield obtained using catalytic triflic acid (TfOH), led Moran and co-workers to propose the possibility of a Brønsted acid mechanism (Scheme 2-23A). With the absence of a hydroxy functional group in the phenylcyclopropane, the activation likely occurs through a Brønsted acid mechanism instead of a Lewis acid or covalent mechanism involving the boronic acid catalyst. Furthermore, inhibition of the reaction with the presence of 2-6-di-*tert*-butylpyridine, a bulky Brønsted base often used to differentiate between Brønsted and Lewis acid catalysis, further supports the Brønsted acid mechanism.[32] Using the Guttman–Beckett method, a procedure to assess the acidity of chemical compound based on the change in the ^{31}P NMR shift of triethylphosphine oxide (TEPO) arising from the interaction of the oxygen atom with the Lewis or Brønsted acid, they discovered that the acidity of this **BA-41/A-1** co-catalytic system in 4:1

HFIP/CH$_3$NO$_2$ (90.3 ppm) appears to be stronger to that of B(C$_6$F$_5$)$_3$ (78.2 ppm) and comparable to that of camphorsulfonic acid (CSA, 91.3 ppm) and HCl (90.7 ppm); this is consistent with their hypothesis.

They then examined the possibility of a Brønsted acid catalyzed mechanism in the Beckmann rearrangement using the **BA-41/A-1** co-catalytic system with four oxime substrates reported by us, and it was found in all cases that the rearrangement was inhibited with 2,6-di-*tert*-butylpyridine.[32] Furthermore, other than oxime **2-1a**, CSA was found capable to promote the rearrangement of oximes **2-1b**, **2-1h** and **2-1ab** with comparable reactivity (Scheme 2-23B). These results indicate that the Brønsted acid mechanism is likely dominant for some of the oxime substrates, such as **2-1b**, **2-1h** and **2-1ab**. Hence, to follow up and verify their claim on the potential Brønsted acid catalyzed mechanism, more mechanistic investigations were performed.
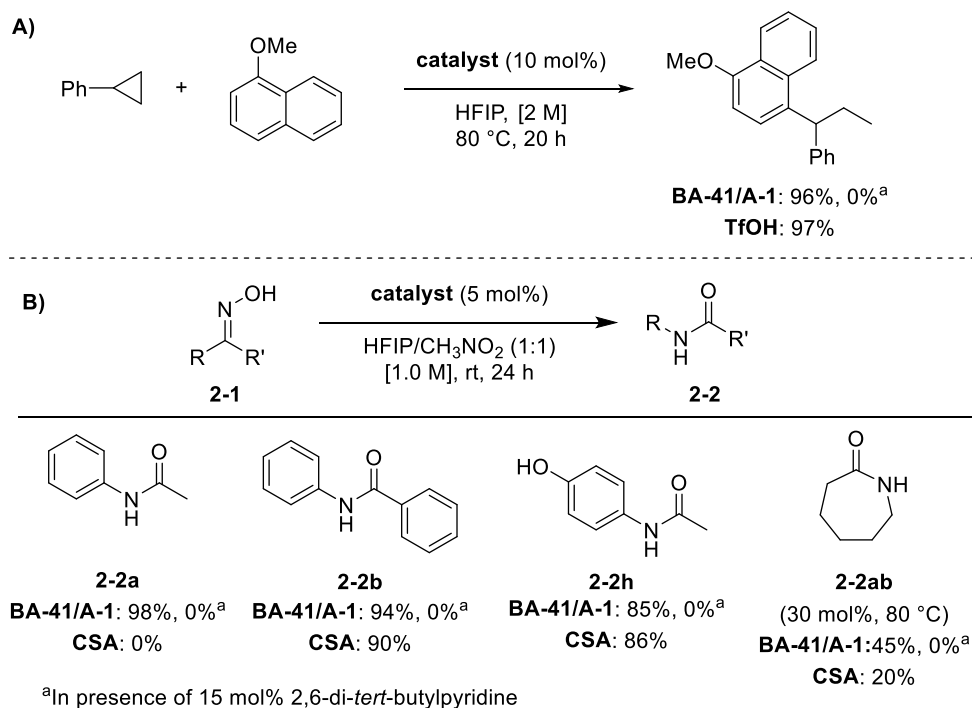
Scheme 2-23 Reported experimental results by Moran and co-workers for A) the hydroarylation of phenylcyclopropane and B) the Beckmann rearrangement.[32]

2.5.3.1 Evaluation of the Beckmann Rearrangement using the Co-Catalytic BA-17/A-1 System

In 2019, we reported a two-component boronic acid catalysis using 2,3,4,5-tetrafluorophenylboronic acid (**BA-17**) and perfluoropinacol (**A-1**) for increased reactivity in challenging Friedel–Crafts alkylations with deactivated benzylic alcohols (see Chapter 3).[33] Based on mechanistic studies, the activation of the hydroxy group is believed to occur via a Brønsted acid mechanism with a hydronium boronate species generated from **BA-17** and **A-1**. Thus, this co-catalytic system was employed in the Beckmann rearrangement to evaluate the possibility of a Brønsted acid catalyzed reaction pathway (Scheme 2-24).
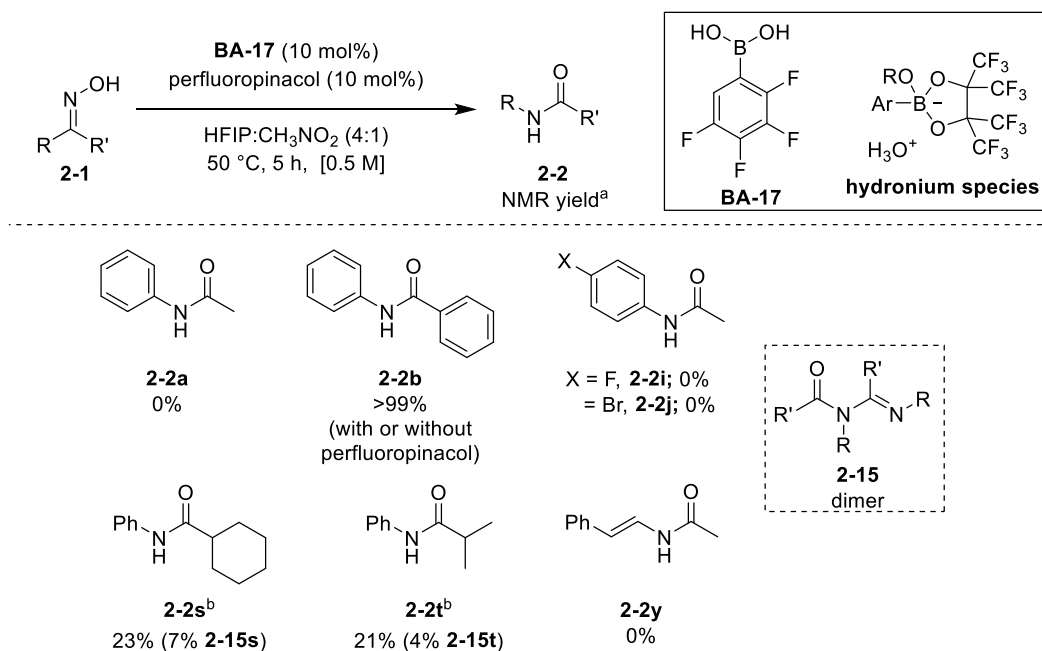
ᵃYields were determined by ^{1}H NMR analysis with 1,4-dinitrobenzene as internal standard.
ᵇOximes were formed as mixture of isomers.

Scheme 2-24 Evaluation of the scope of Beckmann rearrangement using the **BA-17/A-1** system.

Out of six oxime substrates examined, only benzophenone oxime **2-1b** underwent the rearrangement smoothly, yielding the amide product quantitatively, which is in line with the result observed by Moran and co-workers. Moreover, the same efficiency also was obtained without the use of co-catalytic perfluoropinacol. These results strongly suggest that the rearrangement of oxime **2-1b** likely proceeds through a Brønsted acid mechanism; this is unsurprising, as benzophenone oxime

2-1b is an easy substrate for the Beckmann rearrangement. While Moran and co-workers showed that electron rich 4-hydroxy-acetophenone oxime **2-1h** underwent the rearrangement smoothly using catalytic CSA,[32] the rearrangement of electron neutral and poor acetophenone oximes (**2-1a**, **2-1i** and **2-1j**) and alkenyl-alkyl oxime **2-1y** were found to be unsuccessful in the **BA-17/A-1** co-catalytic system.

Other than electronic factors, steric effects also may play a role in dictating the dominant mechanistic pathway for the Beckmann rearrangement. Therefore, oxime substrates with a bigger R' group (**2-2s** and **2-2t**) also were evaluated with the co-catalytic **BA-17/A-1** system. In both cases, the amide products were generated in low yield, along with a small amount of dimer product **2-15**. The formation of dimers **2-15** was supported by LC-MS. The low yield of amide product and formation of dimer **2-15** do not agree with the results obtained with the co-catalytic **BA-41/A-1** protocol, thus suggesting that these oxime substrates undergo the Beckmann rearrangement in our BAC protocol via the proposed oxime ester **2-3** mechanism instead of a Brønsted acid mechanism.

According to all these observations, it is undeniable that there is a competing Brønsted acid catalyzed mechanism with our BAC protocol for Beckmann rearrangement. However, based on additional experiments, it is believed that most of the oxime substrates undergo the rearrangement via our proposed mechanism, and only electron-rich aryl-alkyl and aryl-aryl oximes undergo the Beckmann rearrangement via Brønsted acid catalysis. The ease of electron-rich aryl-alkyl and aryl-aryl oximes to undergo the Beckmann rearrangement with protic acid likely is attributed to the increase in basicity of the hydroxy group due to aryl-aryl substituents and the electron-rich aryl substituent and the stabilization of the positive charge developed in the transition state by the electron rich aryl group.

2.5.3.2 Reaction Progress Analysis of the Rearrangement of Oximes 2-1b and 2-1j

To support further that the rearrangement of aryl-aryl oximes proceeds by a Brønsted acid mechanism, the reaction progress of the rearrangement of benzophenone oxime **2-1b**, an "easy" substrate, and 4-bromo-acetophenone oxime **2-1j**, a difficult one, was

compared. According to our proposed mechanism, where the oxime is activated by the slow transesterification with the boronic acid catalyst, there should be an induction period for the rearrangement, as observed with HFIP ester **2-4** and shown in Scheme 2-16.

In fact, when oxime **2-1b** was subjected to the Beckmann rearrangement with catalyst **BA-41** in the absence of perfluoropinacol, no induction period was observed (Scheme 2-25A). Moran and co-workers also reported the same observations using **BA-41/A-1** and CSA.[32] Whereas, when oxime **2-1j** was subjected to the Beckmann rearrangement with catalyst **BA-42** in the absence of perfluoropinacol, an induction period of 25 min was observed (Scheme 2-25B). Moreover, the formation of oxime ester **2-3j** was observed after 5 min by LC-MS in the negative ion mode as [M+formic acid–H]$^-$ ion (Figure 2-7). According to Moran and co-workers, **2-3j** would not form in the Brønsted acid catalyzed rearrangement. Thus, these results further support our proposed mechanism and confirm the intermediacy of oxime ester **2-3**.
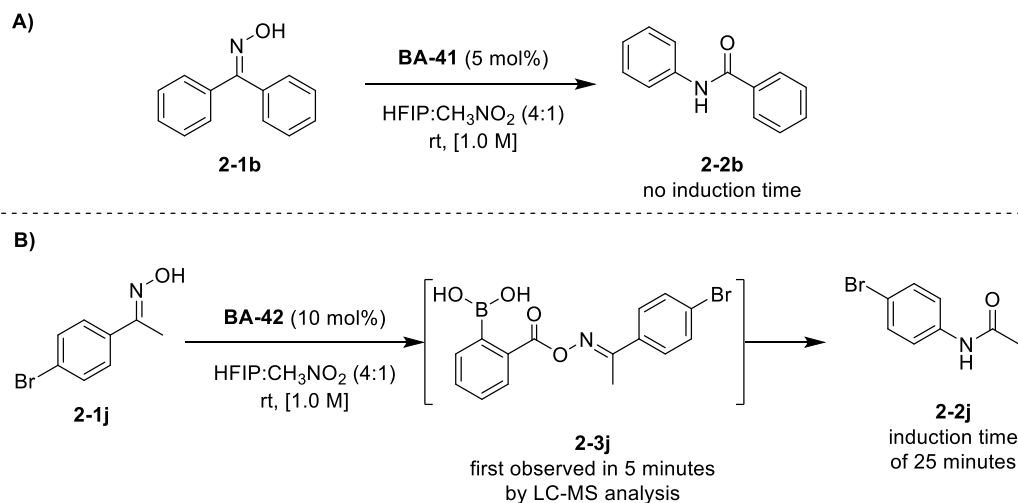
Scheme 2-25 The Beckmann rearrangement of A) oxime **2-1b** with **BA-41** and B) oxime **2-1j** with **BA-42**.
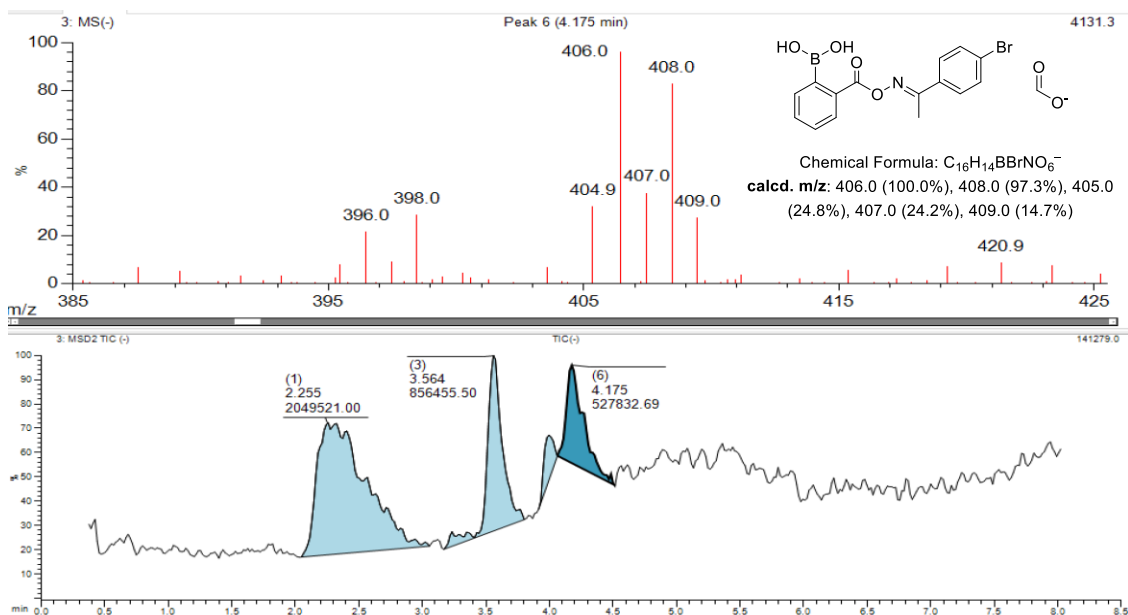
Figure 2-7 LC-MS spectrum of the reaction mixture of the rearrangement of oxime **2-1j** at 20 min with the mass spectrum for oxime ester **2-3j** as [M+formic acid–H]⁻ ion.

2.5.3.3 Effect of Anhydrous Conditions in the Beckmann Rearrangement

As shown by Moran and co-workers, the Beckmann rearrangement was inhibited by 2,6-di-*tert*-butylpyridine, indicating that there is potentially a protic acid-promoted step in the mechanism.[32] Most likely, the oxime transesterification is dependent on the presence of a Brønsted acid. As water is needed in the reaction medium to generate the Brønsted acidic hydronium complex, the Beckmann rearrangement was evaluated in anhydrous conditions using dry solvents with or without molecular sieves to minimize the amount of Brønsted acid (Scheme 2-26).
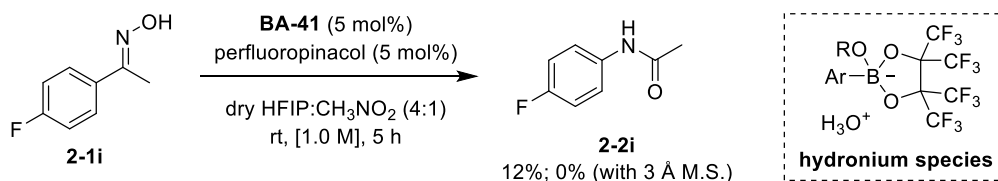
(Yields were determined by ¹H NMR analysis with 1,4-dinitrobenzene as internal standard)

Scheme 2-26 Control experiments for the effect of anhydrous conditions in the Beckmann rearrangement.

Under anhydrous conditions with molecular sieves, the reaction was shut down completely, while without molecular sieves, a small amount of amide product **2-2i** was formed; this could be attributed to the small amount of water generated as

the by-product of the reaction. These results are supportive of the proposed Brønsted acid dependent transesterification of oxime with boronic acid to form the oxime ester **2-3**.

2.6 Improvement of the Synthesis of Catalyst BA-42

The use of the more efficient pre-catalyst **BA-42** is limited by its availability and synthesis. As depicted in Scheme 2-27, the synthetic route for **BA-42,** developed by Xiaobin Mo and Dr. Timothy Morgan, involves four synthetic steps, with an overall yield of 24%. Therefore, improvement of the synthesis of **BA-42** would be beneficial to the utility and practicality of this pre-catalyst.
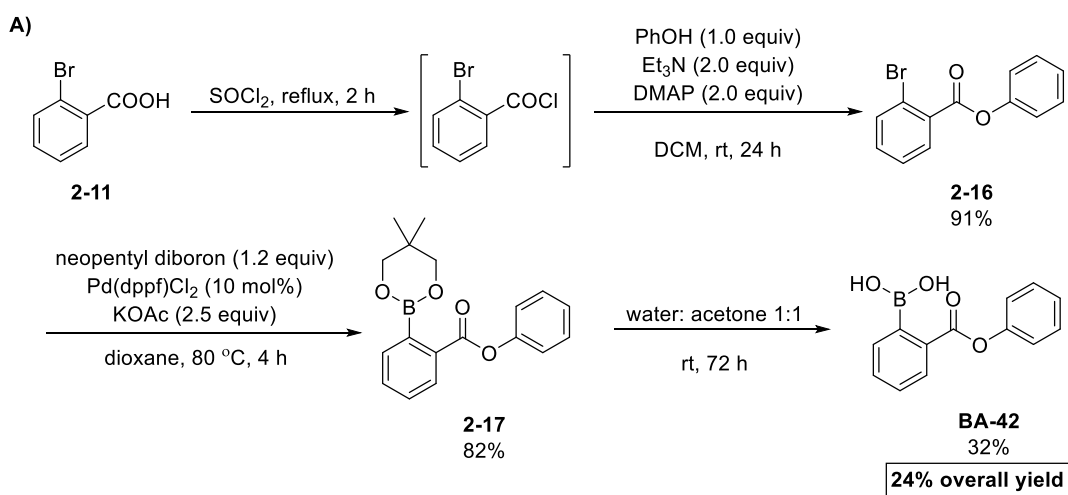
Scheme 2-27 The synthesis of boronic acid **BA-42** by Xiaobin Mo and Dr. Timothy Morgan.

The first approach taken was the esterification of 2-carboxyphenylboronic acid **BA-40** with phenol, which would afford the boronic acid **BA-42** in one step. However, the esterification using different procedures adopted from literatures[34–38] was not successful, and in all cases the starting material was recovered (Scheme 2-28). The failure in the esterification of **BA-40** with phenol could be attributed to the low nucleophilicity of phenol and the potential intramolecular cyclization of **BA-40** to form the cyclic hemiboronic acid **2-18**, which is relatively more stable and unreactive.
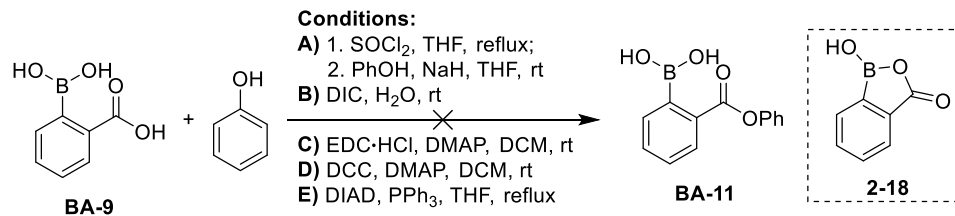
Scheme 2-28 Attempts to synthesize boronic acid **BA-42** from **BA-40** via esterification with phenol.

As the low yielding deprotection of the boronic ester **2-17** is the main problem in the previous synthesis, direct borylation to afford a free boronic acid instead of a boronic ester would be a probable solution. Thus, the palladium-catalyzed borylation of aryl halides using bis-boronic acid ($B_2(OH)_4$), developed by Molander and co-workers in 2012, was attempted.[39] Unfortunately, when the 2-bromo- and 2-chloro-substituted phenyl benzoate were subjected to the Molander's borylation conditions, no desired product was observed, and dehalogenated product **2-19** was isolated as the major product (Scheme 2-29).
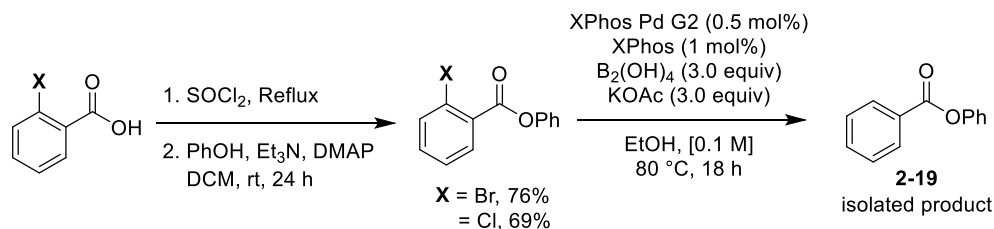
Scheme 2-29 Attempts with the Molander's palladium-catalyzed direct borylation using bis-boronic acid.

Other than transition metal-catalyzed borylation of aryl halides to afford boronic acids/esters, halo-metal exchange, followed by borylation with trialkyl borate, is another common approach for the synthesis of boronic acid from aryl halides. However, butyllithium, which commonly is used in this approach, would be incompatible with the substrate containing a carboxyester group. Fortunately, the report by Senanayake and co-workers in 2006 overcomes this problem by utilizing the fast and mild I/Mg exchange of aromatic iodides bearing a carboxyester and nitrile group with isopropylmagnesium chloride (*i*-PrMgCl).[40] When phenyl 2-iodobenzoate (**2-21**) was subjected to the reported reaction conditions, the desired

product **BA-42** was obtained in a low yield (25%). This low yield is likely due to the hydrolysis of the labile phenoxy ester group during the acidic work-up, as boronic acid **BA-40** and phenol were observed in the crude NMR spectrum. Thankfully, this problem was solved by using a minimal amount of 0.1 M HCl solution instead of 1 M HCl solution in the work-up and by performing the work-up as fast as possible to reduce the exposure of product **BA-42** to acid. Using this modified work-up procedure, the desired product **BA-42** was obtained in a moderate yield of 65% by recrystallization from toluene (Scheme 2-30). Furthermore, the esterification of 2-iodobenzoic acid **2-20** also was simplified to one step using the coupling reagent, *N-N'*-dicyclohexylcarbodiimide (DCC), and 4-dimethylaminopyridine (DMAP), affording the product **2-21** in nearly quantitative yield.
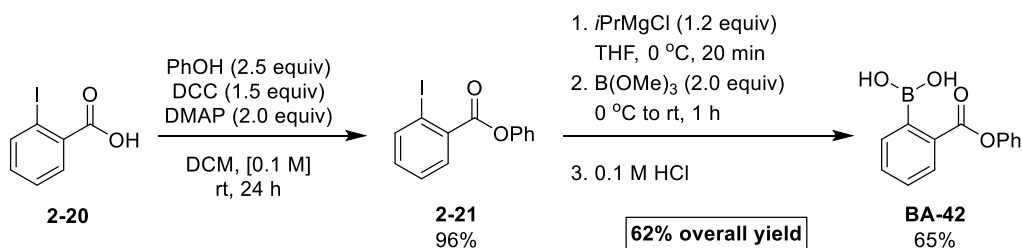
Scheme 2-30 Improved synthesis of boronic acid **BA-42** via I/Mg exchange followed by borylation.

As shown in Scheme 2-30, the synthesis of the pre-catalyst **BA-42** was reduced to two steps, with an overall yield of 62%. Possibly, the synthesis can be improved further by optimizing the work-up procedure of the borylation step to avoid the use of acid to prevent the hydrolysis of the phenoxy ester group. Of note, **BA-42** (CAS: 2211934-51-7) also has been commercialized by Sigma-Aldrich.

2.7 Summary

In conclusion, this chapter describes the efforts in the development of a true organocatalytic Beckmann rearrangement with a boronic acid/perfluoropinacol system. Through extensive screening and optimizations, boronic acid **BA-41** and **BA-42**, bearing an ortho-carboxyester group, were identified as efficient catalysts, along with co-catalytic perfluoropinacol **A-1,** for the Beckmann rearrangement under mild and ambient conditions. This operationally simple procedure requires no pre-

drying of solvents or inert atmosphere and exhibits a broad scope of oxime substrates with good functional group tolerance. Extensive mechanistic studies, including reaction progress monitoring and ^{18}O-labeling experiments, reveal a novel catalytic pathway that is initiated by a boron-assisted transesterification of the pre-catalyst **BA-41** or **BA-42** with oxime to generate the active oxime ester catalyst for the subsequent unimolecular Beckmann rearrangement via an ionic pathway. This proposed catalytic pathway is applicable to most oxime substrates, except for aryl-aryl and electron rich aryl-alkyl oximes, which may undergo the rearrangement via a competitive Brønsted acid catalyzed manifold. The unique role of the boronyl unit in this catalytic system provides new inspiration for the design of boronic acid catalysts in other reactions involving the activation of hydroxy groups.

2.8 Experimental

2.8.1 General Information

The following sections include representative experimental procedures and details for the synthesis and isolation of compounds. Full characterization of all new compounds and partial characterization of known compounds presented in this chapter are described. Unless stated otherwise, all reactions were conducted in regular glassware sealed with a septa or glass stopper and no further precautions to exclude air or moisture. Toluene, tetrahydrofuran (THF), and dichloromethane (DCM) were purified using a cartridge solvent purification system prior to use. All other solvents (including HFIP and nitromethane) were purchased as ACS reagents and used without further purification or drying. 1,1,1,3,3,3-Hexafluoro-2-propanol (HFIP) was purchased from Oakwood Products, Inc. Perfluoropinacol (hexafluoro-2,3-bis(trifluoromethyl)-2,3-butanediol, **A-1**) was purchased from Matrix Scientific. 2-Methoxycarbonyl phenylboronic acid was purchased from Combi-Blocks and used as received. Unless otherwise noted, all other chemicals were purchased from commercial sources and used as received.

Chromatographic separations were performed on silica gel 60 using ACS grade hexanes, ethyl acetate, DCM, and acetone as eluents. Thin layer chromatography (TLC) was performed on silica gel 60 F254 plates, which were

visualized under UV light and with KMnO$_4$, phosphomolybdic acid (PMA), or curcumin (for boron containing compounds) stains. ^{1}H NMR and ^{13}C NMR spectra were recorded on 400 MHz or 500 MHz instruments. The residual solvent protons (^{1}H/CHCl$_3$) or the solvent carbon (^{13}C) were used as internal references. ^{1}H NMR data is presented as follows: chemical shifts in ppm (multiplicity, coupling constant, integration) from downfield to upfield. The following abbreviations are used in reporting NMR data: s, singlet; br s, broad singlet; d, doublet; t, triplet; q, quartet; quin, quintet; sext, sextet; sept, septet; dd, doublet of doublets; m, multiplet. The error of coupling constants from ^{1}H NMR spectra is estimated to be 0.3 Hz. High-resolution mass spectra were recorded by the University of Alberta mass spectrometry services laboratory using either electron impact (EI) or electrospray ionization (ESI) techniques. Infrared (IR) spectra were obtained using cast-film technique with frequencies expressed in cm^{-1}; the intensity of the band is indicated as s (strong), m (medium) and w (weak). The resolution of the IR instrument is 4 wavenumbers. Melting points (Mp) were measured on a melting point apparatus and uncorrected. LC-MS data were acquired from an Agilent 6130 single quadrupole LC-MS system equipped with diode array detector (wavelengths used: 200, 254, 280 nm). Chromatographic separation was achieved on Phenomenex Kinetex® C8 column (50 × 2.1 mm, 1.7 μm/100 Å) with a solvent flow of 0.5 mL/min at 25 °C. The sample injection volume was 2.0 μL. The mobile phase consisted of H$_2$O (solvent A) and acetonitrile with 0.1% formic acid (solvent B). A stepwise gradient of 98% to 5% solvent A over 8 min was employed.

2.8.2 Synthesis and Characterization of Oximes 2-9

2.8.2.1 General Procedure for the Condensation of Ketones with Hydroxylamine
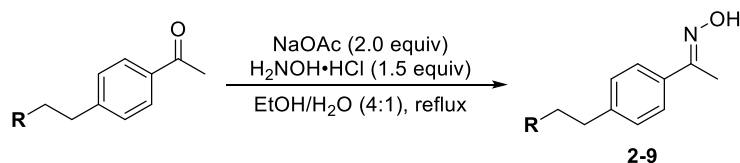
To a 100 mL round bottom flask charged with a stir bar, sodium acetate (2.0 equiv), and hydroxylamine hydrochloride (1.5 equiv) was added a solution of the ketone

(0.3 M) in ethanol/water (4:1). The reaction mixture was heated to reflux until all the ketone starting material was consumed, as indicated by TLC. After reflux, the reaction was allowed to cool to room temperature. The crude mixture was obtained after removal of excess ethanol. To the crude mixture was added 20 mL of water. The resulting aqueous solution was extracted with ethyl acetate (3 × 20 mL). The combined organic layers were washed with water (2 × 20 mL) and brine (1 × 20 mL), dried over anhydrous MgSO₄, filtered, and concentrated. The oxime product was used directly in the next step. In certain cases, the oxime product was obtained after flash column chromatography using the indicated solvent mixture.

2.8.2.2 Characterization of Oximes 2-9
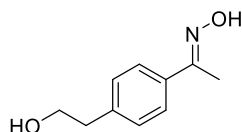
1-[4-(2-Hydroxylethyl)phenyl]ethanone oxime (2-9a): Prepared from 1-[4-(2-hydroxylethyl) phenyl]ethanone[41] (246 mg, 1.52 mmol) using the general procedure. Purified by recrystallization (2:1 hexane:DCM) and isolated as a white solid (228 mg, 85%). **Mp** 98–100 °C; **^{1}H NMR** (CDCl₃, 500 MHz, δ): 7.54 (d, J = 8.4 Hz, 2 H), 7.21 (d, J = 8.4 Hz, 2 H), 3.73 (t, J = 7.0 Hz, 2 H), 2.80 (t, J = 7.0 Hz, 2 H), 2.19 (s, 3 H); **^{13}C NMR** (CDCl₃, 125 MHz, δ): 156.0, 141.3, 136.5, 130.0, 127.0, 64.0, 39.9, 12.1; **IR** (microscope, cm^{-1}): 3209 (br), 2927 (m), 2881 (m), 1909 (w), 1885 (w), 1676 (w), 1629 (m), 1466 (w), 1411 (m), 1348 (m), 1314 (m), 1122 (w), 1055 (s), 1025 (s); **HRMS** (ESI) for C₁₀H₁₃NO₂ [M+H]$^+$: calcd. 180.1019; found 180.1019.
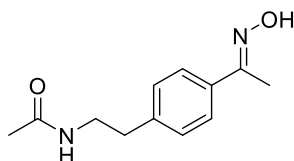
N-[2-(4-Acetylphenyl)ethyl]acetamide oxime (2-9b): Prepared from N-[2-(4-acetylphenyl) ethyl]acetamide[42] (705 mg, 3.43 mmol) using the general procedure. Isolated as a white solid (591 mg, 78%) and used without purification. **Mp** 135–136 °C; **^{1}H NMR** (CD₃OD, 500 MHz, δ): 7.54 (d, J = 8.3 Hz, 2 H), 7.20 (d, J = 8.3

Hz, 2 H), 3.37 (t, J = 7.3 Hz, 2 H), 2.78 (t, J = 7.3 Hz, 2 H), 2.19 (s, 3 H), 1.88 (s, 3 H); ^{13}**C NMR** (CD$_3$OD, 125 MHz, δ): 173.2, 155.9, 141.4, 136.7, 129.8, 127.2, 41.9, 36.2, 22.5, 12.0; **IR** (microscope, cm^{-1}): 3326 (s), 3088 (w), 2932 (w), 2861 (w), 1616 (s), 1549 (s), 1460 (m), 1302 (m), 1292 (m), 1190 (m); **HRMS** (ESI) for C$_{12}$H$_{16}$N$_2$O$_2$ [M+Na]$^+$: calcd. 243.1104; found 243.1105.
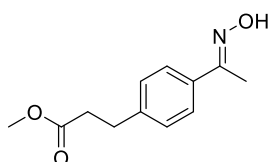
Methyl 3-(4-acetylphenyl)propionate oxime (2-9c): Prepared from 3-(4-acetylphenyl) propionate[43] (861 mg, 4.17 mmol) using the general procedure. Isolated as an off-white solid (884 mg, 95%) and used without purification. **Mp** 90–92 °C; ^{1}**H NMR** (CDCl$_3$, 500 MHz, δ): 8.31 (br s, 1 H), 7.57 (d, J = 8.4 Hz, 2 H), 7.23 (d, J = 8.4 Hz, 2 H), 3.69 (s, 3 H), 2.98 (t, J = 7.8 Hz, 2 H), 2.65 (t, J = 7.8 Hz, 2 H), 2.29 (s, 3 H); ^{13}**C NMR** (CDCl$_3$, 125 MHz, δ): 173.2, 156.0, 141.7, 134.6, 128.4, 126.2, 51.7, 35.5, 30.6, 12.0; **IR** (microscope, cm^{-1}): 3380 (br), 3344 (s), 3021 (w). 2956 (m), 2863 (w), 1709 (s), 1513 (w), 1455 (m), 1434 (m), 1299 (s), 1271 (m), 1247 (s), 1153.19 (m), 1116.45 (m), 1027.65 (m); **HRMS** (ESI) for C$_{12}$H$_{15}$NO$_3$ [M+H]$^+$: calcd. 222.1125; found 222.1129.
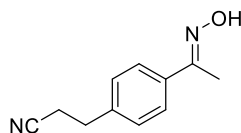
3-(4-Acetylphenyl)propionitrile oxime (2-9d): Prepared from 3-(4-acetylphenyl)propionitrile[44] (433 mg, 2.50 mmol) using the general procedure. Isolated as an off-white solid (383 mg, 81%) and used without purification. **Mp** 105–108 °C; ^{1}**H NMR** (CD$_3$OD, 500 MHz, δ): 7.59 (d, J = 8.4 Hz, 2 H), 7.27 (d, J = 8.5 Hz, 2 H), 2.93 (t, J = 7.2 Hz, 2 H), 2.72 (t, J = 7.2 Hz, 2 H), 2.20 (s, 3 H); ^{13}**C NMR** (CD$_3$OD, 125 MHz, δ): 155.7, 140.8, 137.4, 129.5, 127.4, 120.6, 32.1, 19.4, 12.0; **IR** (microscope, cm^{-1}): 3237 (br), 3135 (s), 2929 (m), 2244 (m), 1918 (w), 1841 (w), 1798 (w), 1645 (w), 1612 (m), 1519 (m), 1442 (m), 1421 (m), 1374 (m), 1311 (m),

1196 (w), 1004 (s); **HRMS** (ESI) for $C_{11}H_{12}N_2O$ [M+H]$^+$: calcd. 189.1022; found 189.1026.

2.8.3 Boronic Acid/Perfluoropinacol Catalyzed Beckmann Rearrangement

2.8.3.1 General Procedure for the Beckmann Rearrangement
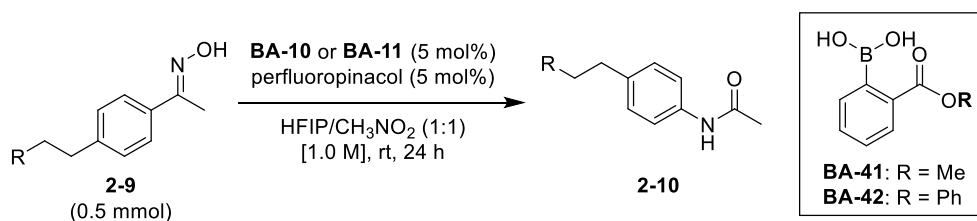
To a 5 mL reaction vial charged with a stir bar was added the oxime substrate **2-9** (0.50 mmol), boronic acid **BA-41** (4.5 mg, 0.025 mmol) or **BA-42** (6.2 mg, 0.025 mmol) and perfluoropinacol (8.4 mg, 0.025 mmol). A solvent mixture of nitromethane and hexafluoroisopropanol (1:4) 0.5 mL was injected. The reaction vial was capped, sealed, and subjected at the room temperature for 24 h. The crude product was obtained after removal of the solvent. The pure amide product **2-10** was isolated after flash column chromatography using the indicated solvent mixtures.

2.8.3.2 Characterization of the Amide Products 2-10
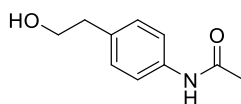
N-**[4-(2-Hydroxylethyl)phenyl]acetamide** (**2-10a**): Prepared from 1-[4-(2-hydroxylethyl)phenyl] ethanone oxime **2-9a** (90 mg, 0.50 mmol) using the general procedure. Purified by flash chromatography (1:1 hexane/acetone) and isolated as a brownish yellow solid (with **BA-41**: 74 mg, 82%; with **BA-42:** 86 mg, 96%). **Mp** 90–93 °C; **^{1}H NMR** (CD$_3$OD, 500 MHz, δ): 7.42 (d, *J* = 8.5 Hz, 2 H), 7.15 (d, *J* = 8.5 Hz, 2 H), 3.70 (t, *J* = 7.1 Hz, 2 H), 2.76 (t, *J* = 7.1 Hz, 2 H), 2.08 (s, 3 H); **^{13}C NMR** (CD$_3$OD, 125 MHz, δ): 171.5, 138.0, 136.3, 130.3, 121.3, 64.2, 39.7, 23.7; **IR** (microscope, cm^{-1}): 3306 (s), 3126 (m), 3045 (m), 2931 (m), 2858 (m), 1898 (w), 1665 (s), 1599 (m), 1531 (s), 1479 (m), 1408 (m), 1375 (m), 1318 (m), 1265 (m),

1234 (m), 1202 (m), 1115 (m), 1043 (s), 1021 (m); **HRMS** (ESI) for $C_{10}H_{13}NO_2$ [M+H]$^+$: calcd. 180.1019; found 180.1020.
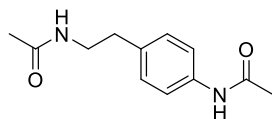
***N*-[4-[2-(Acetylamino)ethyl]phenyl]acetamide (2-10b)**: Prepared from *N*-[2-(4-acetyl-phenyl)ethyl] acetamide oxime **2-9b** (111 mg, 0.504 mmol) using the general procedure. Purified by flash chromatography (1:1 hexane/acetone) and isolated as a pale-yellow solid (with **BA-41**: 94 mg, 85%; with **BA-42:** 102 mg, 91%). **Mp** 176–179 °C; **^{1}H NMR** (CD$_3$OD, 500 MHz, δ): 7.43 (d, J = 8.5 Hz, 2 H), 7.14 (d, J = 8.4 Hz, 2 H), 3.34 (t, J = 7.4 Hz, 2 H), 2.73 (t, J = 7.4 Hz, 2 H), 2.09 (s, 3 H), 1.88 (s, 3 H); **^{13}C NMR** (CD$_3$OD, 125 MHz, δ): 173.2, 171.6, 138.2, 136.4, 130.1, 121.4, 42.1, 35.9, 23.7, 22.5; **IR** (microscope, cm^{-1}): 3294.46 (s), 3117.05 (m), 3089.20 (m), 2972.14 (w), 2934.06 (m), 2861.29 (w), 1892.03 (w), 1665.37 (s), 1611.84 (m), 1596.01 (m), 151129.92 (s), 1442.14 (m), 1411.71 (s), 1366.66 (s), 1306.83 (s), 1267.11 (m), 1193.91 (m); **HRMS** (ESI) for $C_{12}H_{16}N_2O_2$ [M+Na]$^+$: calcd. 243.1104; found 243.1106.
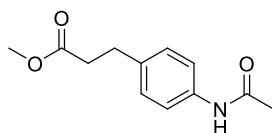
Methyl 3-[4-(acetylamino)phenyl]propanoate (2-10c): Prepared from methyl 3-(4-acetylphenyl) propionate oxime **2-9c** (111 mg, 0.502 mmol) using the general procedure. Purified by flash chromatography (1:1 hexane/EtOAc) and isolated as an off-white solid (with **BA-41**: 111 mg, quantitative). **Mp** 109–111 °C; **^{1}H NMR** (CD$_3$OD, 500 MHz, δ): 7.41 (d, J = 8.4 Hz, 2 H), 7.21 (br s, 1 H), 7.15 (d, J = 8.4 Hz, 2 H), 3.67 (s, 3 H), 2.92 (t, J = 7.7 Hz, 2 H), 2.61 (t, J = 7.7 Hz, 2 H), 2.16 (s, 3 H); **^{13}C NMR** (CD$_3$OD, 125 MHz, δ): 173.3, 168.3, 136.6, 136.1, 128.8, 120.2, 51.6, 35.7, 30.4, 24.5; **IR** (microscope, cm^{-1}): 3282 (s), 3247 (s), 3186 (m), 3121 (m), 3070 (m), 2988 (m), 2948 (m), 2857 (w), 1732 (s), 1660 (s), 1605 (s), 1553 (s), 1516 (s), 1444 (m), 1371 (m), 1235 (m), 1201 (s), 1178 (s), 1159 (m), 1125 (m); **HRMS** (ESI) for $C_{12}H_{15}NO_3$ [M+Na]$^+$: calcd. 244.0944; found 244.0949.
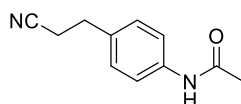
***N*-[4-(2-Cyanoethyl)phenyl]acetamide (2-10d):** Prepared from 3-(4-acetylphenyl)propionitrile oxime **2-9d** (94 mg, 0.50 mmol) using the general procedure. Purified by flash chromatography (2:1 hexane/acetone) and isolated as a yellow solid (with **BA-41**: 79 mg, 83%; with **BA-42:** 87 mg, 92%). **Mp** 60–62 °C; **^{1}H NMR** (CD$_3$OD, 500 MHz, δ): 7.49 (d, J = 8.6 Hz, 2 H), 7.22 (d, J = 8.6 Hz, 2 H), 2.89 (t, J = 7.2 Hz, 2 H), 2.70 (t, J = 7.2 Hz, 2 H), 2.10 (s, 3 H); **^{13}C NMR** (CD$_3$OD, 125 MHz, δ): 171.6, 138.8, 135.8, 129.8, 121.4, 120.7, 31.9, 23.8, 19.6; **IR** (microscope, cm^{-1}): 3309 (s), 3268 (m), 3198 (m), 3133 (m), 3077 (w), 3005 (w), 2945 (w), 2868 (w), 2808 (w), 2243 (m), 1664 (s), 1609 (s), 1541 (s), 1515 (s), 1446 (m), 1412 (s), 1373 (m), 1322 (s), 1269 (m), 1235 (m), 1200 (w), 1049 (w); **HRMS** (ESI) for C$_{11}$H$_{12}$N$_2$O [M+Na]$^+$: calcd. 211.0842; found 211.0845.

2.8.4 Synthesis and Characterization of Oxime Ester 2-3a
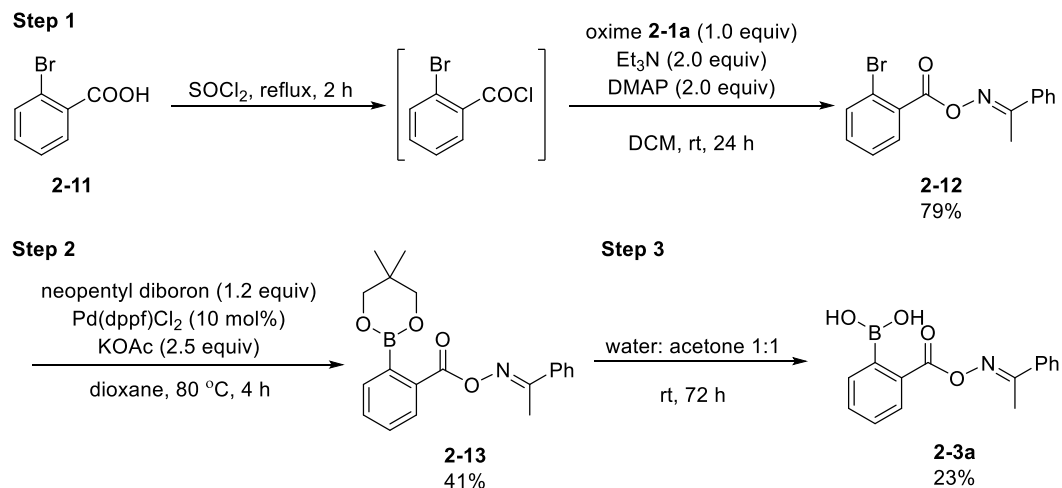
Step 1: To a flame-dried 15 mL round bottom flask was added 2-bromo benzoic acid (8.04 mg, 4.00 mmol) and 4 mL SOCl$_2$. The mixture was brought up to reflux for 2 h under nitrogen. After the indicated time, the reaction was cooled down to room temperature before the removal of excess SOCl$_2$ by vacuum. The resulting crude 2-bromo benzoyl chloride was dissolved in 5 mL of DCM and used without further

purification. To another flame-dried 25 mL round bottom flask charged with triethylamine (816 mg, 8.06 mmol) and DMAP (976 mg, 7.99 mmol) in 15 mL DCM was added the oxime **2-1a** (406 mg, 3.00 mmol) in one-pot. The reaction mixture was cooled down to 0 °C and allowed to stir for 10 min. To the oxime solution was added 2-bromo benzoyl chloride solution carefully over a period of 15 min using a syringe. The reaction was warmed up to room temperature and stirred overnight. The crude 2-bromo benzoate **2-12** was obtained after the removal of DCM. The pure product was isolated by flash column chromatography (40:1 to 10:1 hexanes:EtOAc) and isolated as a white solid (755 mg, 79%).

Step 2: To a flame-dried 15 mL round bottom flask with a stir bar was added Pd(dppf)Cl$_2$ (146 mg, 0.200 mmol), neopentyl diboron (542 mg, 2.40 mmol), and KOAc (491 mg, 5.00 mmol) in 12 mL freshly distilled dioxane under nitrogen. Upon stirring, a solution of the bromo benzoate **2-12** (636 mg, 2.00 mmol) in dioxane (4 mL) from Step 1 was added dropwise via a syringe. After the addition, the reaction mixture was allowed to heat up to 80 °C and stirred for 4 h. Upon cooling down to room temperature, the crude mixture was extracted with EtOAc (2 × 20 mL). The combined organic layers were washed by water (1 × 20 mL) and brine (1 × 20 mL), dried over anhydrous MgSO$_4$, filtered, and concentrated. The boronic ester product **2-13** was isolated by flash column chromatography (10:1 to 3:1 hexanes:EtOAc) and isolated as an off-white solid (282 mg, 40%).

(*E*)-1-Phenylethan-1-one-*O*-(2-(5,5-dimethyl-1,3,2-dioxaborinan-2-yl)benzoyl) oxime (2-13): **Mp** 78–79 °C; **^{1}H NMR** (CDCl$_3$, 500 MHz, δ): 7.99 (d, *J* = 7.8 Hz, 1 H), 7.81 (d, *J* = 6.9 Hz, 2 H), 7.57 (app dt, *J* = 14.6, 7.1 Hz, 2 H), 7.49–7.38 (m, 4 H), 3.81 (s, 4 H), 2.51 (s, 3 H), 1.09 (s, 6 H); **^{13}C NMR** (CDCl$_3$, 125 MHz, δ): 166.0, 163.8, 134.9, 132.3, 132.1, 131.8, 130.6, 128.6, 128.5, 128.4, 127.3, 72.5, 31.8, 22.1, 14.9 (The boron-bound carbon was not detected due to quadrupolar relaxation of boron); **^{11}B NMR** (CDCl$_3$, 160 MHz, δ): 28.3; **IR** (microscope, cm^{-1}): 3012 (w), 2963 (w), 2929 (m), 2885 (m), 1725 (s), 1689 (w), 1565 (w), 1472 (m), 1314 (s), 1253 (s), 1130 (s), 1065 (m); **HRMS** (ESI) for C$_{20}$H$_{22}$BNO$_4$Na [M+Na]$^+$: calcd. 374.1534; found 374.1532.

Step 3: In a 15 mL round bottom flask charged with a stir bar, a solution of the boronic ester **2-13** (282 mg, 0.803 mmol) from Step 2 in a solvent mixture of water:acetone (v:v = 1:1, 0.1 M) was prepared. The reaction was allowed to stir at room temperature for 72 h before removal of acetone by vacuum. The aqueous layer was extracted with EtOAc (3 × 10 mL). The combined organic layers were washed with water (6 × 10 mL) and brine (1 × 10 mL), dried over anhydrous MgSO$_4$, filtered, and concentrated. The pure boronic acid was obtained after recrystallization from 3:1 hexanes:DCM) and isolated as a white solid (52 mg, 23%)

(***E***)-(2-(((((1-Phenylethylidene)amino)oxy)carbonyl)phenyl)boronic acid (**2-3a**): **Mp** decomposed upon heating; **¹H NMR** (CD$_3$COCD$_3$ + 1 drop D$_2$O, 500 MHz, δ): 8.03 (d, *J* = 7.7 Hz, 1 H), 7.87 (dd, *J* = 8.1, 1.5 Hz, 2 H), 7.65–7.54 (m, 2 H), 7.52–7.41 (m, 4 H), 2.54 (s, 3 H); **¹³C NMR** (CD$_3$COCD$_3$ + 1 drop D$_2$O, 125 MHz, δ): 165.9, 164.1, 136.1, 133.2, 132.9, 132.8, 131.4, 129.8, 129.5, 129.1, 127.9, 14.7 (The boron-bound carbon was not detected due to quadrupolar relaxation of boron); **¹¹B NMR** (CD$_3$COCD$_3$ + 1 drop D$_2$O, 160 MHz, δ): 30.1; **IR** (microscope, cm^{-1}): 3423 (w), 3064 (m), 3023 (m), 2930 (w), 2855 (w), 1718 (s), 1596 (m), 1443 (m), 1314 (s), 1268 (s), 1124 (m), 1045 (s), 912 (s); **HRMS** (ESI) for C$_{15}$H$_{13}$BNO$_4$ [M–H]$^-$: calcd. 282.0943; found 282.0943.

2.8.5 Kinetic Profile Analysis
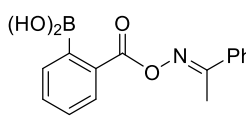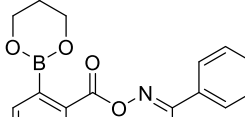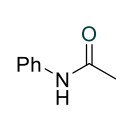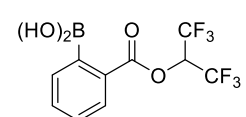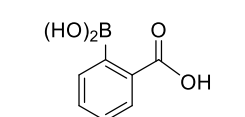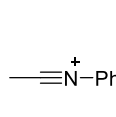
2.8.5.1 The Rearrangement of Oxime Ester 2-3a
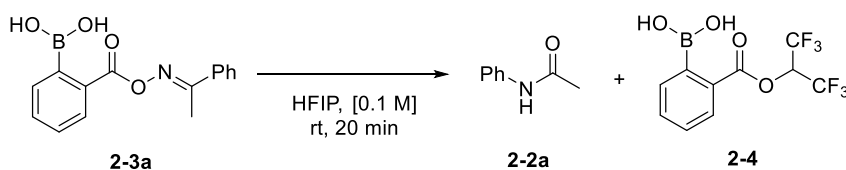
Oxime ester **2-3a** (4.2 mg, 0.015 mmol) was dissolved in 0.15 mL HFIP and stirred at room temperature for 20 min. A 5 μL aliquot was collected and quenched in 1 mL of acetonitrile each minute for 20 min. The aliquots were subjected to LC-MS for analysis. The amount of each compound was determined by the area of their

absorption peak at 254 nm on their respective elution time obtained from MassHunter Analytical Studio Reviewer. The results are given in Table 2-3.

Table 2-3 LC-MS Standard for the Compounds of Interest

compound	retention time	molecular ion	*m/z*
2-3a	4.7 min	[M+H]$^+$	284.1
2-13	5.0 min	[M of **2-13a**+H]$^{+\,a}$	284.1
2-1a	0.9 min	[M+H]$^+$	136.2
2-4	4.9 min	[M–H]$^-$	315.0
BA-40	0.8 min	[M–OH]$^+$	149.1
nitrilium	(no standard)	expected [M]$^+$	118.1

[a]Boronic ester **2-13** was hydrolyzed to boronic acid **2-3a** under the LC-MS conditions

2.8.5.2 The Rearrangement of Oxime Ester 2-3i with or without Oxime
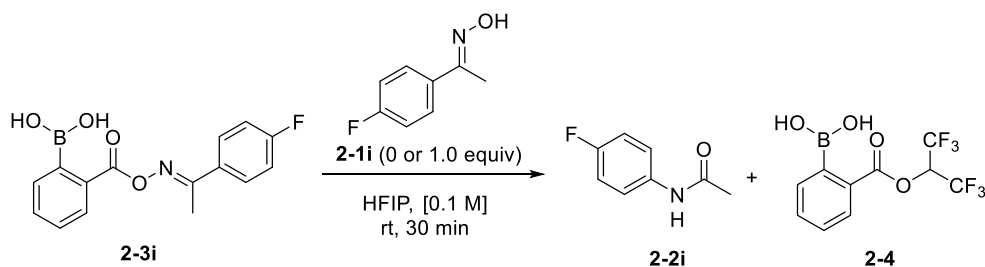
Oxime ester **2-3i** (4.5 mg, 0.015 mmol) with and without oxime **2-1i** (2.3 mg, 0.015 mmol) were dissolved in 0.15 mL HFIP and stirred at room temperature for 30 min. A 5 μL aliquot was collected and quenched with 1 mL of acetonitrile over the 30 min. The aliquots were subjected to LC-MS for analysis. The amount of each compound was determined by the area of their absorption peak at 254 nm on their respective elution time obtained from MassHunter Analytical Studio Reviewer.

2.8.5.3 Procedure for the Control Experiment of HFIP Ester 2-4
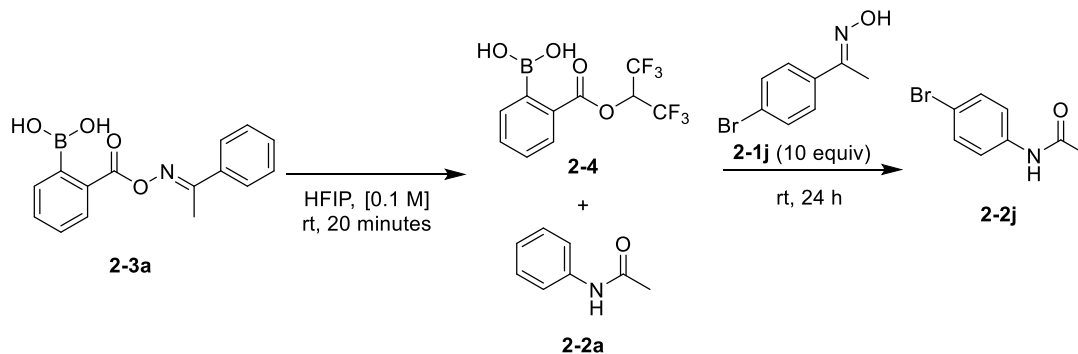
Oxime ester **2-3a** (4.2 mg, 0.015 mmol) was dissolved in 0.15 mL HFIP and stirred at room temperature for 20 min. After the indicated time, oxime **2-1j** (32 mg, 0.15 mmol) was added to the reaction mixture. The reaction was stirred at room temperature another 24 h. A 5 μL aliquot was collected and quenched with 1 mL of acetonitrile a few times over the course of 24 h. The aliquots were subjected to LC-MS and analyzed MassHunter Analytical Studio Reviewer.

2.8.6 ^{18}O-Labeling Studies

2.8.6.1 Synthesis of ^{18}O-Labeled Oxime and Boronic Ester 2-13*
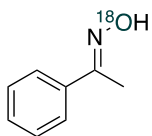
[^{18}O]-Acetophenone oxime (2-1a*): ^{18}O-labeled acetophenone oxime was prepared from acetophenone (0.8 mL, 6.9 mmol) according to the literature procedure of Bode and co-workers[31] and was isolated as a white solid (179 mg, 19%). **HRMS** (ESI) for $C_8H_9N^{18}O$ [M+H]$^+$: calcd 138.0799; found 138.0801. Mass spectral analysis found 65% [18]O isotopic incorporation using SIM mode in LC-MS.
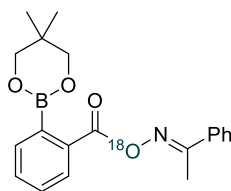
[¹⁸O]-(*E*)-1-Phenylethan-1-one *O*-(2-(5,5-dimethyl-1,3,2-dioxaborinan-2-yl)benzoyl) oxime (2-13*): Prepared from 2-bromo benzoic acid (302 mg, 1.50 mmol) and oxime **2a*** (165 mg, 1.20 mmol) using the procedure, Step 1 and 2 in Section 2.8.4. The crude product was purified by flash column chromatography (10:1 to 3:1 hexanes:EtOAc) and isolated as an off-white solid (83 mg, 24 % for Step 2). **HRMS** (ESI) for $C_{20}H_{22}BNO_3{}^{18}ONa$ [M+Na]$^+$: calcd 376.1573; found 376.1577. Mass spectral analysis found 51% ^{18}O isotopic incorporation using SIM mode in LC-MS.

2.8.6.2 Evaluation of Reaction Condition for the Rearrangement with Boronic Ester 2-13
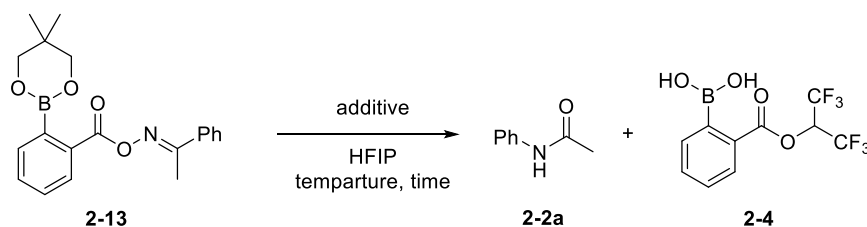
Boronic ester **2-13** (5.3 mg, 0.015 mmol) was dissolved in 0.15 mL HFIP with or without additive. The reaction mixture was stirred at the indicated temperature for about 5 to 24 h. A 5 μL aliquot was collected and quenched in 1 mL of acetonitrile a few times over the course of the reactions. The aliquots were subjected to LC-MS and analyzed MassHunter Analytical Studio Reviewer. The results were summarized in Table 2-4.

Table 2-4 Results from the Mechanistic Studies with LC-MS.

entry	temperature	additive	observation
1	rt	–	no conversion after 16 h
2	50 °C	–	no conversion observed after 5 h
3	rt	perfluoropinacol (1 equiv)	low conversion after 20 h
4	rt	H_2O (10 equiv)	moderate conversion after 16 h
5	50 °C	H_2O (10 equiv)	full conversion after 6 h

2.8.6.3 The Rearrangement of ^{18}O-Labeled Boronic Ester 2-13*
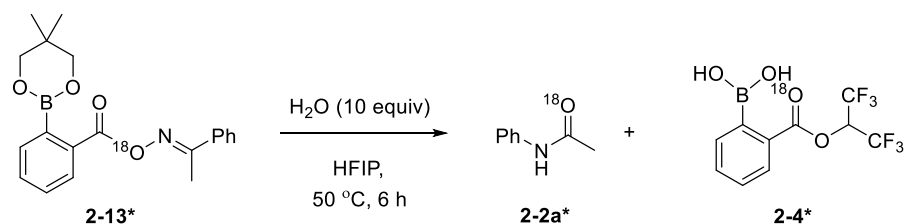
Boronic ester of **2-13*** (5.6 mg, 0.015 mmol) was dissolved in 0.15 mL of HFIP, and water (3 µL, 0.15 mmol) was added. The reaction mixture was stirred at 50 °C for 6 h. The reaction was monitored by LC-MS to ensure complete consumption of the starting material. An aliquot of 5 µL was obtained and quenched in acetonitrile every hour for LCMS analysis. The reaction was completed after 6 h, and the % incorporation of ^{18}O in **2-2a*** and **2-4*** were quantified using LC-MS SIM mode (Figure 2-8).
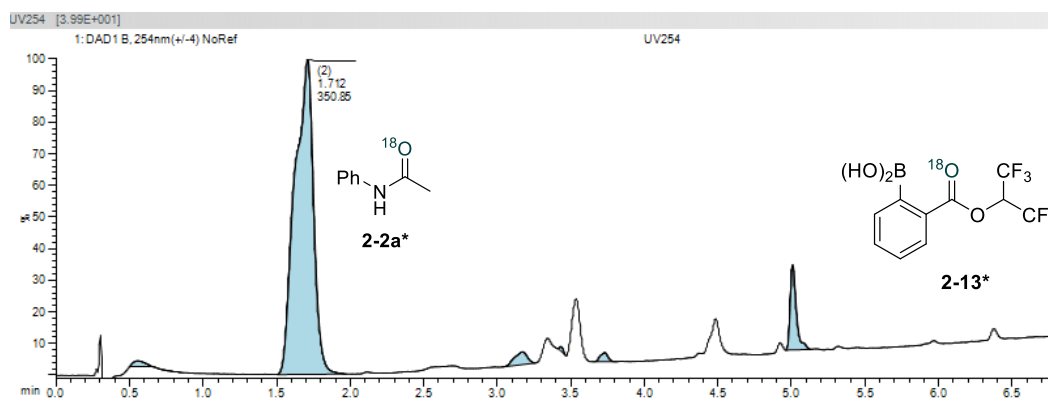
Figure 2-8 LC-MS spectrum at 254 nm of the reaction mixture at 6 h.

2.8.6.4 Control Analysis of 2-Carboxyphenylboronic Acid BA-40
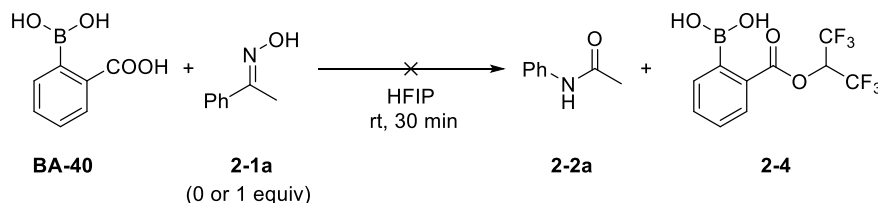
2-Carboxyphenylboronic acid (**BA-40**) (2.5 mg, 0.015 mmol) with or without oxime **2-1a** (2.0 mg, 0.015 mmol) was dissolved in 0.15 mL HFIP. A 5 µL aliquot was

diluted in acetonitrile after 30 min and analyzed by LC-MS. **BA-40** eluted out from the column at 0.6 min and was detected at 200 nm as [M–H$_2$O–H]$^-$, m/z = 147.1. No detectable amount of HFIP ester **2-4** was observed with or without oxime (Figure 2-9).
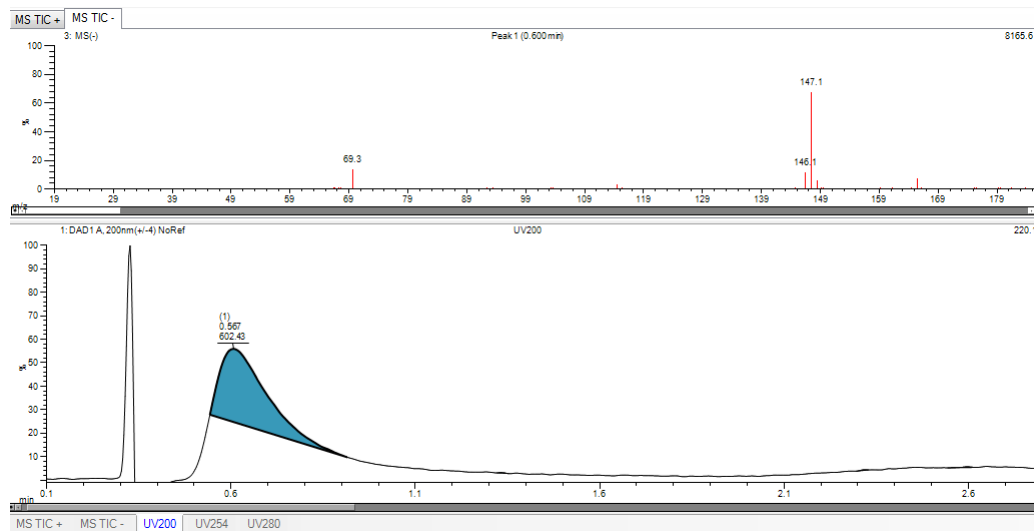
Figure 2-9 LC-MS spectrum at 200 nm of boronic acid **BA-40** in HFIP.

2.8.7 Investigations of Bronsted Acid-Catalyzed Mechanism

2.8.7.1 General Procedure for the Beckmann Rearrangement using the Co-Catalytic BA-17/A-1 System
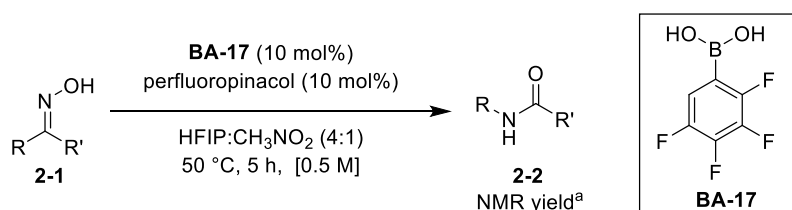
To a 5 mL reaction vial charged with a stir bar was added the oxime substrate **2-1** (0.50 mmol), boronic acid **BA-17** (9.7 mg, 0.050 mmol), and perfluoropinacol (17 mg, 0.050 mmol). A solvent mixture of nitromethane and hexafluoroisopropanol (1:4, 0.5 mL) was added. The reaction vial was capped, sealed, and stirred at 50 °C for 5 h. The crude product was obtained after removal of solvent. 1,4-Dinitrobenzene (21.0 mg, 0.125 mmol) was added as an internal standard, and yields were determined by crude ^{1}H NMR analysis.

2.8.7.2 Procedure of the Beckmann Rearrangement under Anhydrous Conditions
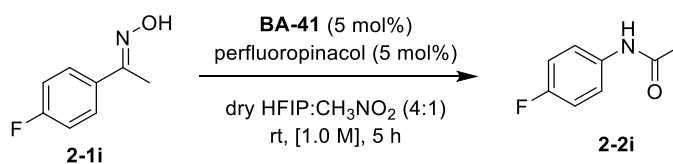
To a flame dried 5 mL reaction flask charged with a stir bar was added the oxime substrate **2-1i** (77 mg, 0.50 mmol), boronic acid **BA-41** (4.5 mg, 0.025 mmol), and perfluoropinacol (8.4 mg, 0.025 mmol). A solvent mixture of 1:4 dry nitromethane (distilled from MgSO$_4$) and hexafluoroisopropanol (distilled and dried over 3 Å molecular sieves) (0.5 mL) was added. The reaction vial was capped, sealed, and left at the room temperature for 24 h. The crude product was obtained after removal of the solvent. The pure amide product was isolated after flash column chromatography using the indicated solvent mixtures. Note: for the reaction with molecular sieves, 100 mg of activated powdered 3 Å molecular sieves was added to the reaction flask before the flame-drying.

2.8.8 Improved Synthesis of Boronic Acid BA-42
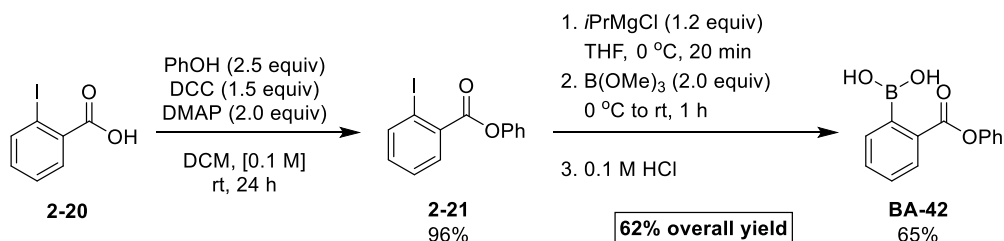
Phenyl 2-iodobenzoate (2-21): A mixture of 2-iodobenzoic acid **2-20** (496 mg, 2.00 mmol), phenol (468 mg, 4.97 mmol), DCC (608 mg, 2.95 mmol), and DMAP (489 mg, 4.00 mmol) was dissolved in DCM (20 mL). The reaction mixture was stirred at room temperature for 24 h, then it was washed with water (2 × 10 mL) and brine (1 × 10 mL). The organic layer was dried over MgSO$_4$, filtered, and concentrated in vacuo. The crude was purified by flash column chromatography (hexanes/EtOAc 20:1) to afford the title compound as a colourless oil (619 mg, 96%). **¹H NMR** (600 MHz, CDCl$_3$, δ) 8.07 (dd, J = 8.0, 1.2 Hz, 1 H), 8.04 (dd, J = 7.8, 1.7

Hz, 1 H), 7.49 (td, J = 7.6, 1.2 Hz, 1 H), 7.46–7.41 (m, 2 H), 7.33–7.25 (m, 3 H), 7.23 (td, J = 7.7, 1.7 Hz, 1 H). Spectral data agree with the literature.[45]

2-(Phenoxycarbonyl)phenylboronic acid (BA-42): To a flame dried flask under nitrogen, was added isopropylmagnesium chloride (0.60 mL, 1.2 mmol, 2 M solution in THF). The solution was diluted with 5 mL THF and cooled to 0 °C with an ice bath. Then, a solution of phenyl 2-iodobenzoate **2-21** (325 mg, 1.00 mmol) in 2 mL THF was added to the flask via a syringe and stirred for 20 min at 0 °C. After the indicated time, trimethylborate (0.23 mL, 2.0 mmol) was added at 0 °C. Then, the reaction flask was removed from the ice bath, and the reaction mixture was allowed to warm up to room temperature with stirring for 1 h. Next, the mixture was extracted with 0.1 M HCl (1 × 2 mL), water (1 × 5 mL) and brine (1 × 5 mL). The organic layer was dried over MgSO$_4$, filtered, and concentrated in vacuo. The crude was purified by crystallization from toluene to afford **BA-42** as beige solid (157 mg, 65%). **^{1}H NMR** (CD$_3$COCD$_3$ + 1 drop D$_2$O, 500 MHz, δ): 8.08 (ddd, J = 7.8, 1.0, 1.0 Hz, 1 H), 7.66–7.57 (m, 2 H), 7.50 (ddd, J = 7.8, 6.6, 2.2 Hz, 1 H), 7.47–7.41 (m, 2 H), 7.30 (d, J =1.2 Hz, 1 H), 7.30–7.20 (m, 3 H); **^{11}B NMR** (CD$_3$COCD$_3$ + 1 drop D$_2$O, 160 MHz, δ): 30.0. Spectral data agree with that obtained by Xiaobin Mo.

2.9 References

(1) Boyes, R. N.; Scott, D. B.; Jebson, P. J.; Godman, M. J.; Julian, D. G. *Clin. Pharmacol. Ther.* **1971**, *12*, 105–116.
(2) O'Connor, S. E.; Brown, R. A. *Vasc. Pharmacol.* **1982**, *13*, 185–193.
(3) Balfour, J. A.; Goa, K. L. *Drugs* **1991**, *42*, 511–539.
(4) Ritz, J.; Fuchs, H.; Kieczka, H.; Moran, W. C. Caprolactam. In *Ullmann's Encyclopedia of Industrial Chemistry*, **2011**.
(5) Gabara, V. High-Performance Fibers. In *Ullmann's Encyclopedia of Industrial Chemistry*; **2016**, 1–22.
(6) Santos, A. S.; Silva, A. M. S.; Marques, M. M. B. *Eur. J. Org. Chem.* **2020**, 2501–2516.
(7) Beckmann, E. *Ber. Dtsch. Chem. Ges.* **1886**, *19*, 988–993.
(8) Aguilar, D. a; Fritch, J. R.; Fruchey, O. S.; Hilton, C. B.; Horlenko, T.; Seeliger, W. J.; Snyder, P. S. Production of Acetaminophen. US5155273A, October 13, 1992.
(9) Yamabe, S.; Tsuchida, N.; Yamazaki, S. *J. Org. Chem.* **2005**, *70*, 10638–10644.
(10) Gawley, R. E. The Beckmann Reactions: Rearrangements, Elimination–Additions, Fragmentations, and Rearrangement–Cyclizations. In *Organic Reactions*, **2004**, 1–420.
(11) Kaur, K.; Srivastava, S. *New J. Chem.* **2020**, *44*, 18530–18572.
(12) Furuya, Y.; Ishihara, K.; Yamamoto, H. *J. Am. Chem. Soc.* **2005**, *127*, 11240–11241.
(13) Zhu, M.; Cha, C.; Deng, W.-P.; Shi, X.-X. *Tetrahedron Lett.* **2006**, *47*, 4861–4863.
(14) Pi, H.-J.; Dong, J.-D.; An, N.; Du, W.; Deng, W.-P. *Tetrahedron* **2009**, *65*, 7790–7793.

(15) Hashimoto, M.; Obora, Y.; Sakaguchi, S.; Ishii, Y. *J. Org. Chem.* **2008**, *73*, 2894–2897.

(16) Vanos, C. M.; Lambert, T. H. *Chem. Sci.* **2010**, *1*, 705–708.

(17) Augustine, J. K.; Kumar, R.; Bombrun, A.; Mandal, A. B. *Tetrahedron Lett.* **2011**, *52*, 1074–1077.

(18) Gao, Y.; Liu, J.; Li, Z.; Guo, T.; Xu, S.; Zhu, H.; Wei, F.; Chen, S.; Gebru, H.; Guo, K. *J. Org. Chem.* **2018**, *83*, 2040–2049.

(19) Chapman, A. W. *J. Chem. Soc.* **1935**, 1223–1229.

(20) An, N.; Tian, B.-X.; Pi, H.-J.; Eriksson, L. A.; Deng, W.-P. *J. Org. Chem.* **2013**, *78*, 4297–4302.

(21) Tian, B.-X.; An, N.; Deng, W.-P.; Eriksson, L. A. *J. Org. Chem.* **2013**, *78*, 6782–6785.

(22) Chandrasekhar, S.; Gopalaiah, K. *Tetrahedron Lett.* **2002**, *43*, 2455–2457.

(23) Ricardo, C. L.; Mo, X.; McCubbin, J. A.; Hall, D. G. *Chem. Eur. J.* **2015**, *21*, 4218–4223.

(24) Mo, X.; Yakiwchuk, J.; Dansereau, J.; McCubbin, J. A.; Hall, D. G. *J. Am. Chem. Soc.* **2015**, *137*, 9694–9703.

(25) Colomer, I.; Chamberlain, A. E. R.; Haughey, M. B.; Donohoe, T. J. *Nat Rev Chem* **2017**, *1,* article number 0088.

(26) Pereira, M.; Santos, P. *The Chemistry of Hydroxylamines, Oximes, and Hydroxamic Acids* **2009**, 343–498.

(27) Pozhydaiev, V.; Power, M.; Gandon, V.; Moran, J.; Lebœuf, D. *Chem. Commun.* **2020**, *56*, 11548–11564.

(28) Kuhara. *Mem. Coll. Sci. Eng. Kyoto Imp. Univ.* **1906**, *1*, 254.

(29) Blatt, A. H. *Chem. Rev.* **1933**, *12*, 215–260.

(30) Yuen, A. K. L.; Hutton, C. A. *Tetrahedron Lett.* **2005**, *46*, 7899–7903.

(31) Pusterla, I.; Bode, J. W. *Angew. Chem. Int. Ed.* **2012**, *51*, 513–516.

(32) Zhang, S.; Lebœuf, D.; Moran, J. *Chem. Eur. J.* **2020**, *26*, 9883–9888.

(33) Ang, H. T.; Rygus, J. P. G.; Hall, D. G. *Org. Biomol. Chem.* **2019**, *17*, 6007–6014.

(34) Wang, H.; Xu, J.; Yang, Q.; Zhang, H.; Zhao, S. Method for Preparing Tert-Butoxycarbonyl Phenylboronic Acid. CN105017301A, November 4, 2015.

(35) Fattahi, N.; Ayubi, M.; Ramazani, A. *Tetrahedron* **2018**, *74*, 4351–4356.

(36) Dhaon, M. K.; Olsen, R. K.; Ramasamy, K. *J. Org. Chem.* **1982**, *47*, 1962–1965.

(37) Neises, B.; Steglich, W. *Angew. Chem. Int. Ed.* **1978**, *17*, 522–524.

(38) Fitzjarrald, V. P.; Pongdee, R. *Tetrahedron Lett.* **2007**, *48*, 3553–3557.

(39) Molander, G. A.; Trice, S. L. J.; Kennedy, S. M.; Dreher, S. D.; Tudge, M. T. *J. Am. Chem. Soc.* **2012**, *134*, 11667–11673.

(40) Wang, X.; Sun, X.; Zhang, L.; Xu, Y.; Krishnamurthy, D.; Senanayake, C. H. *Org. Lett.* **2006**, *8*, 305–307.

(41) Wang, Z.; Tang, J.; Salomon, C. E.; Dreis, C. D.; Vince, R. *Bioorg. Med. Chem.* **2010**, *18*, 4202–4211.

(42) Lafontaine, J. A.; Day, R. F.; Dibrino, J.; Hadcock, J. R.; Hargrove, D. M.; Linhares, M.; Martin, K. A.; Maurer, T. S.; Nardone, N. A.; Tess, D. A. *Bioorg. Med. Chem. Lett.* **2007**, *17*, 5245–5250.

(43) Bair, K.; Baumeister, T.; Buckmelter, A.; Clodfelter, K.; Dragovich, P.; Gosselin, F.; Han, B.; Lin, J.; Reynolds, D. J.; Roth, B.; Smith, C.; Wang, Z.; Yuen, P.-W.; Zheng, X. Novel Compounds and Compositions for the Inhibition of Nampt, March 8, 2012.

(44) Beyer, T. A.; Chambers, R. J.; Lam, K.; Li, M.; Morrell, A. I.; Thompson, D. D. Pyrido[2,3-D]Pyrimidine-2,4-Diamines as Pde 2 Inhibitors. WO2005061497 (A1), July 7, 2005.

(45) Liu, Z.; Larock, R. C. *Org. Lett.* **2004**, *6*, 99–102.

CHAPTER 3

Two-Component Boronic Acid Catalysis for Increased Reactivity in Challenging Friedel–Crafts Alkylations with Deactivated Benzylic Alcohols[‡]

3.1 Introduction

Unsymmetrical diarylmethanes, along with diaryl- and triaryl-alkanes, are a common motif found in the structure of numerous pharmaceutical agents and biologically active natural products,[1] such as lasofoxifene,[2] tolterodine,[3] pimozide,[4] and peperomin B[5] (Figure 3-1). Moreover, in addition to being the structural core of active pharmaceutical agents, triarylmethanes also are a basic motif of many fluorescent organic molecules. The photochemical and photophysical properties of triarylmethanes, along with their applications in various fields, have been studied extensively.[6] Therefore, methods for the facile preparation of these motifs from simple starting materials are desired.

lasofoxifene
(selective estrogen receptor modulator, treatment of osteoporosis)

tolterodine
(antimuscarinic, for urinary incontinence)

pimozide
(antipsychotic, treatment of delusional disorder)

peperomin B
(anti-inflammatory agent)
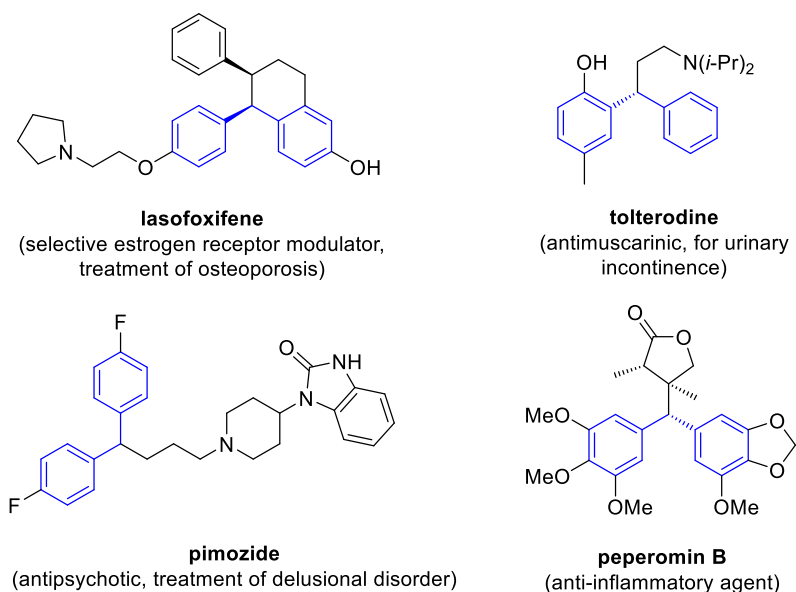
Figure 3-1 Selected examples of biologically active compounds containing a diarylalkane motif.

While numerous synthetic methods have been reported for the construction of such motifs, namely, various transition metal-catalyzed cross-coupling reactions,[7] Friedel–Crafts alkylation chemistry prevails as the most widely used approach because it is operationally simple and does not require the use of expensive and often toxic heavy metal catalysts. Friedel–Crafts alkylation grants rapid access to these compounds from readily available arenes and benzylic electrophiles.[8] Yet, the classical alkylation, invented by Charles Friedel and James Mason Crafts in 1877, uses reactive benzyl halides as starting materials and often requires a stoichiometric amount of a strong Lewis acid as an activator for the reaction.[9] Moreover, the reaction generates irritating haloacid gas (HX) as a by-product (Scheme 3-1). These drawbacks highly limit the practicality of this powerful transformation, mainly in terms of atom-economy and environmental friendliness. Thus, a 'greener' and catalytic Friedel–Crafts alkylation system using benign electrophiles would be greatly beneficial.
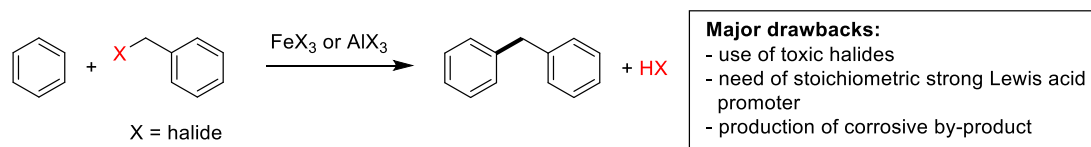
Scheme 3-1 Classic Friedel–Crafts alkylation with benzyl halides and the major drawbacks.

In this regard, direct catalytic benzylation of arenes using readily available benzylic alcohols is highly advantageous due to: (a) their lower toxicity as compared to benzylic halides and (b) the generation of water as the only by-product in the reaction. Not surprisingly, the development of direct catalytic hydroxy group activation for Friedel–Crafts alkylation has drawn significant focus over the past decade, and several strategies using strong Lewis and Brønsted acids as catalysts have been reported (Scheme 3-2). The first catalytic Friedel–Crafts alkylation using benzylic alcohols was disclosed by Fukuzawa and co-workers in 1996 using $Sc(OTf)_3$ as a Lewis acid catalyst.[10] Following this report, other rare earth metal triflates, such as $Gd(OTf)_3$, $Hf(OTf)_3$ and $Yb(OTf)_3$, also were identified as effective Lewis acid catalysts.[11–13]

In 2005, different transition metal chlorides were evaluated by Beller and co-workers for the direct catalytic activation of benzylic alcohols and acetates in Friedel–Crafts alkylation.[14–16] Among all the transition metal Lewis acids tested, IrCl$_3$, H$_2$[PtCl$_6$], HAuCl$_4$, AuCl$_3$, and FeCl$_3$ exhibited excellent catalytic activities.[14–16] In the same year, Roy and co-workers reported the use of a cooperative heterobimetallic catalytic system using [Ir(COD)Cl]$_2$ and SnCl$_4$ to promote Friedel–Crafts alkylation with π-activated alcohols.[17] Later in 2007, NbCl$_5$ also was discovered by Srihari and co-workers as an efficient Lewis acid catalyst.[18] More recently, Floreancig and co-workers demonstrated the use of Re$_2$O$_7$ as an efficient catalyst in the Friedel–Crafts alkylation with benzylic alcohols. Mechanistic studies revealed that Re$_2$O$_7$ is a pre-catalyst for HOReO$_3$ and that the activation of alcohols occurs through the formation of a perrhenate ester intermediate (–OReO$_3$), which is a superior leaving group to halides (Scheme 3-2C).[19] Aside from the expensive and toxic lanthanides and transition metals, a number of main group metal complexes, such as Bi(OTf)$_3$,[20] InCl$_3$,[21,22] Ca(NTf$_2$)$_2$,[23] also were identified as effective catalysts for Friedel–Crafts alkylation with π-activated alcohols.
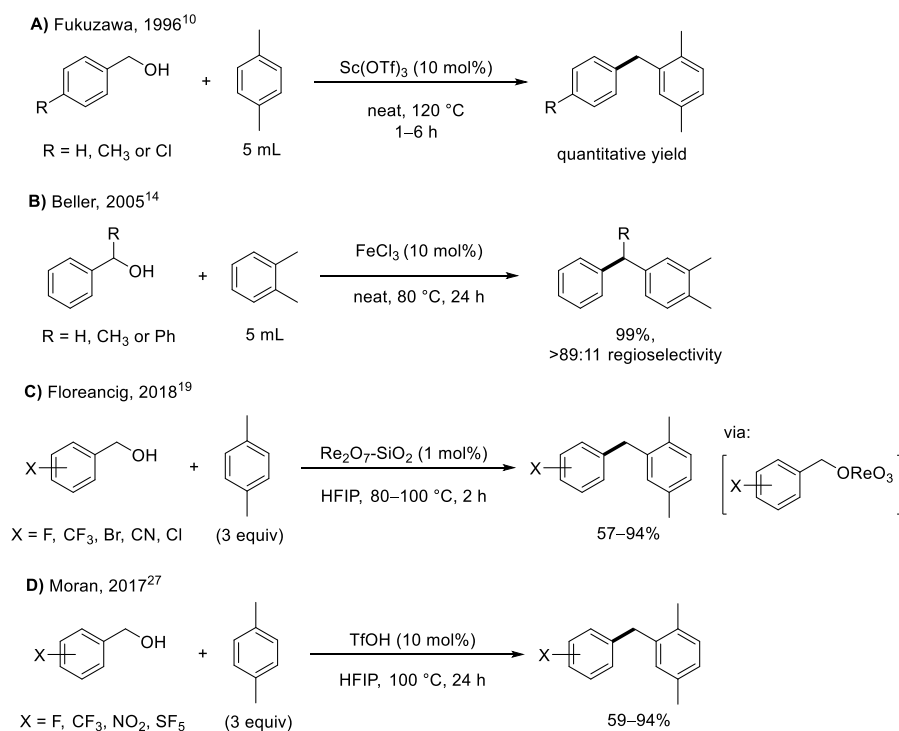
Scheme 3-2 Selected examples of direct catalytic Friedel–Crafts alkylation with benzylic alcohols.

Due to increased environmental awareness and economical concerns, there has been a growing interest in the development of metal-free reactions. The metal-free catalytic systems for the direct Friedel–Crafts alkylation with benzylic alcohols were realized by using molecular iodine[24] as well as some Brønsted acids (TsOH or TfOH).[25–27] Furthermore, a reusable heterogeneous Brønsted acid catalyst based on montmorillonite (mont), a layered hydrophilic clay with ion-exchangeable ability, was developed by Kaneda and co-workers in 2007.[28] It is noteworthy that Paquin and co-workers also reported a non-catalytic metal-free direct Friedel–Crafts alkylation with benzylic alcohols using XtalFluor-E ($[Et_2NSF_2]BF_4$), a stable deoxofluorinating agent.[29]

Although significant progress has been made in the direct catalytic Friedel–Crafts alkylation with benzylic alcohols as benzylic halide surrogates, several limitations remain. Aside from the use of rare, toxic, and expensive metal catalysts in some of the protocols, harsh reaction conditions, including high temperatures (>100 °C) and the use of a large excess of arenes as reaction solvents, generally are required to promote the transformation, which leads to poor functional group tolerability. Furthermore, most of these protocols often are limited to highly activated or electron-rich arene and benzylic alcohol substrates. While this limitation was resolved partially by Moran and co-workers as well as Floreancig and co-workers (Scheme 3-2C and D), where they reported TfOH and Re_2O_7, respectively, as effective catalysts in Friedel–Crafts alkylation with highly electron-deficient benzylic alcohols and neutral arenes using HFIP as solvent, these protocols still required the use of high temperatures and strong acids.[19,27] Therefore, there remains a need for a mild catalytic system with a broader scope, such as acid-sensitive or electron-poor alcohols and arenes.

In this context, boronic acid catalysis (BAC) has emerged as a mild and 'greener' method for direct activation of hydroxy groups.[30,31] In BAC, the C–O bond of alcohols can be activated through a reversible interaction with a boronic acid. Coordination of the hydroxy group with the boron center leads to facile ionization of the C–O bond, which generates a carbocation susceptible to nucleophilic attack to

fashion the desired product and release water as the only by-product (Scheme 3-3). Furthermore, many arylboronic acids are commercially available or can be prepared readily, and they are, generally, shelf stable crystalline solids that are easy to handle,[32] thus making them great candidates for catalysis.
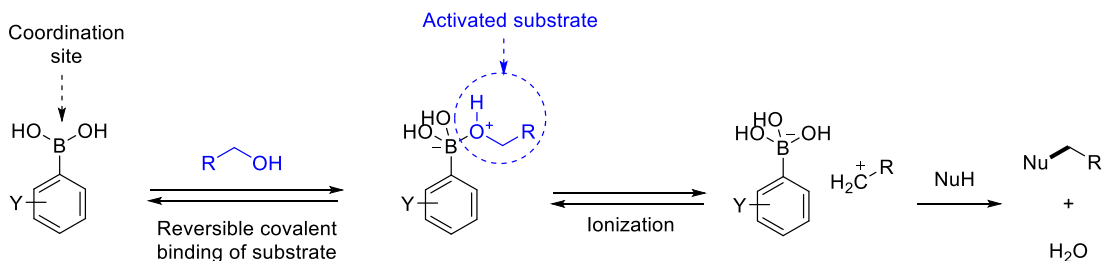
Scheme 3-3 Proposed activation of alcohol C–O bonds by boronic acids.

Indeed, several boronic acid-catalyzed direct Friedel–Crafts alkylation reactions of π-activated alcohols with arenes were developed in the past decade. McCubbin and co-workers, in 2010, established the first example of such a reaction using highly Lewis acidic pentafluorophenylboronic acid (**BA-16**) to effect the ionization of π-activated allylic alcohols.[33] However, this method is limited to strongly activated allylic alcohols and highly electron-rich arenes as suitable starting materials. In 2015, the Hall group disclosed the use of 2,3,4,5-tetrafluorophenyl-boronic acid (**BA-17**) as a more effective catalyst for the direct allylation of arenes.[34] This method reached a major limitation when primary benzyl alcohols were employed, as only moderate yields of the corresponding diarylmethane products were obtained (Scheme 3-4A). The poor reactivity of catalyst **BA-17** toward primary benzyl alcohols clearly limits its practicality for the synthesis of diarylmethane molecules. Gratifyingly, in the same year, the Hall group uncovered a highly effective direct Friedel–Craft alkylation reaction of primary benzylic alcohols and arenes using ferroceniumboronic acid hexafluoroantimonate salt (**BA-20**) as a highly active catalyst (Scheme 3-4B).[35] Although many primary benzylic alcohols containing moderately electron-withdrawing substituents were successful, the most highly electron-deficient benzylic alcohols were poor substrates for this reaction, even at elevated temperature. Presumably, this limitation is caused by an increase in the

barrier to C–O bond activation arising from destabilization of the resulting carbocation intermediate.
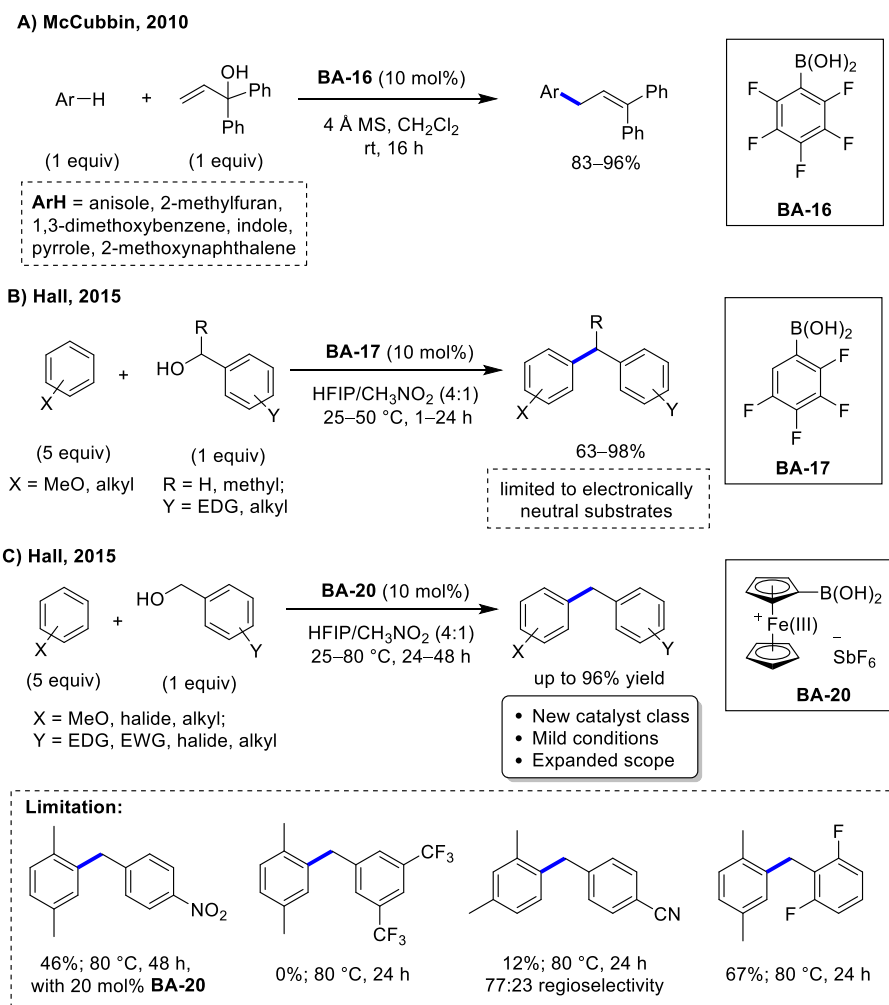
Scheme 3-4 Boronic acid-catalyzed Friedel–Crafts reaction with alcohols and its limitations.

Because the BAC systems developed by the Hall group employ hexafluoroisopropanol (HFIP) as a co-solvent, it was suspected that ionization of the alcohol may proceed with the assistance of a transient, highly electrophilic mono- or di-(hexafluoroisopropoxy) boronic ester intermediate that is more Lewis acidic than the free boronic acid. Therefore, it seemed plausible to improve the reactivity of the BAC systems toward highly electron-deficient benzyl alcohols by utilizing a highly fluorinated diol co-catalyst to increase the Lewis acidity of the boronic acid catalysts through the formation of a cyclic boronic ester. The use of such a diol co-catalyst to

increase the reactivity of the boronic acid catalyst was demonstrated in Chapter 2 by using perfluoropinacol (**A-1**) in the boronic acid catalyzed Beckmann rearrangement (Scheme 3-5A).[36] Mechanistic studies, indeed, suggested that the activating effect of **A-1** occurs by the coordination of **A-1** with **BA-41** forming a more electrophilic boronic ester. Furthermore, Moran and co-workers have demonstrated the concept using oxalic acid as a powerful sub-stoichiometric co-catalyst in Friedel–Crafts chemistry.[37] As highlighted in Scheme 3-5B, the desired diarylmethane product was obtained in excellent yield under a short reaction time when oxalic acid was used in the reaction, while negligible product was observed when oxalic acid was excluded from the reaction. Hence, these studies strongly support the postulation of increased reactivity of boronic acid catalysts in Friedel–Crafts alkylation by using a suitable co-catalyst.
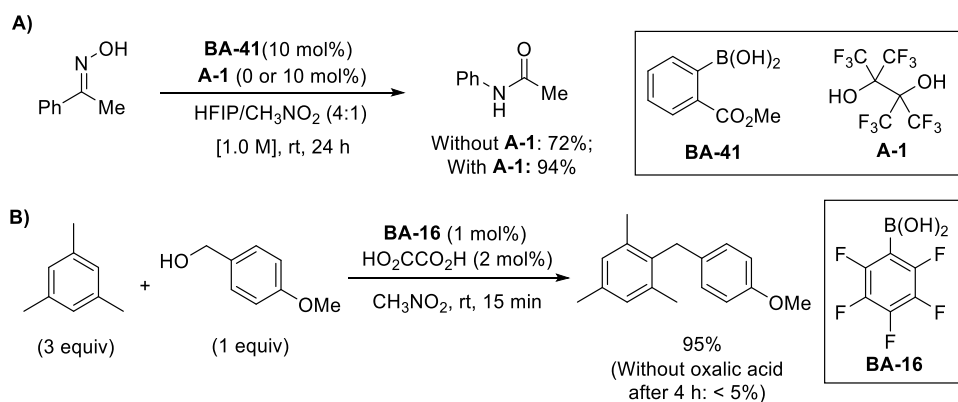
Scheme 3-5 A) Perfluoropinacol as a co-catalyst in Beckmann rearrangement in BAC; B) Oxalic acid as a co-catalyst in Friedel–Crafts alkylation in BAC.

3.2 Objective

Fascinated by the improved reactivity of boronic acid catalysts when perfluoropinacol (**A-1**) was used as a co-catalyst in the Beckmann rearrangement (see Chapter 2), it was envisioned that the boronic acid-catalyzed Friedel–Crafts alkylation using **BA-17** or **BA-20** could be improved further by using an activating diol co-catalyst, such as **A-1**. This chapter will discuss our efforts in a re-examination of the previously reported boronic acid-catalyzed Friedel-Crafts methodology and identification of a co-catalyst that could provide a two-component catalyst with increased reactivity

towards challenging substrates. Mechanistic studies also were performed to investigate the origin of the increased reactivity with the use of such a co-catalyst to provide insights for further possible improvement in other BAC reactions.

3.3 Reaction Development of Two-component Boronic Acid Catalysis for Increased Reactivity in Challenging Friedel–Crafts Alkylations

3.3.1 Screening of Potential Co-catalyst and Reaction Optimization

To discover an effective co-catalyst that would be synergic with the boronic acid catalyst, a small screening of co-catalysts was conducted. First, a primary benzylic alcohol, previously shown to be highly challenging in Friedel–Crafts alkylation, using catalyst **BA-20**, *p*-nitrobenzyl alcohol (**3-1a**),[35] was chosen as the model alcohol substrate. By using such a difficult alcohol substrate, any improvement in yield would be more obvious. Meanwhile, *p*-xylene (**3-2b**) was chosen as the arene nucleophilic partner in order to remove the possibility of regioisomer formation that would complicate analysis of the product yield. Based on the hypothesis that a more electrophilic boronic ester would result in increased reactivity of the boronic acid catalyst, a range of commercially available diols containing electron withdrawing components, such as highly fluorinated diols (**A-1**–**A-3**) and tetrabromocatechol (**A-4**), were selected for the screening. Oxalic acid (**A-5**) and 2,2-bis(trifluoromethyl)glycolic acid (**A-6**) also were included, as oxalic acid previously was shown to be an effective co-catalyst in Friedel–Crafts alkylation, as delineated in Scheme 3-4B above.

The efficacy of compounds **A-1**–**A-6** as potential co-catalysts was examined using the previously optimized reaction conditions in the Friedel–Craft alkylation of primary benzylic alcohols and arenes catalyzed by **BA-20** (Table 3-1).[35] In the absence of any co-catalyst, the desired diarylmethane product **3-3a** was observed in very low yield (entry 1). When 10 mol% of perfluoropinacol (**A-1**) was employed, a notable increase in yield occurred (entry 2). Other electron-deficient diols (**A-2**–**A-4**) tested not only failed to demonstrate a similar efficacy but also suppressed the reaction (entries 3–5). Oxalic acid (**A-5**), which was previously disclosed to be an

effective co-catalyst in the Friedel–Crafts alkylation,[37] unfortunately led to no improvement in yield (entry 6), whereas fluorinated α-hydroxy carboxylic acid **A-6** resulted in a large increase in yield (entry 7). To ensure that the improvement in yield was, in fact, due to the combination of BAC and co-catalyst rather than through the independent activation by the co-catalyst alone, control experiments were executed without catalyst **BA-20** (entries 8 and 9). Satisfactorily, no product formation was observed in both control experiments, thus showing that boronic acid catalyst **BA-20** is, indeed, an essential component for the reaction.

Table 3-1 Screening of Potential Co-catalysts for Improved Reactivity in Challenging Friedel–Crafts Alkylation[a]
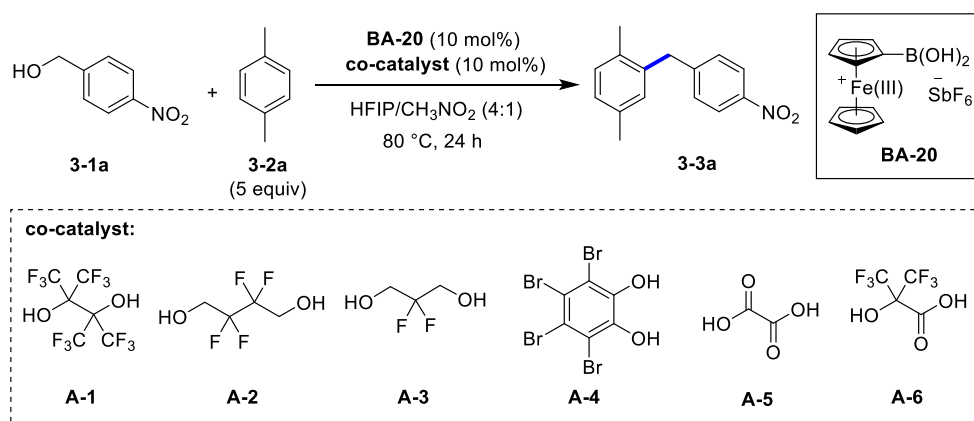
entry	co-catalyst	yield (%)[b]
1	–	10
2	**A-1**	26
3	**A-2**	<5
4	**A-3**	<1
5	**A-4**	6
6	**A-5**	10
7	**A-6**	45
8[c]	**A-1**	0
9[c]	**A-6**	0

[a]Reaction conditions: **3-1a** (0.50 mmol), **3-2a** (2.50 mmol), catalyst **BA-20** (10 mol%), co-catalyst (10 mol%) in HFIP/CH$_3$NO$_2$ (4:1) solvent mixture (1 mL) was stirred at 80 °C for 24 h. [b]NMR yield with 1,4-dinitrobenzene as internal standard. [c]Reaction was performed without catalyst **BA-20**.

With the discovery of two effective co-catalysts, **A-1** and **A-6**, further optimization of other reaction parameters (catalyst loading, temperature, and time), was conducted to improve the yield (Table 3-2). The co-catalytic system with boronic acid **BA-20** and diol **A-1** was examined first (entries 1–5). However, no appreciable

improvement in yield was obtained through increasing the temperature or the reaction time (entries 2 and 3). Although a slight enhancement in yield was observed by increasing the equivalents of boronic acid **BA-20** and co-catalyst to 20 mol%, no increase in yield was detected when employing one equivalent of **A-1** (entries 4 and 5). With the above results in mind, the co-catalytic system of boronic acid **BA-20** and α-hydroxy carboxylic acid **A-6** was inspected briefly with respect to the reaction time or the equivalents of co-catalyst (entries 6–8). Gratifyingly, an impressive improvement in yield was achieved by utilizing one equivalent of co-catalyst **A-6** (entry 8), affording product **3-3a** in 62% yield. No product was obtained in the absence of catalyst **BA-20**, which rules out an acceleration of the reaction from the Brønsted acidic co-catalyst **A-6** alone (entry 9).

Table 3-2 Further Optimization of Reaction Conditions with Co-catalyst **A-1** and **A-6**[a]
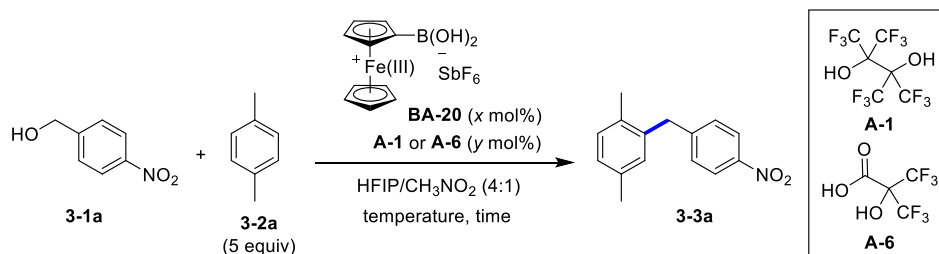
entry	BA-20 (*x* mol%)	co-catalyst (*y* mol%)	temperature (°C)	time	yield (%)[b]
1	10	**A-1** (10)	80	24 h	26
2	10	**A-1** (10)	100	24 h	24
3	10	**A-1** (10)	80	7 days	30
4	20	**A-1** (20)	80	24 h	36
5	20	**A-1** (100)	80	24 h	28
6	10	**A-6** (10)	80	24 h	45
7	10	**A-6** (10)	80	7 days	38
8	10	**A-6** (100)	80	24 h	62
9	0	**A-6** (100)	80	24 h	0

[a]Reaction conditions: **3-1a** (0.50 mmol), **3-2a** (2.50 mmol), catalyst **BA-20** *(x* mol%), co-catalyst **A** (*y* mol%) in HFIP/CH$_3$NO$_2$ (4:1) solvent mixture (1 mL) was stirred at indicated temperature and time. [b]NMR yield with 1,4-dinitrobenzene as internal standard.

Based on the results of co-catalyst screening and reaction optimization, it was determined that the previously published reaction conditions at 80 °C for 24 h with 10 mol% of both the catalyst **BA-20** and co-catalyst **A-1** or **A-6** would be adequate

for most of the moderately challenging primary benzylic alcohol substrates. Furthermore, the use of one equivalent of co-catalyst **A-6** could be implemented for the most challenging primary benzylic alcohol substrates, such as alcohol **3-1a**, to deliver the desired product in an appreciable yield.

Lastly, when expanding the substrate scope to secondary benzylic alcohols, it was found that 2,3,4,5-tetrafluoro-phenylboronic acid **BA-17**, a commercial compound with superior shelf-stability compared to **BA-20**, also can be employed as an effective catalyst with co-catalyst **A-1**. It is postulated that the methyl group on the secondary benzylic alcohols provides extra stabilization to the carbocation intermediate in the reaction, lowering the activation energy so that a weaker catalyst, such as **BA-17,** can be used. A brief investigation was performed on the reaction conditions for improved reactivity of secondary benzylic alcohols using catalyst **BA-17** and a co-catalyst (Table 3-3).

Table 3-3 Investigation of Reaction Conditions for Improved Reactivity with a Secondary Benzylic Alcohol Substrate using Catalyst **BA-17**[a]
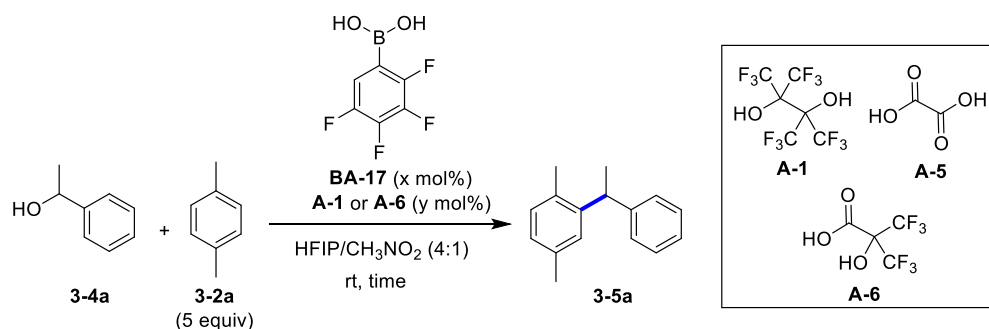
entry	x mol%	co-catalyst (y mol%)	time	yield (%)[b]
1	10	–	24 h	<5
2	10	**A-1** (10)	24 h	89
3	10	**A-6** (10)	1 h	83
4	0	**A-1**(10)	24 h	0
5	0	**A-6** (10)	1 h	75
6	0	**A-5** (10)	1 h	70

[a]Reaction conditions: **3-4a** (0.50 mmol), **3-2a** (2.50 mmol), catalyst **BA-17** (*x* mol%), co-catalyst *(y* mol%) in HFIP/CH$_3$NO$_2$ (4:1) solvent mixture (1 mL) was stirred at room temperature for the indicated time. [b]NMR yield with 1,4-dinitrobenzene as internal standard.

The desired product **3-5a** was observed in less than 5% yield in the absence of any co-catalyst (entry 1), while a substantial improvement in yield was observed in

the presence of co-catalyst **A-1** or **A-6** (entries 2 and 3). However, in control experiments without catalyst **BA-17** (entries 4 and 5), co-catalyst **A-1** alone was ineffective, while a considerable amount of product **3-5a** was generated with co-catalyst **A-6** alone, showing that the carboxylic acid in co-catalyst **A-6** could be strong enough to act as a Brønsted acid to activate the secondary benzylic alcohol for the reaction. Moreover, a similar yield of product **3-5a** was observed when oxalic acid (**A-5**) was utilized as the sole catalyst, which further supports the possibility of Brønsted acid activation of the secondary benzylic alcohol by carboxylic acids (entry 6). Hence, the co-catalytic system of **BA-17** and **A-1** was identified as the optimal system for increased reactivity in Friedel–Crafts alkylation of secondary benzylic alcohol substrates under mild conditions free of a strong protic acid.

3.3.2 Substrate Scope

With the respective optimal co-catalytic systems for primary and secondary benzylic alcohols in hand, the scope of the two-component boronic acid catalyzed procedure was examined in challenging Friedel–Crafts alkylations. The substrate scope also was expanded further to diarylmethanols by Jason P. G. Rygus, a PhD candidate in the Hall Group. Unfortunately, primary and secondary heteroaryl alcohols, such as pyrroles, pyridines, thiophenes, and indoles, are not compatible with this system. With these substrates, complex mixtures often were obtained after the reaction, with no sign of the desired product.

3.3.2.1 Substrate Scope with Primary Benzylic Alcohols

The scope of primary benzylic alcohols was studied first, particularly with respect to electron-deficient benzylic alcohols that proved difficult in the absence of the co-catalyst (Scheme 3-6). It is noteworthy that the use of five equivalents of arene nucleophile and 4:1 HFIP/CH_3NO_2 were adapted from the previously reported optimal reaction conditions without further optimizations.[34,35]

Scheme 3-6 Substrate scope of primary benzyl alcohols with co-catalysts **BA-20** and **A-1/A-6**.

Reaction conditions: **3-1** (0.5 mmol) + **3-2** (5 equiv), **BA-20** (10 mol%), **A-1** or **A-6** (10 mol%), HFIP/CH$_3$NO$_2$ (4:1), [0.5 M], 80 °C, 24 h, giving **3-3**.

3-3b (25 °C)
43% without **A**;
78% with **A-1**;
81% with **A-6**

3-3c (50 °C)
40% without **A**;
76% with **A-1**;
80% with **A-6**

3-3d
48% without **A**;
80% with **A-1**;
83% with **A-6**

3-3e
0% without **A**;
0% with **A-1**;
<5% with **A-6**;
22% with **A-6** (1 equiv)

3-3f (50 °C, 1 h)
40% without **A**;
83% with **A-1**;
87% with **A-6**

3-3g (50 °C)
38% without **A**;
76% with **A-1**;
82% with **A-6**

3-3h
72% without **A**;
80% with **A-1**;
84% with **A-6**

3-3i[a]
33% without **A**;
55% with **A-1**;
67% with **A-6**
(**a:b:c** 61:36:3)[b]

3-3j[a]
20% without **A**;
61% with **A-1**;
68% with **A-6**
(**a:b:c** 61:31:8)[b]

3-3k[a]
35% without **A**;
37% with **A-1**;
67% with **A-6**
(**a:b** 65:35)[b]

3-3l[a]
<5% without **A**;
13% with **A-1**;
18% with **A-6**;
37% with **A-6** (1 equiv)
(**a:b:c** 71:22:7)[b]

3-3m
0% without **A**;
<5% with **A-1**;
9% with **A-6**;
26% with **A-6** (1 equiv)

3-3n[a]
0% without **A**;
23% with **A-1**;
13% with **A-6**
(**a:b:c** 72:20:8)[b]

[a]Reported yields are isolated yields of combined regioisomers; [b]The ratio of regioisomers were determined by ^{1}H NMR analysis.

As fluorine-containing compounds are highly valuable in the pharmaceutical industry, a series of fluorinated benzylic alcohols were examined.[38–40] When employing the co-catalytic system, 4-fluorobenzyl alcohol reacted with *p*-xylene at room temperature for 24 h to afford a yield of product **3-3b** nearly double that of the reaction without the co-catalyst. Likewise, the reactions of 2,5-difluorobenzyl alcohol and 2,4,5-trifluorobenzyl alcohol with *p*-xylene were aided greatly by both co-catalyst **A-1** or **A-6**, with nearly a two-fold increase in yield for the corresponding diarylmethanes **3-3c** and **3-3d**. However, the co-catalytic system reached its limit with the highly electronically deactivated 2,3,5,6-tetrafluorobenzyl alcohol, which

failed to produce diarylmethane **3-3e** with *p*-xylene, even with the use of 10 mol% co-catalysts. Nevertheless, product **3-3e** was obtained in 22% yield when one equivalent of co-catalyst **A-6** was used. Next, other halogenated benzylic alcohols, such as 4-bromobenzyl alcohol and 3,4-dichlorobenzyl alcohol, also provided a substantial improvement in the yield of the corresponding diarylmethane products **3-3f** and **3-3g** with *p*-xylene when the co-catalytic system was implemented. These examples showed that the shorter reaction time and a lower temperature are possible when using the co-catalytic system with moderately deactivated benzylic alcohols. Furthermore, the yield of diarylmethane **3-3h**, from the reaction of 3-bromo-2-fluorobenzyl alcohol with *p*-xylene, was improved further to the range of 80% by using the co-catalytic system.

Other arenes, such as *m*-xylene, bromobenzene, fluorobenzene and 1-bromo-4-isopropylbenzene, also can be employed as the nucleophilic partner in the reaction. The yields of diarylmethane products **3-3i** and **3-3j** were improved with both co-catalysts **A-1** and **A-6**, while the yield of diarylmethane product **3-3k** was enhanced only with co-catalyst **A-6**. It is noteworthy that the corresponding diarylmethane products were obtained as a mixture of inseparable regioisomers, which is an intrinsic feature of many substrates observed in Friedel–Crafts alkylations, regardless of the conditions employed. This is because electrophilic aromatic substitution can occur at different positions on the arene and the rate of substitution at certain positions is affected by the substituents on the arene (ortho-para directing or meta-directing). The ratio of major and minor isomers was determined by ^{1}H NMR analysis of the product mixture.

Lastly, when highly electronically deactivated alcohols, such as 4-nitrobenzyl alcohol and 3,5-bis(trifluoromethyl)benzyl alcohol, were employed, the yield of the corresponding diarylmethane **3-3a**, **3-3l**, and **3-3m** was slightly improved with a co-catalytic amount of **A-1** or **A-6** and substantially increased when one equivalent of co-catalyst **A-6** was used. Diarylmethane **3-3n** was obtained in a comparable yield with the isomeric diarylmethane **3-3m** by using just co-catalytic **A-1**. In general, an improvement in yield was observed with both co-catalytic systems, with co-catalyst

A-6 slightly superior and preferred over co-catalyst **A-1** due to the purportedly high toxicity of **A-1**.[41]

3.3.2.2 Substrate Scope with Secondary Benzylic Alcohols

The scope of secondary benzylic alcohols was examined using the co-catalytic system of **BA-17** and **A-1** (Scheme 3-7).
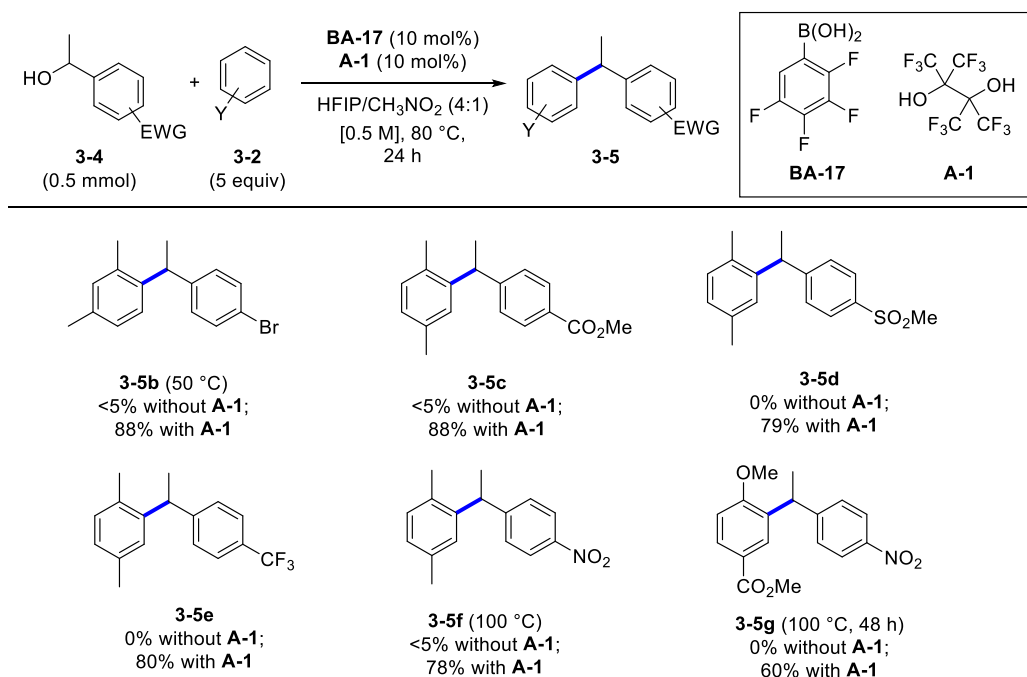
Scheme 3-7 Substrate scope of 1-arylethanols with co-catalysts **BA-17** and **A-1**. Reaction scale: 0.5 mmol of alcohol.

In all cases, a negligible amount of product was observed in the absence of co-catalyst **A-1**, and a significant enhancement in the yield of diarylethane products was achieved by utilizing co-catalyst **A-1**. As with the above primary benzylic alcohols, a brominated substrate was tolerated well, giving high yields of the corresponding diarylethane **3-5b** with *m*-xylene in the presence of co-catalyst **A-1**. It should be mentioned that diarylethane **3-5b** was obtained as a single regioisomer. Substrates containing a carboxyester or a sulphonyl group were also suitable in this co-catalytic system, affording the desired diarylethane products **3-5c** and **3-5d** with *p*-xylene in good yields. Gratifyingly, with the co-catalytic system, highly electronically deactivated 1-(4-(trifluoromethyl)phenyl)ethanol and 1-(4-nitrophenyl)ethanol also

furnished diarylethane products **3-5e** and **3-5f**, respectively, in good yields with *p*-xylene. In the case of 1-(4-nitrophenyl) ethanol, a higher reaction temperature (100 °C) was required to form product **3-5f** in high yield. Moreover, when pairing 1-(4-nitrophenyl)ethanol with *p*-anisate, an electronically less activated arene, a higher reaction temperature (100 °C) and a longer reaction time (48 h) were needed to deliver the corresponding diarylmethane product **3-5g** in a moderate yield of 60%.

3.3.2.3 Substrate Scope with Diarylmethanols

The reaction and substrate scope with diarylmethanols were investigated primarily by Jason Rygus (Scheme 3-8). All results in this subsection, except for substrate **3-7e**, were obtained by Jason. Similar to the reaction of 1-arylethanols, pronounced improvement in the yield of triarylmethane products was noted when employing the co-catalytic system of **BA-17** and **A-1**. A higher reaction temperature (100 °C) was needed to yield product **3-7e** from a diarylmethanol derivative with trifluoromethyl substituents. In contrast with primary benzylic alcohols and 1-arylethanol derivatives, all diarylmethanol starting materials were consumed fully in the absence of co-catalyst **A-1**, giving symmetrical ethers as products of a dehydrative substitution with a second molecule of alcohol, which were obtained in good yield.
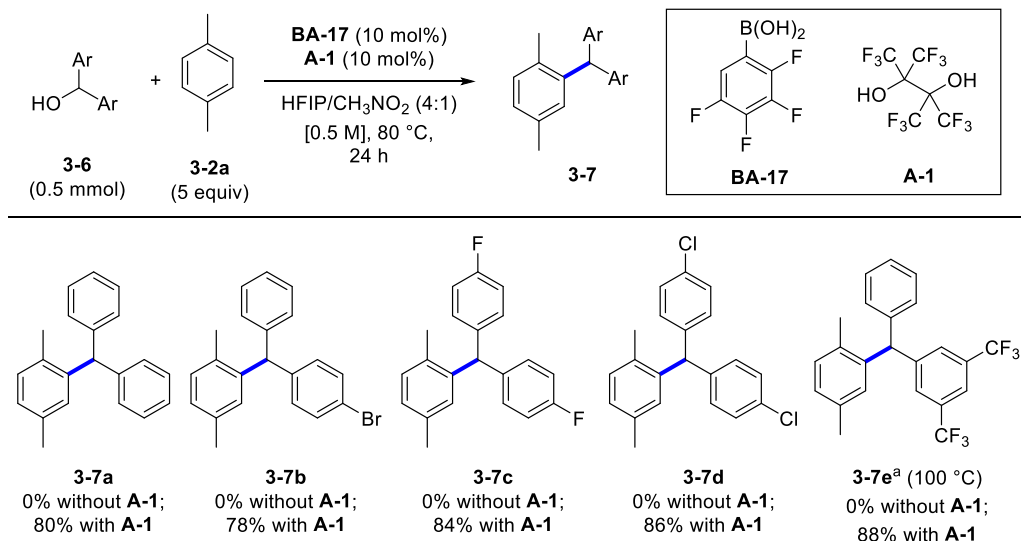
Scheme 3-8 Substrate scope of diarylmethanols with co-catalysts **BA-17** and **A-1**.

When the conversion of alcohol **3-6a** to the Friedel–Crafts alkylation product **3-7a** was monitored by ^{1}H NMR spectroscopy (Figure 3-2), rapid build-up of the symmetrical ether **3-8** was observed in the initial phase of the reaction, along with slow formation of triarylmethane **3-7a**. Over time, further consumption of ether **3-8** was observed, ultimately forming the desired triarylmethane product **3-7a** in good yield. Coincidentally, when Jason was working on the substrate scope, Taylor and co-workers reported the dehydrative synthesis of ether **3-8a** from alcohol **3-6a** using a co-catalytic system with 2,3,4,5,6-pentafluorophenylboronic acid (**BA-16**) and oxalic acid.[42] Thus, this outcome suggests that upon activation of the diarylmethanol **3-6a**, formation of ether **3-8a** by reaction with a second equivalent of alcohol is the kinetically preferred pathway due to the nucleophilicity of oxygen, particularly in the early stages of the reaction where the concentration of unreacted alcohol remains high. However, subsequent decay of ether **3-8a** suggests that it is not an off-cycle side-product but rather an off-cycle intermediate that is capable of further catalytic activation, ultimately delivering the Friedel–Crafts triarylmethane product **3-7a**.
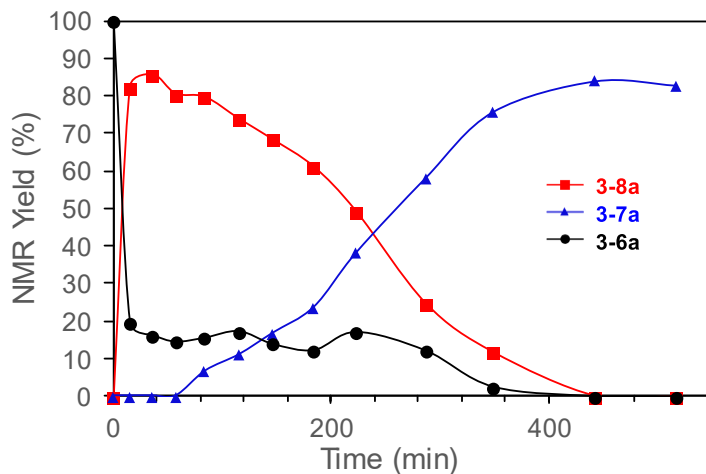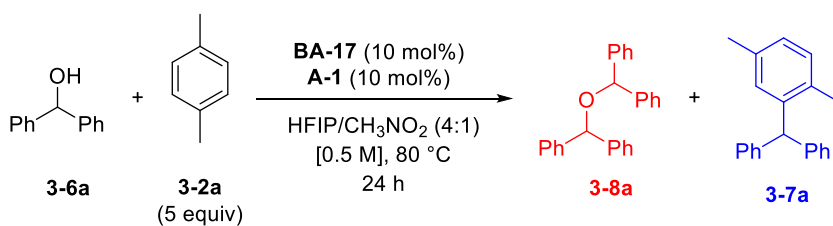
Figure 3-2 Reaction profile for Friedel–Crafts alkylation of alcohol **3-6a** with *p*-xylene **3-2a** (performed by Jason Rygus).

Furthermore, control experiments show that isolated ether **3-8a** is transformed cleanly to the triarylmethane product **3-7a** when subjected to the standard co-catalytic reaction conditions (Scheme 3-9). It should be noted that the 74% yield of product **3-7a** was obtained by taking into account that both diphenylmethyl fragments from ether **3-8** can be transformed into product **3-7a** under the optimal reaction conditions.
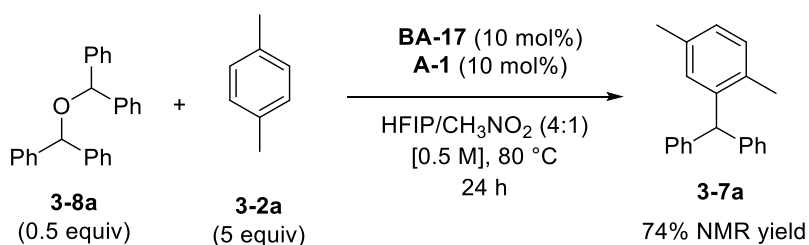
Scheme 3-9 Control experiment to support the formation of ether **3-8** as an intermediate in the reaction (performed by Jason Rygus).

3.4 Mechanistic Studies

With the substrate scope established, several experiments were conducted to probe the mechanism of the reaction, especially regarding the role and effect of the co-catalyst, and to identify the active catalytic species in the reaction. All the mechanistic studies were performed with the use of perfluoropinacol (**A-1**). Part of the studies was performed by Jason Rygus and will be indicated clearly below. Therefore, unless noted otherwise, the experiments were conducted by the author of this thesis.

3.4.1 Role of Perfluoropinacol

Previously, the role of perfluoropinacol (**A-1**) as a co-catalyst in BAC was studied extensively in the Beckmann rearrangement.[36] It was demonstrated that perfluoropinacol reacts with the boronic acid catalyst to form a five-membered boronic ester *in situ*, resulting in a more electrophilic Lewis acidic boron center. Therefore, at the onset, it was suspected that perfluoropinacol plays a similar role in the current Friedel–Crafts BAC system.

To demonstrate the formation of an activated boronic ester, a series of ^{11}B NMR studies were conducted with a boronic acid catalyst and co-catalyst **A-1** in HFIP/CH$_3$NO$_2$/CD$_3$CN (4:1:1). CD$_3$CN was added to the NMR sample mixture only

to lock the NMR field, and it is assumed that it does not affect the interaction of boronic acid and perfluoropinacol occurring under the optimal reaction conditions. When equimolar amounts of co-catalyst **A-1** and **BA-17** or **BA-20** were mixed and subjected to ^{11}B NMR analysis, new ^{11}B NMR signals were detected in the region of 8–14 ppm, corresponding to a tetracoordinate boron species, rather than the expected three-coordinate cyclic boronic ester, which would appear around 25 ppm (Figure-3-3). While **BA-17** remained predominantly as the free boronic acid and only a small amount of corresponding boronate was formed, **BA-20** was converted mostly to two different boronate species. Given the similar pK_a's of **BA-17** (6.0)[34] and **BA-20** (5.8),[43] this contrasting observation may be attributed to the unique cationic nature of **BA-20**. Nevertheless, these results suggest that upon boronic ester formation, the boron center could be sufficiently Lewis acidic to promote coordination by either HFIP or adventitious water, generating a neutral or anionic boronate species in solution that would correspond to the observed boron NMR shifts.
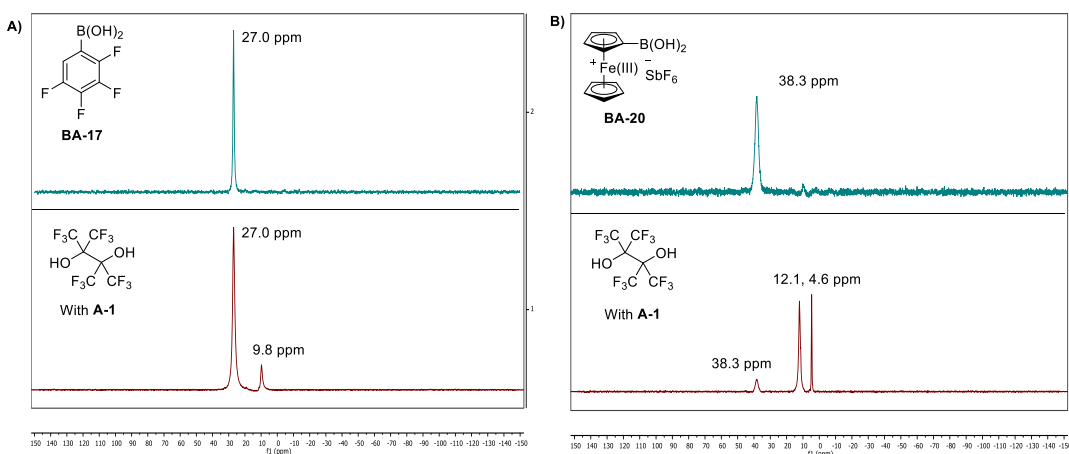
Figure 3-3 ^{11}B NMR spectra of boronic acid **BA-17** or **BA-20** with or without co-catalyst **A-1** in a solvent mixture of HFIP/CH$_3$NO$_2$/CD$_3$CN (4:1:1).

To examine the plausible formation of an anionic tetracoordinate boronate, it was envisioned that such anionic species could be detected with ESI mass spectrometry in the negative mode. Therefore, the mixtures of boronic acids and co-catalyst **A-1** from the NMR studies were subjected to ESI mass spectrometry analysis. In fact, the anionic boronate complexes involving the coordination of hydroxide **3-9**

and hexafluoroisopropoxide (**3-10**) were detected in the mixture of **BA-17** and **A-1** (Figure 3-4A). However, such complexes were not observed in the mixture of ferrocenium boronic acid (**BA-20**) and perfluoropinacol (**A-1**) since the boronate complexes are zwitterionic and overall neutral in charge, thus, they are not detectable by ESI spectrometry. Instead, the perfluoropinacolate boronic ester **3-11** formed between **BA-20** and **A-1** was detected in the positive mode (Figure 3-4B). According to the results obtained from the **BA-17** and **A-1** system, it is assumed that the two upfield ^{11}B shifts (12.1 and 4.6 ppm, see Figure 3-3B) observed in the **BA-20** and **A-1** system corresponded to the two anionic complexes involving the coordination of HFIP and hydroxide. All in all, these results support that a more Lewis acidic cyclic boronic ester was formed in the presence of co-catalyst **A-1**, which is Lewis acidic enough coordinate with HFIP or adventitious water to form the anionic boronate species.
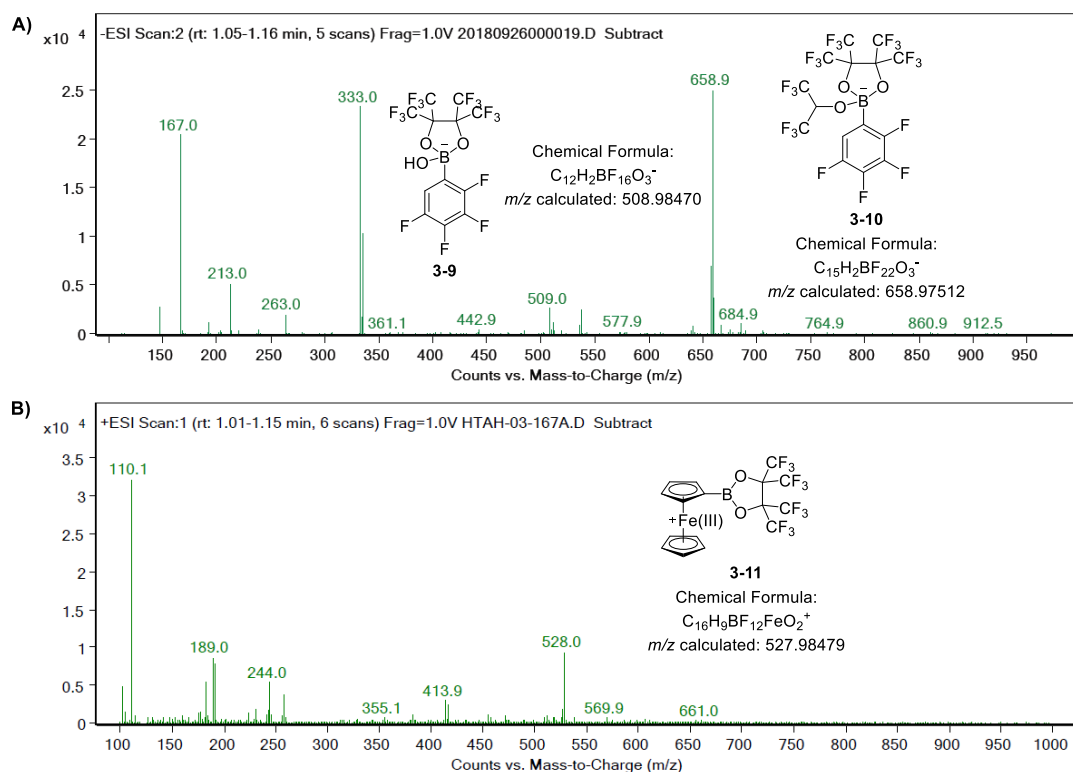
Figure 3-4 ESI mass spectra of A) mixture of boronic acid **BA-17** and co-catalyst **A-1** in negative mode; B) mixture of boronic acid **BA-20** and co-catalyst **A-1** in positive mode.

To support further that the tetracoordinate boron species **3-9** and **3-10** are observed only due to the formation of the highly Lewis acidic perfluoropinacolate boronic ester from boronic acid **BA-17** and co-catalyst **A-1**, control experiments without co-catalyst **A-1** or with pinacol were conducted and analyzed by ^{11}B NMR and ESI mass spectrometry. When boronic acid **BA-17** was stirred in a HFIP/CD$_3$NO$_2$ (4:1) solvent mixture with the absence of co-catalyst **A-1**, the ^{11}B NMR spectrum remained unchanged compared to when **BA-17** was analyzed in CD$_3$CN, and all of the corresponding anionic hexafluoroisopropoxide complexes were not observed in the ESI mass spectrum (Figure 3-5). Similarly, in the presence of pinacol, the non-fluorinated analog of co-catalyst **A-1**, ^{11}B NMR spectroscopy showed formation of the pinacolato-boronic ester **3-12,** with a slight downfield shift (29.6 ppm) relative to the free boronic acid **BA-17** (27.0 ppm), and the corresponding anionic complex **3-13** was not observed in the ESI mass spectra (Figure 3-6).
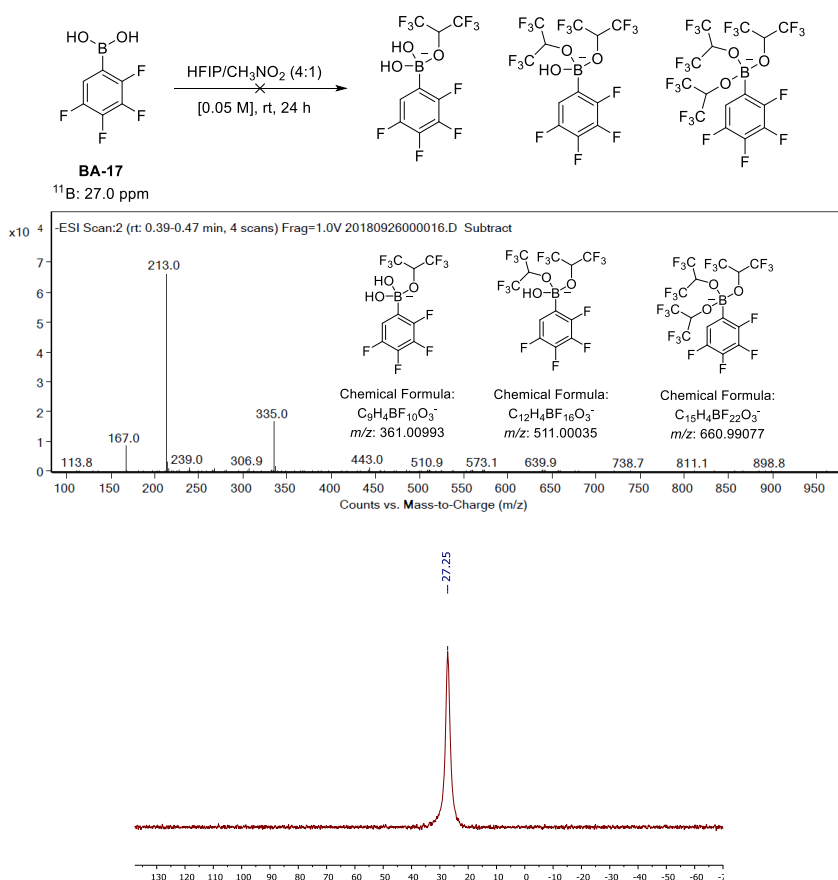
Figure 3-5 ESI mass spectrum and ^{11}B NMR spectrum of **BA-17** in a solution of HFIP/CD$_3$NO$_2$ (4:1) without **A-1.**
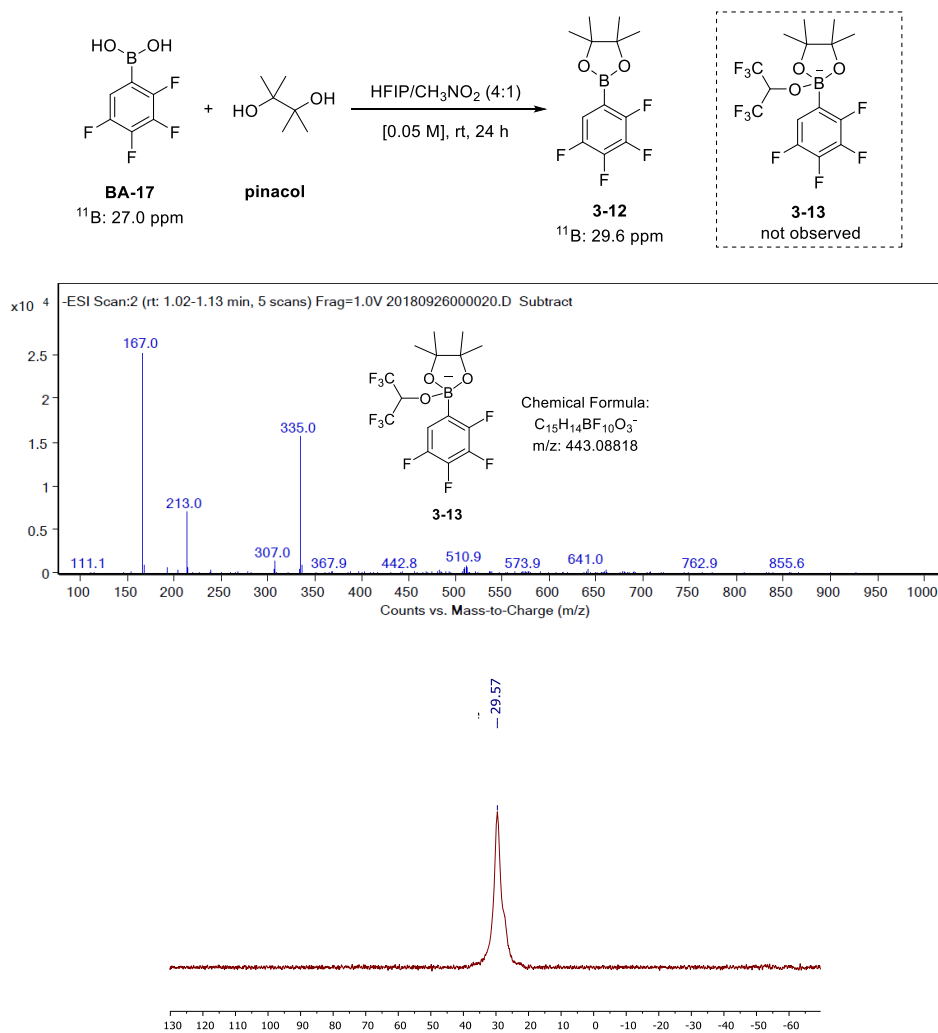
Figure 3-6 ESI mass spectrum and ^{11}B NMR spectrum of **BA-17** with pinacol in a solution of HFIP/CD$_3$NO$_2$ (4:1).

Lastly, an attempt to synthesize the perfluoropinacolate boronic ester from boronic acid **BA-17** with the standard procedure for boronic ester formation using a Dean–Stark apparatus yielded anionic boronate **3-9** instead of the desired perfluoropinacolate boronic ester (Scheme 3-10). Boronate **3-9** was obtained as the sole product after removal of toluene and vacuum drying overnight. The low yield of product **3-9** could be attributed to protodeboronation of the boronic acid forming 1,2,3,4-tetrafluorobenzene, which has a lower boiling point than toluene. With all these results, it was established that perfluoropinacol (**A-1**) indeed reacts with boronic acids to form the highly Lewis acidic five-membered cyclic boronic esters.
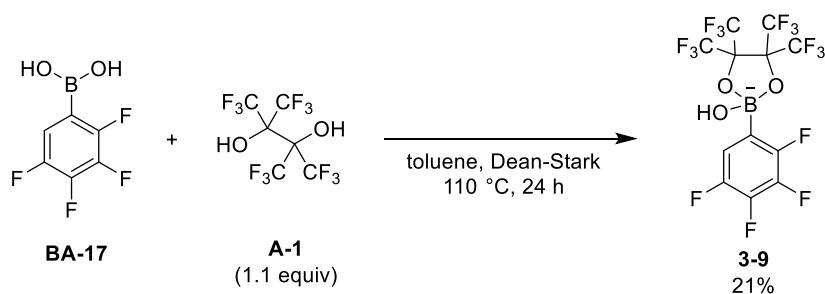
Scheme 3-10 Attempt to synthesize the perfluoropinacolate boronic ester of boronic acid **BA-17**.

3.4.2 Investigation of Plausible Brønsted Acid-mediated Alcohol Activation

Functional group compatibility studies performed by Jason Rygus revealed that the reaction using the co-catalytic system of **BA-20** and **A-1** is moderately tolerant to carboxylic acid, terminal alkyne, aliphatic alcohols, and both unactivated and conjugated alkene moieties. However, complete inhibition was observed upon addition of basic nitrogen-containing compounds, such as 2,6-di-*tert*-butylpyridine (Scheme 3-11).
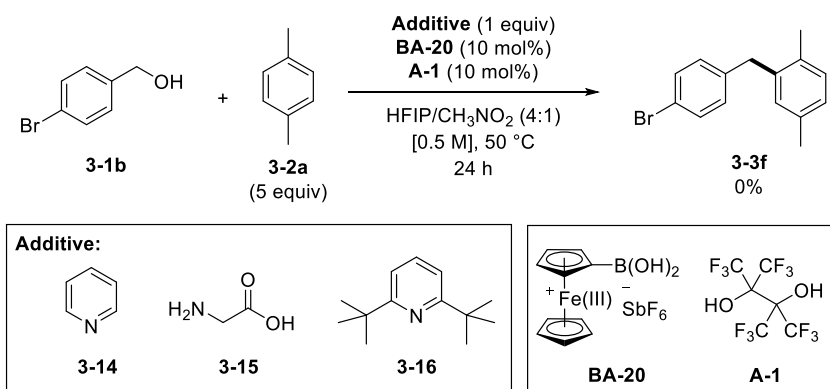
Scheme 3-11 Reaction inhibition by basic nitrogen containing additives (performed by Jason Rygus).

Unless the basic additives play another inhibitory role, such as deprotonation of the solvent generating deleterious species or alteration of the boronic acid–boroxine equilibrium, inhibition by 2,6-di-*tert*-butylpyridine (**3-16**) usually is considered as a strong evidence for a protic acid dependence in the reaction mechanism, as coordination of this highly sterically hindered base to boron Lewis acids is improbable.[44]

In the dehydrative substitution of benzylic alcohols using **BA-16** and the oxalic acid co-catalytic system, Taylor and co-workers proposed that the reaction is likely to proceed via a Brønsted acid alcohol activation mechanism, where the Brønsted acid originates from the formation of hydronium boronate species, as depicted in Scheme 3-12.[42] Hence, it is suspected that a similar hydronium boronate species is formed in our co-catalytic system and acts as the active catalytic species to promote the reaction, which is why basic amine additives inhibit the reaction.
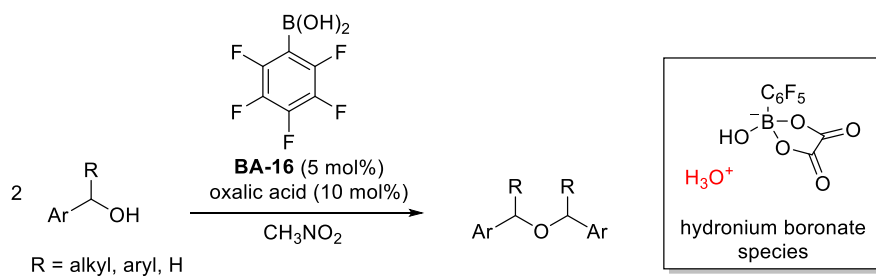
Scheme 3-12 Taylor's work on dehydrative substitution of benzylic alcohols with co-catalytic **BA-16** and oxalic acid.

Assuming that a similar hydronium boronate species **B** is the active catalytic species in the reaction, three plausible modes of benzylic alcohol activation are shown in Scheme 3-13. The activation of alcohols by species **B** can occur through either a Lewis acid, Brønsted acid, or Lewis acid assisted Brønsted acid catalyzed[45–47] mechanism. In the proposed Lewis acid mediated catalysis, it is envisioned that transesterification of the coordinated HFIP with the benzylic alcohol would lead to an activated species **C** that could undergo facile ionization of the C–O bond, resulting in species **D** for subsequent Friedel–Crafts reaction (Scheme 3-13A). In the postulated Brønsted acid catalysis, the hydronium cation in species **B** could act as a strong protic acid to activate the benzylic alcohol by protonation, resulting in ion pair **E**, which leads to species **F** through dissociation of the C–O bond (Scheme 3-13B). Lastly, in the proposed Lewis acid assisted Brønsted acid catalysis, instead of forming a hydronium cation, the acidity of HFIP could be enhanced by the Lewis acidic boronic ester, as delineated in complex **G**, which could be responsible for alcohol activation via a Brønsted acid-catalyzed pathway (Scheme 3-13C). In view of all these

possibilities, various experiments were conducted to gain more insight regarding the activation mode of benzylic alcohols.
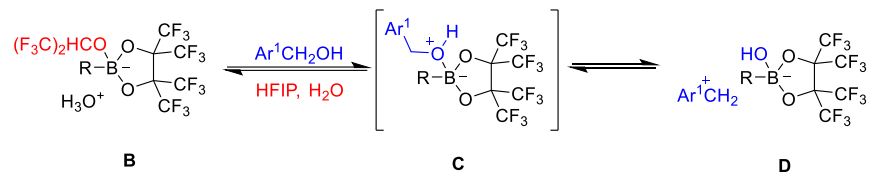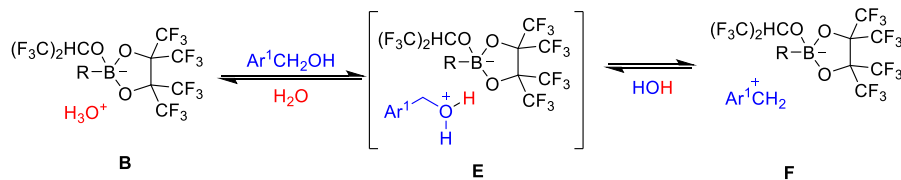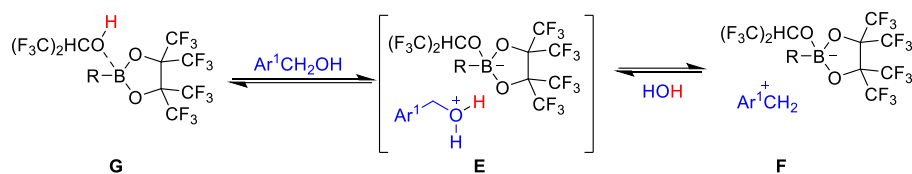
Scheme 3-13 Plausible modes of alcohol activation.

3.4.2.1 Influence of Alcohols on the Catalytic Species

To examine the plausible Lewis acid-catalyzed alcohol activation by coordination of the alcohol substrate on the perfluoropinacolate boronic ester (Scheme 3-13A), 10 equivalents of 3-phenyl-1-propanol (**3-17**), a non-π-activated alcohol, were added to the mixture of **BA-17** and **A-1** in the HFIP/CH$_3$NO$_2$ (4:1) solvent mixture and analyzed by ESI mass spectrometry. Anionic boronate adduct **3-18** with bound alcohol **3-17** was not observed, and only boronate species **3-9** and **3-10** were detected (Scheme 3-14A). Considering that alcohol **3-17** is less acidic than HFIP, it is possible that HFIP boronate adduct **3-10** is formed predominantly when HFIP is present in the system. Hence, a control experiment without HFIP was conducted, however, the anionic species **3-18** still was not detected (Scheme 3-14B).
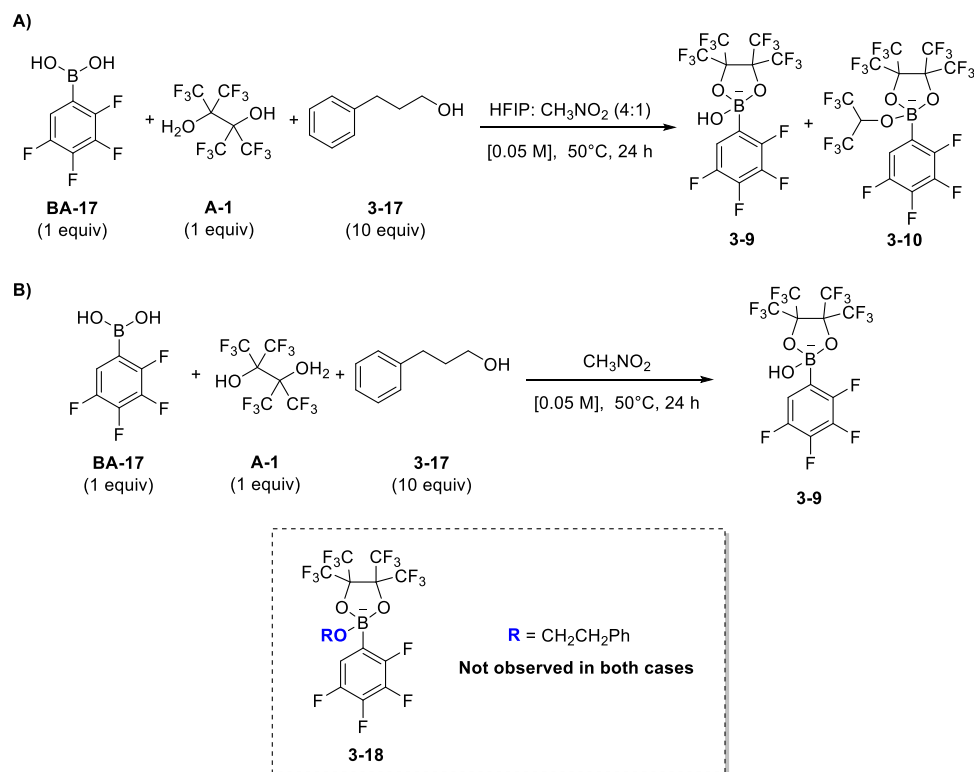
Scheme 3-14 Effect of non-π-activated alcohol **3-17** on anionic boronate species in A) HFIP:CH$_3$NO$_2$ (4:1) solvent mixture and B) CH$_3$NO$_2$ solvent.

These results suggested that the coordination of the alcohol substrate to the boron center is unlikely to happen, especially in the presence of a large excess of HFIP. Thus, it is less likely that the alcohol activation proceeds through Lewis acid mediated catalysis. Nonetheless, the system is always in equilibrium, so some degree of coordination of alcohol substrates to the boron center still may occur and lead to a facile C–O bond dissociation.

3.4.2.2 Influence of 2,6-di-*tert*-butylpyridine on the Catalytic Species

To evaluate further the inhibitory effect of 2,6-di-*tert*-butylpyridine (**3-16**) on the Friedel–Crafts reaction, the influence of this hindered base on the catalytic species was examined using ^{11}B NMR spectroscopy (Figure 3-7). In the absence of 2,6-di-*tert*-butylpyridine, reaction of equimolar boronic acid **BA-17** and co-catalyst **A-1** resulted in a mixture of free boronic acid and a tetracoordinate boron species **3-10**. Upon addition of 1.5 equivalents of 2,6-di-*tert*-butylpyridine, the boronic acid–boronate equilibrium was shifted completely to the tetracoordinate boronate complex

with a pyridinium countercation (**3-19**). The formation of the boronate–pyridinium complex **3-19** also was supported by ESI-mass spectrometry (Figure 3-8). Inhibition of the Friedel–Crafts reaction by 2,6-di-*tert*-butylpyridine indicates that the pyridinium ion pair **3-19** is an ineffective catalytic species. The only difference between ion pair **3-19** and the proposed hydronium boronate species **B** (Scheme 3-13) is their countercation, thus suggesting that the countercation might be a key component in the reaction.
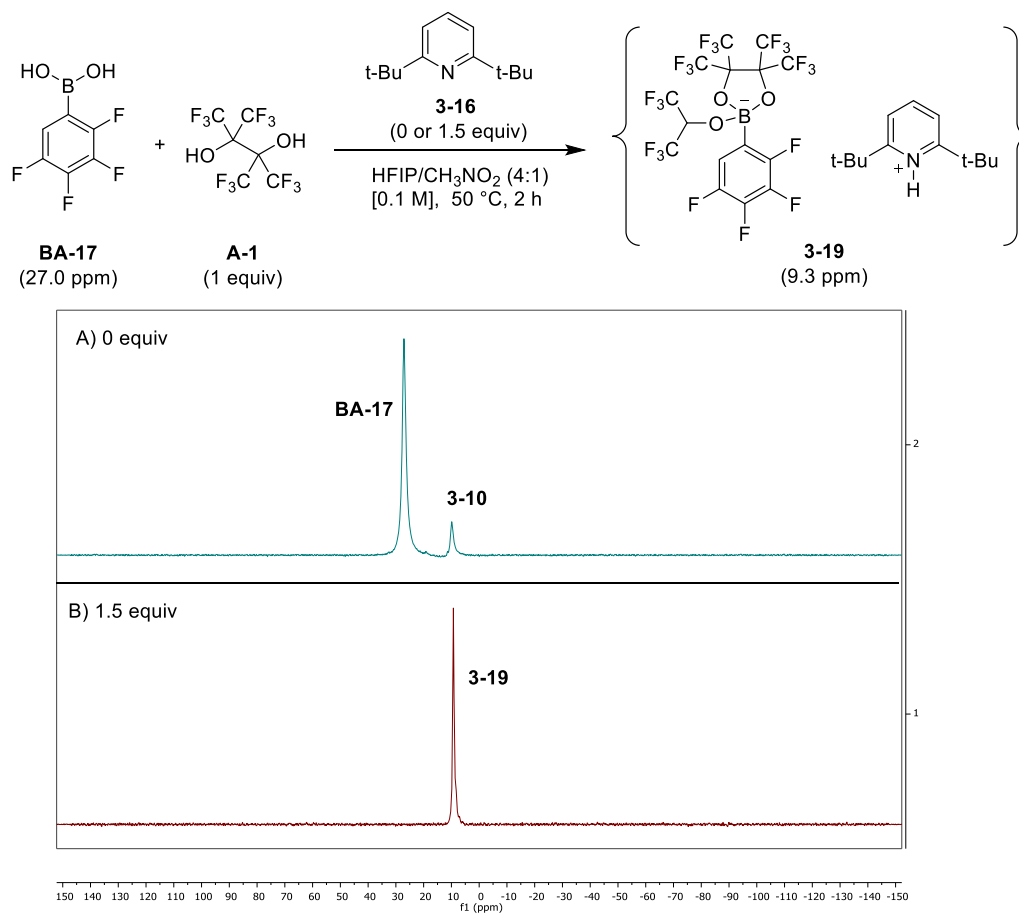
Figure 3-7 Effect of 2,6-di-*tert*-butylpyridine **3-16** on the proposed catalytic species.
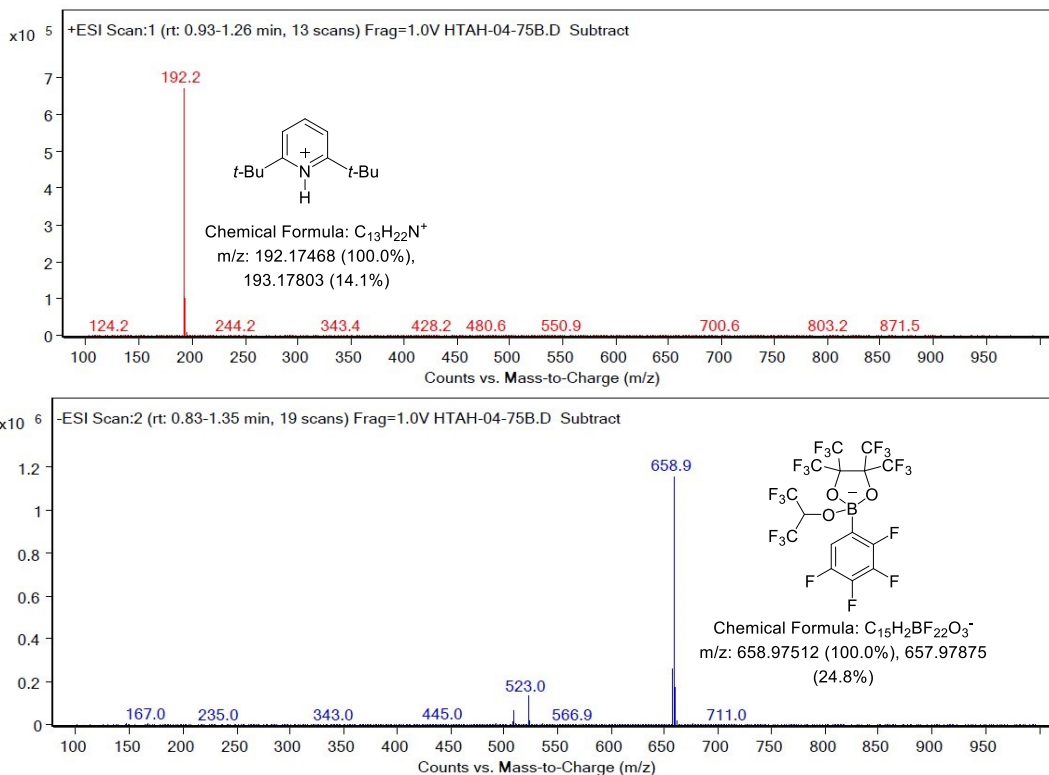
Figure 3-8 ESI mass spectrum of ion pair **3-19**.

3.4.2.3 Effect of Water on the Reaction and Catalytic Species

To study further the possibility of the proposed hydronium boronate catalytic species **B**, the efficiency of the Friedel–Crafts reaction of alcohols **3-1f** and **3-6a** was assessed under anhydrous conditions using carefully dried solvents and glassware, along with the addition of activated 3 Å molecular sieves as a desiccant (Scheme 3-15). The reaction with diphenylmethanol **3-6a** was conducted by Jason Rygus. Under anhydrous conditions, formation of the Friedel–Crafts products **3-3f** and **3-7a** was subdued entirely. While alcohol **3-1f** remained unreacted, alcohol **3-6a** was transformed into ether **3-8** in good yield. Importantly, Jason revealed that addition of 37 mol% water to the Friedel–Crafts reaction of alcohol **3-6a** in dried solvents and glassware restored its catalytic activity, delivering triarylmethane **3-7a** in 71% yield. These results demonstrate that the activation of diarylmethanol **3-6a** is feasible under anhydrous conditions by a weaker acid, either free boronic acid **BA-17** or perfluoropinacol **A-1**, to produce ether **3-8**; however, trace water in the solvents or

water released from the condensation of boronic acid **BA-17** and diol **A-1** is needed to further activate ether **3-8**.
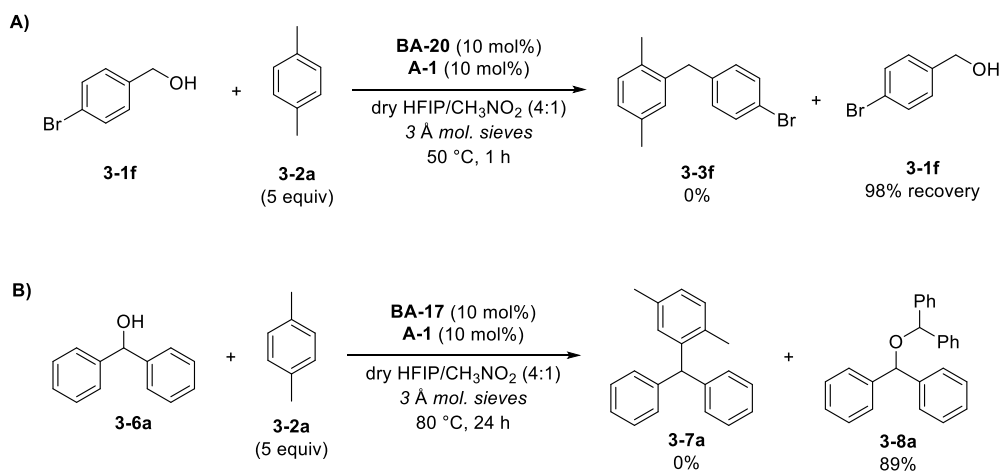
Scheme 3-15 Effect of anhydrous solvents and molecular sieves on the reaction of A) 4-bromobenzyl alcohol **3-1b** and B) diphenylmethanol **3-6a** with *p*-xylene **3-2a**. Experiment with alcohol **3-6a** was performed by Jason Rygus.

Furthermore, the effect of water on the catalytic species was investigated by Jason Rygus using ^{11}B NMR spectroscopy (Figure 3-9). It was found that addition of activated 3 Å molecular sieves only shifted the equilibrium between boronic acid **BA-17** and boronate complex **3-10** slightly towards complex **3-10** but did not appear to generate any significant amount of other unidentified catalytic species that would be accountable for the drastic change in reactivity in the absence of water (Figure 3-6). Hence, based on these results, it is believed that water is necessary to form the hydronium boronate catalytic species **B** (Scheme 3-13), which is sufficiently acidic to activate the C–O bonds of benzylic alcohols and hindered benzylic ethers for a Friedel–Crafts reaction. Along these lines, Yang and coworkers also observed that residual water was essential for the formation of BF_3–H_2O as the active Brønsted acid promoter in the BF_3–OEt_2-promoted Friedel–Crafts benzylation reaction with benzyl ethers.[48]
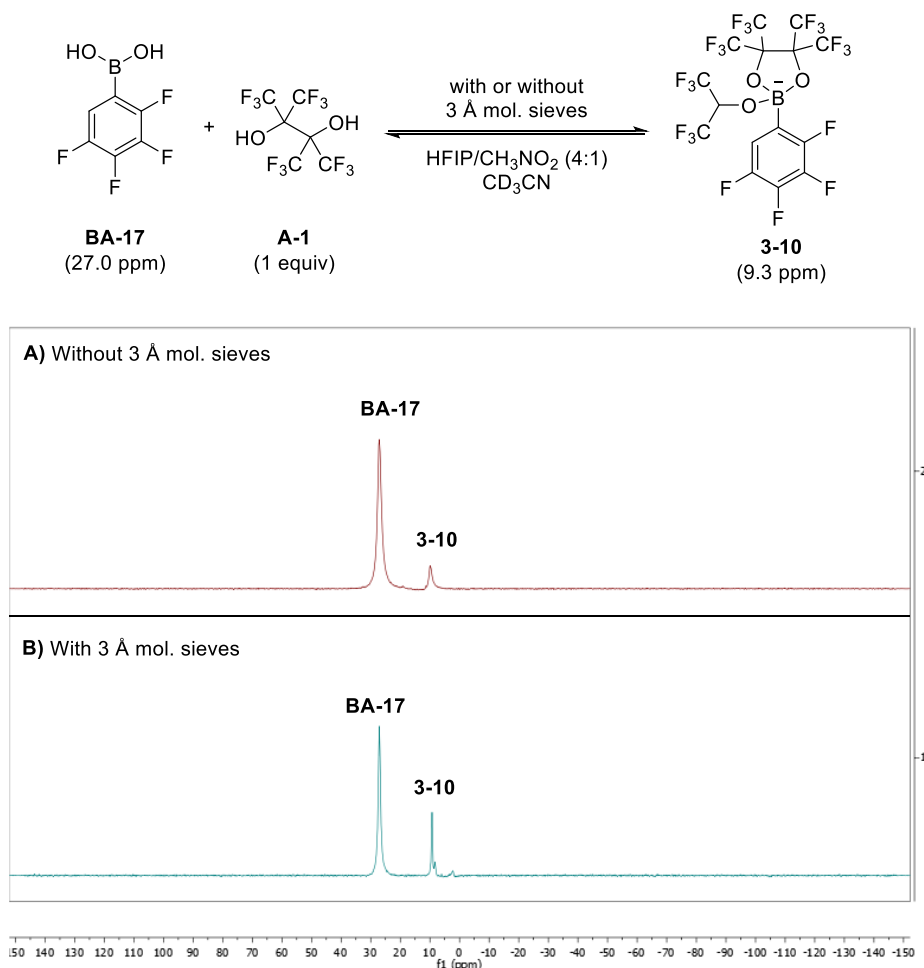
Figure 3-9 Effect of 3Å molecular sieves on the catalytic species (performed by Jason Rygus).

3.5 Proposed Catalytic Cycle

In accordance with the above mechanistic studies, a plausible mechanism for this reaction is delineated in Scheme 3-16. In line with Taylor's study, it is proposed that condensation of the boronic acid catalyst (**BA**) with co-catalyst **A-1** and HFIP solvent forms hydronium boronate complex **B** in equilibrium. Boronate species **B** is deemed to be the active catalyst species that likely activates the alcohol substrate via a Brønsted acid-dependent mechanism (Scheme 3-13B) to generate carbocation ion-pair **D** or **F**. However, at this stage, the other activation modes depicted in Scheme 3-13 cannot be ruled out fully. Thereafter, the complex **D** or **F** undergoes a Friedel–Crafts alkylation by nucleophilic attack of the arene, generating ion-pair **H,** which consisted of a Wheland intermediate stabilized by a weakly coordinating boronate

counteranion. Successive rearomatization of the Wheland intermediate through deprotonation with the boronate counteranion affords the Friedel–Crafts product. Finally, in the presence of HFIP and water, the active catalyst **B** can be regenerated via a zwitterionic intermediate **I**, releasing water or HFIP as a by-product. It is noteworthy that, in the case of diarylmethanols **3-6**, the carbocation in intermediate **D** or **F** can be trapped by a second molecule of alcohol to form ether **3-8**, which appears to be the kinetically favored pathway, as rapid formation of the ether was observed in the initial phases of the reaction (Figure 3-2). It was determined that ether **3-8** is not an off-cycle side-product and can re-enter the catalytic cycle by activation of the ether C–O bond with the active catalytic species **B**.
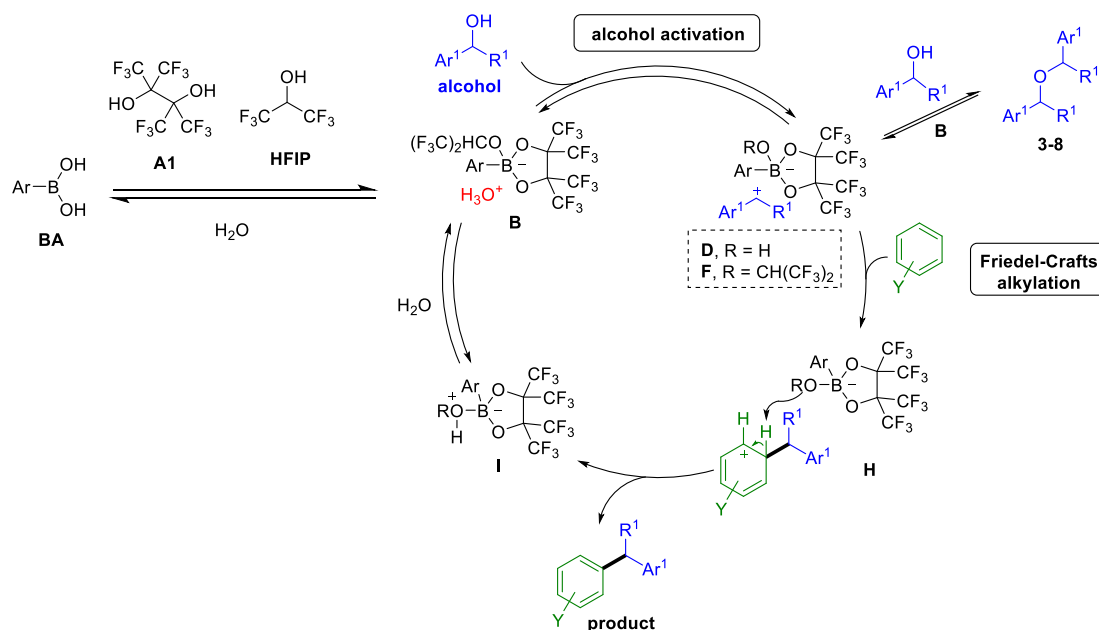
Scheme 3-16 Proposed catalytic cycle for the Friedel–Crafts alkylation catalyzed by two-component boronic acid catalysis.

3.6 Comparison with Other Brønsted Acid Catalysts

As it is proposed that the activation of alcohols in our co-catalytic system may occur through a Brønsted acid-catalyzed mechanism, the efficiency and chemoselectivity of our system in comparison with common Brønsted acid catalysts were examined using alcohol substrate **3-4h** in the alkylation of *p*-xylene **3-2a** (Table 3-4). Substrate **3-4h** contains an acid and hydrolytically labile acetate substituent, thus, it represents a

credible model to assess the mildness of reaction conditions. In all cases, full conversion of the alcohol **3-4h** was observed under the optimal reaction conditions (entries 1–6). However, the co-catalytic system of **BA-17** and **A-1** displayed the highest yield of the desired product **3-5h** (entry 1). The use of a strong Brønsted acid, *p*-toluenesulfonic acid (*p*-TsOH·H$_2$O), resulted in an intractable mixture, with no desired product formation (entry 2). When other relatively mild Brønsted acids were employed as catalysts, a low yield of the desired product **3-5h** (35–56%), along with a complex mixture of by-products, was observed (entries 3–6). Utilizing the conditions from Moran's work for highly deactivated systems using catalytic trifluoromethane-sulfonic acid in HFIP[49] led to full consumption of alcohol **3-4h,** with no desired product **3-5h** detected (entry 7). Additionally, no desired product **3-5h** was observed when dichloroethane (DCE), a common solvent for these classical Brønsted acid catalysts,[50–54] was used (entries 8–11).

Table 3-4 Comparison with Other Brønsted Acid Catalysts[a]
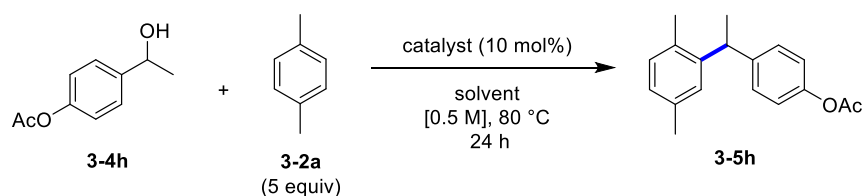
entry	catalyst	solvent	conversion (%)[b]	NMR yield (%)[b]
1	**BA-17** and **A-1**	4:1 HFIP/CH$_3$NO$_2$	>98	80[c]
2	*p*-TsOH·H$_2$O	4:1 HFIP/CH$_3$NO$_2$	>98	0
3	CSA	4:1 HFIP/CH$_3$NO$_2$	>98	35
4	HCl (4.0 M in dioxane)	4:1 HFIP/CH$_3$NO$_2$	>98	50
5	TFA	4:1 HFIP/CH$_3$NO$_2$	>98	56
6	Oxalic acid	4:1 HFIP/CH$_3$NO$_2$	>98	52
7	TfOH	HFIP	>98	0
8	*p*-TsOH·H$_2$O	DCE	>98	0
9	CSA	DCE	>98	0
10	TFA	DCE	28	0
11	Oxalic acid	DCE	81	0

[a]Reaction conditions: **3-4b** (0.50 mmol), **3-2a** (2.50 mmol), catalyst (10 mol%) in solvent mixture (1 mL) were stirred at 80 °C for 24 h. [b]Conversion and yield were determined by ^{1}H NMR analysis with 1,4-dinitrobenzene as internal standard. [c]Isolated yield.

The results above clearly highlight the mildness and high chemoselectivity of the co-catalytic system of **BA-17** and **A-1** and support previous claims regarding the mild reaction conditions offered by boronic acid catalysis.[55] Moreover, the nature of the counteranion in a Brønsted acid catalyst is suspected to have a notable effect on the chemoselectivity of the reaction process. Thus, it is postulated that a large and stable boronate counteranion, such as species **3-10** (Figure 3-4), exhibits a low level of basicity and nucleophilicity that helps minimize undesired side reactions. Along the same lines, such a weakly coordinating boronate counteranion would assist the Friedel–Crafts chemistry effectively by providing an increase of reactivity to its associated carbocation.[35]

3.7 Summary

In summary, this chapter disclosed preliminary results on the use of perfluoropinacol (**A-1**) or 2,2-bis(trifluoromethyl)glycolic acid (**A-6**) as a co-catalyst for increased reactivity of boronic acid catalyzed Friedel–Crafts alkylation with electronically deactivated benzylic alcohols. In general, alkylations with halogenated benzylic alcohols generally were improved, providing yields of Friedel–Crafts products in most cases more than double the yields of reactions conducted in the absence of a co-catalyst. Other electron-withdrawing substituents are well-tolerated under the optimal conditions, with improved yields obtained when the co-catalyst was employed. The co-catalyst is presumed to generate a highly Lewis acidic boronic ester that leads to formation of a hydronium boronate species **B**. Species **B** is inferred to be the active catalyst species that promotes a facile ionization of benzylic alcohols and benzylic ethers into the corresponding carbocations for a Friedel–Crafts reaction. The ionization process likely occurs via a Brønsted acid-dependent mechanism, though further studies are required to determine the exact mode of activation. Furthermore, compared to conventional Brønsted acids, acid-sensitive functional groups were compatible with this dual-catalytic system, which may be attributable to the non-nucleophilic and weakly coordinating boronate counteranion. Lastly, the co-catalytic boronic acid–diol system described in this chapter offers a milder and greener synthetic method for the preparation of di- and triarylalkanes. Moreover, this system

could potentially be applied in other Brønsted acid-catalyzed reactions to provide cleaner and more effective approaches.

3.8 Experimental

3.8.1 General Information

The following materials include the experimental procedures and details for isolation of compounds. Full characterization of all novel compounds and partial characterization of known compounds presented in this chapter are described. All reactions were performed in capped regular glassware without any further precautions, unless otherwise stated. All solvents were purchased as ACS reagents and used with no further purification. 1,1,1,3,3,3-Hexafluoro-2-propanol (HFIP) was purchased from Oakwood Products, Inc. Unless otherwise noted, all other chemicals were purchased from commercial sources and used as received. Hexafluoro-2,3-bis(trifluoromethyl)-2,3-butanediol (perfluoropinacol, **A-1**) was purchased from Matrix Scientific. Catalysts **BA-17**[56] and **BA-20**[35] were synthesized based on literature procedures. Substituted phenylethane-1-ol and substituted diarylmethanol derivatives were prepared according to literature procedures. Chromatographic separations were performed on silica gel 60 using ACS grade hexanes, ethyl acetate, and acetone as eluents. Preparative thin layer chromatography (PTLC) was performed on silica gel 60F 254 plates. Thin layer chromatography (TLC) analysis of reaction mixtures was performed on Silicycle silica gel 60 F254 plates, which were visualized under UV light and with $KMnO_4$ or phosphomolybdic acid (PMA) stains.

^1H, ^{11}B, ^{13}C, and ^{19}F NMR spectra were recorded in $CDCl_3$ or CD_3CN at ambient temperature using Varian DD2 MR two-channel 400 MHz, Varian INOVA-400 MHz, Bruker Avance III 400, Varian VNMRS two-channel 500 MHz, or Varian INOVA-600 MHz spectrometers at 400/500/600, 128, 100/125/150, and 376 MHz, respectively. All NMR chemical shifts are reported in ppm units with residual solvent peak ($CDCl_3$ or CD_3CN) as internal standard. NMR data is reported using the following abbreviations: s, singlet; d, doublet; t, triplet; q, quartet; sept, septet; dd, doublet of doublets; dt, doublet of triplets; tt, triplet of triplets; ddd, doublet of doublet of doublets; m, multiplet. High-resolution mass spectra were recorded by the

University of Alberta Mass Spectrometry Services Laboratory using either electron impact (EI) or electrospray ionization (ESI) techniques. Infrared (IR) spectra were obtained on a Nicolet Magna-IR with frequencies expressed in cm^{-1}.

3.8.2 Preparation of Starting Materials

3.8.2.1 General Procedure for the Synthesis of Secondary Benzylic Alcohols
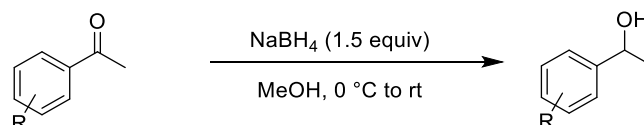
Secondary benzylic alcohol substrates were prepared according to a literature procedure.[57] A round bottom flask equipped with a stir bar was charged with the corresponding acetophenone was dissolved in methanol (10 mL) and cooled to 0 °C in an ice bath. NaBH$_4$ (1.5 equiv) was added slowly in a few portions, and the reaction mixture was stirred at 0 °C for 10 min. The ice bath was removed, and the mixture was allowed to warm to room temperature. TLC analysis was used to monitor the reaction progress. Upon completion, the reaction was quenched by addition of saturated aqueous NH$_4$Cl, and methanol was removed by reduced-pressure evaporation. The mixture was extracted with ethyl acetate (3 × 15 mL), the collected organic phases were dried over anhydrous MgSO$_4$ or Na$_2$SO$_4$, and filtered. After removal of the solvent, the desired alcohols were obtained. If needed, further purification by column chromatography was used to obtain pure alcohol.

3.8.2.2 Characterization of Starting Materials
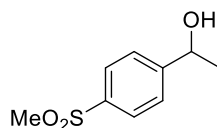
1-(4-(Methylsulfonyl)phenyl)ethan-1-ol (3-4e): Prepared from 4-(methylsulfonyl)-acetophenone (991 mg, 5.01 mmol) and isolated as a pure white solid (681 mg, 68%) without further purification. **^{1}H NMR** (400 MHz, CDCl$_3$, δ): 7.92 (d, J = 8.4 Hz, 2 H), 7.58 (d, J = 8.0 Hz, 2 H), 5.01 (q, J = 6.6 Hz, 1 H), 3.05 (s, 3 H), 1.94 (s, 1 H), 1.52 (d, J = 6.5 Hz, 3 H). Spectral data agree with the literature.[58]
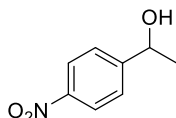
1-(4-Nitrophenyl)ethan-1-ol (3-4f): Prepared from 4-nitroacetophenone (826 mg, 5.02 mmol) and isolated as a yellow oil (677 mg, 81%) without further purification. **^{1}H NMR** (400 MHz, CDCl$_3$, δ): 8.19 (d, J = 8.8 Hz, 1 H), 7.54 (d, J = 8.3 Hz, 1 H), 5.02 (q, J = 6.6 Hz, 1 H), 2.09 (s, 1 H), 1.51 (d, J = 6.5 Hz, 2 H). Spectral data agree with the literature.[59]
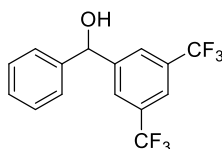
(3,5-Bis(trifluoromethyl)phenyl)(phenyl)methanol (3-6e): A flame dried round bottom flask under nitrogen atmosphere was charged with THF (20 mL) and 1,3-bis(trifluoromethyl)-5-bromobenzene (860 µL, 5.01 mmol). The flask was cooled to −78 °C in a dry ice/acetone bath after which *n*-BuLi (2.5 M solution in hexane, 2.0 mL, 5.0 mmol) was added dropwise. The reaction was stirred for 30 min at −78 °C. A solution of benzaldehyde (460 µL, 4.50 mmol) in THF (5 mL) was added dropwise and the reaction stirred for an additional 30 min at −78 °C. The cold bath was removed, and the reaction stirred for 3.5 h while warming to room temperature. After 3.5 h, the reaction was cooled to 0 °C in an ice bath and quenched with saturated aqueous NH$_4$Cl (20 mL). The reaction mixture was extracted with EtOAc (2 × 30 mL), and the combined organic layers were washed with water (2 × 30 mL) and brine (30 mL). The organic layer was dried with Na$_2$SO$_4$, filtered, and concentrated under reduced pressure. The resulting oil was purified by flash column chromatography (hexane to 8:1 hexane/EtOAc) to afford the title compound (691 mg, 48%) as an ochre solid. **^{1}H NMR** (500 MHz, CDCl$_3$, δ): 7.87 (s, 2 H), 7.79 (s, 1 H), 7.42–7.37 (m, 2 H), 7.37–7.32 (m, 3 H), 5.92 (d, J = 3.0 Hz, 1 H), 2.43 (d, J = 3.1 Hz, 1 H). Spectral data agree with the literature.[60]
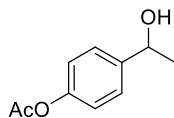
4-(1-Hydroxyethyl)phenyl acetate (3-5h): Prepared from 4-hydroxyacetophenone in two steps according to the literature procedure.[10] To a solution of 4-hydroxyacetophenone (1.36 g, 10.0 mmol) in DCM (20 mL) was added Et$_3$N (2.10 mL, 15.0 mmol) and Ac$_2$O (1.42 mL, 15.0 mmol), and the reaction mixture was stirred for 4 h at room temperature. TLC analysis was used to monitor the reaction progress. Upon completion, water (20 mL) was added to the reaction mixture and extracted with DCM (2 × 10 mL). The combined organic layers were washed with water (2 × 10 mL) and brine (1 × 10 mL), dried over MgSO$_4$, and filtered. The filtrate was concentrated to afford 4-acetylphenyl acetate as colorless oil and was used for the next step without further purification. The title compound was prepared according to the general procedure above from 4-acetylphenyl acetate. The crude mixture was purified by flash column chromatography (5:1 hexanes/EtOAc) to afford the title compound (1.01 g, 56% over two steps) as a colorless oil. **^{1}H NMR** (400 MHz, CDCl$_3$, δ): 7.38 (d, J = 8.4 Hz, 2 H), 7.06 (d, J = 8.6 Hz, 2 H), 4.90 (q, J = 6.5 Hz, 1 H), 2.29 (s, 3 H), 1.48 (d, J = 6.5 Hz, 3 H). Spectral data agree with the literature.[12]

3.8.3 General Procedure for Co-catalyst Screening
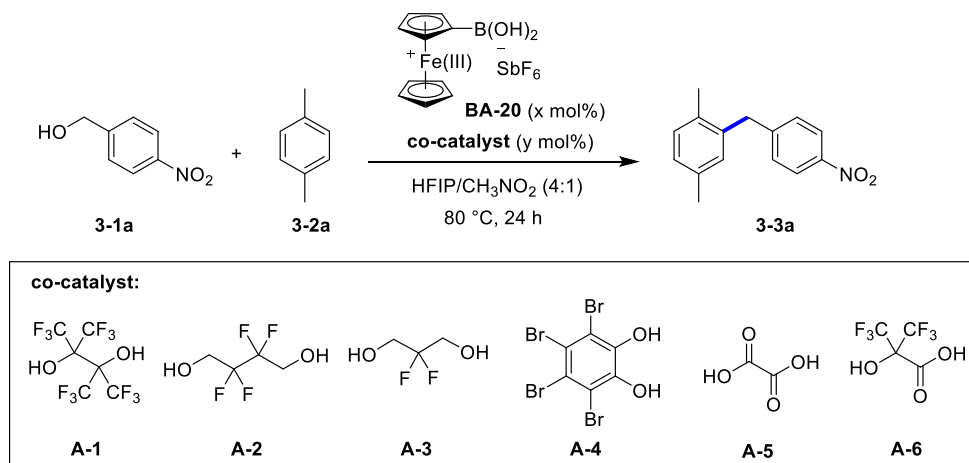
A vial equipped with a stir bar was charged with a solution of 4-nitrobenzyl alcohol (77 mg, 0.50 mmol) and *p*-xylene (0.30 mL, 2.5 mmol) in a solvent mixture of

4:1 HFIP and nitromethane (1 mL), followed by addition of ferrocenium boronic acid catalyst **BA-20** (*x* mol%) and co-catalyst **A-1** (*y* mol%). The vial was capped and stirred at the indicated temperature and time. NMR yield was obtained with 1,4-dinitrobenzene (21 mg, 0.13 mmol) as internal standard.

3.8.4 General Procedure for Friedel–Crafts Alkylation

The boronic acid catalyst **BA** (10 mol%) and/or without the co-catalyst **A-1** or **A-6** (10 mol%) was added to a vial equipped with a stir bar and containing the benzyl alcohol (0.50 mmol) and the arene (1.0–2.5 mmol) dissolved in a solvent mixture of 4:1 hexafluoroisopropanol and nitromethane (1 mL). The vial was capped and stirred at the indicated temperature and time. Upon completion, the reaction mixture was concentrated and purified by flash column chromatography with hexanes/EtOAc to afford the product.

3.8.5 Characterization Data for Friedel–Crafts Alkylation Products
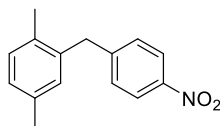
1,4-Dimethyl-2-(4-nitrobenzyl)benzene (3-3a): Prepared from 4-nitrobenzyl alcohol (77 mg, 0.50 mmol) and *p*-xylene (0.30 mL, 2.5 mmol) with boronic acid **BA-20**. Purified by flash column chromatography (10:1 hexane:EtOAc) and isolated as a light yellow solid. NMR yield was obtained with 1,4-dinitrobenzene (21 mg, 0.13 mmol) as internal standard. **^{1}H NMR** (400 MHz, CDCl$_3$, δ): 8.12 (d, *J* = 8.8 Hz, 2 H), 7.27 (d, *J* = 8.8 Hz, 2 H), 7.08 (d, *J* = 7.7 Hz, 1 H), 7.01 (d, *J* =7.7 Hz, 1 H), 6.92 (s, 1 H), 4.04 (s, 2 H), 2.31 (s, 3 H), 2.17 (s, 3 H); **^{13}C NMR** (126 MHz, CDCl$_3$, δ): 148.5, 146.4, 136.9, 135.8, 133.4, 130.8, 130.5, 129.4, 127.8, 123.7, 39.4, 21.0, 19.2; **IR** (cast film, cm^{-1}): 3000 (w), 2922 (w), 1604 (m), 1517 (s), 1347 (s), 1110 (w), 858 (w), 799 (w), 734 (m); **HRMS** (EI) for C$_{15}$H$_{15}$NO$_2$: calcd: 241.1103; found: 241.1099.
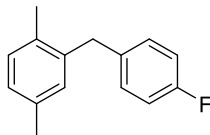
2-(4-Fluorobenzyl)-1,4-dimethylbenzene (3-3b): Prepared from 4-fluorobenzyl alcohol (63 mg, 0.50 mol) and *p*-xylene (0.30 mL, 2.5 mmol) with boronic acid **BA-20** at room temperature for 24 h. Purified by flash column chromatography (hexanes) and isolated as a colourless oil (without **A**: 46 mg, 43%; with **A-1**: 84 mg, 78%, with **A-6**: 87 mg, 81%). ^{1}**H NMR** (400 MHz, CDCl$_3$, δ): 7.10–7.06 (m, 3 H), 7.00–6.95 (m, 3 H), 6.92 (m, 1 H), 3.93 (s, 2 H), 2.31 (s, 3 H), 2.20 (s, 3 H); ^{13}**C NMR** (101 MHz, CDCl$_3$, δ): 161.4 (d, *J* = 241.8 Hz), 138.6, 136.2 (d, *J* = 2.8 Hz), 135.5, 133.4, 130.7, 130.4, 130.0 (d, *J* = 7.8 Hz), 127.3, 115.1 (d, *J* = 20.8 Hz), 38.7, 21.0, 19.2; ^{19}**F NMR** (376 MHz CDCl$_3$, δ): –117.8 (app. sept); **IR** (cast film, cm^{-1}): 3042 (m), 2922 (m), 1603 (m), 1508 (s), 1444 (m) , 1222 (s), 1157 (m), 1092 (w), 811 (s), 770 (m); **HRMS** (EI) for C$_{15}$H$_{15}$F: calcd: 214.1158; found: 214.1154.
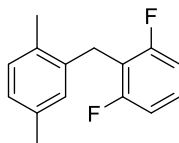
2-(2,5-Dimethylbenzyl)-1,3-difluorobenzene (3-3c): Prepared from 2,6-difluoro-benzyl alcohol (72 mg, 0.50 mmol) and *p*-xylene (0.30 mL, 2.5 mmol) with boronic acid **BA-20** at 50 °C for 24 h. Purified by flash column chromatography (hexanes) and isolated as a white solid (without **A**: 47 mg, 40%; with **A-1**: 91 mg, 76%; with **A-6**: 93 mg, 80%). ^{1}**H NMR** (400 MHz, CDCl$_3$, δ): 7.20 (tt, *J* = 8.3, 6.4 Hz, 1 H), 7.04 (d, *J* = 7.6 Hz, 1 H), 6.96–6.84 (m, 3 H), 6.76 (s, 1 H), 3.95 (s, 2 H), 2.36 (s, 3 H), 2.23 (s, 3 H); ^{13}**C NMR** (126 MHz, CDCl$_3$, δ): 161.7 (dd, *J* = 246.1, 8.5 Hz), 136.7, 135.4, 132.9, 130.0, 128.9, 127.9 (t, *J* = 10.3 Hz), 127.0, 116.1 (t, *J* = 20.1 Hz), 111.2 (dd, *J* = 20.3, 5.9 Hz), 25.4 (t, *J* = 2.5 Hz), 21.0, 19.2; ^{19}**F NMR** (376 MHz, CDCl$_3$, δ): –114.2 (quin, *J* = 6.0 Hz); **IR** (cast film, cm^{-1}): 3007 (w), 2925 (w), 1625 (m), 1592 (m), 1470 (s), 1267 (m), 1012 (m), 809 (m), 771 (m); **HRMS** (EI) for C$_{15}$H$_{14}$F$_2$: calcd: 232.1064; found: 232.1059.
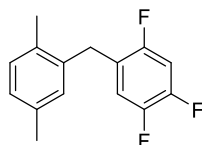
2-(2,5-Dimethylbenzyl)-1,4,5-trifluorobenzene (3-3d): Prepared from 2,4,5-trifluorobenzyl alcohol (81 mg, 0.50 mmol) and *p*-xylene (0.30 mL, 2.5 mmol) with boronic acid **BA-20** at 80 °C for 24 h. Purified by flash column chromatography (hexanes) and isolated as a colorless oil (without **A**: 60 mg, 48%; with **A-1**: 103 mg, 80%, with **A-6**: 104 mg, 83%). **^{1}H NMR** (500 MHz, CDCl$_3$, δ): 7.10 (d, *J* = 7.7 Hz, 1 H), 7.03 (d, *J* = 7.7 Hz, 1 H), 6.96–6.91 (m, 2 H), 6.73 (ddd, *J* = 10.8, 8.8, 7.0 Hz, 1 H), 3.91 (s, 2 H), 2.33 (s, 3 H), 2.21 (s, 3 H); **^{13}C NMR** (126 MHz, CDCl$_3$, δ): 155.63 (ddd, *J* = 244.2, 9.3, 2.7 Hz), 148.4 (ddd, *J* = 249.0, 14.5, 12.3 Hz), 146.8 (ddd, *J* = 244.2, 12.4, 3.6 Hz), 136.2, 135.8, 133.3, 130.6, 130.5, 127.8, 124.0 (ddd, *J* = 18.9, 4.6, 4.5 Hz), 117.9 (dd, *J* = 19.6, 5.9 Hz), 105.1 (dd, *J* = 28.6, 20.9 Hz), 31.3 (d, *J* = 2.8 Hz), 20.9, 18.9; **^{19}F NMR** (469 MHz, CDCl$_3$, δ): −119.30 (dt, *J* = 16.1, 8.2 Hz, 1F), −137.21 (dt, *J* = 19.4, 8.4 Hz, 1F), −143.22 (dddd, *J* = 21.9, 16.6, 10.8, 6.4 Hz, 1F); **IR** (cast film, cm^{-1}): 3054 (w), 2924 (m), 1631 (m), 1516 (s), 1441 (m), 1422 (s), 1333 (m), 1194 (m), 1148 (s), 874 (m), 846 (m), 768 (m), 716 (m); **HRMS** (EI) for C$_{15}$H$_{13}$F$_3$: calcd: 250.0969; found: 250.0967.

2-(4-Bromobenzyl)-1,4-dimethylbenzene (3-3f): Prepared from 4-bromobenzyl alcohol (94 mg, 0.50 mmol) and *p*-xylene (0.30 mL, 2.5 mmol) with boronic acid **BA-20** at 50 °C for 1 h. Purified by flash column chromatography (hexanes) and isolated as a light-yellow oil (without **A**: 56 mg, 40%; with **A-1**: 114 mg, 83%, with **A-6**: 120 mg, 87%). **^{1}H NMR** (400 MHz, CDCl$_3$, δ): 7.42–7.38 (m, 1 H), 7.09–7.07 (m, 1 H), 7.03–7.00 (m, 3 H), 6.92 (s, 1 H), 3.91(s, 2 H), 2.32 (s, 3 H), 2.19 (s, 3 H); **^{13}C NMR** (101 MHz, CDCl$_3$, δ): 139.7, 138.1, 135.6, 133.4, 131.5, 130.8, 130.5, 127.4, 119.7, 38.9, 21.0, 19.2; **IR** (cast film, cm^{-1}): 3040 (m), 2920 (m), 2863 (w), 1503 (m), 1486 (s), 1444 (m), 1071 (m), 1011 (s), 806 (s), 796 (s); **HRMS** (EI) for C$_{15}$H$_{15}{}^{81}$Br: calcd: 276.0337; found: 276.0331.
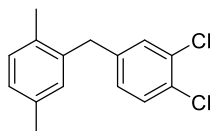
1,2-Dichloro-4-(2,5-dimethylbenzyl)benzene **(3-3g):** Prepared from 3,4-dichlorobenzyl alcohol (89 mg, 0.50 mmol) and *p*-xylene (0.30 mL, 2.5 mmol) with boronic acid **BA-20** at 50 °C for 24 h. Purified by flash column chromatography (hexanes) and isolated as a light-yellow oil (without **A-1**: 50 mg, 38%; with **A-1**: 100 mg, 76%, with **A-6**: 109 mg, 82%). **¹H NMR** (500 MHz, CDCl₃, δ): 7.34 (d, *J* = 8.2 Hz, 1 H), 7.21 (d, *J* = 8.2 Hz, 1 H), 7.08 (d, *J* = 7.7 Hz, 1 H), 7.01 (dd, *J* = 7.7, 2.0 Hz, 1 H), 6.96 (dd, *J* = 8.2, 2.0 Hz, 1 H). 6.92 (s, 1 H), 3.91 (s, 2 H), 2.32 (s, 3 H), 2.19 (s, 3 H); **¹³C NMR** (101 MHz, CDCl₃, δ): 141.0, 137.3, 135.7, 133.3, 132.3, 130.7, 130.5, 130.5, 130.3, 129.9, 128.1, 127.6, 38.6, 21.0, 19.2; **IR** (cast film, cm⁻¹): 3000 (s), 2921 (s), 2861 (m), 1590 (m), 1503 (m), 1470 (s), 1396 (m), 1131 (m), 1031 (m), 810 (s), 763 (m); **HRMS** (EI) for $C_{15}H_{14}Cl_2$: calcd: 264.0472; found: 264.0473.
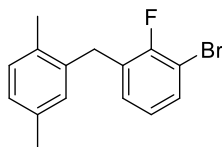
1-Bromo-3-(2,5-dimethylbenzyl)-2-fluorobenzene (3-3h): Prepared from 3-bromo-2-fluorobenzyl alcohol (103 mg, 0.50 mmol) and *p*-xylene (0.30 mL, 2.5 mmol) with boronic acid **BA-20** at 80 °C for 24 h. Purified by flash column chromatography (hexanes) and isolated as a light-yellow oil (without **A**: 105 mg, 72%; with **A-1**: 117 mg, 80%; with **A-6**: 123 mg, 84%).**¹H NMR** (400 MHz, CDCl₃, δ): 7.43–7.35 (m, 1 H), 7.07 (d, *J* = 7.7 Hz, 1 H), 6.99 (dd, *J* = 7.7, 1.9 Hz, 1 H), 6.91–6.82 (m, 3 H), 3.97 (s, 2 H), 2.29 (s, 3 H), 2.20 (s, 3 H); **HRMS** (EI) for $C_{15}H_{14}{}^{79}BrF$: calcd: 292.0262; found: 292.0263.
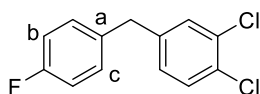
1,2-Dichloro-4-(4-fluorobenzyl)benzene (3-3i): Prepared from 3,4-dichlorobenzyl alcohol (89 mg, 0.50 mmol) and fluorobenzene (0.23 mL, 2.5 mmol) with boronic acid **BA-20** at 80 °C for 24 h. Purified by flash column chromatography (hexanes)

and isolated as a light-yellow oil (without **A**: 42 mg, 33%; with **A-1**: 70 mg, 55%; with **A-6**: 85 mg, 82%, 61:36:3 mixture of inseparable regioisomers). **¹H NMR** (500 MHz, CDCl₃, δ): 7.51 (dd, J = 8.2, 3.6 Hz, 0.04 H), 7.34 (dd, J = 8.2, 3.6 Hz, 0.99 H), 7.29 (d, J = 2.1 Hz, 0.35 H), 7.27–7.19 (m, 1.06 H), 7.16–7.06 (m, 2.07 H), 7.05 (ddd, J = 8.3, 7.3, 1.8 Hz, 0.61 H), 7.02–6.96 (m, 1.87 H), 6.95–6.92 (m, 0.6 H), 3.94 (s, 0.72 H), 3.91 (s, 0.07 H), 3.89 (s, 1.20 H); **¹³C NMR** (126 MHz, CDCl₃, δ): 161.7 (d, J = 245.0 Hz, major), 160.9 (d, J = 245.9 Hz, minor), 141.2 (minor), 140.2 (minor), 135.4 (d, J = 3.5 Hz, minor), 132.5 (minor), 132.4 (minor), 130.94 (d, J = 4.3 Hz, minor), 130.7 (major), 130.6 (major), 130.5 (major), 130.42 (major), 130.36 (major), 130.34 (major), 130.30 (major), 128.57 (d, J = 8.1 Hz, minor), 128.2 (major), 128.2 (minor), 126.8 (minor), 126.7 (minor), 124.35 (d, J = 3.5 Hz, minor), 115.59 (d, J = 21.7 Hz, minor), 115.55 (d, J = 21.6 Hz, major), 113.6 (minor), 40.2 (major), 34.1 (d, J = 3.1 Hz, minor), 29.7 (minor); **¹⁹F NMR** (376 MHz, CDCl₃, δ): −112.9 (td, J = 9.0, 6.3 Hz, 0.02 F), −116.43 (tt, J = 9.4, 4.7 Hz, 0.61 F), −117.61 (dt, J = 8.6, 4.7 Hz, 0.36 F); signals corresponding to all three regioisomers are reported; **IR** (cast film, cm⁻¹): 3042 (m), 2924 (m), 2853 (w), 1602 (s), 1587 (m), 1509 (s), 1472 (s), 1397 (s), 1226 (s), 1157 (s), 1093 (m), 1032 (s), 925 (m), 850 (s); **HRMS** (EI) for $C_{13}H_9{}^{35}Cl_2F$: calcd: 254.0064; found: 254,0063.
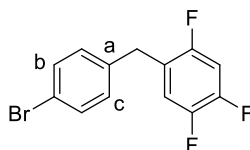
1-(4-Bromobenzyl)-2,4,5-trifluorobenzene **(3-3j):** Prepared from 2,4,5-trifluorobenzyl alcohol (81 mg, 0.50 mmol) and bromobenzene (0.26 mL, 2.5 mmol) with boronic acid **BA-20** at 80 °C for 24 h. Purified by flash column chromatography (hexanes) and isolated as a colorless oil (without **A-1**: 31 mg, 20%; with **A-1**: 92 mg, 61%; with **A-6**: 102 mg, 68%, 61:31:8 mixture of inseparable regioisomers). **¹H NMR** (500 MHz, CDCl₃, δ): 7.62 (d, J = 7.9 Hz, 0.35 H), 7.46 (d, J = 7.0 Hz, 1.24 H), 7.40 (d, J = 8.6 Hz, 0.08 H), 7.36 (s, 0.08 H), 7.33–7.26 (m, 0.47 H), 7.24–7.12 (m, 0.83 H), 7.09 (d, J = 8.1 Hz, 1.24 H), 7.01–6.83 (m, 2 H), 4.10 (s, 0.65 H), 3.93 (s, 0.14 H), 3.91 (s, 1.21 H); **¹³C NMR** (126 MHz, CDCl₃, δ): 155.7 (dd,

$J = 247.1$, 9.1 Hz, major), 148.7 (dd, $J = 246.0$, 10.6 Hz, major), 146.78 (dd, $J = 244.0$, 9.0 Hz, major), 138.0 (minor), 137.7 (minor), 133.2 (major), 131.9 (major), 131.7 (minor), 131.0 (minor), 130.5 (major), 130.3 (minor), 129.9 (minor), 128.6 (major), 127.8 (major), 127.4 (minor), 124.8 (minor), 124.0 (minor), 123.9 (ddd, $J = 18.1$, 4.5, 4.4 Hz, minor), 120.6 (major), 118.0 (dd, $J = 19.1$, 5.8 Hz, major), 105.4 (ddd, $J = 28.4$, 24.2, 20.9 Hz, minor), 34.2 (d, $J = 2.7$ Hz, minor), 33.8 (d, $J = 2.3$ Hz, minor), 33.7 (d, $J = 2.4$ Hz, major); **^{19}F NMR** (376 MHz, CDCl$_3$, δ): −118.8 (dt, $J = 15.0$, 6.7 Hz, 0.32 F), −119.2 (s, 0.05 F), −119.3 (dt, $J = 15.0$,7.5 Hz, 0.62 F), −136.0 (dt, $J = 20.0$, 9.5 Hz, 0.32 F), −136.1 (dt, $J = 20.4$, 9.7 Hz, 0.62 F), −136.4 (dt, $J = 20.6$, 9.6 Hz, 0.06 F), −142.7 (m, 0.06 F), −142.8 (dddd, $J = 20.8$, 15.6, 10.0, 5.9 Hz, 0.63 F), −143.0 (dddd, $J = 20.9$, 15.7, 10.3, 4.7 Hz, 0.32 F); signals corresponding to all three regioisomers are reported; **IR** (cast film, cm^{-1}): 3061 (w), 2928 (w), 1631 (s), 1511 (s), 1426 (s), 1229 (s), 1150 (s), 1012 (m), 881 (m), 748 (m), 690 (m); **HRMS** (EI) for C$_{13}$H$_8$^{81}BrF$_3$: calcd: 301.9741; found: 301.9736.
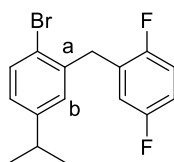
1-Bromo-2-(2,5-difluorobenzyl)-4-isopropylbenzene (3-3k): Prepared from 2,5-difluorobenzyl alcohol (72 mg, 0.50 mmol) and 4-bromo-isopropylbenzene (0.40 mL, 2.5 mmol) with boronic acid **BA-20** at 80 °C for 24 h. Purified by flash column chromatography (hexanes) and isolated as a clear oil. (without **A**: 58 mg, 35%; with **A-1**: 59 mg, 37%; with **A-6**: 111 mg, 67%, 65:35 mixture of inseparable regioisomers). **^{1}H NMR** (400 MHz, CDCl$_3$, δ): 7.51 (d, $J = 8.2$ Hz, 0.57 H), 7.48–7.37 (m, 0.50 H), 7.26–7.18 (m, 0.73 H), 7.09–6.96 (m, 2.29 H), 6.95–6.84 (m, 1.08 H), 6.75 (ddd, $J = 9.0$, 5.9, 3.2 Hz, 0.59 H), 6.61 (ddd, $J = 9.0$, 5.9, 3.2 Hz, 0.35 H), 4.11 (s, 1.32 H), 4.00 (s, 0.74 H), 3.04 (hept, $J = 6.8$ Hz, 0.35 H), 2.86 (hept, $J = 6.9$ Hz, 0.65 H), 1.23 (d, $J = 6.9$ Hz, 3.63 H), 1.17 (d, $J = 6.9$ Hz, 2.22 H); signals corresponding to two regioisomers are reported.

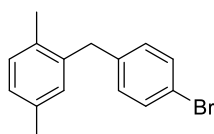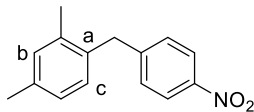**2,4-Dimethyl-1-(4-nitrobenzyl)benzene (3-3l)**: Prepared from 4-nitrobenzyl alcohol (77 mg, 0.50 mmol) and *m*-xylene (0.30 mL, 2.5 mmol) with boronic acid **BA-20**. Purified by flash column chromatography (10:1 hexanes/EtOAc) and isolated as a light-yellow solid (without **A**: <5%; with **A-1**: 16 mg, 13%; with **A-6**: 22 mg, 18%; with 1 equivalent **A-6**: 45 mg, 37%, 71:22:7 mixture of inseparable regioisomers). **^{1}H NMR** (400 MHz, CDCl$_3$, δ): 8.11 (dd, *J* = 8.8, 6.9 Hz, 1.89 H), 7.34 (d, *J* = 8.5 Hz, 0.13 H), 7.30–7.22 (m, 1.35 H), 7.20–7.06 (m, 1.04 H), 7.04–6.95 (m, 1.92 H), 6.89 (s, 0.06 H), 6.78 (s, 0.14 H), 4.15 (s, 0.43 H), 4.04 (s, 1.37 H), 3.99 (s, 0.14 H), 2.32 (s, 1.98 H), 2.28 (s, 0.42H), 2.22 (s, 1.21 H), 2.17 (s, 2.00 H); signals corresponding to all three regioisomers are reported.
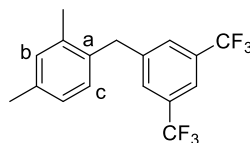
1-(3,5-Bis(trifluoromethyl)benzyl)-2,4-dimethylbenzene (3-3n): Prepared from 3,4-bis-(trifluoromethyl)benzyl alcohol (122 mg, 0.50 mmol) and *m*-xylene (0.30 mL, 2.50 mmol) with boronic acid **BA-20** at 80 °C for 24 h. Purified by flash column chromatography (hexanes) and isolated as a colorless oil (without **A**: 0 mg, 0%; with **A-1**: 38 mg, 23%; with **A-6**: 22 mg, 13%, 72:20:8 mixture of inseparable regioisomers). **^{1}H NMR** (500 MHz, CDCl$_3$, δ): 7.77–7.70 (m, 1.4 H), 7.66 (s, 0.3 H), 7.59 (s, 2 H), 7.47 (s, 0.5 H), 7.22–7.11 (m, 1 H), 7.07–6.97 (m, 3 H), 6.93 (s, 0.2 H), 6.81 (s, 0.3 H), 4.20 (s, 0.6 H), 4.09 (s, 2 H), 4.04 (s, 0.2 H), 2.35 (s, 3 H), 2.32 (s, 0.7 H), 2.25 (s, 1.5 H), 2.21 (s, 3 H); **^{13}C NMR** (126 MHz, CDCl$_3$, δ): 143.4 (major), 142.7 (minor), 138.5 (minor), 137.0 (minor), 136.9 (major), 136.2 (major), 134.5 (minor), 133.6 (major), 131.8 (minor), 131.7 (q, *J* = 32.7 Hz, major), 131.6 (major), 129.9 (major), 128.7 (d, *J* = 3.8 Hz, major), 128.6 (d, *J* = 3.8 Hz, minor), 127.9 (d, *J* = 3.8 Hz, minor), 127.3 (minor), 127.1 (major), 126.7 (minor), 123.3 (q *J* = 271.5 Hz, major), 120.1(ap. quint, *J* = 3.8 Hz, major), 41.5 (minor), 38.7 (major), 34.8 (minor), 29.7 (minor), 21.3 (minor), 21.0 (major), 20.2 (minor), 19.6

(major); **¹⁹F NMR** (376 MHz, CDCl₃, δ): −62.9 (s, minor, 0.7 F), −62.8 (s, major, 6 F), −62.7 (s, minor, 1.9 F); signals corresponding to all three regioisomers are reported; **IR** (cast film, cm^{-1}): 2926 (w), 1620 (w), 1375 (s), 1279 (s), 1172 (s), 897 (m), 706 (w), 682 (m); **HRMS** (EI) for $C_{17}H_{14}F_6$: calcd: 332.1000; found: 332.0999.
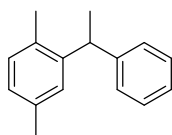
1,4-Dimethyl-2-(1-phenylethyl)benzene (3-5a): Prepared from 1-phenylethan-1-ol (61 mg, 0.50 mmol) and *p*-xylene (0.30 mL, 2.5 mmol) with boronic acid **BA-17** at room temperature for 24 h. Purified by flash column chromatography (hexane) and isolated as a colorless oil (without **A-1**: 0%; with **A-1**: 94 mg, 89%). **¹H NMR** (500 MHz, CDCl₃, δ): 7.32–7.24 (m, 2 H), 7.22–7.14 (m, 3 H), 7.10 (s, 1 H), 7.04 (d, *J* = 7.6 Hz, 1 H), 6.97 (d, *J* = 7.7 Hz, 1 H), 4.32 (q, *J* = 7.2 Hz, 1 H), 2.34 (s, 3 H), 2.21 (s, 3 H), 1.63 (d, *J* = 7.2 Hz, 3 H); **¹³C NMR** (126 MHz, CDCl₃, δ): 146.4, 143.7, 135.3, 132.9, 130.3, 128.3, 127.7, 127.5, 126.8, 125.8, 40.9, 22.1, 21.3, 19.3; **IR** (cast film, cm^{-1}): 3024 (m), 2967 (s), 2929 (m), 1601 (m), 1496 (s), 1450 (s), 1372 (m), 1030 (m), 810 (s), 699 (s); **HRMS** (EI) for $C_{16}H_{18}$: calcd: 210.1409; found: 210.1413.
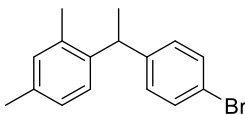
1-(1-(4-Bromophenyl)ethyl)-2,4-dimethylbenzene (3-5b): Prepared from 1-(4-bromophenyl)-ethan-1-ol (101 mg, 0.501 mmol) and *m*-xylene (0.30 mL, 2.50 mmol) with boronic acid **BA-17** at 50 °C for 24 h. Purified by flash column chromatography (hexanes) and isolated as a colorless oil (without **A-1**: 0%; with **A-1**: 127 mg, 88%). **¹H NMR** (500 MHz, CDCl₃, δ): 7.38 (d, *J* = 8.0 Hz, 2 H), 7.14 (dd, *J* = 7.9, 1.9 Hz, 1 H), 7.07–7.00 (m, 3 H), 6.98 (s, 1 H), 4.25 (q, *J* = 7.1 Hz, 1 H), 2.32 (s, 3 H), 2.20 (s, 3 H), 1.58 (d, *J* = 7.2 Hz, 3 H); **¹³C NMR** (126 MHz, CDCl₃, δ): 145.6, 140.3, 135.9, 135.8, 131.41, 131.39, 129.4, 126.8, 126.5, 119.6, 40.3, 22.1, 20.9, 19.7; **IR** (cast film, cm^{-1}): 3012 (m), 2968 (s), 2873 (m), 1487 (s), 1452 (m), 1403 (m),

1074 (s), 1010 (s), 822 (s), 793 (m); **HRMS** (EI) for C$_{16}$H$_{17}$^{81}Br: calcd: 290.0493; found: 290.0493.
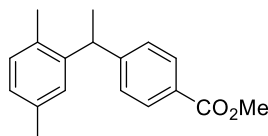
Methyl 4-(1-(2,5-dimethylphenyl)ethyl)benzoate (3-5c): Prepared from methyl 4(1-hydroxyethyl)benzoate (90 mg, 0.50 mmol) and *p*-xylene (0.30 mL, 2.5 mmol) with boronic acid **BA-17** at 80 °C for 24 h. Purified by flash column chromatography (10:1 hexanes/EtOAc) and isolated as a yellow oil (without **A-1**: 10 mg, 5%; with **A-1**: 197 mg, 88%). **^{1}H NMR** (500 MHz, CDCl$_3$, δ): 7.96 (d, *J* = 8.3 Hz, 2 H), 7.25 (d, *J* = 8.4 Hz, 2 H), 7.10–7.03 (m, 2 H), 6.99 (dd, *J* = 7.6, 1.8 Hz, 1 H), 4.36 (q, *J* = 7.2 Hz, 1 H), 3.92 (s, 3 H), 2.35 (s, 3 H), 2.19 (s, 3 H), 1.64 (d, *J* = 7.2 Hz, 3 H); **^{13}C NMR** (126 MHz, CDCl$_3$, δ): 167.1, 151.9, 142.9, 135.5, 132.9, 130.5, 129.7, 127.8, 127.7, 127.5, 127.1, 52.0, 41.1, 21.8, 21.3, 19.3; **IR** (cast film, cm^{-1}): 2968 (m), 2950 (m), 1723 (s), 1609 (m), 1501 (w), 1435 (m), 1280 (s), 1019 (m), 857 (w); **HRMS** (EI) for C$_{18}$H$_{20}$O$_2$: calcd: 264.8.1463; found: 268.1462.
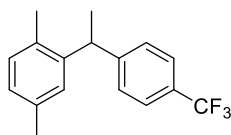
1,4-Dimethyl-2-(1-(4-(trifluoromethyl)phenyl)ethyl)benzene (3-5d): Prepared from 1-(4-(trifluoromethyl)phenyl)ethan-1-ol (95 mg, 0.50 mmol) and *p*-xylene (0.30 mL, 2.5 mmol) at 80 °C for 24 h. Purified by flash column chromatography (10:1 hexanes/EtOAc) and isolated with boronic acid **BA-17** as a colorless oil (without **A-1**: 0%; with **A-1**: 111 mg, 80%). **^{1}H NMR** (500 MHz, CDCl$_3$, δ): 7.51 (d, *J* = 7.3 Hz, 2 H), 7.26 (d, *J* = 8.3 Hz, 2 H), 7.05 (d, *J* = 1.8 Hz, 1 H), 7.04 (d, *J* = 7.6 Hz, 1 H), 6.97 (dd, *J* = 7.8, 1.8 Hz, 1 H), 4.34 (q, *J* = 7.2 Hz, 1 H), 2.33 (s, 3 H), 2.17 (s, 3 H), 1.62 (d, *J* = 7.2 Hz, 3 H); **^{13}C NMR** (126 MHz, CDCl$_3$, δ): 150.5, 142.7, 135.6, 132.9, 130.5, 128.1 (q, *J* = 32.3 Hz), 128.0, 127.4, 127.2, 125.3 (q, *J* = 3.9 Hz), 124.3 (q, *J* = 272.0 Hz), 121.1, 40.9, 21.9, 21.3, 19.3; **^{19}F NMR** (376 MHz, CDCl$_3$, δ): –62.3; **IR** (cast film, cm^{-1}): 2971 (m), 2933 (w), 1617 (m),

1500 (w), 1417 (w), 1354 (s), 1164 (s), 1123 (s), 1071 (s), 1018 (m), 842 (m), 812 (w); **HRMS** (EI) for $C_{17}H_{17}F_3$: calcd: 278.1282; found: 278.1280.
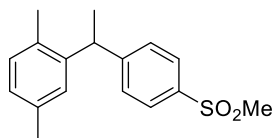
1,4-Dimethyl-2-(1-(4-(methylsulfonyl)phenyl)ethyl)benzene (3-5e): Prepared from 1-(4-(methylsulfonyl)phenyl)ethan-1-ol (100 mg, 0.50 mmol) and *p*-xylene (0.30 mL, 2.5 mmol) with boronic acid **BA-17** at 80 °C for 24 h. Purified by flash column chromatography (10: 1 hexanes/EtOAc) and isolated as a colorless oil (without **A-1**: 0%; with **A-1**: 114 mg, 79%). **¹H NMR** (500 MHz, CDCl₃, δ): 7.85 (d, *J* = 8.5 Hz, 2 H), 7.38 (d, *J* = 8.0 Hz, 2 H), 7.07 (dd, *J* = 4.7, 3.0 Hz, 3 H), 7.03–6.97 (m, 1 H), 4.40 (q, *J* = 7.2 Hz, 1 H), 3.06 (s, 3 H), 2.36 (s, 3 H), 2.19 (s, 3 H), 1.65 (d, *J* = 7.2 Hz, 3 H); **¹³C NMR** (126 MHz, CDCl₃, δ): 153.1, 142.2, 138.0, 135.7, 132.8, 130.6, 128.7, 127.5, 127.4, 77.29, 77.0, 76.8, 44.6, 41.1, 21.8, 21.2, 19.3; **IR** (cast film, cm⁻¹): 3019 (w), 2969 (m), 1596 (m), 1500 (m), 1406 (m), 1308 (s), 1151 (s), 956 (m), 814 (m), 796 (m); **HRMS** (EI) for $C_{17}H_{20}O_2S$: calcd: 288.1184; found: 288.1185.
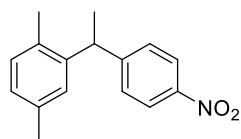
1,4-Dimethyl-2-(1-(4-nitrophenyl)ethyl)benzene (3-5f): Prepared from 1-(4-nitrophenyl)ethan-1-ol (84 mg, 0.50 mmol) and *p*-xylene (0.30 mL, 2.5 mmol) with boronic acid **BA-17** at 100 °C for 24 h. Purified by flash column chromatography (10:1 hexane:EtOAc) and isolated as a colorless oil (without **A-1**: 6.4 mg, 5%; with **A-1**: 100 mg, 78%). **¹H NMR** (500 MHz, CDCl₃, δ): 8.14 (d, *J* = 8.8 Hz, 2 H), 7.33 (d, *J* = 8.3 Hz, 2 H), 7.11–7.03 (m, 2 H), 7.01 (dd, *J* = 7.8, 1.9 Hz, 1 H), 4.41 (q, *J* = 7.2 Hz, 1 H), 2.35 (s, 3 H), 2.18 (s, 3 H), 1.66 (d, *J* = 7.2 Hz, 3 H); **¹³C NMR** (126 MHz, CDCl₃, δ): 154.2, 146.3, 142.0, 135.8, 132.8, 130.6, 128.5, 127.4, 127.4, 123.7, 41.0, 21.8, 21.2, 19.3; **IR** (cast film, cm⁻¹): 3102 (w), 2970 (m), 1601 (m), 1510 (s), 1346 (s), 857 (m), 820 (m); **HRMS** (EI) for $C_{16}H_{17}NO_2$: calcd: 255.1259; found: 255.1260.
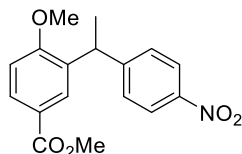
Methyl 4-methoxy-3-(1-(4-nitrophenyl)ethyl)benzoate (3-5g): Prepared from 1-(4-nitro-phenyl)ethan-1-ol (84 mg, 0.50 mmol) and methyl 4-methoxybenzoate (249 mg, 1.50 mmol) with 20 mol% of co-catalysts **BA-17** and **A-1** at 100 °C for 24 h. Purified by flash column chromatography (10:1 hexane:EtOAc) and isolated as a white solid (without **A-1**: 0%; with **A-1**: 95 mg, 60%). **^{1}H NMR** (500 MHz, CDCl$_3$, δ): 8.10 (d, J = 8.8 Hz, 2 H), 7.99–7.91 (m, 2 H), 7.34 (d, J = 8.3 Hz, 2 H), 6.86 (d, J = 8.5 Hz, 1 H), 4.58 (q, J = 7.2 Hz, 1 H), 3.89 (s, 3 H), 3.79 (s, 3 H), 1.64 (d, J = 7.3 Hz, 3 H); **^{13}C NMR** (126 MHz, CDCl$_3$, δ): 166.9, 160.6, 153.9, 146.3, 132.8, 130.3, 128.9, 128.3, 123.5, 122.6, 110.1, 77.3, 77.0, 76.8, 55.6, 52.0, 38.0, 20.5; **IR** (cast film, cm^{-1}): 3079 (w), 2972 (m), 1715 (s), 1606 (s), 1520 (s), 1374 (s), 1298 (m), 1374 (s), 1299 (m), 1257 (s), 1132 (m), 856 (m), 769 (m), 699 (m); **HRMS** (EI) for C$_{17}$H$_{17}$O$_5$N: calcd: 315.1107; Found: 315.1100.
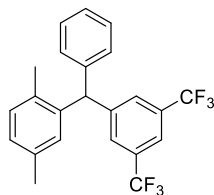
2-((3,5-Bis(trifluoromethyl)phenyl)(phenyl)methyl)-1,4-dimethylbenzene (3-7e): Prepared from (3,5-bis(trifluoromethyl)phenyl)(phenyl)methanol (160 mg, 0.502 mmol) and p-xylene (0.31 mL, 2.5 mmol) with 20 mol% boronic acid **BA-17** at 100 °C for 24 h. Purified by flash column chromatography (hexane) and isolated as a white solid (without **A-1**: 0%, with **A-1**: 180 mg, 88%). **^{1}H NMR** (600 MHz, CDCl$_3$, δ): 7.77 (s, 1 H), 7.52 (s, 2 H), 7.33 (t, J = 7.4 Hz, 2 H), 7.30–7.26 (m, 1 H), 7.10 (d, J = 7.7 Hz, 1 H), 7.04–7.00 (m, 3 H), 6.52 (s, 1 H), 5.76 (s, 1 H), 2.23 (s, 3 H), 2.17 (s, 3 H); **^{13}C NMR** (151 MHz, CDCl$_3$, δ): 146.6, 141.6, 140.3, 135.8, 133.5, 131.7 (q, J = 33.0 Hz) 130.9, 129.9, 129.7 (m), 129.6, 128.9, 128.0, 127.2, 123.5 (q, J = 271.0 Hz), 120.7 (sept, J = 3.7 Hz), 53.3, 21.3, 19.6. **^{19}F NMR** (376 MHz, CDCl$_3$, δ): −62.7 (s, 6F); **IR** (cast film, cm^{-1}): 3063 (w), 2983 (w), 1496 (m), 1372 (s),

1278 (s), 1170 (s), 1134 (s), 1110 (m), 899 (m), 701 (m); **HRMS** (EI) for C$_{23}$H$_{18}$F$_6$: calcd: 408.1313; found: 408.1317.
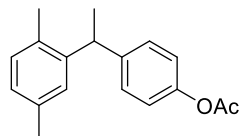
4-(1-(2,5-Dimethylphenyl)ethyl)phenyl acetate (3-5h): Prepared from 4-(1-hydroxy-ethyl)phenyl acetate **3-4h** (90 mg, 0.50 mmol) and *p*-xylene (0.30 mL, 2.5 mmol) at 80 °C for 24 h. Purified by flash column chromatography (hexanes) and isolated as a light-yellow oil (102 mg, 76%). **^{1}H NMR** (500 MHz, CDCl$_3$, δ): 7.21–7.17 (m, 2 H), 7.09 (s, 1 H), 7.05 (d, *J* = 7.6 Hz, 1 H), 7.03–7.00 (m, 2 H), 6.99–6.96 (m, 1 H), 4.32 (q, *J* = 7.2 Hz, 1 H), 2.35 (s, 3 H), 2.31 (s, 3 H), 2.22 (s, 3 H), 1.62 (d, *J* = 7.2 Hz, 3 H); **^{13}C NMR** (126 MHz, CDCl$_3$, δ): 169.6, 148.7, 143.8, 143.5, 135.4, 132.9, 130.4, 128.6, 127.4, 126.9, 121.2, 40.4, 22.1, 21.3, 21.2, 19.3; **IR** (cast film, cm^{-1}): 3027 (w), 2968 (m), 2930 (m), 1768 (s), 1612 (w), 1505 (s), 1369 (m), 1219 (s), 1200 (s), 1167 (m), 1018 (m), 911 (m), 849 (m), 810 (m); **HRMS** (EI) for C$_{18}$H$_{20}$O$_2$: calcd: 264.8.1463; found: 268.1464.

3.8.6 Mechanistic Studies

3.8.6.1 Procedure for ^{11}B NMR Studies with Boronic Acid Catalyst and Co-catalyst A-1

A solution of boronic acid catalyst **BA** (0.05 mmol) in HFIP/CH$_3$NO$_2$ (4:1, 0.5 mL) with 1.0 equivalent or without co-catalyst **A-1** was stirred at room temperature for 24 h. The solvent was removed under reduced pressure. The reaction mixture was dissolved in CD$_3$CN (0.7 mL) and analysed by ^{11}B NMR analysis.

3.8.6.2 Control Experiments to Assess a Potential Role for Co-catalyst A-1

Boronic acid **BA-17** (4.7 mg, 0.025 mmol) and diol (1 equiv) in a solution of HFIP/CH$_3$NO$_2$ (4:1, 0.5 mL) were stirred at room temperature for 24 h. After 24 h, a 5 μL aliquot of the reaction mixture was diluted with CH$_3$CN (1 mL) and submitted for low resolution ESI analysis. A 0.2 mL sample of CD$_3$CN was added to the remaining reaction mixture and submitted for ^{11}B NMR analysis.

3.8.6.3 Effect of 2,6-Di-*tert*-butylpyridine on the Catalytic Species

Boronic acid **BA-17** (9.4 mg, 0.050 mmol) and co-catalyst **A-1** (8.5 µL, 0.050 mmol) in a solution of HFIP/CH$_3$NO$_2$ (4:1, 0.5 mL) with 1.5 equivalents or without 2,6-di-*tert*-butylpyridine were stirred at 50 °C for 2 h. After 2 h, a 5 µL aliquot of the reaction mixture was diluted with CH$_3$CN (1 mL) and submitted for low resolution ESI analysis. A 0.2 mL sample of CD$_3$CN was added to the remaining reaction mixture and submitted for ^{11}B NMR analysis.

3.8.6.4 Effect of Molecular Sieves and Anhydrous Solvents

A flask charged with activated powdered 3 Å molecular sieves (250 mg) and a magnetic stir bar was flame-dried and allowed to cool to room temperature under vacuum three times. After cooling to room temperature the final time, the flask was back-filled with nitrogen and charged with 4-bromobenzyl alcohol (94 mg, 0.50 mmol), dry *p*-xylene (distilled and dried over 3 Å molecular sieves) (0.3 mL, 2.50 mmol), catalyst **BA-20** (23 mg, 0.050 mmol), additive **A-1** (9.0 µL, 0.050 mmol), anhydrous HFIP (distilled and dried over 3 Å molecular sieves) (0.80 mL), and anhydrous CH$_3$NO$_2$ (distilled from MgSO$_4$ and dried over calcium sulfate) (0.20 mL). The flask was sealed with a septum and stirred at 50 °C for 1 h. After cooling to room temperature, the crude reaction mixture was filtered through a pipette of silica gel with EtOAc (50 mL). The reaction mixture was concentrated under reduced pressure, followed by addition of 1,4-dinitrobenzene (21 mg, 0.13 mmol) and analysed by ^{1}H NMR spectroscopy. The Friedel–Crafts product **3-3f** was not observed and alcohol **3-1f** was detected in 98% recovery.

3.8.7 Comparison with other Brønsted Acid Catalysts
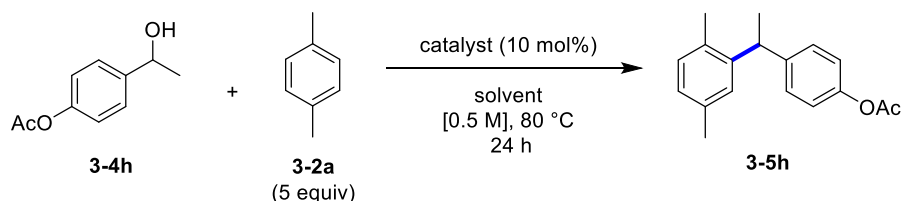
In a vial equipped with a stir bar, 4-(1-hydroxyethyl)phenyl acetate **3-4h** (90 mg, 0.50 mmol), *p*-xylene (0.30 mL, 2.5 mmol), and catalyst (10 mol%) were dissolved in HFIP/CH$_3$NO$_2$ (4:1, 1 mL). The reaction was stirred at 80 °C for 24 h, after which,

the reaction mixture was concentrated and dried under vacuum. 1,4-Dinitrobenzene (10 mg, 0.060 mmol) was added as an internal standard and yields were determined by crude ^{1}H NMR analysis.

3.9 References

(1)   Mondal, S.; Panda, G. *RSC Adv* **2014**, *4*, 28317–28358.

(2)   Gennari, L.; Merlotti, D.; Martini, G.; Nuti, R. *Expert Opin. Investig. Drugs* **2006**, *15*, 1091–1103.

(3)   Rovner, E. S. *Expert Opin. Pharmacother.* **2005**, *6*, 653–666.

(4)   Finder, R. M.; Brogden, R. N.; Sawyer, P. R.; Speight, T. M.; Spencer, R.; Avery, G. S. *Drugs* **1976**, *12*, 1–40.

(5)   Tsutsui, C.; Yamada, Y.; Ando, M.; Toyama, D.; Wu, J.; Wang, L.; Taketani, S.; Kataoka, T. *Bioorg. Med. Chem. Lett.* **2009**, *19*, 4084–4087.

(6)   Nair, V.; Thomas, S.; Mathew, S. C.; Abhilash, K. G. *Tetrahedron* **2006**, *62*, 6731–6747.

(7)   Nambo, M.; Crudden, C. M. *ACS Catal.* **2015**, *5*, 4734–4742.

(8)   Olah, G. A.; Kobayashi, S.; Tashiro, M. *J. Am. Chem. Soc.* **1972**, *94*, 7448–7461.

(9)   Friedel, C. R.; Crafts, J. M. *Compt. Rend.* **1877**, *84*, 1450–1454.

(10)   Tsuchimoto, T.; Tobita, K.; Hiyama, T.; Fukuzawa, S. *Synlett* **1996**, 557–559.

(11)   Sarca, V. D.; Laali, K. K. *Green Chem.* **2006**, *8*, 615–620.

(12)   Noji, M.; Ohno, T.; Fuji, K.; Futaba, N.; Tajima, H.; Ishii, K. *J. Org. Chem.* **2003**, *68*, 9340–9347.

(13)   Bonrath, W.; Dittel, C.; Giraudi, L.; Netscher, T.; Pabst, T. *Catal. Today* **2007**, *121*, 65–70.

(14)   Iovel, I.; Mertins, K.; Kischel, J.; Zapf, A.; Beller, M. *Angew. Chem. Int. Ed.* **2005**, *44*, 3913–3917.

(15)   Mertins, K.; Iovel, I.; Kischel, J.; Zapf, A.; Beller, M. *Angew. Chem. Int. Ed.* **2005**, *44*, 238–242.

(16)   Mertins, K.; Iovel, I.; Kischel, J.; Zapf, A.; Beller, M. *Adv. Synth. Catal.* **2006**, *348*, 691–695.

(17)   Choudhury, J.; Podder, S.; Roy, S. *J. Am. Chem. Soc.* **2005**, *127*, 6162–6163.

(18)   Yadav, J. S.; Bhunia, D. C.; Vamshi Krishna, K.; Srihari, P. *Tetrahedron Lett.* **2007**, *48*, 8306–8310.

(19)   Qin, Q.; Xie, Y.; Floreancig, P. E. *Chem. Sci.* **2018**, *9*, 8528–8534.

(20)   Rueping, M.; Nachtsheim, B. J.; Ieawsuwan, W. *Adv. Synth. Catal.* **2006**, *348*, 1033–1037.

(21)   Yasuda, M.; Somyo, T.; Baba, A. *Angew. Chem. Int. Ed.* **2006**, *45*, 793–796.

(22)   Sun, H.-B.; Li, B.; Chen, S.; Li, J.; Hua, R. *Tetrahedron* **2007**, *63*, 10185–10188.

(23)   Niggemann, M.; Meel, M. J. *Angew. Chem. Int. Ed.* **2010**, *49*, 3684–3687.

(24)   Sun, G.; Wang, Z. *Tetrahedron Lett.* **2008**, *49*, 4929–4932.

(25)   Sanz, R.; Martínez, A.; Miguel, D.; Álvarez-Gutiérrez, J. M.; Rodríguez, F. *Adv. Synth. Catal.* **2006**, *348*, 1841–1845.

(26)   Le Bras, J.; Muzart, J. *Tetrahedron* **2007**, *63*, 7942–7948.

(27)   Vuković, V. D.; Richmond, E.; Wolf, E.; Moran, J. *Angew. Chem. Int. Ed.* **2017**, *56*, 3085–3089.

(28)   Motokura, K.; Nakagiri, N.; Mizugaki, T.; Ebitani, K.; Kaneda, K. *J. Org. Chem.* **2007**, *72*, 6006–6015.

(29)   Desroches, J.; Champagne, P. A.; Benhassine, Y.; Paquin, J.-F. *Org. Biomol. Chem.* **2015**, *13*, 2243–2246.

(30)   Zheng, H.; Hall, D. G. *Aldrichimica Acta* **2014**, *47*, 41–51.

(31)   Hall, D. G. *Chem. Soc. Rev.* **2019**, *48*, 3475–3496.

(32)   Hall, D. G., Ed. *Boronic Acids: Preparation and Applications in Organic Synthesis*, 2nd edn.; Wiley-VCH: Weinheim, 2011.

(33)   McCubbin, J. A.; Hosseini, H.; Krokhin, O. V. *J. Org. Chem.* **2010**, *75*, 959–962.

(34)   Ricardo, C. L.; Mo, X.; McCubbin, J. A.; Hall, D. G. *Chem. - Eur. J.* **2015**, *21*, 4218–4223.

(35)   Mo, X.; Yakiwchuk, J.; Dansereau, J.; McCubbin, J. A.; Hall, D. G. *J. Am. Chem. Soc.* **2015**, *137*, 9694–9703.

(36)   Mo, X.; Morgan, T. D. R.; Ang, H. T.; Hall, D. G. *J. Am. Chem. Soc.* **2018**, *140*, 5264–5271.

(37)   Wolf, E.; Richmond, E.; Moran, J. *Chem. Sci.* **2015**, *6*, 2501–2505.

(38)   Gillis, E. P.; Eastman, K. J.; Hill, M. D.; Donnelly, D. J.; Meanwell, N. A. *J. Med. Chem.* **2015**, *58*, 8315–8359.

(39)   Purser, S.; Moore, P. R.; Swallow, S.; Gouverneur, V. *Chem. Soc. Rev.* **2008**, *37*, 320–330.

(40)   Ojima, I. *Fluorine in Medicinal Chemistry and Chemical Biology*; John Wiley & Sons, 2009.

(41)   Laird, T. *Org. Process Res. Dev.* **2003**, *7*, 225–225.

(42)   Estopiñá-Durán, S.; Donnelly, L. J.; Mclean, E. B.; Hockin, B. M.; Slawin, A. M. Z.; Taylor, J. E. *Chem. Eur. J.* **2019**, *25*, 3950–3956.

(43)   Moore, A. N.; Wayner, D. *Can. J. Chem.* **1999**, *77*, 681–686.

(44)   Brown, H. C.; Kanner, B. *J. Am. Chem. Soc.* **1966**, *88*, 986–992.

(45)   Ishihara, K.; Nakamura, S.; Kaneeda, M.; Yamamoto, H. *J. Am. Chem. Soc.* **1996**, *118*, 12854–12855.

(46)   Ishihara, K.; Kaneeda, M.; Yamamoto, H. *J. Am. Chem. Soc.* **1994**, *116*, 11179–11180.

(47)   Jiang, Z.-Y.; Wu, J.-R.; Li, L.; Chen, X.-H.; Lai, G.-Q.; Jiang, J.-X.; Lu, Y.; Xu, L.-W. *Cent. Eur. J. Chem.* **2010**, *8*, 669–673.

(48)   Li, Y.; Xiong, Y.; Li, X.; Ling, X.; Huang, R.; Zhang, X.; Yang, J. *Green Chem.* **2014**, *16*, 2976–2981.

(49)   Vuković, V. D.; Richmond, E.; Wolf, E.; Moran, J. *Angew. Chem. Int. Ed.* **2017**, *56*, 3085–3089.

(50)   Jin, T.; Himuro, M.; Yamamoto, Y. *Angew. Chem. Int. Ed.* **2009**, *48*, 5893–5896.

(51)   Gonzalez-Rodriguez, C.; Escalante, L.; Varela, J. A.; Castedo, L.; Saa, C. *Org. Lett.* **2009**, *11*, 1531–1533.

(52)   Sato, Y.; Aoyama, T.; Takido, T.; Kodomari, M. *Tetrahedron* **2012**, *68*, 7077–7081.

(53)   Kuznetsov, A.; Makarov, A.; Rubtsov, A. E.; Butin, A. V.; Gevorgyan, V. *J. Org. Chem.* **2013**, *78*, 12144–12153.

(54)   Patil, D. V.; Kim, S. W.; Nguyen, Q. H.; Kim, H.; Wang, S.; Hoang, T.; Shin, S. *Angew. Chem. Int. Ed.* **2017**, *56*, 3670–3674.

(55)   Zheng, H.; Ghanbari, S.; Nakamura, S.; Hall, D. G. *Angew. Chem. Int. Ed.* **2012**, *51*, 6187–6190.

(56)   Verdelet, T.; Ward, R. M.; Hall, D. G. *Eur. J. Org. Chem.* **2017**, 5729–5738.

(57)   Soni, R.; Hall, T. H.; Mitchell, B. P.; Owen, M. R.; Wills, M. *J. Org. Chem.* **2015**, *80*, 6784–6793.

(58)   Jeyakumar, K.; Chakravarthy, R. D.; Chand, D. K. *Catal. Commun.* **2009**, *10*, 1948–1951.

(59)   Saito, T.; Nishimoto, Y.; Yasuda, M.; Baba, A. *J. Org. Chem.* **2006**, *71*, 8516–8522.

(60)   Munoz, S. B.; Ni, C.; Zhang, Z.; Wang, F.; Shao, N.; Mathew, T.; Olah, G. A.; Prakash, G. S. *Eur. J. Org. Chem.* **2017**, 2322–2326.

CHAPTER 4

Development of Enantioselective Desymmetrization of Prochiral 1,3-Diols Using a Rationally Designed Chiral Hemiboronic Acid Catalyst §

4.1 Introduction

4.1.1 Enantioselective Desymmetrization of 2-Substituted 1,3-Propanediols

Enantioselective desymmetrization of simple symmetrical substrates, such as meso- and prochiral diols, is a powerful strategy for the preparation of useful optically active building blocks in organic synthesis.[1,2] Unlike kinetic resolution strategies, where only a maximum yield of 50% can be achieved, enantioselective desymmetrization methodologies, in theory, can provide an enantioenriched product in quantitative yields (Figure 4-1).
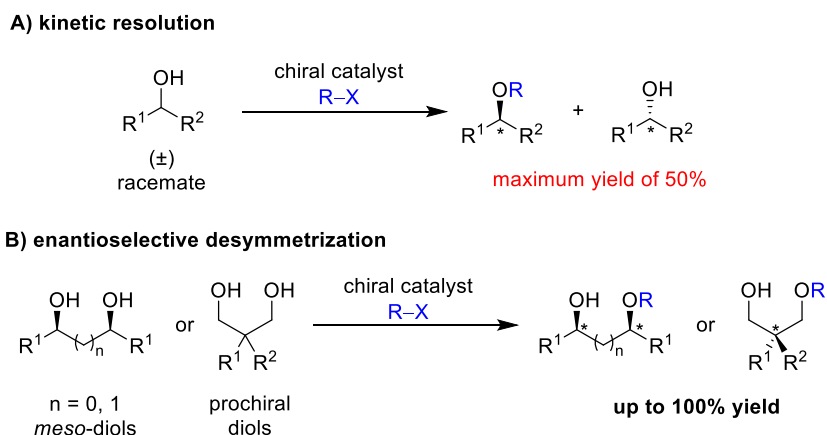
Figure 4-1 Catalytic asymmetric synthesis of optically enriched alcohols.

Traditionally, enzymatic methods have been employed for such transformations. While excellent enantioselectivities can be achieved, their uses often

---

§ A version of this chapter has been published as Estrada, C. D.; Ang, H. T.; Vetter, K.-M.; Ponich, A. A.; Hall, D. G. *J. Am. Chem. Soc.* **2021**, *143*, 4162–4167.

are restricted by numerous limitations, such as substrate specificity, accessibility to only one enantiomeric form, and irreproducibility. In this regard, non-enzymatic catalytic methods, which demonstrate a broader substrate scope, have emerged as promising alternatives for the direct and selective desymmetrization of symmetrical diols. Furthermore, with non-enzymatic methods, both enantiomers of the product can be accessed easily from the same starting material simply by switching the chirality of the catalyst.

While enantioselective desymmetrization of *meso*-1,2-diols has been studied widely, only a limited number of procedures are available for 1,3-diols, particularly 2-substituted 1,3-propanediols. Desymmetrization of 2-substituted 1,3-propanediols is inherently challenging, as the prochirality center is positioned further away from the reaction site. Thus, it is more difficult for the prochirality center to exert a differentiation of the enantiotopic hydroxy groups. Furthermore, primary alcohols are more reactive than secondary alcohols, thus difunctionalization often is observed with such 1,3-diols. Despite the challenges, numerous efforts toward the desymmetrization of such diols have been reported, which mostly include indirect,[3,4] intramolecular,[5–9] and other catalytic methods[10–16] for the desymmetrization of specific classes of substrates, such as 2-heteroatom substituted 1,3-diols (Figure 4-2).
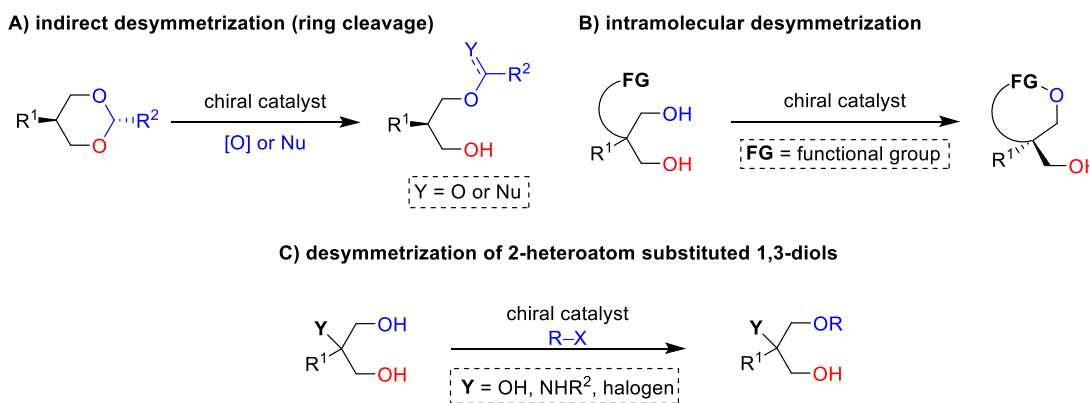
Figure 4-2 Common catalytic strategies for enantioselective desymmetrization of 2-substituted 1,3-diols.

Among the reported catalytic systems, there is only a few examples of direct intermolecular desymmetrization of 2-alkyl/aryl 1,3-propanediols. In 2002, Oriyama and co-workers reported the first non-enzymatic direct desymmetrization of 2-alkyl-

1,3-propanediols with a proline-derived diamine catalyst affording the desymmetrized product in high enantioselectivity (Scheme 4-1A).[17] However, in all cases, the desymmetrized products were obtained in a low yield, as the reaction proceeds via a non-selective monofunctionalization of diols to afford a racemic mixture of monoacetate first, then a subsequent kinetic resolution of the monoacetate to furnish the desymmetrized products, along with a substantial amount of diester as a by-product.

A) Oriyama, 2002 (proline-derived diamine catalyst)

(0.5 mol%)
i-Pr$_2$NEt (1.5 equiv)

4Å MS, CH$_2$Cl$_2$
−78 °C, 3 h

R-OH / R-OH + R^{1}COCl (1.5 equiv) → [R–OCOR^1 / OH] (±) → R–OCOR^1 / OH (22–33% yield; 85–98% ee) + R–OCOR^1 / OCOR^1 (50–67% yield)
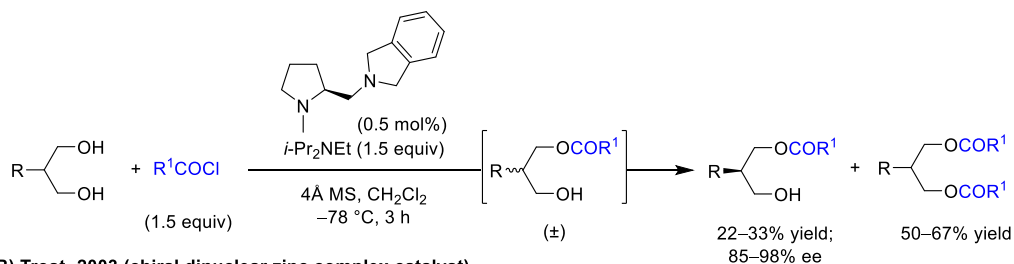
B) Trost, 2003 (chiral dinuclear zinc complex catalyst)

4-1 (5 mol%)
Et$_2$Zn (10 mol%)

toluene, −15 °C

R-OH / R-OH + vinyl OCOPh (5 equiv) → R–OCOPh / OH (78–99% yield; 59–93% ee) + R–OCOPh / OCOPh (<5% yield)

dinuclear zinc complex
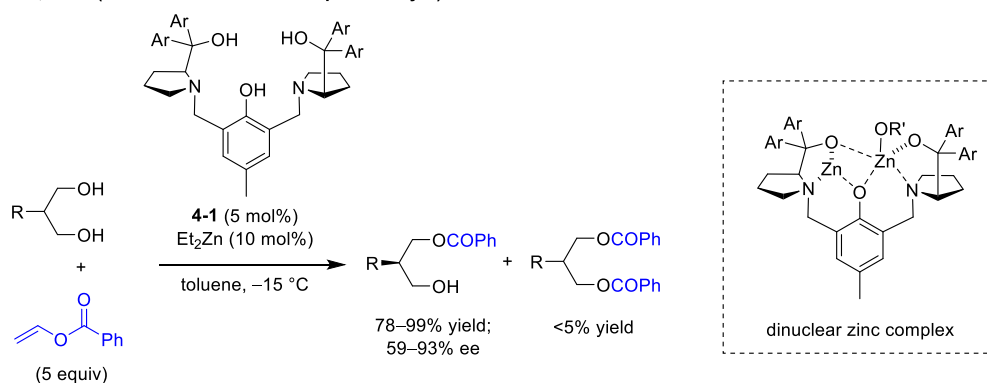
C) Fujimoto, 2012 (chiral aminophosphonite catalyst)

OPPh$_2$
NMe$_2$ (5 mol%)

i-Pr$_2$NEt (1.5 equiv)

4Å MS, toluene
0 °C

R-OH / R-OH + R^{1}COCl (1.5 equiv) → R–OCOR^1 / OH (55–78% yield; 42–67% ee) + R–OCOR^1 / OCOR^1 (7–19% yield)
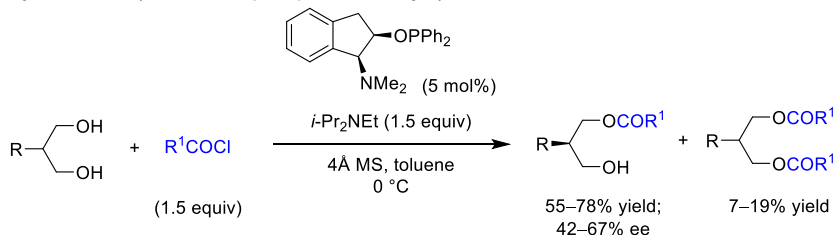
D) Suga, 2018 (chiral DMAP catalyst)

chiral DMAP (0.1 mol%)
TMEDA (1.5 equiv)

toluene, −60 °C

R^1/R^2-OH / OH + (i-PrCO)$_2$CO (1.1 equiv) → R^1/R^2–OCOi-Pr / OH (48–90% yield; 8–90% ee) + R^1/R^2–OCOi-Pr / OCOi-Pr (3–28% yield)

chiral DMAP

149

A more generic desymmetrization protocol was introduced by Trost and co-workers using a chiral dinuclear zinc catalyst generated *in situ* from diethyl zinc and ProPhenol **4-1** (Scheme 4-1B).[18,19] Using the dinuclear zinc catalyst, a series of 2-aryl-1,3-proponediols was desymmetrized, with good to excellent enantioselectivity and minimal difunctionalization (<5 mol%) via esterification with vinyl benzoate at −15 °C. It was proposed that the diarylcarbinol moieties in ligand **4-1** establish the chiral environment responsible for the good enantioselectivity. Fujimoto and co-workers also developed a chiral aminophosphonite catalytic system for the enantioselective desymmetrization of symmetrical diols via acylation (Scheme 4-1C).[20] While excellent enantioselectivity and minimal difunctionalization were observed with *meso*-1,2-diols, desymmetrization of 2-substituted 1,3-propanediols resulted in moderate enantioselectivity and a considerable amount of difunctionalized by-product. More recently, Suga and co-workers discovered a chiral 4-dimethylaminopyridine (DMAP) derivative bearing a 1,1'-binaphthyl unit as a suitable catalyst for the desymmetrization of prochiral 1,3-propanediols via acylation with isobutyric anhydride at −60 °C (Scheme 4-1D).[21] However, a large deviation in enantioselectivity and moderate difunctionalization were observed across the 14 substrates examined. In general, it was found that this catalytic system is more efficient for 2,2-disubstituted 1,3-propanediols as compared to 2-substituted 1,3-propanediols.

While these protocols generate monofunctionalized 2-substituted 1,3-propanediols with moderate to high enantioselectivities, their uses are restricted by the large variation in enantioselectivity, competing difunctionalization, and the need of cryogenic conditions. Moreover, these desymmetrization procedures are limited also to acylation reactions, which result in base-sensitive acylated products. Therefore, there is still a need for mild and general organocatalytic strategies for the desymmetrization of 2-substituted 1,3-propanediols to access optically enriched *O*-functionalized products with complementary groups. For instance, due to their

stability and ease of removal by hydrogenolysis or Lewis acids, benzylic ethers would be an ideal option.

4.1.2 Boronic Acid Catalysis in Monofunctionalization of Diols

In this context, it was envisioned that boronic acids, which are known to provide nucleophilic activation to diols, would offer a potential solution to the paucity of methodologies for the desymmetrization of 2-substituted 1,3-propanediols. Nucleophilic activation of diols by boronic acids can be achieved under basic conditions by forming a transient tetravalent anionic boronate complex, which increases the nucleophilicity of the oxygen atoms of the diol moiety, as the negative charge is distributed across the heteroatom substituents on the boron center (Chapter 1). Compared to boronic acids, greater advances have been achieved in regioselective monofunctionalization of polyols using diarylborinic acid catalysts,[22] as exemplified by the benchmark diphenylborinic acid catalyst introduced by Taylor and co-workers in 2012 (Scheme 4-2A).[23]
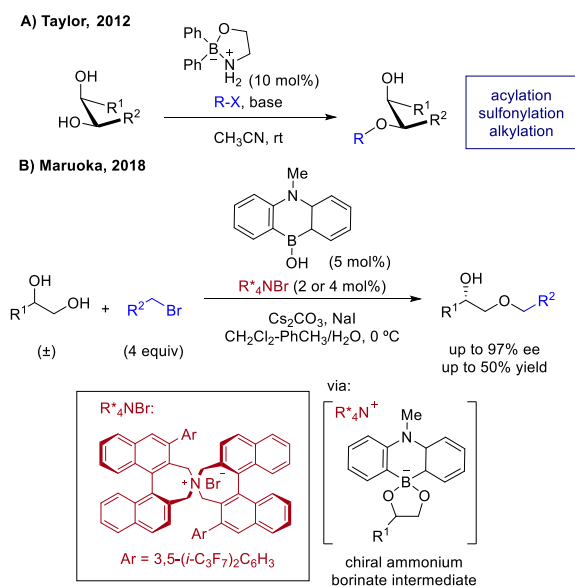
Scheme 4-2 A) Borinic acid catalyzed regioselective monofunctionalization of polyols. B) Alkylative kinetic resolution of vicinal diols via chiral ammonium-borinate catalysis.

However, the use of borinic acids comes with its own limitations. Apart from the instability of borinic acids toward oxidation, another major drawback of the use of borinic acids in asymmetric transformations is the lack of methods to render this

scaffold chiral. Although examples of enantioselective functionalization of vicinal diols were reported, these systems typically require a chiral co-catalyst in addition to the achiral borinic acid catalyst.[24,25] For instance, Maruoka and co-workers disclosed the use of a chiral ammonium salt, along with a borinic acid catalyst, in the alkylative kinetic resolution of vicinal diols via the formation of a chiral ammonium-borinate intermediate (Scheme 4-2B).[24]

On the other hand, owing to their increased stability toward oxidation as compared to borinic acids, boronic acids have emerged as an attractive alternative catalyst for the monofunctionalization of polyols. Several boronic acids, including hemiboronic acids, have been reported as suitable catalysts for such transformations in the past decade (Figure 4-3A).[26–30]
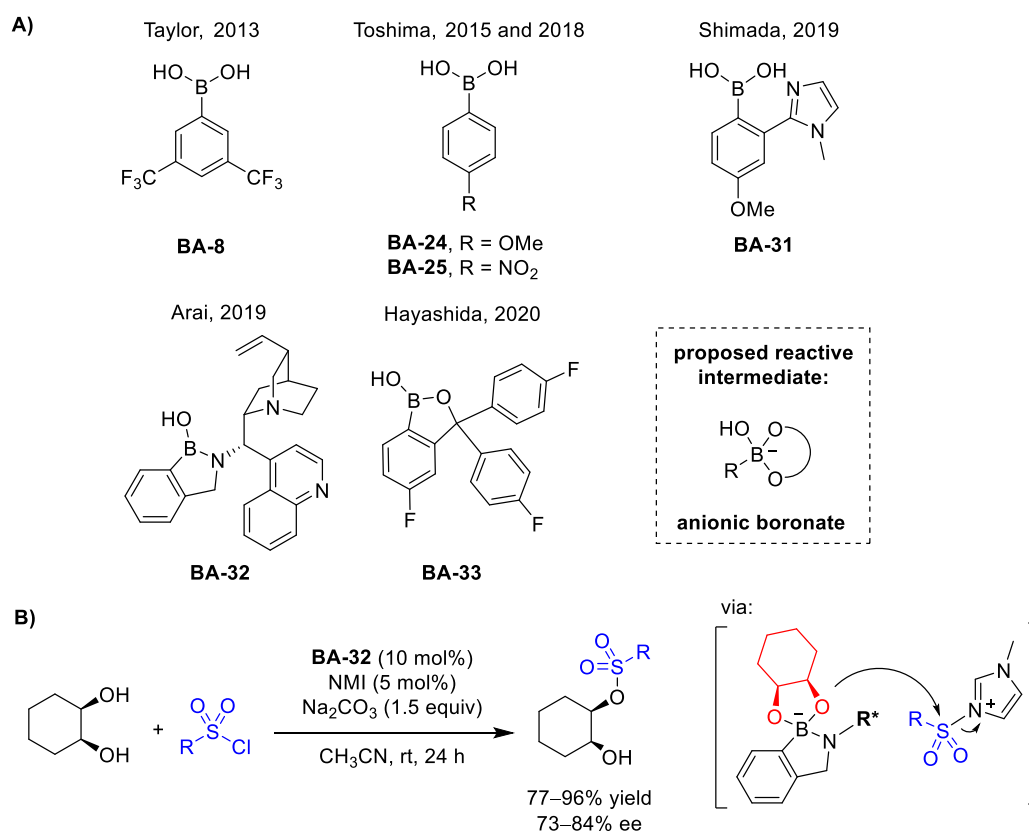
Figure 4-3 A) Examples of boronic acid catalysts for the monofunctionalization of polyols. B) Enantioselective desymmetrization of *meso*-1,2-diols with chiral benzazaborole **BA-32** catalyst.

Another notable advantage offered by boronic acids, as compared to borinic acids, is the ease of scaffold modifications, which may make it possible to embed

chirality into boronic acids. To date, however, asymmetric transformations of diols using a chiral organoboron catalyst are scarce. The only example was disclosed by Arai and co-workers, where they successfully rendered the benzazaborole scaffold of catalyst **BA-32** chiral for the enantioselective desymmetrization of *meso*-1,2-diols via sulfonylation (Figure 4-3B).[29] This asymmetric system, however, is limited to *cis*-1,2-cyclohexanediol to deliver the corresponding products in high yield and moderate to good enantioselectivities. Therefore, there remains a challenge to develop chiral boronic acid derivatives as catalysts for enantioselective transformation of diols.

4.2 Preliminary Discovery of a Chiral Hemiboronic Acid Catalyst by Previous Group Members

Motivated by the high demand for highly selective methodologies for the desymmetrization of 2-substituted-1,3-propanediols, this project was instigated by Kim-Marie Vetter, a visiting research intern, then followed up and further expanded by Carl D. Estrada, a Masters student, with the help of Ashley A. Ponich, an undergraduate summer research student. This section will describe their efforts toward the discovery of the first generation chiral hemiboronic acid catalyst for the enantioselective desymmetrization of 2-aryl-1,3-propanediols via *O*-alkylation. Therefore, all experiments disclosed in this section were conducted by these three colleagues.

4.2.1 Discovery of 9-Hydroxy-9,10-boroxarophenanthrene for Catalytic Monofunctionalization of Diols

The initial exploration of an improved boronic acid catalyst scaffold for the monofunctionalization of diols was performed by Kim-Marie Vetter. To identify potential organoboron acid catalysts, a range of cyclic hemiboronic acids was screened in the monosulfonylation of pinanediol with tosyl chloride using the reaction conditions reported by Taylor and co-workers for their diphenylborinic acid catalytic system (Scheme 4-3).[23] Only the 9-hydroxy-9,10-boroxarophenanthrene **BA-43** was found to exhibit a comparable catalytic activity to Taylor's diphenylborinic acid ethanolamine ester catalyst. Boroxarophenanthrene **BA-43** was reported first by Dewar in 1959,[31] and its ability to undergo rapid and reversible exchange with

alcohols was studied by Philp and co-workers.[32,33] While **BA-43** has been reported as a useful synthetic intermediate to prepare triaryls, 3,4-benzocoumarins, and *o*-phenylene oligomers,[34,35] its use in catalysis has not been reported yet.
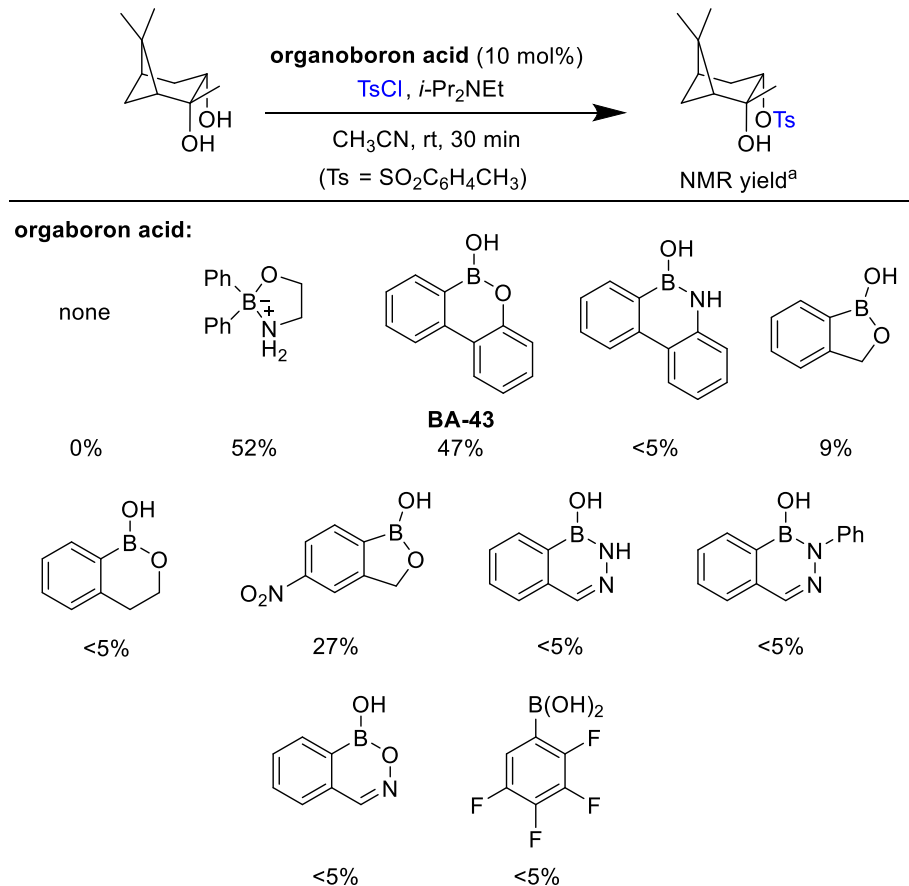
Scheme 4-3 Screening of organoboron acids in the monosulfonylation of pinanediol.

Next, the efficacy of catalyst **BA-43** in the monobenzylation of diols was assessed in comparison with that of diphenylborinic acid by Carl Estrada and Ashley Ponich. Using the reaction conditions reported by Taylor and co-workers,[23] monobenzylation of a series of 1,2- and 1,3-diols was realized with good yields and high selectivities (Scheme 4-4). In general, the efficiency of **BA-43** was on par with diphenylborinic acid. Notably, catalyst **BA-43** was found to be more efficient than diphenylborinic acid in effecting the monobenzylation of 2-phenyl-1,3-propanediol.

This result strongly suggested a potential for enantioselective desymmetrization of 2-aryl-1,3-propanediol via *O*-benzylation using a chiral variant of **BA-43**.
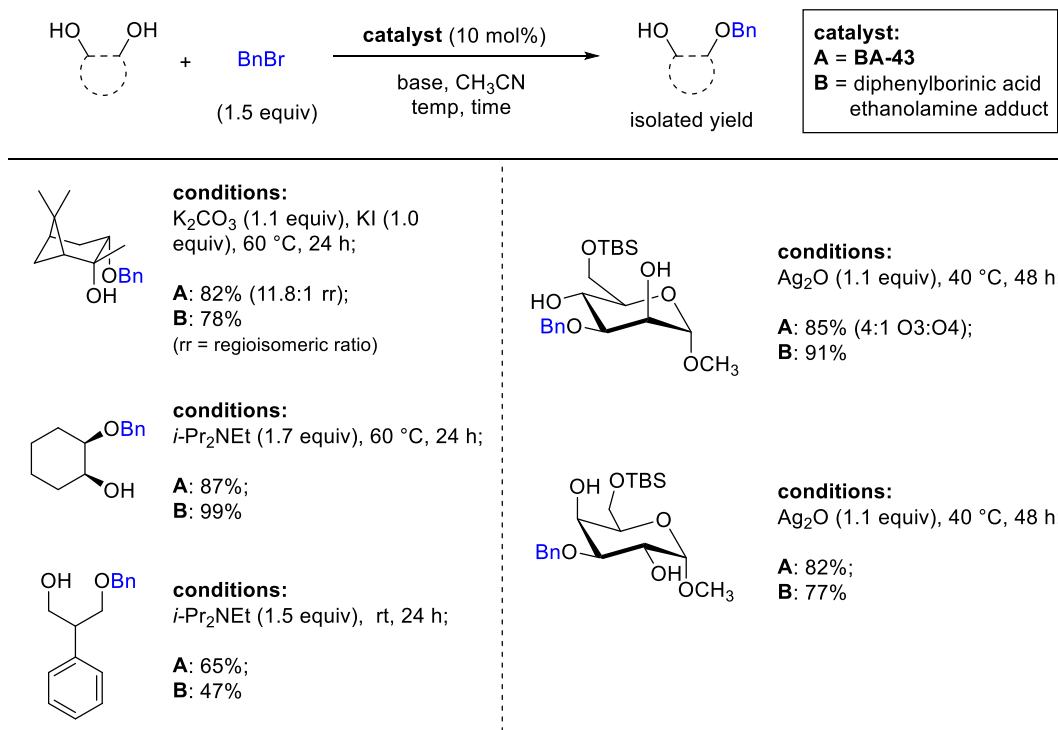
Scheme 4-4 Comparison of boroxarophenanthrene **BA-43** and diphenylborinic acid in the monobenzylation of 1,2- and 1,3-diols.

As mentioned above, diol activation of catalyst **BA-43** is expected to occur through a tetravalent anionic boronate intermediate. The ability of **BA-43** to form a tetrahedral anionic boronate species with 1,3-propanediol in solution was suggested previously by Philp and co-workers, where they observed an upfield ^{11}B NMR shift (–0.4 ppm, in d_6-acetone).[33] To confirm the formation of a tetravalent boronate intermediate under the BAC conditions for *O*-alkylation further, ^{11}B NMR analysis of a mixture of equimolar **BA-43**, 2-phenyl-1,3-propanediol **4-2a** and potassium carbonate in CD₃CN was conducted (Figure 4-4). Expectably, an upfield shift of 2.8 ppm, corresponding to a tetravalent intermediate **4-3a,** was observed. The formation of intermediate **4-3a** was supported also by ESI-HRMS analysis.
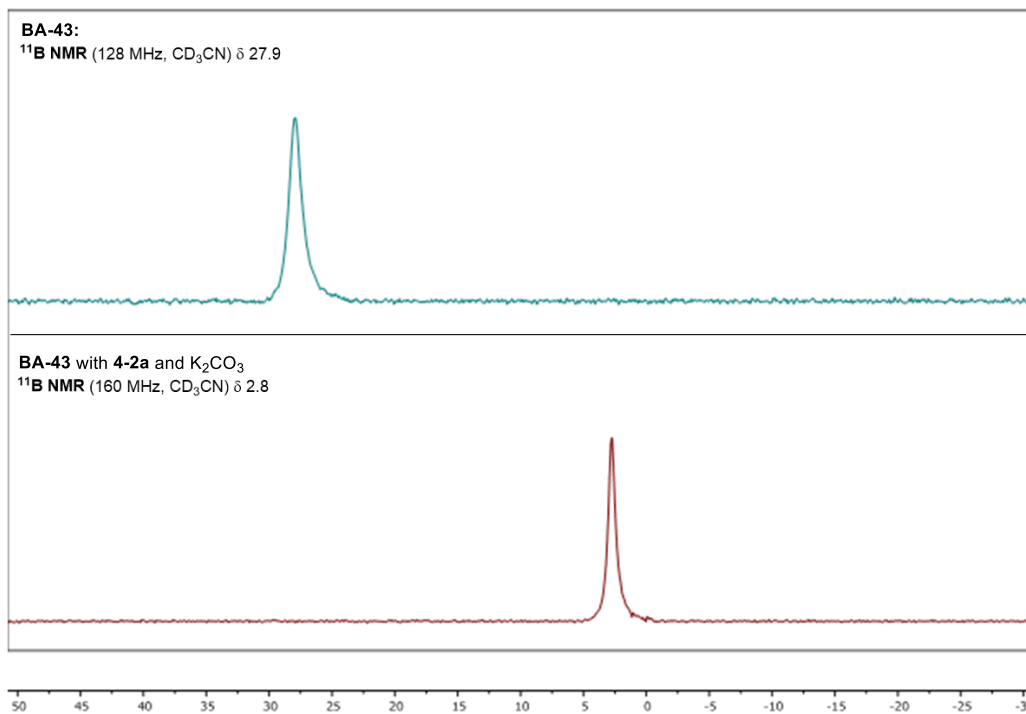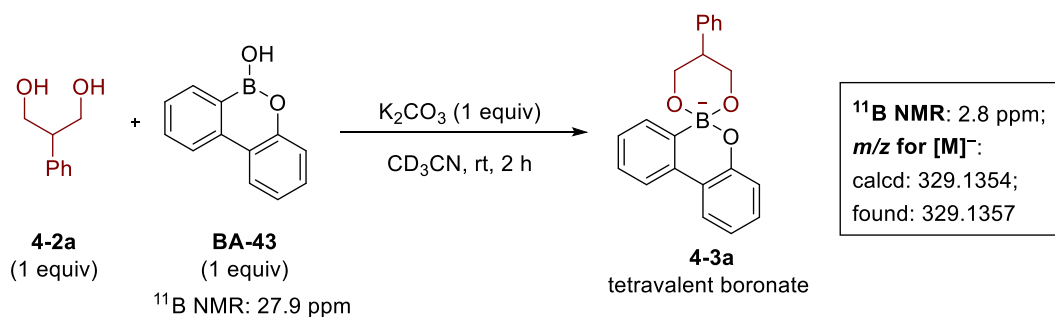
Figure 4-4 ^{11}B NMR spectra of **BA-43** without and with diol **4-2a** along with potassium carbonate.

Using 1,3-diol **4-2a** as an example, the proposed catalytic cycle for the monofunctionalization of diols with **BA-43** is depicted in Scheme 4-5. Complexation of diol **4-2a** with **BA-43** in the presence of base generates the activated anionic intermediate **4-3a**. One of the bound oxygen atoms in **4-3a** then reacts with the electrophile to form a boronic ester intermediate, which undergoes exchange with another molecule of diol **4-2a** to release the monofunctionalized product **4-4a** and close the catalytic cycle. It is notable that functionalization of one of the two alkoxy ligands from the diol is much more preferred, as compared to the less nucleophilic phenoxy ligand from **BA-43**. Furthermore, as two hydroxy groups are required for effective activation by the boronic acid catalyst, the undesired difunctionalization that

was observed in previously reported methodologies for the desymmetrization of 1,3-diols (Scheme 4-1) is prevented with the BAC protocol.
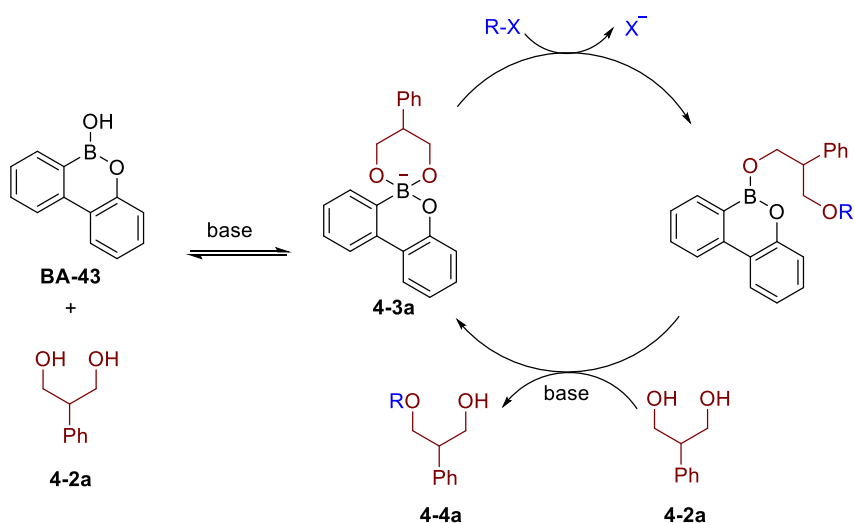
Scheme 4-5 Proposed catalytic cycle for the monofunctionalization of diols catalyzed by boroxarophenanthrene **BA-43**.

4.2.2 Development of the First-generation Chiral Boroxarophenanthrene Catalyst for Enantioselective Desymmetrization of Prochiral 1,3-Diols

Realizing the possibility for enantioselective desymmetrization of prochiral 1,3-diols, a literature search for reported chiral variants of boroxarophenanthrene **BA-43** was conducted. Delightfully, an axially chiral 1,1'-bi-2-naphthol (BINOL)-derived bis-boroxarophenanthrene **BA-44** had been disclosed by Hosoya and co-workers as a substrate using their reported methodology.[36] As a starting point, (*R*)-**BA-44** was prepared from (*R*)-BINOL using the procedure reported by Hosoya and co-workers and was employed as a chiral catalyst for the enantioselective desymmetrization of model substrate **4-2a** under the monobenzylation conditions (Scheme 4-6). Fortunately, the desymmetrized product **4-4a** was obtained in good yield, with moderate enantioselectivity. Further optimization of reaction parameters revealed that a slight improvement in enantioselectivity was achieved by changing the electrophile and base from benzyl bromide and *N,N*-diisopropylethylamine to benzyl chloride and potassium carbonate, with potassium iodide as an additive (Scheme 4-6, conditions B). This new set of conditions was then selected for future reaction development.
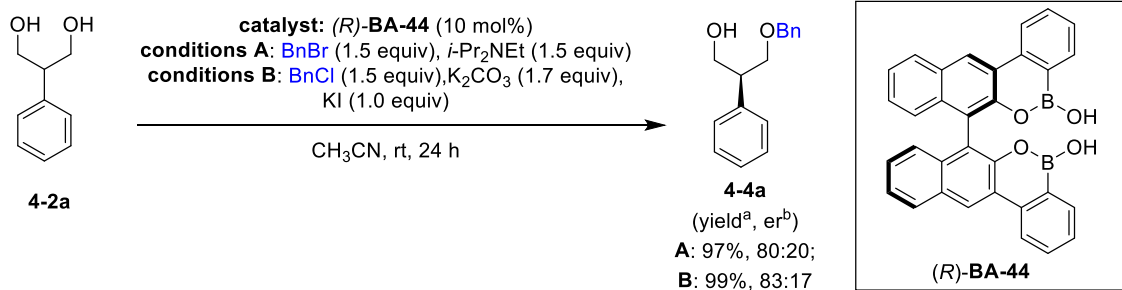
Scheme 4-6 Preliminary results in the enantioselective desymmetrization of diol **4-2a** by direct benzylation using chiral boroxarophenanthrene (*R*)-**BA-44**.

Next, structural modifications of the catalyst were attempted in hopes to improve the enantioselectivity of the desymmetrization reaction. Taking into account the dimeric structure of catalyst **BA-44**, it was postulated that one boronyl unit would be sufficient to complex the diol and the other boronyl unit may serve as a "steric shield" to induce the differentiation of the two hydroxy groups. To probe this hypothesis, three chiral mono-boroxarophenanthrenes (**BA-45–47**) with different levels of steric properties (phenol, benzyl ether, and trityl ether) were prepared from (*R*)-BINOL and evaluated in the enantioselective desymmetrization of diol **4-2a** (Scheme 4-7).
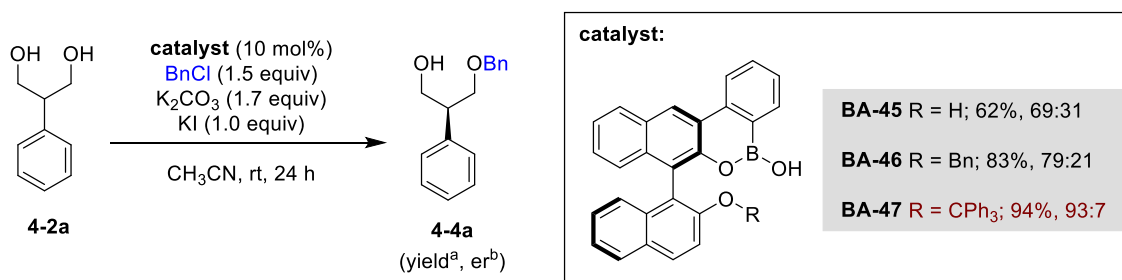
Scheme 4-7 Optimization of chiral boroxarophenanthrene for the enantioselective desymmetrization of diol **4-2a** via monobenzylation.

While lower enantioselectivities were observed with catalysts **BA-45** and **BA-46** bearing a smaller "steric shield", a significant improvement in enantioselectivity was achieved by catalyst **BA-47** bearing a larger trityl ether unit. Further optimizations of the catalyst with bulkier ether moieties were attempted by

introducing alkyl substituents on the trityl fragment, however, only a marginal improvement of enantioselectivity was observed. Using catalyst **BA-47**, a final round of optimization was attempted to improve the enantioselectivity of the reaction further. However, no improvement was observed by lowering the reaction temperature, switching to other polar solvents and carbonate bases, or slow addition of the electrophile.

Based on the results above, **BA-47** was identified as a "proof-of-concept" and the first-generation chiral catalyst for the enantioselective desymmetrization of 2-substituted-1,3-diols via *O*-benzylation. A small scope of 2-substituted 1,3-propanediols was examined using the optimal reaction conditions by Carl Estrada (Scheme 4-8).
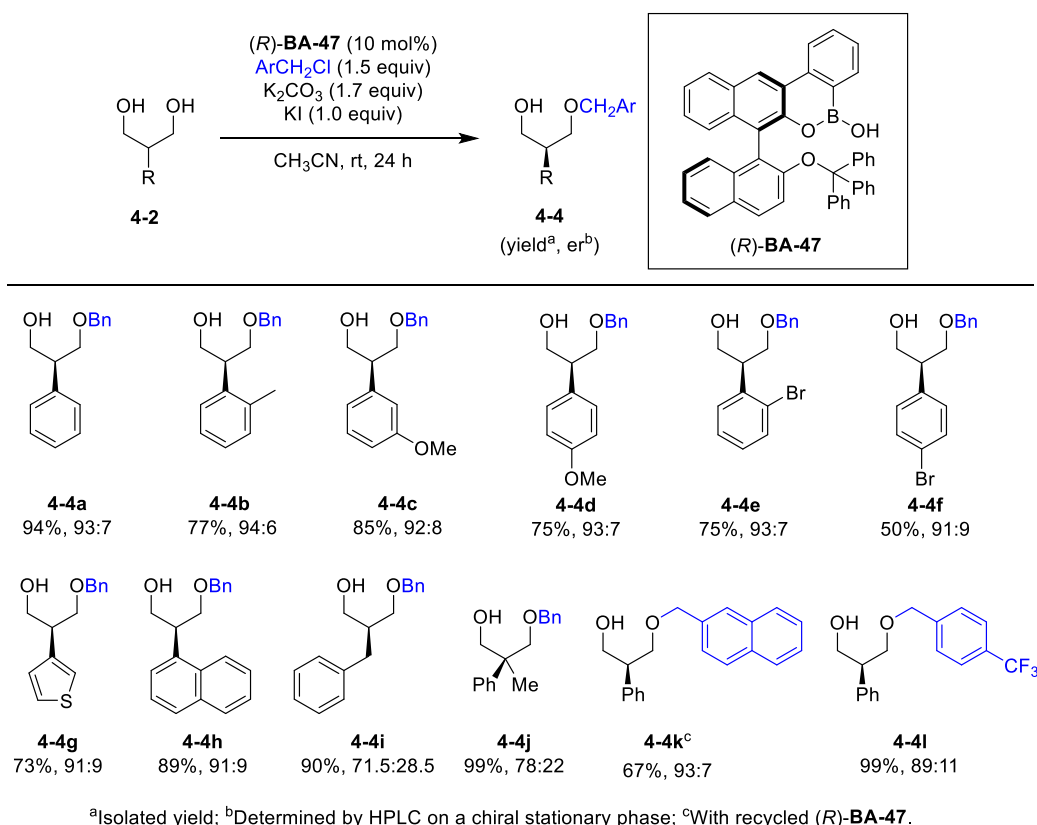
Scheme 4-8 Scope of 2-substituted 1,3-propanediols and electrophiles with catalyst (*R*)-**BA-47**.

In general, high yields and consistently good enantioselectivities were achieved for 2-aryl/heteroaryl-1,3-propanediols (**4-2a–h**). On the other hand, 2-alkyl- (**4-2i**)

and 2,2-disubstituted-1,3-propanediols (**4-2j**) resulted in significantly lower enantioselectivities. Furthermore, other functionalized benzylic chlorides were found to be compatible in this protocol, furnishing the desymmetrized products **4-4k** and **4-4l** in good enantioselectivity. Note that the absolute stereochemistry of the major enantiomer of products **4-4** was assigned to be *(S)* based on X-ray crystallographic analysis of a derivative of product **4-4a** obtained by me (see Section 4.4.1 for details).

4.3 Objective

In short, based on preliminary investigations, a novel axially chiral boroxarophenanthrene **BA-47** was discovered as an efficient catalyst for the enantioselective desymmetrization of 2-aryl-1,3-propanediols via benzylation, resulting in desymmetrized products in good enantioselectivity (up to 94:6 enantiomeric ratio (er)). However, it was believed strongly that there was still room for improvement, especially in terms of enantioselectivity. Thus, the objectives of this chapter are to investigate the factors responsible for the observed enantioselectivity in this transformation and to use this information for the development of a better catalyst with improved selectivity. Note that, unless noted otherwise, the work described from hereon were conducted by the author of this thesis.

4.4 Investigations of the Factors Responsible for Enantioselectivity

The observations from the catalyst optimization studies described above strongly suggest that the differentiation of the enantiotopic hydroxy groups arises from the sterically hindered trityl moiety of **BA-47** in the reactive boronate intermediate, which blocks the electrophile from attacking one of the hydroxy groups. However, it is believed that there is another factor playing a role in the enantioselectivity of this system, as attempts to increase the enantioselectivity through further catalyst modifications with alkyl-substituted trityl ethers and various reaction parameters were unfruitful. Furthermore, when the reaction was performed by Carl Estrada with a slow addition of diol **4-2a** to maximize the concentration of the reactive boronate intermediate relative to the free diol (as there was not enough **BA-47** in hand for a

stoichiometric study), the same enantioselectivity was observed as when the diol was not slowly added (Scheme 4-9). These results suggest that there is no competing uncatalyzed background reaction under these conditions and that the observed enantioselectivity is restricted truly by the structure of the catalyst. Thus, to design a better catalyst, it is crucial to identify the other factors accountable for the observed enantioselectivity with catalyst **BA-47**.
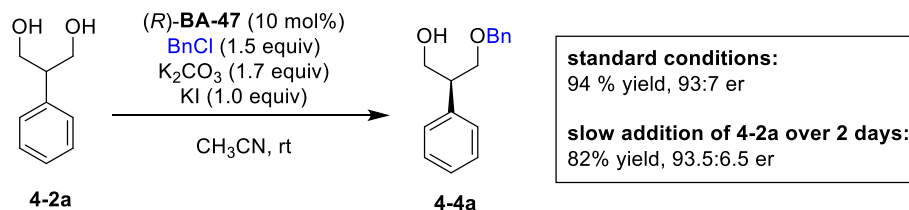
Scheme 4-9 Control experiment to examine the possibility of a competing background reaction (performed by Carl Estrada).

4.4.1 X-Ray Crystallographic Analysis and Stereochemical Model of the Tetravalent Boronate Complex

To gain structural information on the reactive intermediate, a tetravalent boronate complex between boroxarophenanthrene **BA-43** and neopentyl alcohol was synthesized as the tetrabutylammonium salt **4-5**, and a suitable crystal was subjected to X-ray crystallographic analysis (Figure 4-5).
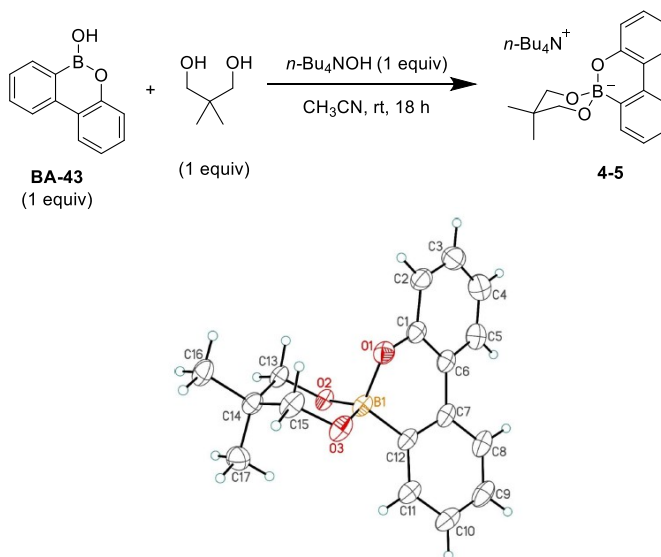
Figure 4-5 Synthesis and ORTEP of the X-ray crystallographic structure of the tetrahedral boronate complex **4-5** (Note: the tetrabutylammonium ion was omitted for clarity).

The X-ray crystallographic structure of **4-5** shows that the tetravalent boronate adopted a defined six-membered chair-like conformation, where the phenoxy B−O bond of **BA-43** is placed axially and the larger aryl B−C unit occupies the equatorial position. Using the information obtained from the X-ray crystallographic structure of adduct **4-5**, a stereochemical induction model for the monobenzylation of 1,3-diol **4-2a** with catalyst (*R*)-**BA-47** was generated using MacSpartan 18 by Prof. Dennis Hall (Figure 4-6).
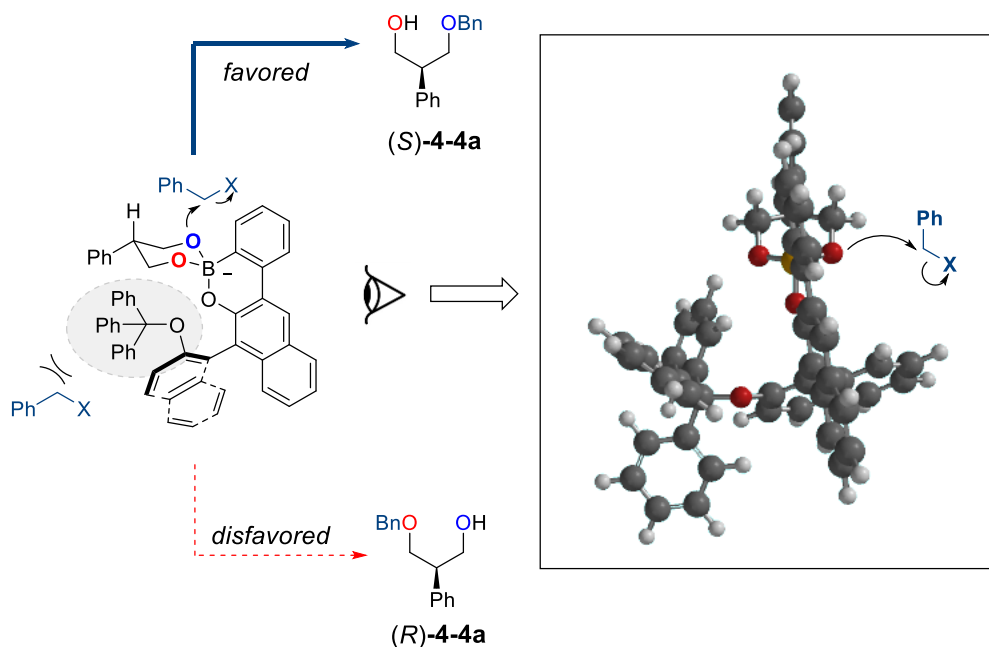
Figure 4-6 Stereochemical model for the benzylation of diol **4-2a** using catalyst (*R)*-**BA-47** generated with MacSpartan 18 (semi-empirical (PM3), equilibrium geometry).

According to the stereochemical model where the 2-phenyl group of diol **4-2a** is positioned equatorially in the chair-like complex, benzylation would occur at the most accessible oxygen atom, away from the trityl group of **BA-47**, resulting in the formation of (*S*)-**4-4a**. To verify the absolute stereochemistry of the major enantiomer, the 3,5-dinitrobenzoyl derivative of **4-4a** (**4-6**) was synthesized, a single crystal was obtained for X-ray crystallographic analysis, and the (*S*) absolute stereochemistry of the major enantiomer was confirmed (Figure 4-7).
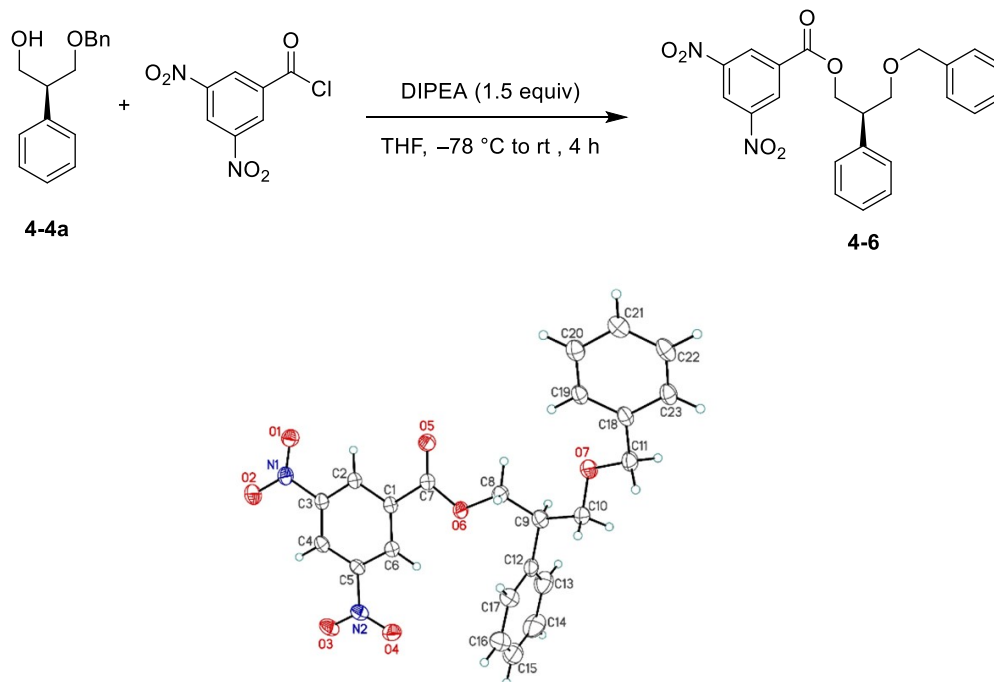
Figure 4-7 Synthesis and ORTEP of the X-ray crystallographic structure of the 3,5-dinitrobenzyl derivative **4-6**.

These results further support the role of the trityl ether group of the catalyst as a "steric shield" for the discrimination of the enantiotopic hydroxy groups. However, they do not provide explanation for the formation of minor enantiomeric products.

4.4.2 Conformational Studies of the Tetravalent Boronate Intermediate

An important clue for explaining the observed enantioselectivity using chiral boroxarophenanthrene **BA-47** emerged from the ^{1}H NMR analysis of tetravalent boronate complex **4-3a**. A close inspection of the ^{1}H NMR spectrum of the boronate complex **4-3a** in CD$_3$CN revealed a minor set of resonances, which is likely attributable to another slow exchanging conformer (Figure 4-8).
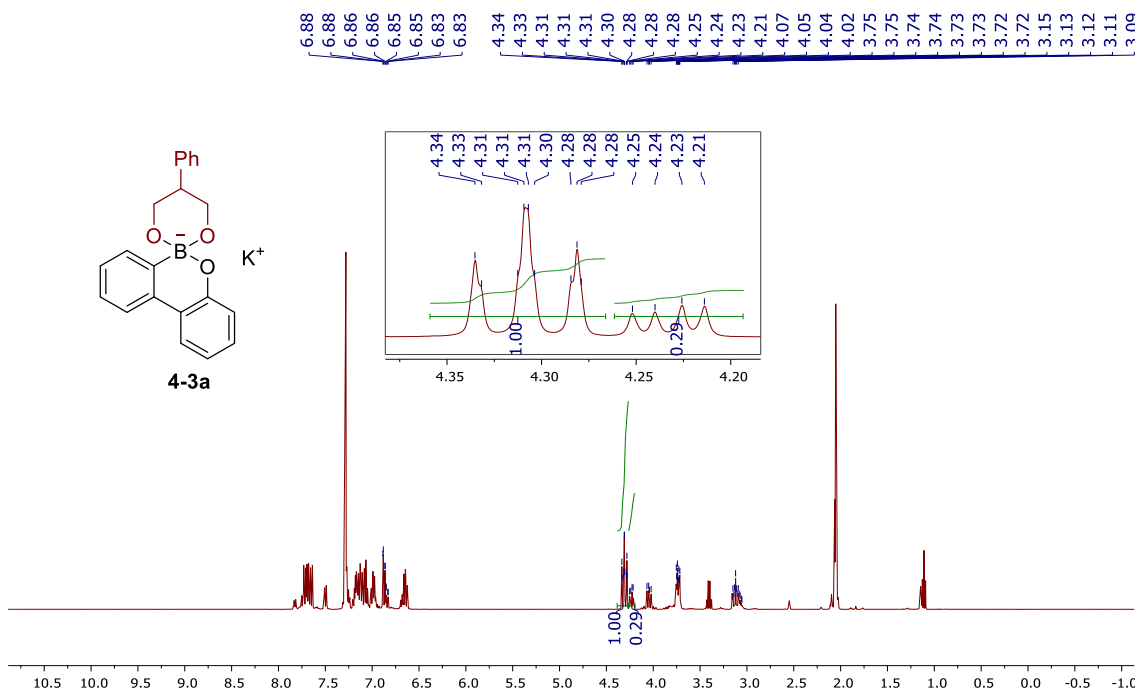
Figure 4-8 ^{1}H NMR spectrum of tetravalent boronate complex **4-3a**.

As informed by the X-ray crystallographic structure of **4-5**, while the conformer of **4-3a** with the phenoxy group of **BA-43** in the axial position is expected to be favored, the 2-phenyl group of diol **4-2a** may be placed either equatorially or axially in the chairlike intermediate. Unlike phenylcyclohexane, the all-carbon analog, there are no H⇔Ph 1,3-diaxial interactions in the six-membered ring of complex **4-3a**; this may cause the conformer with the 2-phenyl group axial (**II**) to be very close in energy to that with the 2-phenyl group equatorial (**I**). To support this hypothesis, density functional theory (DFT) calculations (B3LYP/6-31G*) were used to approximate the relative energies of the four possible conformers of **4-3a** (Figure 4-9). The calculations were performed by Prof. Dennis Hall without extensive conformation optimization, thus the optimal conformation identified may not represent the global minimum. The calculations corroborated the high preference for the two conformers with the axial phenoxy group (**I** and **II**); this is likely due to the unfavorable 1,3-diaxial steric interactions between the aryl B−C unit within the six-membered ring in conformers **III** and **IV**, as well as a possible anomeric effect of the exocyclic B−O bond in conformers **I** and **II**. Furthermore, it was found that

164

conformers **I** and **II** are, indeed, very close in energy, with a difference of ~0.5 kJ/mol.
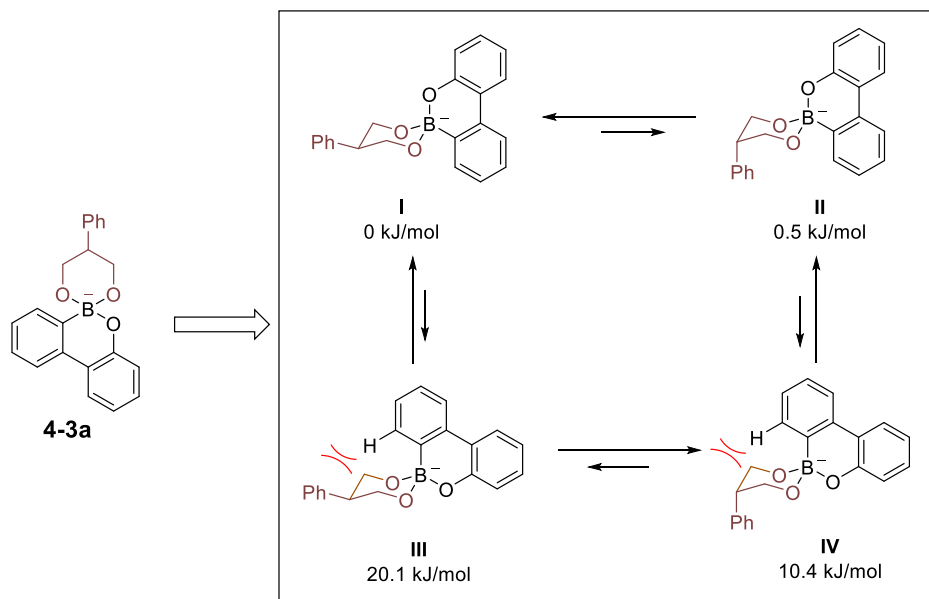
Figure 4-9 Computational analysis of possible conformers of tetravalent boronate complex **4-3a** (DFT calculations (B3LYP/6-31G*) were performed by Prof. Dennis Hall).

The formation of the minor conformer **II** with the chiral catalyst can lead to a significant erosion of the enantioselectivity in the desymmetrization reaction. As shown in Scheme 4-10 with catalyst (*R*)-**BA-47**, alkylation of the least hindered O atom in the minor conformer **II** leads to formation of product (*R*)-**4-4a**, the antipode of the isomer expected from conformer **I**.
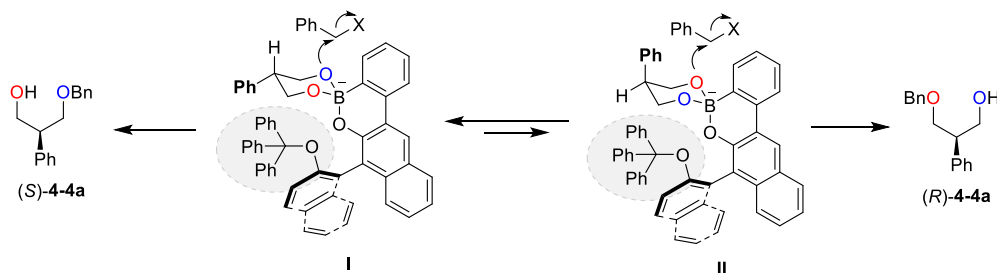
Scheme 4-10 Stereochemical implications of the possible conformers of (*R*)-**BA-47** complexed with diol **4-2a**.

4.5 Rational Design and Synthesis of Chiral Boroxarophenanthrene Catalyst BA-49

Having determined the deleterious effect of minor conformer **II** of the reactive intermediate on the enantioselectivity of the reaction, it was envisioned that the addition of a substituent ortho to the boronyl group (an "ortho-blocker") in the boroxarophenanthrene scaffold would help minimize the impact of this undesired conformer by creating unfavorable steric interactions with the axial 2-phenyl group.

4.5.1 NMR and Computational Investigation of the Effect of the "Ortho-blocker"

The effect of the proposed "ortho-blocker" on the conformational equilibrium was examined first by DFT calculations (B3LYP/6-31G*) with an ortho-methyl substituent (Figure 4-10). Expectedly, a greater energy difference of 7.8 kJ/mol in favor of conformer **I** was observed with the "methyl-blocker", as opposed to 0.5 kJ/mol without the blocker (Figure 4-9).
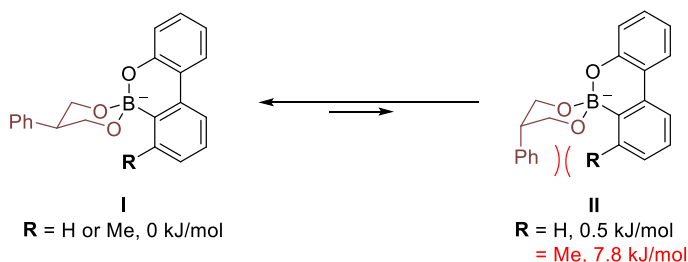
Figure 4-10 DFT Computational analysis of the effect of a "methyl-blocker" on the conformational equilibrium.

To support the proposal further with experimental data, an ortho-methylated derivative of catalyst **BA-43** (**BA-48**) was prepared by Carl Estrada from 2-bromoanisole and 3,5-dimethylphenylboronic acid via a Suzuki–Miyaura coupling reaction, followed by a one-pot demethylation and electrophilic borylation with BBr_3 (Scheme 4-11A). With **BA-48** in hand, the effect of the "methyl-blocker" on the conformational equilibrium was examined experimentally using ^{1}H NMR spectroscopic studies to compare the ratio of conformers **I** and **II** between **BA-43** and **BA-48** (Scheme 4-11B). Although the formation of undesired conformer **II** still is observed with methylated **BA-48**, the proportion is significantly lower than that with **BA-43**, 1:10 (Figure 4-11) as compared to 1:3.5 (Figure 4-8).
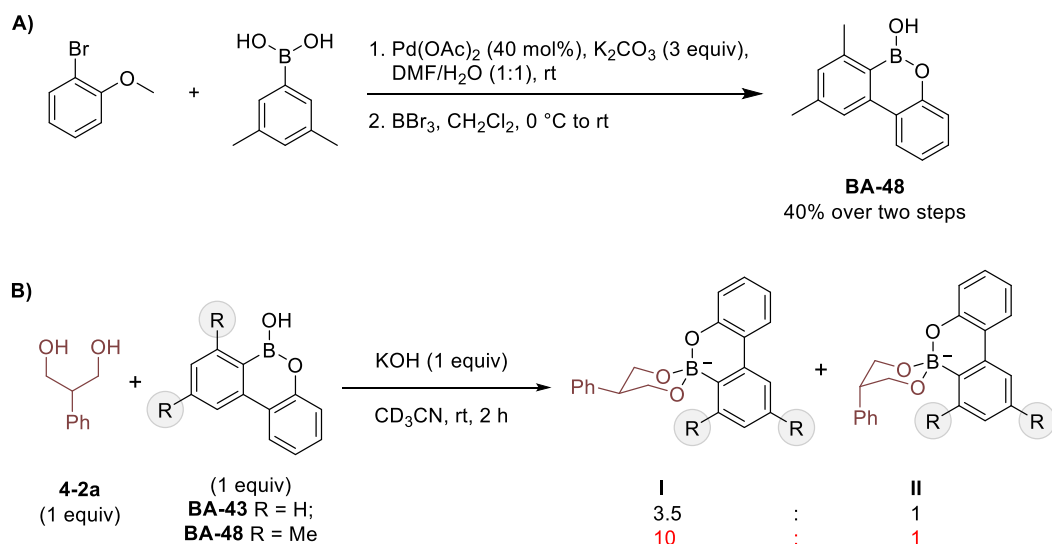
Scheme 4-11 A) Synthesis of boroxarophenanthrene with "methyl-blocker" **BA-48** (performed by Carl Estrada. B) ^{1}H NMR study of the effect of the "methyl-blocker" on the conformational equilibrium.
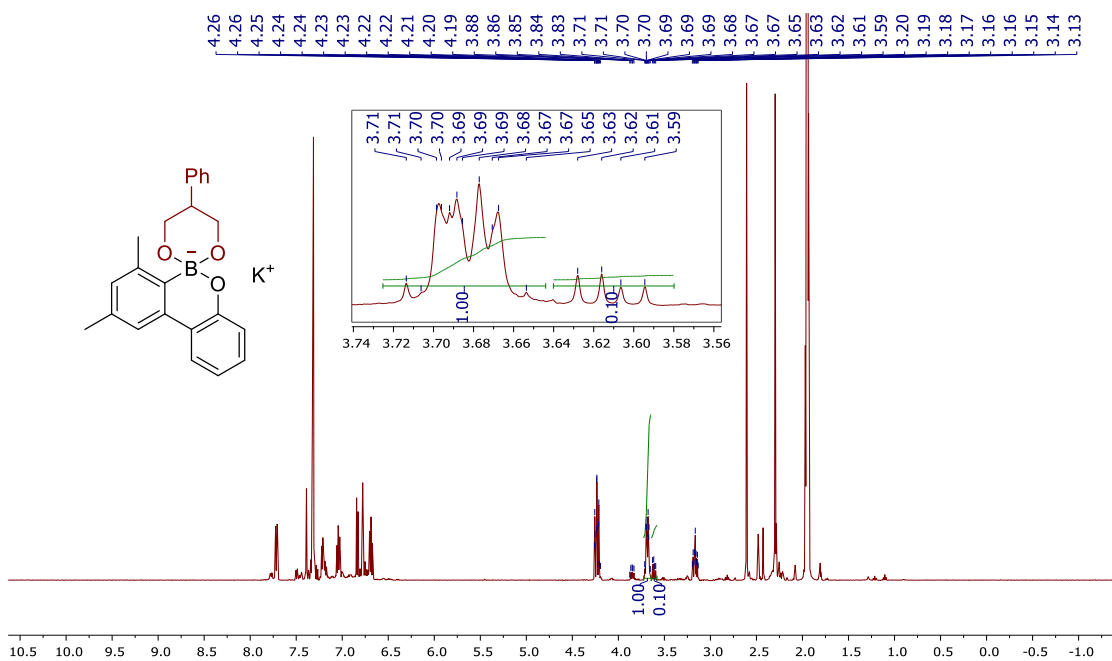
Figure 4-11 ^{1}H NMR spectrum for determination of the conformer ratio for boroxarophenanthrene **BA-48**.

4.5.2 Synthesis of Chiral Boroxarophenanthrene Catalyst with a "Methyl-blocker"

Encouraged by the promising effect of the "methyl-blocker" in substrate conformational control, as shown above, chiral methylated boroxarophenanthrene **BA-49** was prepared and examined for its catalytic properties in the enantioselective

desymmetrization of 2-aryl-1,3-propanediols. As depicted in Scheme 4-12, boroxarophenanthrene (R)-**BA-49** was synthesized from (R)-(2,2'-dimethoxy-[1,1'-binaphthalen]-3-yl)boronic acid (**4-7**) and 5-bromo-*m*-xylene via a sequence similar to that employed in the synthesis of **BA-48**. Specifically, the synthesis commenced with a Suzuki–Miyaura coupling, followed by a one-pot demethylation and electrophilic borylation, and subsequent etherification. While boronic acid **4-7** is not available commercially, it can be prepared easily from (R)-BINOL following a literature procedure.[37]
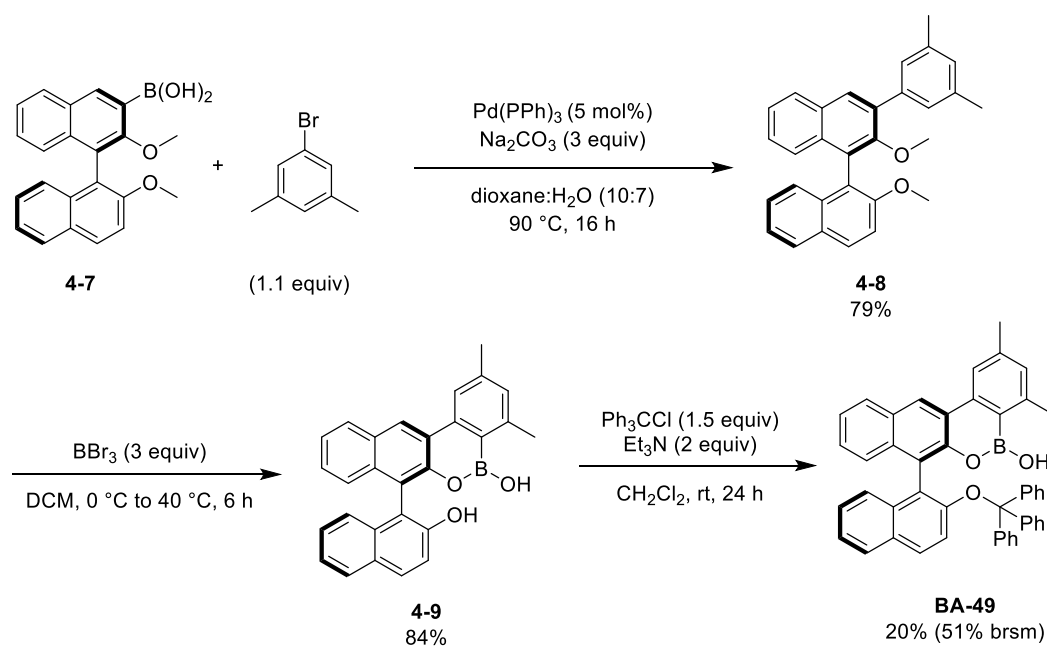
Scheme 4-12 Synthesis of chiral boroxarophenanthrene **BA-49** with a "methyl-blocker".

The lower-than-expected isolated yield of **BA-49** (51% brsm) was due to a similar R_f value of **BA-49** and triphenylmethanol, a side product from the unreacted trityl chloride, making the isolation by silica column chromatography difficult. Purification of a mixture of **BA-49** and triphenylmethanol obtained after column chromatography by HPLC was attempted using 95:5 acetonitrile/water containing 0.1% formic acid as eluent. However, partial cleavage of the trityl group was observed, resulting in a mixture of **4-9** and **BA-49** after the purification. The preparation and isolation of **BA-49** are areas for improvement in future work.

4.5.3 Comparison of the Performance between Catalyst BA-47 and BA-49

With boroxarophenanthrene (*R*)-**BA-49** in hand, its performance in the enantioselective desymmetrization of 2-aryl-1,3-propanediols via *O*-benzylation was examined in comparison with catalyst (*R*)-**BA-47** (Scheme 4-13). Gratifyingly, the methylated derivative **BA-49** resulted in an increase of enantioselectivity from 93:7 to 95:5 er for diol substrate **4-2a**. Furthermore, the methylated catalyst **BA-49** was found to outperform **BA-47** in all 2-substituted-1,3-propanediol substrates and electrophiles studied by Carl Estrada (Scheme 4-8). These results strongly support the ability of catalyst **BA-49** with a "methyl-blocker" to control the substrate's conformation.
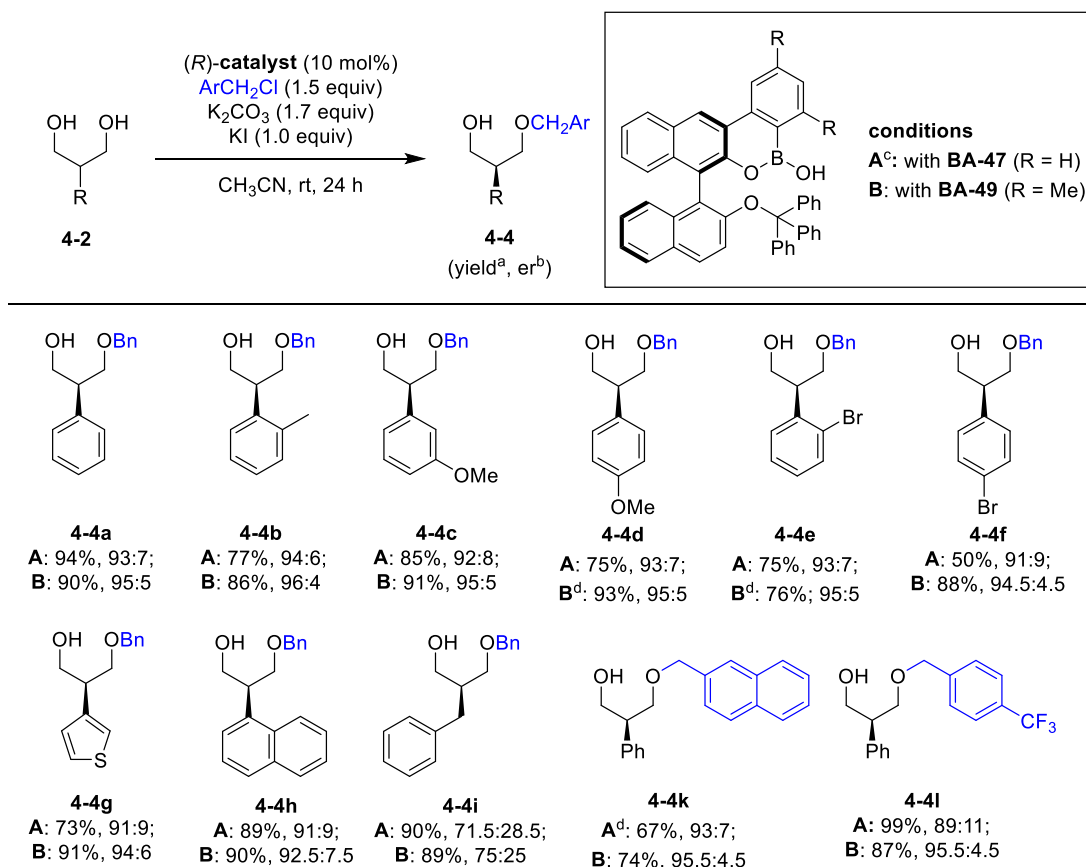
^{a}Isolated yield; ^{b}Determined by HPLC on a chiral stationary phase; ^{c}Performed by Carl D. Estrada; ^{d}With recycled catalyst.

Scheme 4-13 Comparison of catalysts (*R*)-**BA-47** and (*R*)-**BA-49** for the enantioselective desymmetrization of 1,3-diols by *O*-alkylation.

Although the enantioselectivity was improved with catalyst **BA-49**, 2-benzyl-1,3-propanediol (**4-2i**) still resulted in significantly lower er as compared to 2-aryl-1,3-propanediol substrates. These results were expected, as a benzyl group has a smaller A value (0.45 kJ/mol) in comparison with a phenyl group (0.72 kJ/mol). Furthermore, as illustrated by substrates **4-4a**, **4-4k** and **4-4l**, the structure of benzylic chlorides were found to have little to no effect on the enantioselectivity; this is because benzylic chlorides have a planar structure, and the benzylic group is situated away from the reaction centre thus has little to no effect on the facial selectivity. Notably, as shown with substrates **4-4d** and **4-4e**, catalyst **BA-49** can be recovered by silica column chromatography and reused for the desymmetrization without loss of catalytic performance; this is a great advantage of BAC over other catalytic systems.

4.6 Scope for the Enantioselective Desymmetrization of Prochiral 1,3-Diols by Direct *O*−Alkylation with Catalyst BA-49

To explore the potential of this catalytic system, the scope for the enantioselective desymmetrization of prochiral 1,3-diols with the optimal catalyst (*R*)-**BA-49** was expanded further.

4.6.1 Scope of 2-Substituted-1,3-Propanediols

The scope of 2-substituted 1,3-propanediols and electrophiles was examined first (Scheme 4-14). Delightfully, consistently high yields and enantioselectivity ratios were obtained for a wide range of 2-aryl substituents (**4-4m** to **4-4s**). Electron-donating (methoxy and methyl) and moderately electron-withdrawing (halides) aryl substituents were found to be compatible, regardless of the position of the substituent, providing an average er of 95:5. On the other hand, strong electron-withdrawing substituents, such as trifluoromethyl (**4-4t**) and nitro (**4-4u**) groups, lead to slightly decreased enantioselectivities (93.5:6.5 er). Other nitrogen-containing heteroaryl substituents, like 3-indolyl and 4-pyridinyl, were examined also. While free 3-indolyl substituted diol (**4-2v**) is a suitable substrate with a slightly lower enantioselectivity, 4-pyridinyl substituted diol (**4-2w**) was found to be incompatible; this is likely due to the higher nucleophilicity of pyridine, which can coordinate to the boron center

rendering the catalyst inactive. Furthermore, 2-amino-1,3-propanediol protected with phthalimide (**4-2x**) also underwent desymmetrization, with moderate yield and good enantioselectivity.
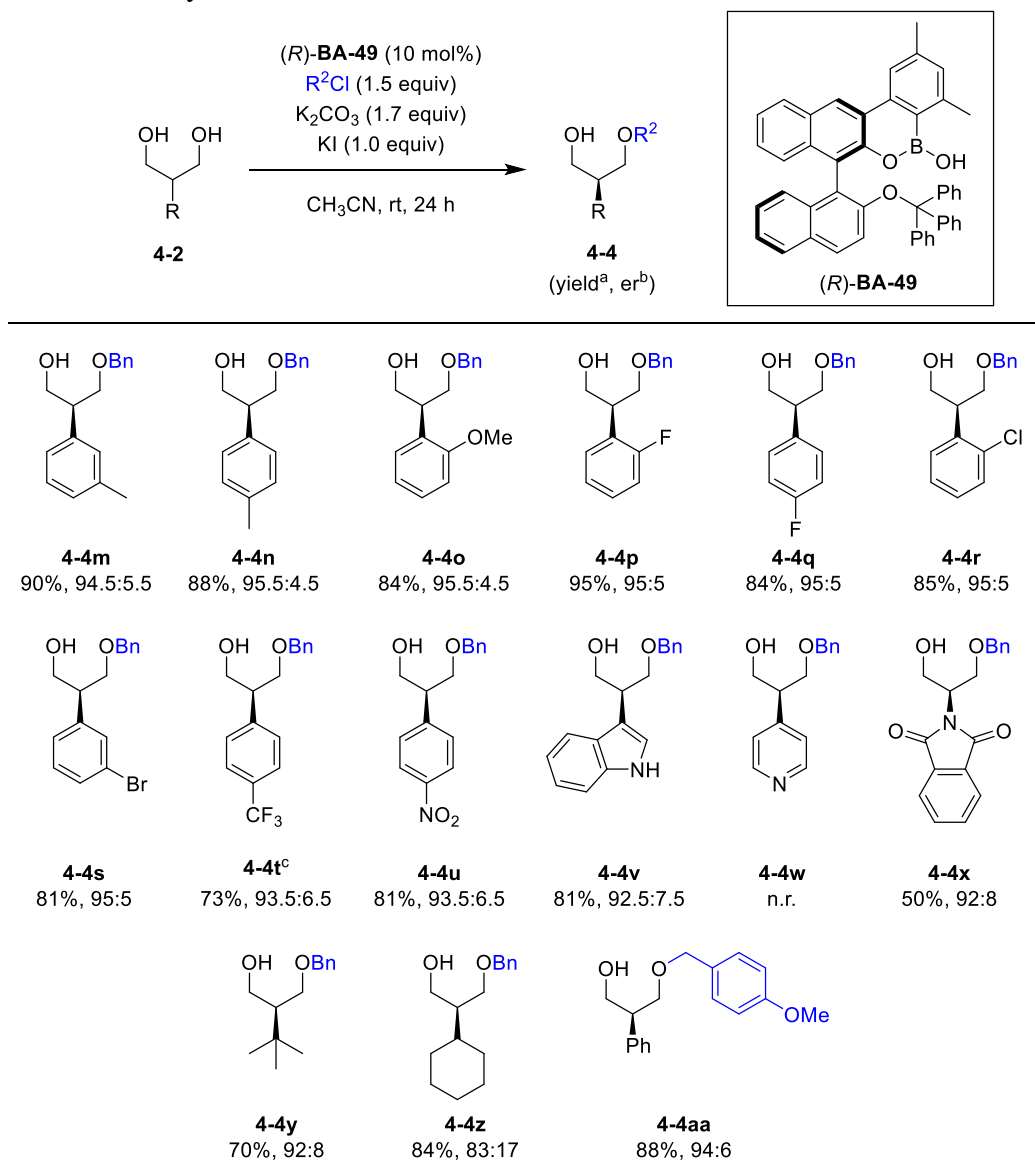
Scheme 4-14 Scope of enantioselective desymmetrization of 2-substituted-1,3-propanediols via *O*-benzylation using (*R*)-**BA-49**.

In contrast to the higher A value (>1 kJ/mol), a lower enantiomeric ratio (92:8) was obtained with 2-*tert*-butyl-1,3-propanediol (**4-2y**), in comparison with 2-aryl-1,3-propanediols (~95:5). This counterintuitive result suggests that there might be secondary π-π interactions between the 2-aryl group of the diol and one of the phenyl

171

groups of the trityl ether moiety, which further favor the formation of conformer **I,** leading to a higher enantioselectivity. Moreover, 2-cyclohexyl-substituent (**4-2z**), the fully saturated analog of the phenyl group, also resulted in a lower enantioselectivity, which is in agreement with the moderate enantioselectivities observed with 2-alkyl-1,3-propanediol substrates. Lastly, as shown by substrate **4-4aa**, a *p*-methoxybenzyl (PMB) group, a commonly used protecting group for alcohols, can also be installed while maintaining high selectivity.

4.6.2 Scope with Catalyst (*S*)-BA-49

To demonstrate the advantage of non-enzymatic catalytic systems, where the opposite enantiomeric products can be accessed easily by switching the chirality of the catalyst, (*S*)-**BA-49** was synthesized from (*S*)-BINOL via the same synthetic route depicted in Scheme 4-12 above and employed in the desymmetrization of diols **4-2a** and **4-2b**. As shown in Scheme 4-15, when (*S*)-**BA-49** was used as the catalyst, the opposite enantiomeric products were, indeed, obtained with same level of selectivity as (*R*)-**BA-49**.
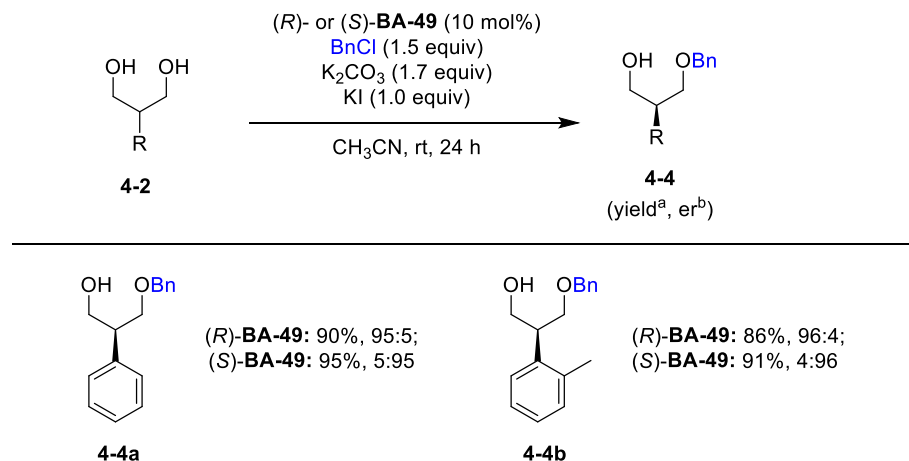
Scheme 4-15 Comparison of catalytic performance between (*R*)-BA-49 and (*S*)-BA-49 in the enantioselective desymmetrization of 2-aryl-1,3-propanediols.

4.6.3 Desymmetrization of 1,3-Disubstituted 1,3-Diols

To expand the potential of this catalytic system toward other classes of prochiral diol substrates, the desymmetrization of *syn*-1,3-diphenyl-1,3-propanediol (**4-10**) was examined (Scheme 4-16). Using the optimal reaction conditions described above, the

desymmetrized product **4-11** was obtained in excellent enantioselectivity (98.5:1.5 er), albeit, in very poor yield. The excellent enantioselectivity is believed to arise from the unfavorable 1,3-diaxial interactions of the two phenyl groups of the 1,3-diol in the minor conformer **VII**, which is consistent with the proposed substrate conformational control of enantioselectivity with catalyst **BA-49**. On the other hand, the poor yield may be attributed to the difficulty in the complexation of catalyst **BA-49** and diol **4-10** due to increased steric interactions with the two substituents in the 1,3-positions of diol **4-11**. Satisfactorily, it was found that the yield of desymmetrized product **4-11** can be increased to 67% by increasing the reaction temperature to 40 °C without affecting the enantioselectivity. These results demonstrate the great potential of this catalytic system to effect the enantioselective desymmetrization of *meso*-1,3-disubstituted 1,3-propanediols.
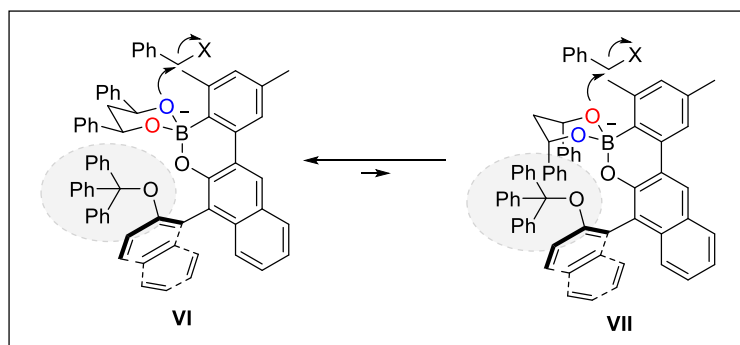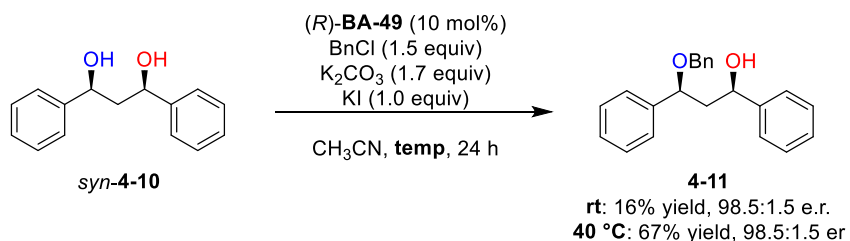
Scheme 4-16 Enantioselective desymmetrization of *syn*-**4-10** with (*R*)-**BA-49** and conformational equilibrium of the reactive intermediate.

Based on the stereochemical model, the absolute stereochemistry of the major enantiomer of product **4-11** is expected to be (1*R*, 3*S*). Other than X-ray crystallography analysis, the absolute stereochemistry can be determined by comparing it with the reported specific rotation of the compound of interest. As there

is no previously reported specific rotation for both enantiomers of **4-11**, the specific rotation of **4-11** was compared with the known specific rotation of the opposite enantiomer of (1*S*,3*R*)-1,3-dialkyl-substituted 1,3-propanediols (Figure 4-12).[4] As expected, the specific rotation of product **4-11** showed an opposite sign, as compared to the (1*S*,3*R*)-1,3-dialkyl-substituted analogs, supporting the (1*R*,3*S*) absolute stereochemistry assignment of the major enantiomer of **4-11**.

Experimental:

OBn OH

(1*R*,3*S*)-**4-11**
[α]$_D$: −50 (*c* 0.71, CHCl$_3$)

Literature:

OH OBn

(1*S*,3*R*)

R	[α]$_D$
Me	+57.4 (*c* 0.70)
Bu	+49.6 (*c* 1.00)
i-Pr	+58.6 (*c* 1.00)
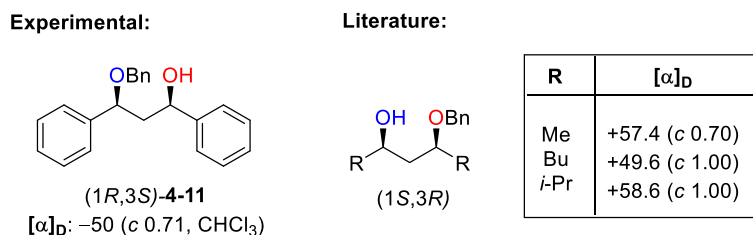
Figure 4-12 Determination of the absolute chemistry of **4-11** by comparing the optical rotation with reported analogs.

Inspired by the excellent enantioselectivity for the *syn*-1,3-disubstituted-1,3-propanediol substrate, it is envisioned that the chiral boroxarophenanthrene catalytic system could be employed for the diastereomeric kinetic resolution of an *anti*- and *syn*-1,3-disubstituted-1,3-diol mixture by selectively functionalizing the syn-isomer; this is because the anti-isomer would position a phenyl group axially in the reactive boronate intermediate, which is less favored. A preliminary screening was conducted using the 1:1 mixture of *syn*- and *anti*-2,4-pentanediol **4-12** with catalyst (*R*)-**BA-49** (Table 4-1). When subjected to the optimal reaction conditions described above, only a trace amount of product was observed by TLC after 24 h (entry 1). The reaction mixture was allowed to stir for another 24 h at ambient temperature, but the monobenzylated product **4-13** was isolated in a poor yield and low diastereoselectivity (entry 2). To improve the reactivity, the reaction was performed at a higher temperature; while the yield was increased, the diastereoselectivity, unfortunately, dropped significantly (entry 3). To ensure that the decrease in diastereoselectivity at higher temperature was not due to the background reaction, a control reaction without catalyst **BA-49** was conducted; indeed, a negligible amount of product was observed by TLC (entry 4).

Table 4-1 Preliminary Screening of Diastereomeric Kinetic Resolution of 2,4-Pentanediol **4-12** via *O*-Benzylation with Catalyst (*R*)-**BA-49**
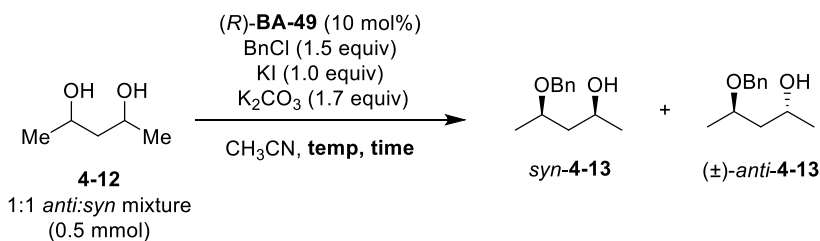
entry	temp, time	yield[a]	dr[b]
1	rt, 24 h	trace[c]	–
2	rt, 48 h	12%	2.0:1
3	40 °C, 24 h	37%	1.2:1
4[d]	40 °C, 24 h	trace[c]	–

[a]Isolated yield. [b]Diastereomeric ratio was determined using ^{1}H NMR analysis. [c]Reaction was monitored with TLC. [d]Without **BA-49**.

Despite the low diastereomeric ratio (2:1), the chiral boroxarophenanthrene **BA-49**, without a doubt, has a small preference toward one of the diol's diastereomers. Further optimization of reaction parameters and modification of the catalyst, potentially, could lead to an optimal BAC system for this application.

4.7 Attempts at Synthesis of a Chiral Boroxarophenanthrene with a Larger "Ortho-blocker"

Encouraged by the positive effect of the "methyl-blocker" on the enantioselectivity of the desymmetrization, attempts to install a larger ortho-substituent, such as isopropyl or tert-butyl groups, were made to improve the enantioselectivity of the benzylation reaction further. The efforts toward the synthesis of a chiral boroxarophenanthrene bearing an "*i*-Pr-blocker" was made primarily by me, while the synthesis of a boroxarophenanthrene with a "*t*-Bu-blocker" was attempted by Carl Estrada and will not be discussed in detail in this section.

The synthesis of a chiral boroxarophenanthrene with an "*i*-Pr-blocker" was explored first as the achiral variant using the standard two-step protocol for the preparation of boroxarophenanthrene derivatives employed in this work (Scheme 4-11A and 4-12). As shown in Scheme 4-17A, the Suzuki–Miyaura coupling of 2-methoxyphenylboronic acid and 2-iodo-4-isopropyl-1-methylbenzene, which was prepared by iodination of *p*-cymene,[38] delivered the biaryl intermediate **4-14** in good

yield. However, the subsequent treatment of **4-14** with BBr$_3$ did not result in the desired boroxarophenanthrene **BA-50**, and only demethylated product **4-15** was obtained. Electrophilic borylation of 2-arylphenol **4-15** with BCl$_3$ and catalytic AlCl$_3$ using the conditions reported by Dolle and co-workers was attempted (Scheme 4-17B).[34] Unfortunately, the desired product **BA-50** was not observed even when the reaction was conducted with 50 mol% of AlCl$_3$. The failure of electrophilic borylation is likely due to the increased steric hinderance of the isopropyl group. The same results were observed by Carl Estrada for the synthesis of the catalyst with a "*t*-Bu-blocker".
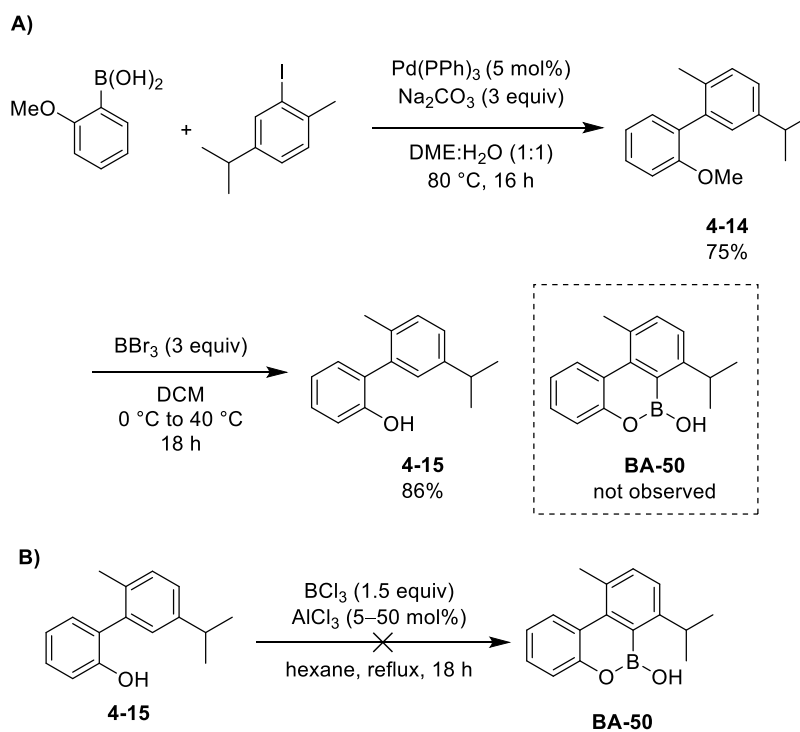
Scheme 4-17 Attempts to synthesize boroxarophenanthrene **BA-50** via electrophilic borylation.

Realizing the difficulty of the late-stage electrophilic borylation, another approach involving the use of substrates containing a pre-installed boryl group was attempted for the preparation of the catalyst with an "*i*-Pr-blocker". Such an approach was employed by Carl Estrada in the preparation of chiral boroxarophenanthrene **BA-45** using 1,2-diborylbenzene **4-17** (Scheme 4-18). The diboryl compound **4-17** was coupled with brominated (*R*)-BINOL **4-16** via a Suzuki–Miyaura cross-coupling

to generate intermediate **4-18** bearing a boryl group. Treatment of intermediate **4-18** with BBr$_3$ resulted in demethylation and *in situ* cyclization of the phenol with the boryl group to afford **BA-45**. Thus, it was envisioned that a chiral boroxarophenanthrene with an "*i*-Pr-blocker" can be prepared in similar fashion using an isopropyl-substituted diboryl derivative.
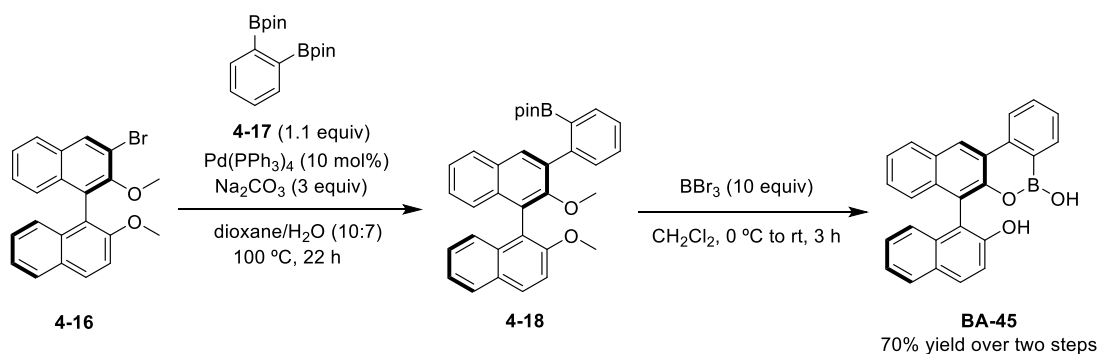
Scheme 4-18 Synthesis of chiral boroxarophenanthrene **BA-45** by Carl Estrada.

As the preparation of the isopropyl-substituted diboryl derivative **4-19** was not reported previously, the synthesis of such diboryl compound was attempted first (Scheme 4-19). After an extensive search of chemical databases, 2-bromo-6-isopropylphenol (**4-20**), which is prepared from electrophilic bromination of 2-isopropylphenol with NBS,[39] was found to be a suitable starting material toward the synthesis of precrusor **4-19**. Starting from arene **4-20**, two different approaches toward the synthesis of **4-19** were investigated. A double Miyaura borylation strategy was attempted by Carl Estrada (Scheme 4-19A). The phenol moiety of arene **4-20** was transformed first into a triflate group, which is an excellent leaving group. The triflate intermediate **4-21** was subjected to the double Miyaura borylation using 2.1 equivalents of B$_2$pin$_2$, which resulted in the desired diboryl compound **4-19** in poor yield, along with other mono-borylated side products. Aside from the double Miyaura borylation strategy, the preparation of intermediate **4-19** was attempted using the platinum-catalyzed aryne diborylation protocol reported by Yoshida and co-workers.[40] As shown in Scheme 4-19B, the aryne precursor **4-22** was prepared in moderate yield from the arene **4-20** and was subjected to the platinum-catalyzed diborylation, which afforded the desired product **4-19** in poor yield.

A)

B)
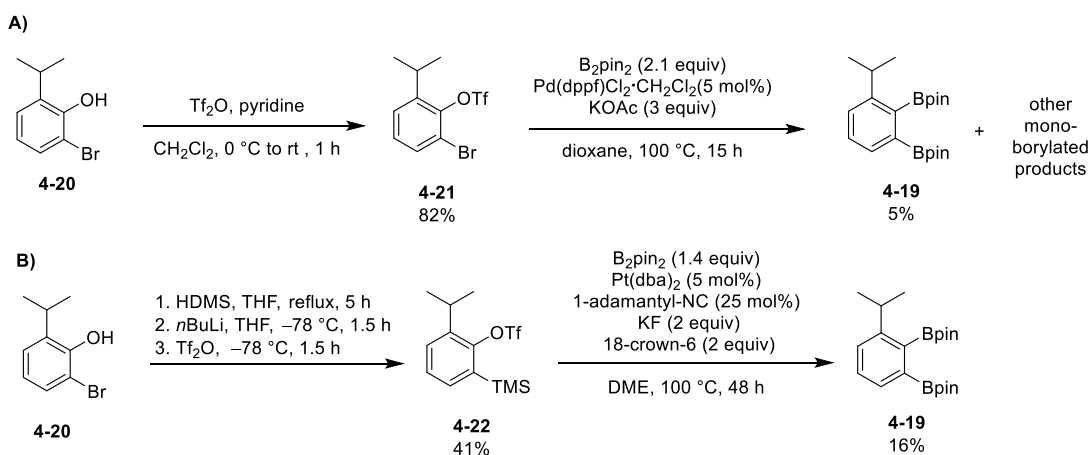
Scheme 4-19 Synthesis of diboryl compound **4-19** from arene **4-20** using A) double Miyaura borylation approach (performed by Carl Estrada) and B) platinum-catalyzed diborylation of arynes.

Using the small amount of diboryl compound **4-19** isolated from the above approaches, the Suzuki–Miyaura cross-coupling with iodinated (*R*)-BINOL **4-23** was conducted (Scheme 4-20). Unfortunately, a complex mixture was obtained; LC-MS analysis of the crude reaction mixture revealed that no desired product **4-24** was formed, instead deiodinated BINOL **4-25** was generated.
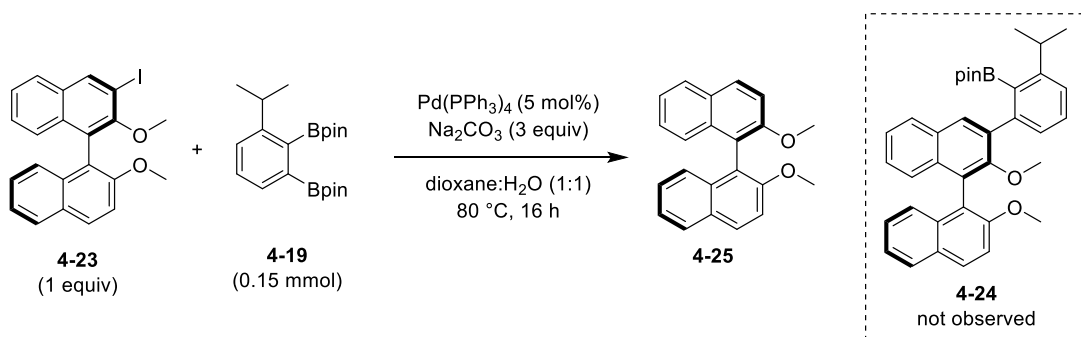
Scheme 4-20 Attempt for the synthesis of intermediate **4-24** via Suzuki–Miyaura cross-coupling.

Regretfully, the attempts to install a larger "ortho-blocker" on the chiral boroxarophenanthrene catalyst so far have been unsuccessful. However, these attempts only covered two commonly used strategies for the preparation of boroxarophenanthrenes. Other strategies may exist for the synthesis of such compounds. Furthermore, numerous Suzuki–Miyaura cross-coupling conditions have been reported, and there may be conditions that are suitable for the cross-coupling of

diboryl precursor **4-19** with iodinated **4-23**. Therefore, it can be anticipated that continuous efforts toward the synthesis of a chiral boroxarophenanthrene with a larger "ortho-blocker" eventually would result in a better boroxarophenanthrene catalyst.

4.8 Summary

In summary, a novel class of chiral boroxarophenanthrene catalysts derived from BINOL was discovered for the enantioselective desymmetrization of 2-aryl-1,3-propanediols by direct *O*-benzylation under mild and ambient conditions. Differentiation of the enantiotopic hydroxy groups on the diol was found to occur via a tetrahedral anionic boronate complex with a defined, chair-like six-membered ring conformation, where one of the hydroxy groups is effectively shielded by a large trityl group from the catalyst. Further investigations revealed the existence of a minor conformer that led to an erosion in the enantioselectivity of the desymmetrization process. Based on this information, the optimal catalyst **BA-49**, which features a strategically placed "methyl-blocker" to disfavor the minor conformer, was rationally designed and synthesized. Using catalyst **BA-49**, monoalkylated products were obtained in high enantiomeric ratios for a wide range of 2-aryl/heteroaryl-1,3-propanediols. Preliminary investigations of the desymmetrization of 1,3-disubstituted-1,3-diols demonstrate the potential of this BAC system toward other substrate classes. Besides that, it is anticipated that this BAC system can be amenable to other electrophiles and transformations such as phosphorylation, silylation and sulfonylation. Further optimization of potential catalysts with a larger "ortho-blocker" and a larger "steric shield" should be explored to increase the enantioselectivity.

4.9 Experimental

4.9.1 General Methods

The following section includes experimental procedures and details for the synthesis and isolation of compounds. Full characterization of all new compounds and partial characterization of known compounds presented in this chapter are described. Unless otherwise stated, all reactions were performed in capped regular glassware open to air

with no further precautions. Tetrahydrofuran (THF), dichloromethane (DCM), and *N,N*-dimethylformamide (DMF) were purified using an MBraun MS solvent purification system prior to use. 1,4-Dioxane was distilled from a sodium–benzophenone ketyl still, which was prepared from commercial sodium and benzophenone. All other solvents were purchased as ACS reagents and used without further purification. (*R*)-(2,2'-dimethoxy-[1,1'-binaphthalen]-3-yl)boronic acid (**4-7**) was prepared based on the literature procedure.[37] Unless otherwise noted, all other chemicals were purchased from commercial sources (Strem, Sigma Aldrich, Oakwood Chemicals, Tokyo Chemical Industry, or Combi-Blocks) and used as received. Flash chromatographic separations were performed on silica gel 60 using ACS grade hexanes, ethyl acetate, dichloromethane, and diethyl ether as eluents. Thin layer chromatography (TLC) was performed on silica gel 60 F254 plates, which were visualized under UV light and with potassium permanganate ($KMnO_4$), phosphomolybdic acid (PMA), or curcumin (for organoboron compounds) stains.

^{1}H NMR, ^{13}C NMR, ^{19}F NMR, and ^{11}B NMR spectra were recorded on 400, 500, 600, or 700 MHz instruments. The residual solvent ($CDCl_3$, CD_3OD, CD_3CN, or CD_3COCD_3) protons (^{1}H) and carbons (^{13}C) were used as internal references. ^{1}H NMR data are presented as follows: chemical shifts in ppm downfield from tetramethylsilane (multiplicity, coupling constant, integration). The following abbreviations are used in reporting the ^{1}H NMR data: s, singlet; br s, broad singlet; d, doublet; t, triplet; dd, doublet of doublet; dddd, doublet of doublet of doublet of doublet; tt, triplet of triplet; m, multiplet; comp m, complex multiplet. The error of coupling constants from ^{1}H NMR spectra is estimated to be 0.3 Hz. High-resolution mass spectra were recorded by the University of Alberta mass spectrometry services laboratory using either electron impact (EI) or electrospray ionization (ESI) techniques. Infrared (IR) spectra were obtained using cast film (for solid sample) or thin film (for liquid sample) techniques with frequencies expressed in cm^{-1}; the intensity of the band is indicated as br (broad), s (strong), m (medium), or w (weak). The resolution of the IR instrument is 4 wavenumbers. Optical rotations were measured using a 1 mL cell with a 10 cm length on a polarimeter by the University of

Alberta Analytical and Instrumentation Laboratory. Melting points (Mp) were measured on an uncalibrated melting point apparatus and are uncorrected. The enantiomeric ratio for chiral compounds were determined using an Agilent HPLC instrument with Chiralpak IB, IC, or AS columns, as specified in the following individual procedures.

4.9.2 Preparation of Crystals of Complex 4-5 Suitable for X-Ray Crystallographic Analysis

BA-43
(1 equiv)

(1 equiv)

4-5
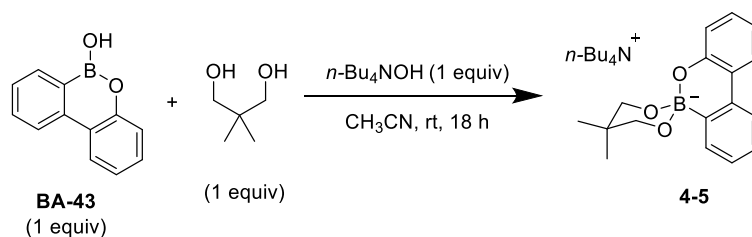
Tetrabutylammonium 5',5'-dimethylspiro[dibenzo[1,2]oxaborinine-6,2'-[1,3,2] dioxaborinan]-6-uide (4-5): A mixture of boroxarophenanthrene catalyst **BA-43** (25 mg, 0.13 mmol) and neopentyl glycol (13 mg, 0.13 mmol) was dissolved in CH_3CN (1 mL), then tetrabutylammonium hydroxide (40% in H_2O, 81 µL, 0.13 mmol) was added to this mixture. The reaction mixture was stirred at room temperature for 18 h, after which time, it was concentrated in vacuo; a sticky crude solid was obtained. Then, the crude was triturated with diethyl ether to give complex **4-5** as a white solid (50 mg, 76%). A single crystal of compound **6** for X-ray crystallographic analysis was obtained through slow diffusion method using the following procedure. A 20 mg sample of compound **4-5** was dissolved in 0.2 mL acetonitrile and filtered through a cotton bud into a ½ dram vial. The ½ dram vial (without a lid) was placed into a 3-dram vial containing diethyl ether as the anti-solvent for the crystallization, and the 3-dram vial was capped and left inside the fume hood. After three days, a clear long needle-like crystal was obtained and subjected to X-ray crystallographic analysis.

^{1}H NMR (400 MHz, CD₃CN, δ): 7.70 (dd, J = 7.7, 1.7 Hz, 1 H), 7.65–7.58 (m, 1 H), 7.58–7.53 (m, 1 H), 7.15–7.09 (m, 1 H), 7.06 (td, J = 7.1, 1.3 Hz, 1 H), 6.99 (ddd, J = 8.1, 7.1, 1.7 Hz, 1 H), 6.71 (dd, J = 8.1, 1.4 Hz, 1 H), 6.63 (ddd, J = 7.7, 7.1, 1.4 Hz, 1 H), 3.83 (d, J = 9.4 Hz, 2 H), 3.11 (d, J = 9.5 Hz, 2 H), 3.08–3.00 (m, 8 H),

1.68–1.47 (m, 8 H), 1.44–1.26 (m, 8 H), 1.21 (s, 3 H), 0.96 (t, J = 7.3 Hz, 12 H), 0.68 (s, 3 H); **^{11}B NMR** (128 MHz, CD$_3$CN, δ): 2.4.

4.9.3 Verification of the Absolute Stereochemistry of Product 4-4a by X-Ray Crystallographic Analysis
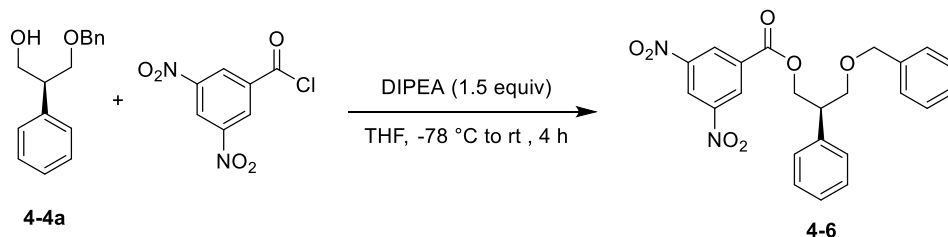
(*R*)-3-(Benzyloxy)-2-phenylpropyl 3,5-dinitrobenzoate (4-5): A mixture of compound **4-4a** (41 mg, 0.17 mmol) and *N,N*-diisopropylethylamine (45 µL, 0.26 mmol, 1.5 equiv) in 5 mL dry THF was cooled to –78 °C. Then, 3,5-dinitrobenzoyl chloride (58 mg, 0.26 mmol, 1.5 equiv) was added portion-wise to the reaction mixture at –78 °C and stirred at –78 °C for 30 min before removing it from the cooling bath. The reaction mixture was allowed to warm up to room temperature and stirred for another 3 h, after which time, it was quenched by addition of water (10 mL) and extracted by ethyl acetate (3 × 5 mL). The combined organic layers were washed with brine, dried with MgSO$_4$, filtered, and concentrated in vacuo. The crude mixture was purified by flash column chromatography (20:1 to 10:1 hexanes/EtOAc) to afford the desired product as a white solid (53 mg, 73%). A single crystal of compound **4-6** for X-ray crystallographic analysis was obtained through a slow diffusion technique in a closed system using the following procedures. A 10 mg sample of compound **4-6** was dissolved in 0.2 mL chloroform and filtered through a cotton bud into a ½ dram vial. The ½ dram vial (without a lid) was placed into a 3-dram vial containing pentane as the anti-solvent for the crystallization, and the 3-dram vial was capped and left inside the fume hood. After two days, a clear crystal was obtained and subjected to X-ray crystallographic analysis.

Mp: 77.1–78.0 °C; **^{1}H NMR** (500 MHz, CDCl$_3$, δ): 9.14 (t, J = 2.2 Hz, 1 H), 8.96 (d, J = 2.2 Hz, 2 H), 7.39–7.34 (m, 2 H), 7.34–7.27 (comp m, 3 H), 7.25–7.23 (comp m, 4 H), 7.20–7.18 (comp m, 1 H), 4.85 (dd, J = 10.9, 6.6 Hz, 1 H), 4.69 (dd, J = 10.9,

7.0 Hz, 1 H), 4.52 (d, J = 11.8 Hz, 1 H, A part of AB), 4.51 (d, J = 12.0 Hz, 1 H, B part of AB), 3.87–3.78 (m, 2 H, AB part of AB), 3.50 (dddd, J = 7.0, 7.0, 7.0, 5.0 Hz, 1 H); **^{13}C NMR** (126 MHz, CDCl$_3$, δ): 162.4, 148.6, 138.7, 137.9, 134.0, 129.3, 128.9, 128.3, 128.0, 127.70, 127.66, 127.6, 122.2, 73.4, 71.3, 68.0, 45.1; **IR** (KBr, cast film, cm^{-1}): 3100 (m), 3030 (m), 2861 (m), 1733 (s), 1629 (m), 1545 (s), 1454 (m), 1345 (s), 1278 (s), 1168 (s), 1100 (m), 921 (m), 730 (s); **HRMS** (ESI-TOF) *m/z* for C$_{23}$H$_{20}$N$_2$NaO$_7$ (M+Na)$^+$: calcd 459.1163; found 459.1163; $[\alpha]_D^{20}$ –21.5 (*c* 1.02, CHCl$_3$).

4.9.4 NMR Studies of the Effect of the "Methyl-blocker" on the Conformational Equilibrium
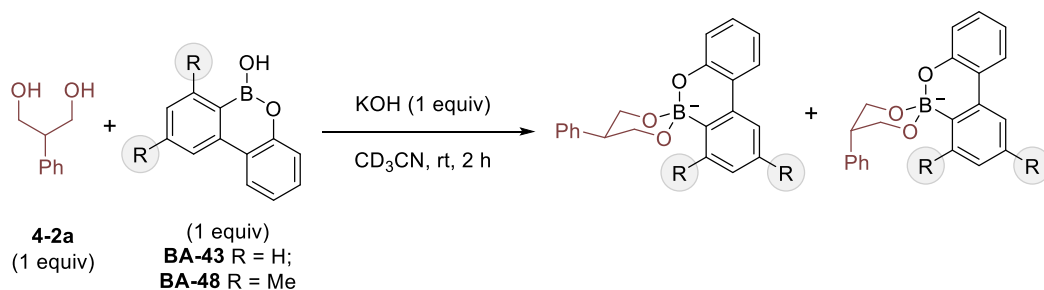
A mixture of boroxarophenanthrene catalyst **BA-43** (10 mg, 0.050 mmol) or **BA-48** (11 mg, 0.050 mmol) and 2-phenyl-1,3-propanediol **4-2a** (8 mg, 0.05 mmol) was dissolved in CD$_3$CN or *d*-acetone (0.7 mL), then potassium hydroxide (45% in H$_2$O, 7 µL, 0.05 mmol) was added to the reaction mixture. The reaction mixture was stirred at room temperature for 2 h, after which time, it was filtered through a celite plug into an NMR tube and subjected to NMR spectroscopic analysis. The ratio of the two conformers were determined using ^{1}H NMR spectroscopy.

4.9.5 Synthesis and Characterization of Boroxarophenanthrene BA-49
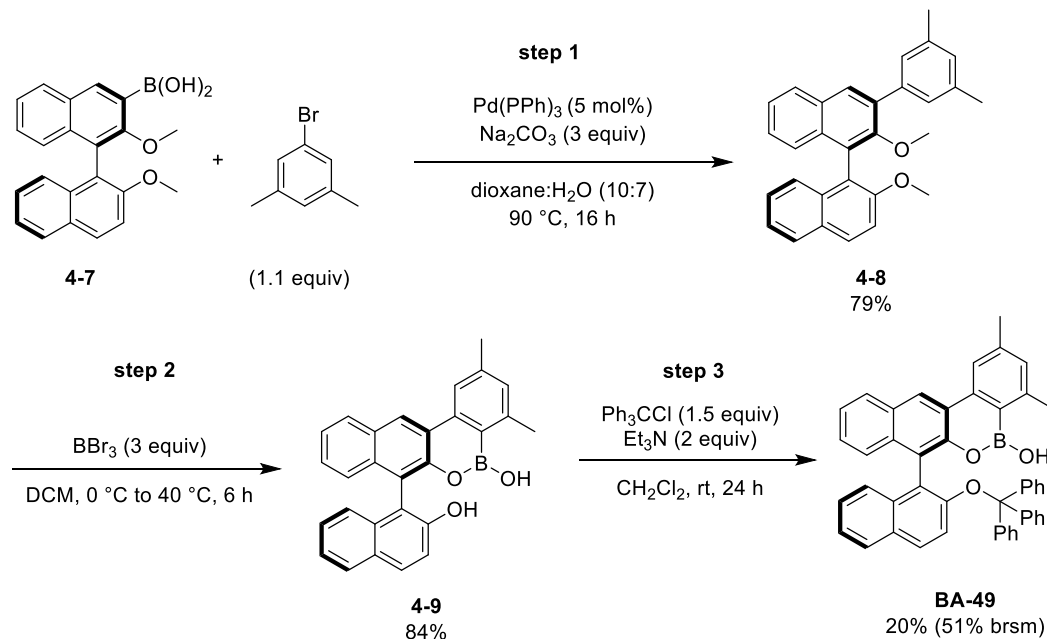
Step 1: To a 15 mL pressure tube equipped with a stir bar was added (*R*)-(2,2'-dimethoxy-[1,1'-binaphthalen]-3-yl)boronic acid (**4-7**) (419 mg, 1.17 mmol), 5-bromo-*m*-xylene (191 μL, 1.41 mmol), sodium carbonate (373 mg, 3.51 mmol), and Pd(PPh$_3$)$_4$ (68 mg, 0.059 mmol). The reaction flask was sealed with a septum, evacuated, and back-filled with nitrogen three times before dioxane (8 mL) and H$_2$O (5.6 mL, degassed with N$_2$) were added. Then, the reaction mixture was stirred at 90 °C for 18 h, after which time, it was removed from the oil bath and allowed to cool to room temperature. The reaction mixture was filtered, and the filtrate was extracted with ethyl acetate (3 × 5 mL). The combined organic layers were washed with H$_2$O (2 × 10 mL) followed by brine (10 mL), dried with MgSO$_4$, filtered, and concentrated in vacuo. The crude oil was purified by silica gel chromatography (40:1 to 20:1 hexanes/ethyl acetate), and the intermediate **4-8** was isolated as a beige solid foam (387 mg, 79% yield).

Step 2: The intermediate **4-8** (387 mg, 0.925 mmol) was added to a flame-dried 15 mL pressure tube equipped with a stir bar and dissolved in CH$_2$Cl$_2$ (5 mL). The flask was sealed with a septum and cooled to 0 °C. BBr$_3$ (neat, 270 μL, 2.80 mmol)

was added dropwise with a gas-tight syringe. The reaction mixture was removed from the ice bath and gradually warmed to room temperature, then stirred at 45 °C in an oil bath for 19 h. Then, the reaction was quenched with a slow addition of H_2O (5 mL) followed by saturated aqueous $NaHCO_3$ (5 mL) at 0 °C with a venting needle connected to an open syringe filled with solid Na_2CO_3 and Na_2SO_4. Next, the reaction mixture was removed from the ice bath and was stirred for an additional 30 min and then extracted with CH_2Cl_2 (2 × 10 mL). The combined organic layers were washed with saturated aqueous $NaHCO_3$ solution (10 mL) followed by brine (10 mL), dried with $MgSO_4$, filtered, and concentrated in vacuo. The residue was purified by silica gel chromatography (20:1 to 10:1 hexanes/EtOAc) to yield the intermediate **4-9** as a beige solid foam (322 mg, 84 % yield).

Step 3: Intermediate **4-9** (320 mg, 0.769 mmol) and triphenylmethyl chloride (324 mg, 1.16 mmol, 1.50 equiv) were dissolved with CH_2Cl_2 (5 mL) in a 10 mL round-bottom flask equipped with a stir bar, then triethylamine (130 µL, 0.924 mmol, 1.20 equiv) was added. The flask was sealed with a glass stopcock, and the reaction mixture was stirred at room temperature for 17 h, after which time, it was transferred to a separatory funnel, followed by addition of H_2O (5 mL), and then extracted with CH_2Cl_2 (2 × 5 mL). The combined organic layers were washed with brine, dried with $MgSO_4$, filtered, and concentrated in vacuo. The residue was purified by silica gel chromatography (20:1 to 10:1 hexanes/diethyl ether with slow elution) to afford the desired product **BA-49** as a yellow solid foam (102 mg, 20% yield). **Note:** Slow elution and long column packing were needed to separate compound **BA-49** from triphenylmethanol, a side product from the excess trityl chloride. The TLC was performed with 4:1 hexanes/diethyl ether to give the optimal R_f and separation of the two compounds, and the TLC plate was stained with 10% H_2SO_4 to visualize triphenylmethanol as a bright yellow spot better. Some of the product co-eluted with triphenylmethanol and was not collected, thus resulting in a lower yield than expected (51% brsm).
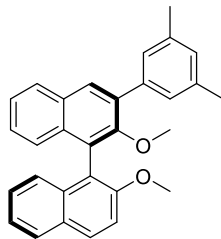
(*R*)-3-(3,5-Dimethylphenyl)-2,2'-dimethoxy-1,1'-binaphthalene (**4-8**): **Mp**: 80.3–83.1°C; **¹H NMR** (500 MHz, CDCl₃, δ): 8.00 (d, *J* = 9.0 Hz, 1 H), 7.94 (s, 1 H), 7.91–7.84 (comp m, 2 H), 7.48 (d, *J* = 9.1 Hz, 1 H), 7.42–7.35 (comp m, 3 H), 7.33 (ddd, *J* = 8.1, 6.5, 1.4 Hz, 1 H), 7.29 – 7.24 (m, 1 H), 7.23–7.19 (m, 2 H), 7.15–7.10 (m, 1 H), 3.82 (s, 3 H), 3.13 (s, 3 H), 2.39 (s, 6 H); **¹³C NMR** (126 MHz, CDCl₃, δ): 154.9, 154.1, 138.9, 137.7, 135.3, 134.2, 133.4, 130.9, 130.3, 129.6, 129.1, 128.9, 128.0, 127.9, 127.2, 126.6, 126.0, 125.6, 125.3, 124.9, 123.6, 119.7, 113.7, 60.5, 56.6, 21.4; **IR** (KBr, Cast film, cm⁻¹): 3007 (m), 2934 (m), 1621 (m), 1594 (s), 1509 (m), 1268 (s), 1247 (s), 1091 (m), 1068 (m), 751 (s); **HRMS** (EI) *m/z* for C₃₀H₂₆O₂ (M⁺•): calcd 418.1933; found 418.1930.
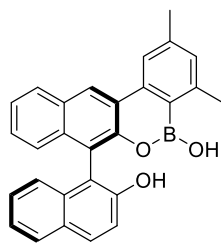
(*R*)-7-(2-Hydroxynaphthalen-1-yl)-2,4-dimethyl-5*H*-benzo[*c*]naphtho[2,3-*e*][1,2] oxaborinin-5-ol (4-9): **Mp:** 184–189 °C; **¹H NMR** (400 MHz, CD₃COCD₃, D₂O drop, δ): 8.99 (s, 1 H), 8.30 (s, 1 H), 8.11 (d, *J* = 8.1 Hz, 1 H), 7.96 (d, *J* = 9.0 Hz, 1 H), 7.92 (d, *J* = 8.2 Hz, 1 H), 7.44–7.36 (comp m, 2 H), 7.32–7.22 (comp m, 2 H), 7.19–7.13 (comp m, 2 H), 7.12 (d, *J* = 8.6 Hz, 1 H), 6.99 (d, *J* = 8.5 Hz, 1 H), 2.65 (s, 3 H), 2.51 (s, 3 H); **¹³C NMR** (101 MHz, CD₃COCD₃, D₂O drop, δ): 153.4, 148.7, 146.6, 142.5, 142.2, 135.0, 134.1, 131.6, 130.3, 129.7, 129.24, 129.16, 128.5, 126.8, 126.6, 125.5, 125.1, 124.9, 124.6, 124.4, 123.2, 121.02, 120.03, 119.0, 116.1, 22.8, 21.6; the boron-bound carbon was not detected due to the quadrupolar relaxation of boron; **¹¹B NMR** (128 MHz, CD₃COCD₃, D₂O drop, δ): 27.8 (br s); **IR** (KBr, Cast film, cm⁻¹): 3538 (br), 3057 (m), 3011 (m), 2923 (m), 1608 (s), 1553 (m), 1427 (m),

1324 (s), 1217 (s), 1144 (m), 1075 (m), 750 (s), 628 (m); **HRMS** (ESI-TOF) *m/z* for $C_{28}H_{22}^{11}BO_3$ (M+H)$^+$: calcd 417.1657; found 417.1655.
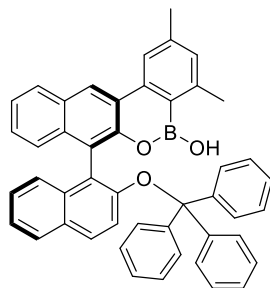
(*R*)-2,4-Dimethyl-7-(2-(trityloxy)naphthalen-1-yl)-5*H*-benzo[*c*]naphtho[2,3-e][1,2] oxaborin-in-5-ol (BA-49): Mp: 129–132 °C; **^{1}H NMR** (500 MHz, CD$_3$COCD$_3$, D$_2$O drop, δ): 9.03 (s, 1 H), 8.37 (s, 1 H), 8.09 (d, *J* = 8.3 Hz, 1 H), 7.82 (d, *J* = 8.2 Hz, 1 H), 7.56 (d, *J* = 9.1 Hz, 1 H), 7.36 (t, *J* = 7.5 Hz, 1 H), 7.30 (t, *J* = 7.3 Hz, 1 H), 7.25 (dd, *J* = 8.5, 6.7 Hz, 1 H), 7.23–7.11 (comp m, 9 H), 7.10–7.00 (comp m, 9 H), 6.95 (d, *J* = 8.5 Hz, 1 H), 6.89 (d, *J* = 9.2 Hz, 1 H), 2.69 (s, 3 H), 2.54 (s, 3 H); **^{13}C NMR** (126 MHz, CD$_3$COCD$_3$, D$_2$O drop, δ): 152.7, 149.0, 147.1, 145.3, 142.92, 142.89, 135.0, 134.1, 132.1, 130.8, 129.7, 129.6, 129.2, 128.7, 128.5, 127.85, 127.82, 126.9, 126.8, 126.4, 126.2, 125.2, 125.0, 124.5, 124.4, 122.8, 122.1, 121.5, 121.1, 90.0, 23.3, 22.1; the boron-bound carbon was not detected due to the quadrupolar relaxation of boron; **^{11}B NMR** (128 MHz, CD$_3$COCD$_3$, D$_2$O drop, δ): 27.9 (br s); **IR** (KBr, thin film, cm^{-1}): 3546 (br), 3058 (s), 2975 (m), 2924 (m), 1608 (s), 1554 (m), 1490 (s), 1447 (s), 1374 (s), 1285 (s), 1239 (s), 1155 (m), 1089 (m), 1057 (m), 1011 (s), 901 (m), 851 (m), 811 (m), 758 (s), 703 (s), 635 (s); **HRMS** (ESI-TOF) *m/z* for $C_{47}H_{35}BO_3Na$ (M+Na)$^-$: calcd 681.2571; found 681.2608; $[\alpha]_{20}^{D}$ +62.1 (*c* 2.04, CHCl$_3$).

(*S*)-2,4-Dimethyl-7-(2-(trityloxy)naphthalen-1-yl)-5*H*-benzo[*c*]naphtho[2,3-*e*][1,2] oxaborin-in-5-ol ((*S*)-BA-49): Synthesized following the same procedure as compound **BA-49** starting from (*S*)-(2,2'-dimethoxy-[1,1'-binaphthalen]-3-yl)boronic acid. Isolated as yellow foam solid (52 mg, 7% yield for Step 3); $[\alpha]_{20}^{D}$ –71.8 (*c* 1.18, CHCl$_3$).

4.9.6 Preparation and Characterization of 2-Substituted 1,3-Propanediols

2-Phenyl-1,3-diol **4-2a** was purchased from Combi Blocks and used directly without prior purifications. Other 1,3-diols were synthesized using one of the following methods depending on the commercial availability of starting materials.

4.9.6.1 General Procedure 1 (GP1): Preparation of Diols from Arylacetic Acid
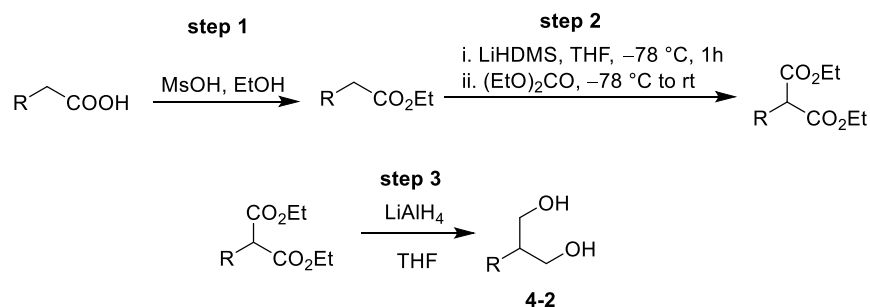
Step 1: The arylacetic acid (3.0 mmol) was dissolved with 5 mL ethanol in a 25 mL round bottom flask equipped with a stir bar. Methanesulfonic acid (1.5 equiv) was added, and the reaction mixture was stirred for 4–20 h (monitored by TLC). The solvent was removed in vacuo, the crude mixture was diluted with ethyl acetate, and washed with saturated aqueous NaHCO$_3$ and then brine. The organic layer was dried over MgSO$_4$, filtered, and concentrated to yield ethyl 2-arylacetate. The ethyl 2-arylacetate was used without any further purification.

Step 2: To a solution of ethyl 2-arylacetate (from Step 1) in THF (0.25 M) at –78 °C under nitrogen atmosphere was added 1 M solution of lithium hexamethyldisilazane in THF (1.2 equiv) using a syringe, and the mixture was stirred at –78 °C for 1 h. Then, carbonate (1.5 equiv) was added, the mixture was stirred for an additional 30 min at –78 °C, the cooling bath was removed, and the reaction mixture was allowed to warm up to room temperature and stirred for 14 h. Next, the reaction was quenched by addition of a saturated aqueous ammonium chloride solution (10 mL), and the mixture was extracted with ethyl acetate (3 × 10 mL). The combined organic layers were washed with brine, dried over MgSO$_4$, filtered, and concentrated in vacuo. The crude mixture was purified by flash column chromatography (20:1 to 10:1 hexanes/ethyl acetate), affording diethyl 2-arylmalonate.

Step 3: To a suspension of lithium aluminum hydride (5 equiv) in dry THF (0.50 M) at 0 °C, a solution of diethyl 2-arylmalonate (from Step 2, 1 equiv) in 2 mL THF was added slowly over 5 min. Then, the cooling bath was removed, and the resultant mixture was allowed to warm up to room temperature and stirred for 18 h, after which time, it was cooled to 0 °C. The reaction was quenched using the Fieser workup, and the reaction mixture was concentrated in vacuo to afford the crude mixture. The crude product was purified by flash column chromatography (2:1 CH$_2$Cl$_2$/ethyl acetate), yielding the desired 1,3-propanediols.

4.9.6.2 General Procedure 2 (GP2): Preparation of Diols from Substituted Iodobenzene
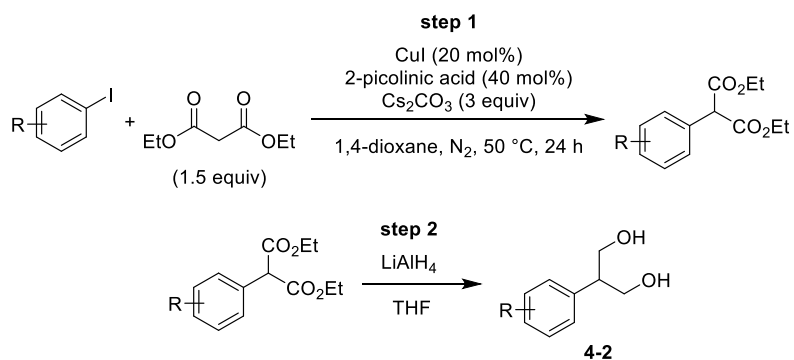
Step 1: To a flame dried 100 mL round bottom flask charged with a stir bar was added CuI (0.2 equiv), 2-picolinic acid (0.4 equiv), and cesium carbonate (3 equiv), and the flask was purged with nitrogen. To another flame dried flask was added the substituted iodobenzene (3.0 mmol), diethyl malonate (1.5 equiv), and dioxane (30 mL). The reaction mixture was degassed vigorously with nitrogen for 10 min, cannula transferred to the 100 mL round bottom flask containing solid reagents, and vigorously stirred under nitrogen at 50 °C for 24 h. Then, the reaction mixture was removed from the heating bath and allowed to cool to room temperature. Next, the reaction was quenched with addition of a saturated aqueous ammonium chloride solution (10 mL), stirred for 15 min, and extracted with ethyl acetate (3 × 10 mL). The combined organic phases were washed with brine, dried over MgSO$_4$, filtered, and concentrated in vacuo. The reaction crude was purified by flash column

chromatography (20:1 to 10:1 hexanes/ethyl acetate), affording diethyl 2-arylmalonate.

Step 2: To a suspension of lithium aluminum hydride (5 equiv) in dry THF (0.50 M) at 0 °C, a solution of diethyl 2-arylmalonate (from step 2, 1 equiv) in 2 mL THF was added slowly over 5 min. Then, the cooling bath was removed, and the resultant mixture was allowed to warm up to room temperature and stirred for 18 h, after which time, it was cooled to 0 °C. The reaction was quenched using the Fieser workup, and the reaction mixture was concentrated in vacuo to afford the crude mixture. The crude was purified by flash column chromatography (2:1 CH_2Cl_2/ethyl acetate), yielding the desired 1,3-propanediols.

4.9.6.3 Characterization of 2-Substituted 1,3-Propanediols
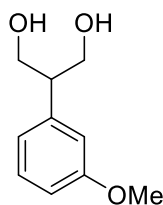
2-(3-Methoxyphenyl)propane-1,3-diol (4-2c): Prepared according to **GP1** from 3-methoxyphenylacetic acid and isolated as a white solid. **Mp**: 40.2–43.6 °C; **^{1}H NMR** (400 MHz, CDCl₃, δ): 7.26 (t, J = 7.6 Hz, 1 H), 6.86–6.76 (comp m, 3 H), 4.05–3.89 (comp m, 4 H, AB part of ABX), 3.81 (s, 3 H), 3.08 (tt, J = 7.4, 5.7 Hz, 1 H, X part of ABX), 1.96 (t, J = 5.4 Hz, 2 H); **^{13}C NMR** (101 MHz, CDCl₃, δ): 159.5, 140.5, 129.5, 119.9, 113.7, 111.9, 65.6, 54.8, 49.6.
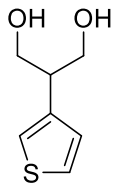
2-(Thiophen-3-yl)propane-1,3-diol (4-2g): Prepared from 3-thiophenemalonic acid using step 1 and 3 of **GP1**, and isolated as a white solid. **Mp**: 37.0–39.2 °C; **^{1}H NMR** (500 MHz, CDCl₃, δ): 7.32 (dd, J = 5.0, 2.9 Hz, 1 H), 7.12 (dd, J = 2.9, 1.3 Hz, 1 H), 7.01 (dd, J = 5.0, 1.3 Hz, 1 H), 3.97 – 3.93 (comp m, 4 H, AB part of ABX), 3.23

(app p, J = 6.2 Hz, 1 H, X part of ABX), 2.17 (s, 2 H); ^{13}C NMR (126 MHz, CDCl$_3$, δ): 139.6, 127.2, 126.2, 121.6, 65.7, 45.2.

2-(*m*-Tolyl)propane-1,3-diol (4-2m): Prepared according to **GP1** from 3-methylphenylacetic acid and isolated as a white solid. **Mp**: 54.3–55.5 °C; ^{1}**H NMR** (500 MHz, CDCl$_3$, δ): 7.23 (t, J = 7.5 Hz, 1 H), 7.08 (d, J = 7.6 Hz, 1 H), 7.06–7.01 (comp m, 2 H), 4.00 (dd, J = 10.8, 7.6 Hz, 2 H, A part of AB), 3.93 (dd, J = 10.8, 5.7 Hz, 2 H, B part of ABX), 3.08 (tt, J = 7.5, 5.7 Hz, 1 H, X part of ABX), 2.35 (s, 3 H), 1.91 (s, 2 H); ^{13}**C NMR** (101 MHz, CDCl$_3$, δ): 138.7, 138.1, 128.4, 128.3, 127.6, 124.6, 65.7, 49.5, 21.1.
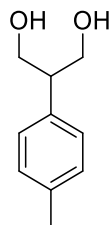
2-(*p*-Tolyl)propane-1,3-diol (4-2n): Prepared according to **GP2** from 4-iodotoluene and isolated as a white solid. **Mp**: 43.7–45.5 °C; ^{1}**H NMR** (500 MHz, CDCl$_3$, δ): 7.18–7.10 (comp m, 4 H), 3.99 (dd, J = 10.8, 7.6 Hz, 2 H, A part of ABX), 3.92 (dd, J = 10.8, 5.6 Hz, 2 H, B part of ABX), 3.08 (tt, J = 7.6, 5.6 Hz, 1 H, X part of ABX), 2.33 (s, 3 H), 1.90 (s, 3 H); ^{13}**C NMR** (126 MHz, CDCl$_3$, δ): 136.9, 136.1, 129.6, 127.9, 66.2, 49.5, 21.1.
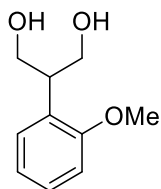
2-(2-Methoxyphenyl)propane-1,3-diol (4-2o): Prepared according to **GP2** from 2-iodoanisole and isolated as a white solid. **Mp**: 64.9–66.4 °C; ^{1}**H NMR** (500 MHz,

CDCl$_3$, δ): 7.24 (ddd, J = 8.3, 7.5, 1.8 Hz, 1 H), 7.17 (dd, J = 7.5, 1.7 Hz, 1 H), 6.94 (td, J = 7.5, 1.2 Hz, 1 H), 6.90 (dd, J = 8.2, 1.2 Hz, 1 H), 4.02 (dd, J = 10.7, 7.5 Hz, 2 H, A part of ABX), 3.95 (dd, J = 10.7, 5.3 Hz, 2 H, B part of ABX), 3.83 (s, 3 H), 3.55 (tt, J = 7.4, 5.2 Hz, 1 H, X part of ABX), 2.04 (s, 3 H); **^{13}C NMR** (126 MHz, CDCl$_3$, δ): 157.4, 128.3, 128.1, 127.5, 120.8, 110.8, 65.3, 55.4, 43.3.
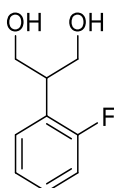
2-(2-Fluorophenyl)propane-1,3-diol (4-2p): Prepared according to **GP2** from 1-fluoro-2-iodobenzene and isolated as a white solid. **Mp**: 45.6–46.7 °C; **^{1}H NMR** (500 MHz, CDCl$_3$, δ): 7.32–7.20 (comp m, 2 H), 7.12 (td, J = 7.5, 1.3 Hz, 1 H), 7.06 (ddd, J = 10.5, 8.2, 1.2 Hz, 1 H), 4.06 (dd, J = 10.9, 7.5 Hz, 2 H, A part of ABX), 3.99 (dd, J = 10.8, 5.2 Hz, 2 H, B part of ABX), 3.45 (tt, J = 7.6, 5.2 Hz, 1 H, X part of ABX), 1.93 (br s, 2 H); **^{13}C NMR** (126 MHz, CDCl$_3$, δ): 161.0 (d, J = 245.6 Hz), 129.2 (d, J = 4.6 Hz), 128.6 (d, J = 8.4 Hz), 126.3 (d, J = 14.9 Hz), 124.4 (d, J = 3.6 Hz), 115.8 (d, J = 22.9 Hz), 65.1, 43.0; **^{19}F NMR** (376 MHz, CDCl$_3$, δ): –117.6 (dt, J = 11.5, 6.3 Hz).
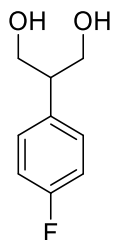
2-(4-Fluorophenyl)propane-1,3-diol (4-2q): Prepared according to **GP1** from 4-fluorophenylacetic acid and isolated as a white solid. **Mp**: 34.2–36.3 °C; **^{1}H NMR** (400 MHz, CDCl$_3$, δ): 7.25–7.17 (m, 2 H), 7.08–6.98 (m, 2 H), 4.03–3.88 (comp m, 4 H, AB part of ABX), 3.09 (tt, J = 7.4, 5.5 Hz, 1 H, X part of ABX), 2.01 (t, J = 4.6 Hz, 2 H); **^{13}C NMR** (101 MHz, CDCl$_3$, δ): 134.7, 129.1 (d, J = 7.8 Hz), 115.3 (d, J = 21.0 Hz), 65.6, 48.6; **^{19}F NMR** (376 MHz, CDCl$_3$, δ): –115.48 (ddd, J = 13.9, 8.8, 5.3 Hz).
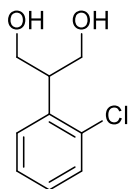
2-(2-Chlorophenyl)propane-1,3-diol (4-2r): Prepared according to **GP1** from 2-chlorophenylacetic acid and isolated as a white solid. **Mp**: 45.7–47.9 °C; **^{1}H NMR** (400 MHz, CDCl$_3$, δ): 7.40 (dd, J = 7.8, 1.6 Hz, 1 H), 7.29 (dd, J = 7.6, 2.0 Hz, 1 H), 7.24 (td, J = 7.4, 1.6 Hz, 1 H), 7.19 (td, J = 7.5, 2.0 Hz, 1 H), 4.02 (dd, J = 10.8, 7.1 Hz, 2 H, A part of ABX), 3.99 (dd, J = 10.8, 5.3 Hz, 2 H, B part of ABX), 3.66 (tt, J = 7.0, 5.3 Hz, 1 H, X part of ABX), 2.38 (s, 2 H); **^{13}C NMR** (101 MHz, CDCl$_3$, δ): 136.5, 134.0, 129.5, 127.9, 127.8, 126.7, 64.5, 44.8.
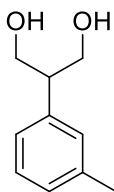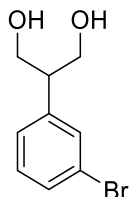

2-(3-Bromophenyl)propane-1,3-diol (4-2s): Prepared according to **GP1** from 3-bromophenylacetic acid and isolated as a white solid. **Mp**: 42.3–44.7 °C; **^{1}H NMR** (500 MHz, CDCl$_3$, δ): 7.34 (comp m, 2 H), 7.30–7.22 (comp m, 2 H), 4.02 (dd, J = 10.8, 7.5 Hz, 2 H, A part of ABX), 3.95 (dd, J = 10.8, 5.7 Hz, 2 H, B part of ABX), 3.12 (tt, J = 7.7, 5.6 Hz, 1 H, X part of ABX), 1.88 (s, 2 H); **^{13}C NMR** (126 MHz, CDCl$_3$, δ): 139.3, 128.9, 128.1, 127.3, 66.1, 49.9.
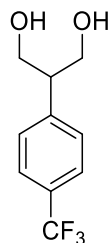
2-(4-(Trifluoromethyl)phenyl)propane-1,3-diol (4-2n): Prepared according to **GP1** from 4-(trifluoromethyl)phenylacetic acid and isolated as a white solid. **Mp**: 38.7–40.7 °C; **^{1}H NMR** (400 MHz, CDCl$_3$, δ): 7.60 (d, J = 8.1 Hz, 2 H), 7.38 (d, J = 8.1 Hz,

2 H), 4.03 (dd, $J = 10.8$, 7.2 Hz, 2 H, A part of ABX), 3.98 (dd, $J = 10.7$, 5.5 Hz, 2 H, B part of ABX), 3.16 (tt, $J = 7.2$, 5.4 Hz, 1 H, X part of ABX), 2.01 (s, 2 H); ^{13}**C NMR** (101 MHz, CDCl$_3$, δ): 143.4, 128.1, 125.3 (q, $J = 3.5$ Hz), 65.2, 49.1; ^{19}**F NMR** (376 MHz, CDCl$_3$, δ): –62.5.
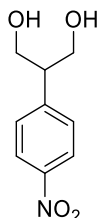
2-(4-Nitrophenyl)propane-1,3-diol (4-2u): Prepared from 1-iodo-4-nitrobenzene using Step 1 from **GP2** and reduced by NaBH$_4$ instead of LiAlH$_4$ using the following procedure. To a suspension of sodium borohydride (10 equiv) in THF (0.50 M) at 0 °C, a solution of diethyl 2-(4-nitro-phenyl)malonate (1 equiv) in 1 mL THF was added dropwise over 5 min, followed by methanol (5 mL). Then, the cooling bath was removed, and the resultant mixture was allowed to warm up to room temperature. The reaction mixture was heated to reflux for 18 h, after which time, it was removed from the heating bath and allowed to cool to room temperature and then to 0 °C. The reaction was quenched by addition of 1 M aqueous HCl (10 mL) and stirred for 15 min. The reaction mixture was extracted with ethyl acetate (3 × 10 mL), and the combined organic phases were washed with brine, dried over MgSO$_4$, filtered, and concentrated in vacuo. The product was isolated as an orange solid from flash column chromatography (1:1 DCM/ethyl acetate). **Mp**: 82.4–84.0 °C; ^{1}**H NMR** (500 MHz, CDCl$_3$, δ): 8.20 (d, $J = 8.7$ Hz, 2 H), 7.46 (d, $J = 8.7$ Hz, 2 H), 4.07–3.99 (comp m, 4 H, AB part of ABX), 3.20 (app p, $J = 6.1$ Hz, 1 H, X part of ABX), 1.95 (t, $J = 5.2$ Hz, 2 H); ^{13}**C NMR** (126 MHz, CDCl$_3$, δ): 147.6, 147.2, 129.1, 123.9, 65.2, 49.4.
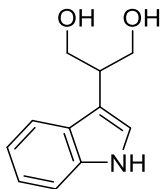
2-(1*H*-Indol-3-yl)propane-1,3-diol (4-2v): Prepared according to a slightly modified **GP1** from indole-3-acetic acid and isolated as a white solid. After Step 1 in **GP1**, the

ethyl 2-(1*H*-indol-3-yl) acetate was protected by a Boc-group using the following procedure. To a solution of ethyl 2-(1*H*-indol-3-yl) acetate in DCM (10 mL) at room temperature was added triethylamine (1.1 equiv) and Boc$_2$O (1.3 equiv). The resultant mixture was stirred for 17 h, after which time, it was washed with saturated aqueous sodium bicarbonate (10 mL) and then brine, dried with MgSO$_4$, filtered, and concentrated in vacuo. The crude mixture was purified by flash column chromatography (9:1 hexanes/ethyl acetate) before subjecting it to step 2 and 3. **Mp**: 73.3–75.8 °C; **^{1}H NMR** (400 MHz, CD$_3$COCD$_3$, δ): 10.01 (br s, 1 H), 7.59 (d, *J* = 8.0, 1 H), 7.36 (dt, *J* = 8.1, 1.0 Hz, 1 H), 7.20 (d, *J* = 2.4 Hz, 1 H), 7.07 (ddd, *J* = 8.2, 7.0, 1.2 Hz, 1 H), 6.99 (ddd, *J* = 8.0, 7.0, 1.1 Hz, 1 H), 4.01–3.87 (comp m, 4 H, AB part of ABX), 3.30 (tt, *J* = 7.1, 5.3 Hz, 1 H, X part of ABX), 2.80 (s, 2 H); **^{13}C NMR** (126 MHz, CD$_3$COCD$_3$, δ): 137.6, 128.5, 123.0, 122.1, 119.5, 119.4, 114.8, 112.2, 65.5, 42.6.
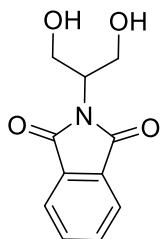
2-(1,3-Dihydroxypropan-2-yl)isoindoline-1,3-dione (4-2x): Prepared from serinol using the following procedure and isolated as a beige solid. A mixture of serinol (329 mg, 3.61 mmol) and phthalic anhydride (535 mg, 3.61 mmol) in 10 mL of toluene was heated at reflux for 18 h, after which time, it was concentrated in vacuo to afford a crude solid chunk. MTBE (5 mL) was added to the crude solid, and the heterogenous mixture was stirred for 1 h at room temperature. The heterogenous mixture was filtered, and the residue was washed with 20 mL MTBE to afford compound **4-2x** as a beige solid (591 mg, 74% yield). **Mp**: 116.8–118.2 °C; **^{1}H NMR** (600 MHz, CDCl$_3$, δ): 7.88 (dd, *J* = 5.4, 3.1 Hz, 2 H), 7.77 (dd, *J* = 5.5, 3.0 Hz, 2 H), 4.48 (tt, *J* = 5.9, 4.4 Hz, 1 H, X part of ABX), 4.12 (dd, *J* = 12.2, 6.0 Hz, 2 H, A part of ABX), 4.07 (dd, *J* = 12.1, 4.4 Hz, 2 H, B part of ABX), 3.12 (br s, 2 H); ^{13}C NMR (126 MHz, CDCl$_3$, δ): 169.4, 134.4, 131.7, 123.6, 61.9, 54.7.
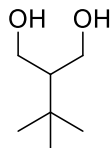
2-(*Tert*-butyl)propane-1,3-diol (4-2y): Prepared according to **GP1** from *tert*-butylacetic acid and isolated as a white flaky solid. Note: Ethyl 3,3-dimethylbutanoate has a low boiling point and should not be left under high vacuum for prolonged periods. **Mp**: 51.0–52.3 °C; **^{1}H NMR** (500 MHz, CDCl$_3$, δ): 4.02–3.98 (m, 2 H, A part of AB), 3.78 (ddd, *J* = 10.2, 9.1, 2.5 Hz, 2 H, B part of ABX), 2.47 (s, 2 H), 1.64 (tt, *J* = 9.1, 3.5 Hz, 1 H, X part of ABX), 0.92 (s, 9 H); **^{13}C NMR** (126 MHz, CDCl$_3$, δ): 65.0, 51.3, 31.5, 28.2.

4.9.7 General Procedure for the Enantioselective Desymmetrization of 1,3-Diols using Chiral Catalyst BA-49
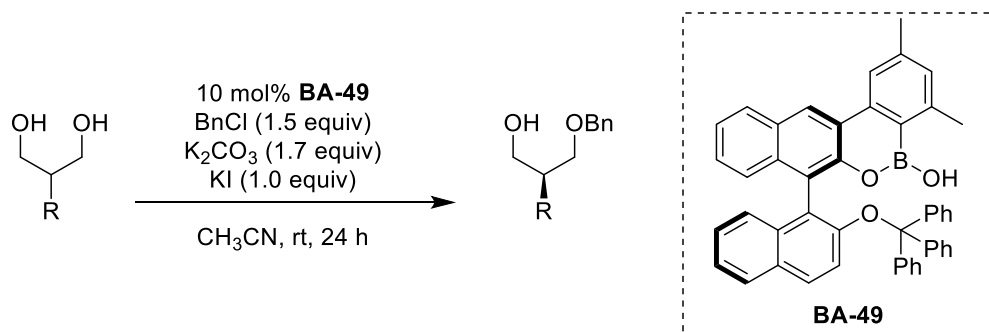
To a 5 mL round-bottom flask was added the 1,3-diol **4-2** (0.1 mmol), organoboron catalyst **BA-49** (0.01 mmol), potassium carbonate (23.5 mg, 0.170 mmol), and potassium iodide (16.6 mg, 0.100 mmol). Then, acetonitrile (0.5 mL) was added, followed by benzyl chloride (17 µL, 0.15 mmol). The flask was sealed with a glass stopper, and the reaction was stirred at room temperature for 24 h, after which time, it was filtered through a celite plug with ethyl acetate as solvent and concentrated in vacuo. Unless noted otherwise, the crude mixture was purified by flash column chromatography (10:1 to 5:1 hexanes/EtOAc). The catalyst **BA-49** can be recovered from the flash column chromatography and reused for another desymmetrization reaction.

4.9.7.1 Characterization of Desymmetrized Products
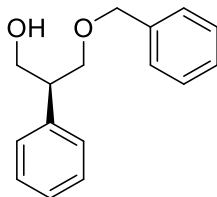
(S)-2-Phenyl-3-(benzyloxy)propan-1-ol (4-4a): Prepared from 1,3-diol **4-2a** (16 mg, 0.10 mmol) using the general procedure. Isolated as a yellow oil (22.5 mg, 90%). **^{1}H NMR** (400 MHz, CDCl$_3$, δ): 7.41–7.29 (comp m, 7 H), 7.29–7.19 (comp m, 3 H), 4.57 (s, 2 H), 4.02 (dd, J = 10.9, 7.4 Hz, 1 H, A part of ABX), 3.89 (dd, J = 10.9, 7.4 Hz, 1 H, B part of ABX), 3.86–3.75 (comp m, 2 H, AB part of ABX), 3.23 (dddd, J = 7.8, 7.8, 5.3, 5.3 Hz, 1 H, X part of ABX), 2.45 (br s, 1 H); **^{13}C NMR** (101 MHz, CDCl$_3$, δ): 139.6, 137.9, 128.7, 128.5, 128.0, 127.8, 127.7, 127.1, 118.0, 73.6, 73.5, 66.5, 47.8; **IR** (KBr, Cast film, cm^{-1}): 3409 (br), 3061 (m), 3028 (s), 2863 (s), 1952 (w), 1875 (w), 1810 (w), 1603 (m), 1495 (s), 1453 (s), 1364 (s), 1205 (m), 1093 (s), 1029 (s), 909 (m), 848 (w), 739 (s), 699 (s); **HRMS** (EI-TOF) m/z for C$_{16}$H$_{18}$O$_2$ (M$^{+\bullet}$): calcd 242.1307; found 242.1307; $[\alpha]_D^{20}$ –22.0 (c 1.14, CHCl$_3$); **HPLC** (Chiralpak IC): 5:95 iPrOH/Hex, 20 °C, 0.5 mL/min, λ = 211 nm, T$_{(S)}$ = 14.1 min, T$_{(R)}$ = 15.2 min, er = 94.9: 5:1.
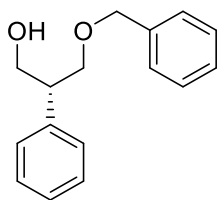
(R)-2-Phenyl-3-(benzyloxy)propan-1-ol ((R)-4-4a): Prepared from 1,3-diol **4-2a** (15 mg, 0.099 mmol) with catalyst **(S)-BA-49** (6.5 mg, 9.9 µmol) using the general procedure. Isolated as a yellowish oil (22.7 mg, 95%). $[\alpha]_D^{20}$ +21.7 (c 2.24, CHCl$_3$); **HPLC** (Chiralpak IC): 5:95 i-PrOH/Hex, 20 °C, 0.5 mL/min, λ = 221 nm, T$_{(S)}$ = 14.2 min, T$_{(R)}$ = 15.3 min, er = 5.1:94.9.
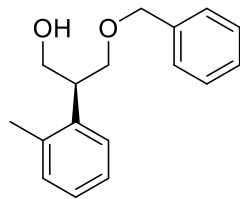
(*S*)-3-(Benzyloxy)-2-(*o*-tolyl)propan-1-ol (4-4b): Prepared from 1,3-diol **4-2b** (17 mg, 0.10 mmol) using the general procedure. Isolated as clear oil (22.6 mg, 86%). **¹H NMR** (500 MHz, CDCl$_3$, δ): 7.39–7.28 (comp m, 5 H), 7.21–7.12 (comp m, 3H), 7.12–7.07 (m, 1 H), 4.57 (s, 2 H), 4.04 (dd, *J* = 10.9, 7.7 Hz, 1 H, A part of ABX), 3.86 (dd, *J* = 11.0, 4.9 Hz, 1 H, B part of ABX), 3.81 (dd, *J* = 9.2, 9.2 Hz, 1 H, A part of ABX), 3.74 (dd, *J* = 9.2, 4.5 Hz, 1 H, B part of ABX) 3.51 (dddd, *J* = 9.3, 7.6, 4.7, 4.7 Hz, 1 H, X part of ABX), 2.54 (br s, 1 H), 2.38 (s, 3 H); **¹³C NMR** (126 MHz, CDCl$_3$, δ): 137.9, 137.6, 136.5, 130.7, 128.5, 127.8, 127.7, 126.8, 126.3, 126.2, 73.9, 73.5, 66.5, 43.0, 19.7; **IR** (KBr, Cast film, cm^{-1}): 3412 (br), 3062 (s), 3027 (s), 2863 (s), 1736 (w), 1604 (m), 1493 (s), 1454 (s), 1363 (s), 1205 (s), 1098 (s), 908 (m), 737 (s), 699 (s), 610 (m); **HRMS** (ESI-TOF) *m/z* for C$_{17}$H$_{20}$NaO$_2$ (M+Na)$^+$: calcd 279.1356; found 279.1355; $[\alpha]_D^{20}$ –21.0 (*c* 0.76, CHCl$_3$); **HPLC** (Chiralpak IC): 5:95 *i*-PrOH/Hex, 20 °C, 0.5 mL/min, λ = 221 nm, T$_{(S)}$ = 12.0 min, T$_{(R)}$ = 13.6 min, er = 96.0:4.0.

(*S*)-3-(Benzyloxy)-2-(3-methoxyphenyl)propan-1-ol (4-4c): Prepared from 1,3-diol **4-2c** (18 mg, 0.10 mmol) using the general procedure. Isolated as a clear oil (24.7 mg, 91%). **¹H NMR** (500 MHz, CDCl$_3$, δ): 7.38–7.27 (comp m, 5 H), 7.23 (t, *J* = 7.9 Hz, 1 H), 6.83–6.75 (comp m, 3 H), 4.56 (s, 2 H), 4.00 (ddd, *J* = 10.9, 7.2, 4.8 Hz, 1 H, A part of ABX), 3.86 (ddd, *J* = 11.0, 7.2, 5.4 Hz, 1 H, B part of ABX), 3.85 – 3.80 (m, 1 H, A part of ABX), 3.79 (s, 3 H), 3.77 (dd, *J* = 9.3, 5.3 Hz, 1 H, B part of ABX), 3.19 (dddd, *J* = 8.5, 7.2, 5.3, 5.3 Hz, 1 H, X part of ABX), 2.35 (dd, *J* = 7.3, 4.9 Hz, 1 H); **¹³C NMR** (126 MHz, CDCl$_3$, δ): 159.8, 141.2, 137.9, 129.7, 128.5, 127.8, 127.7,

120.3, 114.0, 112.2, 73.6, 73.5, 66.5, 55.2, 47.9; **IR** (KBr, Cast film, cm^{-1}): 3418 (br), 3029 (m), 2865 (s), 1601 (s), 149 (s), 1454 (s), 1363 (m), 1260 (s), 1157 (s), 1102 (s), 1042 (s), 908 (w), 873 (w), 783 (m), 738 (s), 699 (s); **HRMS** (EI-TOF) *m/z* for C$_{17}$H$_{20}$O$_3$ (M$^{+\bullet}$): calcd 272.1412; found 272.1413; $[\alpha]_D^{20}$ –21.3 (*c* 2.43, CHCl$_3$); **HPLC** (Chiralpak IC): 10:90 *i*-PrOH/Hex, 20 °C, 0.5 mL/min, λ = 211 nm, T$_{(S)}$ = 16.2 min, T$_{(R)}$ = 19.5 min, er = 95.0:5.0.

(*S*)-3-(Benzyloxy)-2-(4-methoxyphenyl)propan-1-ol (4-4d): Prepared from 1,3-diol **4-2d** (18 mg, 0.10 mmol) and recovered catalyst **BA-49** using the general procedure. Isolated as a clear oil (25.1 mg, 93%). **^{1}H NMR** (500 MHz, CDCl$_3$, δ): 7.38–7.26 (comp m, 5 H), 7.14 (d, *J* = 8.4 Hz, 2 H), 6.86 (d, *J* = 8.6 Hz, 2 H), 4.55 (s, 2 H), 3.98 (dd, *J* = 10.9, 7.3 Hz, 1 H, A part of ABX), 3.83 (dd, *J* = 10.9, 5.4 Hz, 1 H, B part of ABX), 3.79 (s, 3 H), 3.78–3.73 (comp m, 2 H, AB part of ABX), 3.17 (ddd, *J* = 13.4, 7.9, 5.4 Hz, 1 H, X part of ABX), 2.41 (br s, 1 H); **^{13}C NMR** (126 MHz, CDCl$_3$, δ): 158.7, 137.9, 131.6, 129.0, 128.5, 127.8, 127.7, 114.1, 73.9, 73.5, 66.7, 55.3, 47.0; **IR** (KBr, Cast film, cm^{-1}): 3416 (br), 3004 (w), 2930 (m), 1611 (m), 1583 (w), 1513 (s), 1454 (m), 1363 (w), 1301 (w), 1249 (s), 1179 (m), 1099 (s), 1035 (s), 830 (m), 752 (s), 698 (m); **HRMS** (EI-TOF) *m/z* for C$_{17}$H$_{20}$O$_3$ (M$^{+\bullet}$): calcd 272.1412; found 272.1410; $[\alpha]_D^{20}$ –17.6 (*c* 1.87, CHCl$_3$); **HPLC** (Chiralpak IC): 7:93 *i*-PrOH/Hex, 20 °C, 0.5 mL/min, λ = 221 nm, T$_{(S)}$ = 23.0 min, T$_{(R)}$ = 24.2 min, er = 95.0:5.0.

(*S*)-3-(Benzyloxy)-2-(2-bromophenyl)propan-1-ol (4-4e): Prepared from 1,3-diol **4-2e** (23.4 mg, 0.10 mmol) and recovered catalyst **BA-49** using the general procedure. Isolated as a clear oil (24.4 mg, 76%). **^{1}H NMR** (500 MHz, CDCl$_3$, δ): 7.41–7.27 (comp m, 7 H), 7.29–7.20 (comp m, 2 H), 4.57 (s, 2 H), 4.03 (dd, *J* = 10.9, 7.3 Hz, 1 H, A part of ABX), 3.89 (dd, *J* = 10.9, 5.3 Hz, 1 H, B part of ABX), 3.85–3.77 (comp m, 2 H, AB part of ABX), 3.23 (dddd, *J* = 13.1, 7.9, 5.3, 5.3 Hz, 1 H, X part of ABX), 2.26 (br s, 1 H); **^{13}C NMR** (126 MHz, CDCl$_3$, δ): 139.6, 137.9, 128.7, 128.5, 128.0, 127.8, 127.7, 127.1, 73.7, 73.5, 66.6, 47.8; **IR** (KBr, Cast film, cm^{-1}): 3411 (br), 3062 (m), 3029 (s), 2863 (s), 1951 (w), 1810 (w), 1603 (m), 1495 (s), 1453 (s), 1363 (s), 1206 (m), 1097 (s), 1029 (s), 909 (w), 739 (s), 699 (s), 607 (w), 550 (m); **HRMS** (EI-TOF) *m/z* for C$_{16}$H$_{18}$O$_2$^{81}Br (M$^{+\bullet}$): calcd 322.0392; found 322.0391; [α]$_D^{20}$ –23.5 (*c* 2.72, CHCl$_3$); **HPLC** (Chiralpak IC): 5:95 *i*-PrOH/Hex, 20 °C, 0.5 mL/min, λ = 221 nm, T$_{(S)}$ = 14.8 min, T$_{(R)}$ = 16.0 min, er = 94.9:5.1.
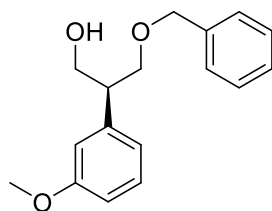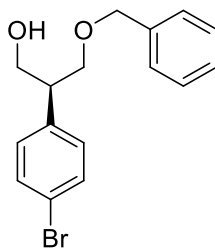

(*S*)-3-(Benzyloxy)-2-(4-bromophenyl)propan-1-ol (4-4f): Prepared from 1,3-diol **4-2f** (23 mg, 0.10 mmol) using the general procedure. Isolated as a clear oil (28.7 mg, 88%). **^{1}H NMR** (500 MHz, CDCl$_3$, δ): 7.43 (d, *J* = 8.4 Hz, 2 H), 7.38–7.33 (comp m, 2 H), 7.31–7.29 (comp m, 3 H), 7.11 (d, *J* = 8.4 Hz, 2 H), 4.54 (s, 2 H), 3.96 (dd, *J* = 10.9, 7.0 Hz, 1 H, A part of ABX), 3.85 (dd, *J* = 10.9, 5.3 Hz, 1 H, B part of ABX), 3.81–3.71 (comp m, 2 H, AB part of ABX), 3.15 (dddd, *J* = 7.5, 7.5, 5.3, 5.3 Hz, 1 H, X part of ABX), 2.12 (br s, 1 H); **^{13}C NMR** (176 MHz, CDCl$_3$, δ): 138.8, 137.8, 131.7, 129.8, 128.6, 127.9, 127.7, 120.9, 73.6, 73.0, 66.0, 47.4; **IR** (KBr, Cast film, cm^{-1}): 3399 (br), 3029 (m), 2862 (s), 1613 (m), 1489 (s), 1453 (m), 1407 (m),

1362 (m), 1205 (w), 1073 (s), 1010 (s), 821 (m), 739 (s), 698 (s); **HRMS** (ESI-TOF) *m/z* for $C_{16}H_{17}{}^{79}BrNaO_2$ (M+Na)$^+$: calcd 343.0304; found 343.0304; $[\alpha]_D^{20}$ –17.1 (*c* 2.95, CHCl$_3$); **HPLC** (Chiralpak IC): 5:95 *i*-PrOH/Hex, 20 °C, 0.5 mL/min, λ = 230 nm, $T_{(S)}$ = 12.0 min, $T_{(R)}$ = 13.0 min, er = 94.5:5.5.
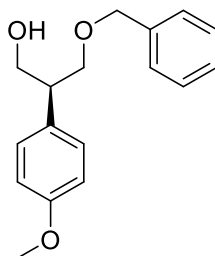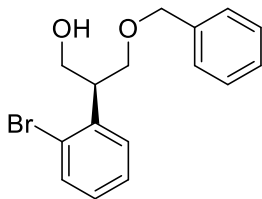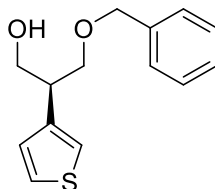

(*S*)-3-(Benzyloxy)-2-(thiophen-3-yl)propan-1-ol (4-4g): Prepared from 1,3-diol **4-2g** (16 mg, 0.10 mmol) using the general procedure. Isolated as a clear oil (23.1 mg, 91%). **^{1}H NMR** (500 MHz, CDCl$_3$, δ): 7.39–7.31 (comp m, 4 H), 7.31–7.27 (comp m, 2 H), 7.08 (dd, *J* = 3.4, 1.1 Hz, 1 H), 7.00 (dd, *J* = 5.0, 1.3 Hz, 1 H), 4.56 (s, 2 H), 3.96 (dd, *J* = 10.9, 7.0 Hz, 1 H, A part of ABX), 3.88 (dd, *J* = 10.9, 5.0 Hz, 1 H, B part of ABX), 3.84–3.75 (comp m, 2 H, AB part of ABX), 3.34 (ddd, *J* = 12.6, 7.0, 5.3 Hz, 1 H, X part of ABX), 2.27 (br s, 1 H); **^{13}C NMR** (126 MHz, CDCl$_3$, δ): 139.9, 137.9, 128.5, 127.8, 127.7, 127.4, 125.7, 121.4, 73.5, 73.2, 66.2, 43.3; **IR** (KBr, Cast film, cm^{-1}): 3412 (br), 3088 (m), 3029 (m), 2863 (s), 1495 (m), 1453 (s), 1411 (m), 1361 (s), 1250 (m), 1206 (m), 1100 (s), 1028 (s), 918 (m), 854 (m), 782 (s), 738 (s), 698 (s), 654 (s); **HRMS** (EI-TOF) *m/z* for $C_{14}H_{16}O_2S$ (M$^{+\bullet}$): calcd 248.0871; found 248.0869; $[\alpha]_D^{20}$ –20.1 (*c* 2.31, CHCl$_3$); **HPLC** (Chiralpak IB): 2:98 *i*-PrOH/Hex, 20 °C, 0.5 mL/min, λ = 220 nm, $T_{(S)}$ = 25.1 min, $T_{(R)}$ = 28.0 min, er = 94.0:6.0.
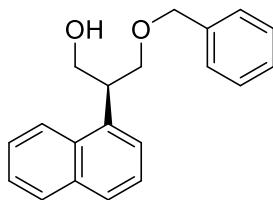
(*S*)-3-(Benzyloxy)-2-(naphthalen-1-yl)propan-1-ol (4-4h): Prepared from 1,3-diol **4-4h** (19 mg, 0.094 mmol) using the general procedure. Isolated as a clear oil (24.6 mg, 90%). **^{1}H NMR** (500 MHz, CDCl$_3$, δ): 8.15 (d, *J* = 8.4 Hz, 1 H), 7.87 (dd, *J* = 7.9, 1.6 Hz, 1 H), 7.76 (d, *J* = 8.2 Hz, 1 H), 7.57–7.47 (comp m, 2 H), 7.42 (dd, *J* = 8.2, 7.2 Hz, 1 H), 7.38–7.33 (comp m, 4 H), 7.32–7.30 (comp m, 2 H), 4.61 (s,

2 H), 4.18 (dd, $J = 10.0$, 6.9 Hz, 1 H, A part of ABX), 4.11 (m, 1 H, X part of ABX), 4.05 (dd, $J = 10.0$, 3.8 Hz, 1 H, B part of ABX), 3.98 (dd, $J = 8.7$, 8.7 Hz, 1 H, A part of ABX), 3.94 (dd, $J = 9.1$, 4.5 Hz, 1 H, B part of ABX), 2.65 (br s, 1 H); **^{13}C NMR** (126 MHz, CDCl$_3$, δ): 137.8, 135.4, 134.1, 131.8, 129.1, 128.6, 127.9, 127.8, 127.6, 126.4, 125.7, 125.4, 124.0, 123.0, 74.1, 73.7, 66.8, 42.0; **IR** (KBr, Cast film, cm^{-1}): 3416 (br), 3060 (m), 2863 (s), 1597 (m), 1511 (m), 1453 (s), 1370 (s), 1363 (s), 1260 (w), 1206 (m) 1074 (s), 1028 (s), 799 (s), 779 (s), 738 (s), 698 (s); **HRMS** (ESI-TOF) m/z for C$_{20}$H$_{20}$NaO$_2$ (M+Na)$^+$: calcd 315.1356; found 315.1356; $[\alpha]_D^{20}$ –49.6 (c 2.27, CHCl$_3$); **HPLC** (Chiralpak IC): 5:95 i-PrOH/Hex, 20 °C, 0.5 mL/min, λ = 221 nm, T$_{(S)}$ = 15.8 min, T$_{(R)}$ = 20.5 min, er = 92.4:7.6.
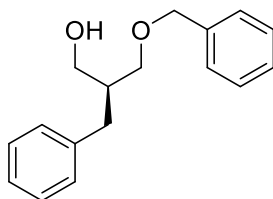
(S)-2-Benzyl-3-benzyloxypropan-1-ol (4-4i): Prepared from 1,3-diol **4-2i** (17 mg, 0.10 mmol) using the general procedure. Isolated as a clear oil (23.5 mg, 89%). **^{1}H NMR** (700 MHz, CDCl$_3$, δ): 7.35 (dd, $J = 8.0$, 6.8 Hz, 2 H), 7.33–7.25 (comp m, 5 H) 7.20 (app t, $J = 7.4$ Hz, 1 H), 7.16 (app d, $J = 7.9$ Hz, 2 H), 4.51 (d, $J = 11.9$ Hz, 1 H), 4.47 (d, $J = 11.9$ Hz, 1 H), 3.74 (dd, $J = 10.9$, 3.7 Hz, 1 H, A part of ABX), 3.65 (dd, $J = 10.9$, 6.5 Hz, 1 H, B part of ABX), 3.59 (dd, $J = 9.2$, 4.2 Hz, 1 H, A part of ABX), 3.49 (dd, $J = 9.2$, 6.7 Hz, 1 H, B part of ABX), 2.68 (dd, $J = 13.7$, 7.5 Hz, 1 H, A part of ABX), 2.65 (dd, $J = 13.7$, 7.6 Hz, 1 H, B part of ABX), 2.44 (br s, 1 H), 2.15 (dddddd, $J = 7.3$, 7.3, 6.6, 6.6, 3.9, 3.9 Hz, 1 H, X part of ABX); **^{13}C NMR** (176 MHz, CDCl$_3$, δ): 140.0, 138.0, 129.1, 128.5, 128.4, 127.8, 127.7, 126.1, 73.5, 72.9, 65.4, 42.6, 34.6; **IR** (KBr, Cast film, cm^{-1}): 3409 (br), 3061 (m), 3027 (s), 2860 (s), 1602 (m), 1495 (s), 1453 (s), 1363 (m), 1206 (m), 1098 (s), 1030 (s), 910 (w), 816 (w), 740 (s), 699 (s); **HRMS** (EI-TOF) m/z for C$_{17}$H$_{20}$O$_2$ (M$^{+\bullet}$): for calcd 256.1463; found 256.1464; $[\alpha]_D^{20}$ –15.6 (c 2.31, CHCl$_3$); **HPLC** (Chiralpak IC): 5:95 i-PrOH/Hex, 20 °C, 0.5 mL/min, λ = 221 nm, T$_{(S)}$ = 14.0 min, T$_{(R)}$ = 12.8 min, er = 75.2:24.8.
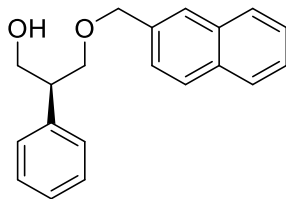
(*S*)-3-(Naphthalen-2-ylmethoxy)-2-phenylpropan-1-ol **(4-4k):** Prepared from 1,3-diol **4-2a** (16 mg, 0.10 mmol) and 2-(chloromethyl) naphthalene (28 μL, 0.15 mmol) using the general procedure. Isolated as a yellowish oil (22.3 mg, 74%). **^{1}H NMR** (500 MHz, CDCl$_3$, δ): 7.86 – 7.79 (comp m, 3 H), 7.74 (s, 1 H), 7.52–7.44 (comp m, 2 H), 7.44 (dd, *J* = 8.4, 1.7 Hz, 1 H), 7.35–7.29 (comp m, 2 H), 7.29–7.19 (comp m, 4 H), 4.72 (s, 2 H), 4.04 (ddd, *J* = 10.8, 7.2, 4.8 Hz, 1 H, A part of ABX), 3.89 (ddd, *J* = 10.9, 7.2, 5.4 Hz, 1 H, B part of ABX), 3.88–3.79 (m, 2 H, AB part of ABX), 3.25 (dddd, *J* = 7.6, 7.6, 5.3, 5.3 Hz, 1 H, X part of ABX), 2.36 (dd, *J* = 7.2, 4.9 Hz, 1 H); **^{13}C NMR** (126 MHz, CDCl$_3$, δ): 139.6, 135.4, 133.3, 133.1, 128.7, 128.4, 128.1, 127.9, 127.8, 127.1, 126.5, 126.2, 126.0, 125.6, 73.64, 73.60, 66.5, 47.9; **IR** (KBr, Cast film, cm^{-1}): 3410 (br), 3057 (s), 2862 (s), 1602 (m), 1508 (m), 1453 (s), 1368 (m), 1271 (w), 1089 (s), 1032 (s), 856 (m), 818 (s), 754 (s), 701 (s); **HRMS** (ESI-TOF) *m/z* for C$_{20}$H$_{20}$NaO$_2$ (M+Na)$^+$**:** calcd 315.1355; found 315.1356; **$[\alpha]_D^{20}$** – 29.4 (*c* 2.01, CHCl$_3$); **HPLC** (Chiralpak AS): 15:85 *i*-PrOH/Hex, 20 °C, 0.5 mL/min, λ = 221 nm, T$_{(S)}$ = 14.8 min, T$_{(R)}$ = 16.1 min, er = 95.7:4.3.
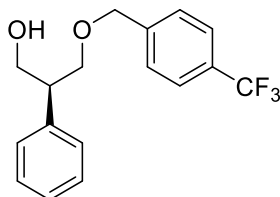

(*S*)-2-Phenyl-3-(*p*-trifluoromethylbenzyloxy)propan-1-ol **(4-4l)**: Prepared from 1,3-diol **4-2a** (14 mg, 0.091 mmol) and 4-(trifluoromethyl)benzyl chloride (20 μL, 0.13 mmol) using the general procedure. Isolated as a clear oil (24.5 mg, 87%). **^{1}H NMR** (700 MHz, CDCl$_3$, δ): 7.59 (d, *J* = 7.9 Hz, 2 H), 7.40 (d, *J* = 7.9 Hz, 2 H), 7.33 (dd, *J* = 8.2, 6.9 Hz, 2 H), 7.28–7.25 (m, 1 H), 7.23 (d, *J* = 8.4 Hz, 2 H), 4.60 (s, 2 H), 4.02 (dd, *J* = 10.9, 7.0 Hz, 1 H, A part of ABX), 3.90 (dd, *J* = 10.9, 5.6 Hz, 1 H, B part of ABX), 3.84 (dd, *J* = 9.3, 8.2 Hz, 1 H, A part of ABX), 3.79 (dd, *J* = 9.2,

5.3 Hz, 1H, B part of ABX), 3.22 (dddd, J = 7.8, 7.8, 5.6, 5.6 Hz, 1 H, X part of ABX), 2.17 (br s, 1 H); **^{13}C NMR** (176 MHz, CDCl$_3$, δ): δ 142.1, 139.5, 130.0 (q, J = 32.3 Hz), 128.8, 128.1, 127.5, 127.2, 125.4 (q, J = 3.8 Hz), 124.2 (q, J = 271.8 Hz), 73.6, 72.6, 66.1, 48.0; **^{19}F NMR** (376 MHz, CDCl$_3$, δ): –62.5; **IR** (KBr, Cast film, cm^{-1}): 3409 (br), 3030 (m), 2867 (s), 1620 (m), 1494 (m), 1453 (m), 1419 (m), 1326 (s), 1123 (s), 1066 (s), 1019 (s), 823 (s), 759 (s), 701 (s), 593 (m); **HRMS** (EI-TOF) m/z for C$_{17}$H$_{17}$O$_2$F$_3$ (M$^{+\bullet}$): calcd 310.1181; found 310.1179; $[\alpha]_D^{20}$ –17.6 (c 2.19, CHCl$_3$); **HPLC** (Chiralpak IC): 2:98 i-PrOH/Hex, 20 °C, 0.5 mL/min, λ = 220 nm, T$_{(S)}$ = 16.9 min, T$_{(R)}$ = 17.9 min, er = 95.6:5.4.
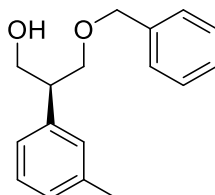

(S)-3-(Benzyloxy)-2-(m-tolyl)propan-1-ol (4-4m): Prepared from 1,3-diol **4-2m** (17 mg, 0.10 mmol) using the general procedure. Isolated as a clear oil (23.4 mg, 90%). **^{1}H NMR** (400 MHz, CDCl$_3$, δ): 7.40–7.27 (comp m, 5 H), 7.21 (td, J = 7.3, 1.3 Hz, 1 H), 7.07 (d, J = 7.6 Hz, 1 H), 7.04–6.98 (comp m, 2 H), 4.57 (s, 2 H), 4.02 (ddd, J = 11.3, 7.2, 4.3 Hz, 1 H, A part of ABX), 3.87 (ddd, J = 11.3, 6.2, 5.2 Hz, 1 H, B part of ABX), 3.86–3.71 (m, 2 H, AB part of ABX), 3.19 (dddd, J = 8.6, 7.3, 5.2, 5.2 Hz, 1 H, X part of ABX), 2.39 (app t, J = 6.0 Hz, 1 H), 2.34 (s, 3 H); **^{13}C NMR** (101 MHz, CDCl$_3$, δ): 139.0, 137.9, 137.5, 128.4, 128.2, 128.1, 127.5, 127.4, 127.3, 124.6, 73.4, 73.1, 66.2, 47.4, 21.0; **IR** (KBr, Cast film, cm^{-1}): 3429 (br), 3009 (s), 2863 (s), 1607 (m), 1492 (s), 1453 (s), 1362 (s), 1309 (m), 1217 (s), 1095 (s), 1029 (s), 906 (w), 755 (s), 701 (s), 667 (m); **HRMS** (EI-TOF) m/z for C$_{17}$H$_{20}$O$_2$ (M$^{+\bullet}$): calcd 256.1463; found 256.1464; $[\alpha]_D^{20}$ –21.5 (c 2.31, CHCl$_3$); **HPLC** (Chiralpak IC): 5:95 i-PrOH/Hex, 20 °C, 0.5 mL/min, λ = 211 nm, T$_{(S)}$ = 13.6 min, T$_{(R)}$ = 15.9 min, er = 94.5:5.5.
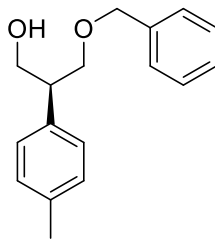
(*S*)-3-(Benzyloxy)-2-(*p*-tolyl)propan-1-ol (4-4n): Prepared from 1,3-diol **4-2n** (17 mg, 0.10 mmol) using the general procedure. Isolated as a yellowish oil (22.7 mg, 88%). **^{1}H NMR** (400 MHz, CDCl$_3$, δ): 7.39–7.26 (comp m, 5 H), 7.16–7.07 (comp m, 4 H), 4.56 (s, 2 H), 4.00 (ddd, J = 11.3, 7.3, 4.3 Hz, 1 H; A part of ABX), 3.90–3.83 (m, 1 H, B part of ABX), 3.83–3.71 (comp m, 2 H, AB part of ABX), 3.19 (dddd, J = 8.5, 7.4, 5.2, 5.2 Hz, 1 H, X part of ABX), 2.41 (t, J = 6.0 Hz, 1 H), 2.33 (s, 3 H); **^{13}C NMR** (101 MHz, CDCl$_3$, δ): 137.5, 136.3, 136.0, 129.0, 128.1, 127.5, 127.4, 127.3, 73.5, 73.1, 66.3, 47.0, 20.6; **IR** (KBr, Cast film, cm^{-1}): 3425 (br), 3028 (m), 2862 (s), 1735 (m), 1605 (m), 1515 (s), 1452 (s), 1350 (s), 1308 (m), 1099 (s), 1029 (s), 815 (m), 737 (m), 698 (m); **HRMS** (EI-TOF) *m/z* for C$_{17}$H$_{20}$O$_2$ (M$^{+\bullet}$): calcd 256.1463; found 256.1468; $[\alpha]_D^{20}$ –28.3 (*c* 2.06, CHCl$_3$); **HPLC** (Chiralpak IC): 5:95 *i*-PrOH/Hex, 20 °C, 0.5 mL/min, λ = 221 nm, T$_{(S)}$ = 16.2 min, T$_{(R)}$ = 17.2 min, er = 95.4:4.6.
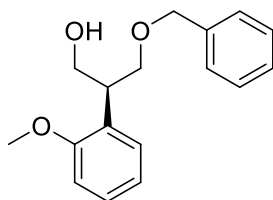
(*S*)-3-(Benzyloxy)-2-(2-methoxyphenyl)propan-1-ol (4-4o): Prepared from 1,3-diol **4-2o** (19 mg, 0.10 mmol) using the general procedure. Isolated as a clear oil (23.3 mg, 84%). **^{1}H NMR** (400 MHz, CDCl$_3$, δ): 7.38–7.26 (comp m, 5 H), 7.22 (ddd, J = 8.2, 7.4, 1.7 Hz, 1 H), 7.15 (dd, J = 7.6, 1.7 Hz, 1 H), 6.91 (td, J = 7.5, 1.2 Hz, 1 H), 6.87 (dd, J = 8.2, 1.1 Hz, 1 H), 4.57 (s, 2 H), 4.02 (dd, J = 10.7, 7.2 Hz, 1 H, A part of ABX), 3.92–3.74 (comp m, 6 H), 3.70 (dddd, J = 9.1, 7.1, 4.7, 4.7 Hz, 1 H, X part of ABX), 2.50 (br s, 1 H); **^{13}C NMR** (101 MHz, CDCl$_3$, δ): 156.8, 137.7, 128.0, 127.8, 127.5, 127.4, 127.30, 127.26, 120.2, 110.3, 72.9, 72.7, 65.5, 55.0, 40.4; **IR** (KBr, Cast film, cm^{-1}): 3428 (br), 3030 (m), 2864 (s), 1600 (s), 1585 (m), 1494 (s), 1456 (s),

1364 (m), 1290 (m), 1243 (s), 1171 (m), 1029 (s), 804 (w), 753 (s), 699 (s); **HRMS** (EI-TOF) *m/z* for $C_{17}H_{20}O_3$ (M$^{+\bullet}$): calcd: 272.1412; found: 272.1410; $[\alpha]_D^{20}$ –27.4 (*c* 2.30, CHCl$_3$); **HPLC** (Chiralpak IC): 10:90 *i*-PrOH/Hex, 20 °C, 0.5 mL/min, λ = 220 nm, T$_{(S)}$ = 13.7 min, T$_{(R)}$ = 18.8 min, er = 95.6:4.4.

(S)-3-(Benzyloxy)-2-(2-fluorophenyl)propan-1-ol (4-4p): Prepared from 1,3-diol **4-2p** (17 mg, 0.10 mmol) using the general procedure. Isolated as a clear oil (25.3 mg, 95%). **¹H NMR** (500 MHz, CDCl$_3$, δ): 7.37 – 7.27 (comp m, 5H), 7.28–7.24 (m, 1H), 7.24–7.18 (m, 1H), 7.09 (td, *J* = 7.5, 1.3 Hz, 1 H), 7.04 (ddd, *J* = 10.5, 8.2, 1.3 Hz, 1 H), 4.56 (s, 2 H), 4.04 (dd, *J* = 10.8, 7.2 Hz, 1 H, A part of ABX), 3.91 (dd, *J* = 10.9, 5.0 Hz, 1 H, B part of ABX), 3.85 (ddd, *J* = 9.2, 8.2, 0.9 Hz, 1 H, A part of ABX), 3.80 (dd, *J* = 9.3, 5.1 Hz, 1 H, B part of ABX), 3.56 (dddd, *J* = 8.1, 7.3, 5.0, 5.0 Hz, 1 H, X part of ABX), 2.13 (br s, 1 H); **¹³C NMR** (126 MHz, CDCl$_3$, δ): 161.9 (d, *J* = 245.6 Hz), 137.9, 129.3 (d, *J* = 4.7 Hz), 128.5, 128.4, 127.8, 127.7, 126.6 (d, *J* = 14.9 Hz), 124.2 (d, *J* = 3.5 Hz), 115.6 (d, *J* = 22.8 Hz), 73.4, 72.4, 65.3, 41.0; **¹⁹F NMR** (469 MHz, CDCl$_3$, δ): –117.60 (ddd, *J* = 11.9, 6.3, 6.3 Hz); **IR** (KBr, Cast film, cm^{-1}): 3401 (br), 3031 (m), 2865 (s), 1583 (m), 1492 (s), 1454 (s), 1364 (s), 1226 (s), 1099 (s), 1035 (s), 824 (m), 756 (s), 699 (s); **HRMS** (EI-TOF) *m/z* for $C_{16}H_{17}FO_2$ (M$^{+\bullet}$): calcd 260.1213; found 260.1218; $[\alpha]_D^{20}$ –23.9 (*c* 2.02, CHCl$_3$); **HPLC** (Chiralpak IC): 5:95 *i*-PrOH/Hex, 20 °C, 0.5 mL/min, λ = 255 nm, T$_{(S)}$ = 14.2 min, T$_{(R)}$ = 17.7 min, er = 95.1:4.9.

(S)-3-(Benzyloxy)-2-(4-fluorophenyl)propan-1-ol (4-4q): Prepared from 1,3-diol **4-2q** (17 mg, 0.099 mmol) using the general procedure. Isolated as a colorless oil (21.7 mg, 84%). **^{1}H NMR** (400 MHz, CDCl$_3$, δ): 7.40–7.27 (comp m, 5 H), 7.19 (dd, J = 8.3, 5.1 Hz, 2 H), 7.07–6.95 (comp m, 2 H), 4.55 (s, 2 H), 4.02–3.93 (m, 1 H, A part of ABX), 3.85 (dt, J = 10.4, 5.1 Hz, 1 H, B part of ABX), 3.81–3.71 (comp m, 2 H, AB part of ABX), 3.18 (dddd, J = 7.5, 7.5, 5.4, 5.4 Hz, 1 H, X part of ABX), 2.30 (br s, 1 H); **^{13}C NMR** (101 MHz, CDCl$_3$, δ): 136.2 (d, J = 240.0 Hz), 129.1 (d, J = 7.8 Hz), 128.1, 127.4 (d, J = 18.2 Hz), 115.1 (d, J = 21.2 Hz), 73.1, 73.0, 65.9, 46.7; **^{19}F NMR** (376 MHz, CDCl$_3$, δ): –115.79 (ddd, J = 14.1, 9.0, 5.4 Hz); **IR** (KBr, Cast film, cm^{-1}): 3400 (br), 3032 (s), 2864 (s), 1886 (w), 1604 (s), 1510 (s), 1454 (s), 1363 (s), 1223 (s), 1160 (s), 1098 (s), 834 (s), 737 (s), 698 (s); **HRMS** (EI-TOF) *m/z* for C$_{16}$H$_{17}$FO$_2$ (M$^{+•}$): calcd 260.1213; found 260.1213; $[\alpha]_D^{20}$ –22.7 (*c* 1.94, CHCl$_3$); **HPLC** (Chiralpak IC): 5:95 *i*-PrOH/Hex, 20 °C, 0.5 mL/min, λ = 221 nm, T$_{(S)}$ = 11.8 min, T$_{(R)}$ = 13.1 min, er = 95.1:4.9.
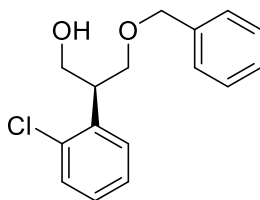
(S)-3-(Benzyloxy)-2-(2-chlorophenyl)propan-1-ol (4-4r): Prepared from 1,3-diol **4-2r** (17 mg, 0.099 mmol) using the general procedure. Isolated as a clear oil (22.9 mg, 85%). Catalyst **1g** was recovered by flash column chromatography (5.8 mg, 92% recovery) and re-used. **^{1}H NMR** (400 MHz, CDCl$_3$, δ): 7.41–7.29 (comp m, 6 H), 7.29–7.15 (comp m, 3 H), 4.56 (s, 2 H), 4.02 (ddd, J = 11.4, 7.3, 4.3 Hz, 1 H, A part of ABX), 3.93–3.85 (m, 1 H, B part of ABX), 3.85–3.64 (comp m, 2 H, AB part of ABX), 3.28–3.17 (m, 1 H, X part of ABX), 2.39 (dd, J = 7.2, 4.8 Hz, 1 H); **^{13}C NMR** (101 MHz, CDCl$_3$, δ): 139.2, 137.5, 128.3, 128.1, 127.6, 127.4, 127.3, 126.7, 73.3,

73.1, 66.2, 47.4; **IR** (KBr, Cast film, cm^{-1}): 3414 (br), 3028 (s), 2863 (s), 1735 (m), 1603 (m), 1495 (s), 1453 (s), 1364 (m), 1205 (m), 1094 (s), 1029 (s), 910 (m), 737 (s), 699 (s); **HRMS** (EI-TOF) *m/z* for C$_{18}$H$_{19}$O$_2$^{35}Cl (M$^{+•}$): calcd 276.0917; found 276.0914; $[\alpha]_D^{20}$ –31.1 (*c* 2.14, CHCl$_3$); **HPLC** (Chiralpak IC): 5:95 *i*-PrOH/Hex, 20 °C, 0.5 mL/min, λ = 221 nm, T$_{(S)}$ = 14.8 min, T$_{(R)}$ = 16.1 min, er = 95.0:5.0.
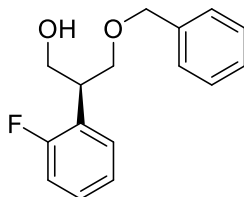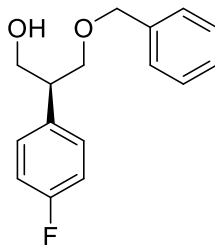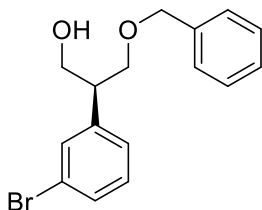

(*S*)-3-(Benzyloxy)-2-(3-bromophenyl)propan-1-ol (4-4s): Prepared from 1,3-diol **4-2s** (23 mg, 0.10 mmol) using the general procedure. Isolated as a clear oil (26.3 mg, 81%). **^{1}H NMR** (500 MHz, CDCl$_3$, δ): 7.41–7.28 (comp m, 6 H), 7.28–7.19 (comp m, 3 H), 4.56 (s, 2 H), 4.02 (dd, *J* = 10.9, 7.3 Hz, 1 H, A part of ABX), 3.88 (dd, *J* = 10.9, 5.3 Hz, 1 H, B part of ABX), 3.82 (dd, *J* = 9.3, 8.5 Hz, 1 H, A part of ABX), 3.79 (dd, *J* = 9.3, 5.2 Hz, 1 H, B part of ABX), 3.22 (dddd, *J* = 8.5, 7.4, 5.2, 5.2 Hz, 1 H, X part of ABX), 2.17 (s, 1 H); **^{13}C NMR** (126 MHz, CDCl$_3$, δ): 139.6, 137.9, 128.7, 128.5, 128.0, 127.8, 127.7, 127.1, 73.7, 73.5, 66.6, 47.8; **IR** (KBr, Cast film, cm^{-1}): 3417 (br), 3029 (m), 2863 (s), 1736 (m), 1603 (w), 1495 (m), 1453 (s), 1361 (m), 1243 (m), 1094 (s), 1030 (s), 738 (m), 699 (s); **HRMS** (EI-TOF) *m/z* for C$_{16}$H$_{18}$O$_2$^{81}Br (M$^{+•}$): calcd 322.0392; found 322.0390; $[\alpha]_D^{20}$ –25.6 (*c* 2.08, CHCl$_3$); **HPLC** (Chiralpak IC): 5:95 *i*-PrOH/Hex, 20 °C, 0.5 mL/min, λ = 255 nm, T$_{(S)}$ = 14.8 min, T$_{(R)}$ = 16.0 min, er = 95.0:5.0.
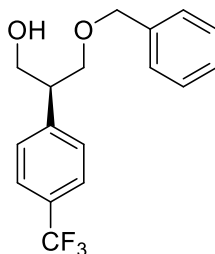
(*S*)-3-(Benzyloxy)-2-(4-(trifluoromethyl)phenyl)propan-1-ol (4-4t): Prepared from 1,3-diol **4-2t** (23 mg, 0.10 mmol) and recovered catalyst **BA-49** using the general procedure. Isolated as a colorless oil (23.5 mg, 73%). **^{1}H NMR** (400 MHz, CDCl$_3$, δ):

7.57 (d, J = 8.0 Hz, 2 H), 7.41–7.27 (comp m, 7 H), 4.55 (s, 2 H), 4.01 (ddd, J = 11.3, 6.9, 4.7 Hz, 1 H, A part of ABX), 3.90 (ddd, J = 11.3, 5.9, 5.9 Hz, 1 H, B part of ABX), 3.85–3.74 (comp m, 2 H, AB part of ABX), 3.24 (dddd, J = 7.2, 7.2, 5.5, 5.5 Hz, 1 H, X part of ABX), 2.21 (t, J = 6.0 Hz, 1 H); **^{13}C NMR** (126 MHz, CDCl$_3$, δ): 144.1, 137.7, 129.35 (q, J = 32.4 Hz), 128.6, 128.5, 127.9, 127.7, 125.51 (q, J = 3.8 Hz), 124.19 (d, J = 271.9 Hz), 73.6, 72.7, 65.7, 47.8; **^{19}F NMR** (376 MHz, CDCl$_3$, δ): –62.5; **IR** (KBr, Cast film, cm^{-1}): 3400 (br), 3032 (w), 2866 (m), 1619 (m), 1454 (m), 1421 (m), 1327 (s), 1164 (s), 1121 (s), 1068 (s), 1018 (m), 839 (m), 739 (m), 699 (m); **HRMS** (EI-TOF) m/z for C$_{17}$H$_{17}$F$_3$O$_2$ (M$^{+•}$): calcd 310.1181; found 310.1181; $[\alpha]_D^{20}$ –16.5 (c 2.14, CHCl$_3$); **HPLC** (Chiralpak IC): 5:95 i-PrOH/Hex, 20 °C, 0.5 mL/min, λ = 211 nm, T$_{(S)}$ = 8.2 min, T$_{(R)}$ = 8.9 min, er = 93.6:6.4.
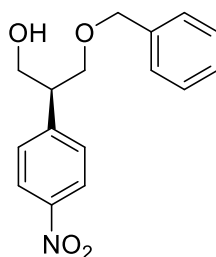
(S)-3-(Benzyloxy)-2-(4-nitrophenyl)propan-1-ol (4-4u): Prepared from 1,3-diol **4-2u** (20 mg, 0.10 mmol) using the general procedure. Purified by flash column chromatography (10:1 to 2:1 hexanes/ethyl acetate) and isolated as an orangish oil (23.4 mg, 81%). **^{1}H NMR** (400 MHz, CDCl$_3$, δ): 8.17 (d, J = 8.8 Hz, 2 H), 7.44 (d, J = 8.7 Hz, 2 H), 7.40–7.24 (comp m, 5 H), 4.55 (s, 2 H), 4.01 (ddd, J = 10.8, 6.5, 4.2 Hz, 1 H, A part of ABX), 3.93 (ddd, J = 11.0, 5.4, 5.4 Hz, 1 H, B part of ABX), 3.86–3.78 (comp m, 2 H, AB part of ABX), 3.28 (app p, J = 6.1 Hz, 1 H, X part of ABX), 2.14 (t, J = 5.7 Hz, 1 H); **^{13}C NMR** (101 MHz, CDCl$_3$, δ): 147.5, 146.6, 137.1, 128.7, 128.2, 127.6, 127.3, 123.3, 73.2, 71.6, 64.8, 47.4; **IR** (KBr, Cast film, cm^{-1}): 3412 (br), 3029 (w), 2863 (m), 1601 (m), 1517 (s), 1454 (m), 1347 (s), 1215(w), 1108 (m), 855 (m), 752 (s), 699 (s); **HRMS** (EI-TOF) m/z for C$_{16}$H$_{17}$NO$_4$ (M$^{+•}$): calcd 287.1158; found 287.1156; $[\alpha]_D^{20}$ –17.2 (c 2.17, CHCl$_3$); **HPLC** (Chiralpak IC): 15:85 i-PrOH/Hex, 20 °C, 0.5 mL/min, λ = 221 nm, T$_{(S)}$ = 12.9 min, T$_{(R)}$ = 14.3 min, er = 93.2:6.8.
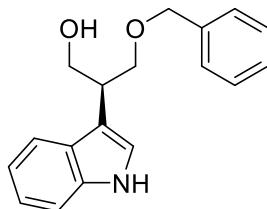
(S)-3-(Benzyloxy)-2-(1H-indol-3-yl)propan-1-ol (4-4v): Prepared from 1,3-diol **4-2v** (19 mg, 0.10 mmol) using the general procedure. Purified by flash column chromatography (10:1 dichloromethane/ethyl acetate) and isolated as a sticky oil (23.6 mg, 81%). **¹H NMR** (400 MHz, CDCl₃, δ): 8.08 (s, 1 H), 7.64 (d, J = 7.9 Hz, 1 H), 7.40–7.34 (comp m, 4 H), 7.34–7.28 (m, 1 H), 7.21 (ddd, J = 8.2, 7.0, 1.2 Hz, 1 H), 7.13 (ddd, J = 8.0, 7.0, 1.1 Hz, 1 H), 7.07 (d, J = 2.5 Hz, 1 H), 4.60 (s, 2 H), 4.12–3.96 (comp m, 2 H, AB part of ABX), 3.97–3.85 (comp m, 2 H, AB part of ABX), 3.59 (ddd, J = 12.8, 7.1, 5.2 Hz, 1 H, X part of ABX), 2.54 (dd, J = 7.3, 4.9 Hz, 1 H); **¹³C NMR** (101 MHz, CDCl₃, δ): 137.6, 135.7, 128.1, 127.4, 127.3, 126.5, 121.9, 121.1, 119.2, 118.5, 113.2, 110.8, 76.9, 76.6, 76.3, 73.1, 73.0, 65.7, 38.7; **IR** (KBr, Cast film, cm⁻¹): 3471 (m), 3418 (m), 3322 (m), 3010 (m), 2925 (m), 2866 (m), 1455 (m), 1420 (w), 1361 (w), 1216 (s), 1093 (s), 1028 (s), 755 (s), 699 (m), 667 (w); **HRMS** (EI-TOF) *m/z* for C₁₈H₁₉NO₂ (M⁺•): calcd 281.1416; found 281.1415; $[\alpha]_D^{20}$ − 29 (*c* 0.61, CHCl₃); **HPLC** (Chiralpak IC): 15:85 *i*-PrOH/Hex, 20 °C, 0.5 mL/min, λ = 221 nm, T(S) = 11.2 min, T(R) = 12.4 min, er = 92.5:7.5.
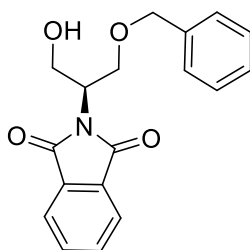
(S)-2-(1-(Benzyloxy)-3-hydroxypropan-2-yl)isoindoline-1,3-dione (4-4x): Prepared from 1,3-diol **4-4x** (22 mg, 0.10 mmol) using the general procedure. Isolated as a colorless oil (17 mg, 50%). **¹H NMR** (400 MHz, CDCl₃, δ): 7.84 (dd, J = 5.6, 3.2 Hz, 2 H), 7.73 (dd, J = 5.5, 3.0 Hz, 2 H), 7.30–7.18 (comp m, 5 H), 4.67 (dddd, J = 8.1, 6.3, 6.3, 3.8 Hz, 1 H, X part of ABX), 4.57 (d, J = 12.1 Hz, 1 H), 4.48 (d, J = 12.0 Hz, 1 H), 4.09 (ddd, J = 14.8, 8.3, 6.2 Hz, 1 H, A part ABX), 4.04–3.96 (m, 1 H, B part of

ABX), 3.97–3.78 (comp m, 2 H, AB part of ABX), 2.98–2.71 (m, 1 H); **^{13}C NMR** (126 MHz, CDCl$_3$, δ): 169.0, 137.8, 134.2, 131.8, 128.4, 127.7, 127.6, 123.5, 73.1, 67.2, 62.0, 53.0; **IR** (KBr, Cast film, cm^{-1}): 3470 (br), 3066 (w), 2926 (w), 1774 (m), 1709 (s), 1468 (m), 1390 (s), 1101 (m), 1029 (m), 876 (m), 722 (s); **HRMS** (ESI-TOF) *m/z* for C$_{18}$H$_{17}$NNaO$_4$ (M+Na)$^+$: calcd 334.1055; found 334.1048; $[\alpha]_D^{20}$ +27.7 (*c* 1.46, CHCl$_3$); **HPLC** (Chiralpak IC): 30:70 *i*-PrOH/Hex, 20 °C, 0.5 mL/min, λ = 211 nm, T$_{(S)}$ = 16.9 min, T$_{(R)}$ = 26.6 min, er = 91.8:8.2.
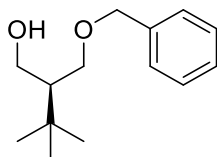
**(*S*)-2-((Benzyloxy)methyl)-3,3-dimethylbutan-1-ol (4-4y):** Prepared from 1,3-diol **4-2y** (14 mg, 0.10 mmol) using the general procedure. Isolated as a clear oil (16.0 mg, 70%). **^{1}H NMR** (400 MHz, CDCl$_3$, δ): 7.39–7.27 (comp m, 5 H), 4.53 (d, *J* = 2.1 Hz, 2 H), 3.88–3.81 (comp m, 2 H, AB part of ABM), 3.72 (ddd, *J* = 10.9, 8.4, 2.4 Hz, 1 H), 3.61 (t, *J* = 9.2 Hz, 1 H), 3.00 (dd, *J* = 8.7, 2.9 Hz, 1 H), 1.73 (dddd, *J* = 9.4, 8.5, 4.0, 2.9 Hz, 1 H, M part of ABM), 0.92 (s, 9 H); **^{13}C NMR** (101 MHz, CDCl$_3$, δ): 137.5, 128.1, 127.4, 127.2, 73.3, 72.4, 64.1, 49.4, 31.1, 27.8; **IR** (KBr, Cast film, cm^{-1}): 3419 (br), 3030 (w), 2956 (m), 2870 (m), 1605 (w), 1453 (w), 1396 (w), 1365 (m), 1208 (w), 1071 (m), 1029 (m), 736 (m), 697 (m); **HRMS** (EI-TOF) *m/z* for C$_{14}$H$_{22}$O$_2$ (M$^{+•}$): calcd 222.1620; found 222.1622; $[\alpha]_D^{20}$ –19.0 (*c* 1.39, CHCl$_3$); **HPLC** (Chiralpak IB): 2:98 *i*-PrOH/Hex, 20 °C, 0.5 mL/min, λ = 220 nm, T$_{(S)}$ = 10.4 min, T$_{(R)}$ = 11.4 min, er = 92.2:7.8.
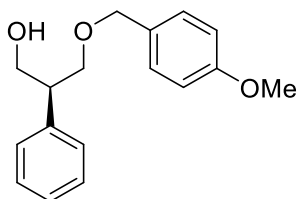
(*S*)-3-((4-Methoxybenzyl)oxy)-2-phenylpropan-1-ol (4-4aa): Prepared from 1,3-diol **4-2a** (13 mg, 0.085 mmol) and 4-methoxybenzyl chloride (22 μL, 0.13 mmol) using the general procedure. Isolated as a colorless oil (20.4 mg, 88%). **^{1}H NMR** (500 MHz, CDCl$_3$, δ): 7.35–7.28 (m, 2 H), 7.26–7.18 (comp m, 5 H), 6.88

(d, J = 8.1 Hz, 2 H), 4.49 (s, 2 H), 4.00 (dd, J = 10.9, 7.4 Hz, 1 H, A part of ABX), 3.86 (dd, J = 10.9, 5.2 Hz, 1 H, B part of ABX), 3.81 (s, 3 H), 3.79–3.73 (m, 2 H, AB part of ABX), 3.24–3.16 (m, 1 H, X part of ABX); **^{13}C NMR** (126 MHz, CDCl$_3$, δ): 159.4, 139.6, 129.9, 129.3, 128.7, 128.0, 127.1, 113.9, 73.5, 73.2, 66.8, 55.3, 47.8; **IR** (KBr, Cast film, cm^{-1}): 3425 (br), 2929 (m), 1612 (m), 1513 (s), 1454 (m), 1247 (s), 1086 (s), 1034 (s), 820 (m), 757 (s), 701 (s); **HRMS** (EI-TOF) *m/z* for C$_{17}$H$_{20}$O$_3$ (M$^{+\bullet}$): calcd 272.1414; found 272.1414; $[\alpha]_D^{20}$ –25.9 (*c* 1.48, CHCl$_3$); **HPLC** (Chiralpak IC): 2:98 *i*-PrOH/Hex, 20 °C, 0.5 mL/min, λ = 221 nm, T$_{(S)}$ = 22.2 min, T$_{(R)}$ = 23.2 min, er = 94.2:5.8.
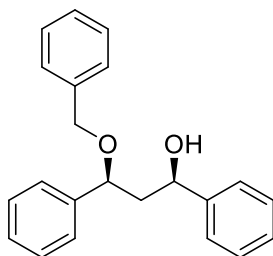

(1*R*,3*S*)-3-(Benzyloxy)-1,3-diphenylpropan-1-ol (4-11): Prepared from *syn*-1,3-diphenyl propane-1,3-diol (**4-10**) (23 mg, 0.10 mmol) using the general procedure at 40 °C. Isolated as a colorless oil (21 mg, 67%). **^{1}H NMR** (700 MHz, CDCl$_3$, δ): 7.39–7.27 (comp m, 14 H), 7.25–7.19 (m, 1 H), 4.94 (dd, J = 9.6, 2.9 Hz, 1 H), 4.67 (dd, J = 10.2, 3.4 Hz, 1 H), 4.50 (d, J = 11.4 Hz, 1 H), 4.31 (d, J = 11.4 Hz, 1 H), 3.96 (s, 1 H), 2.30 (dt, J = 14.8, 9.9 Hz, 1 H), 1.95 (dt, J = 14.8, 3.2 Hz, 1 H); **^{13}C NMR** (176 MHz, CDCl$_3$, δ): 144.2, 141.3, 137.6, 128.7, 128.6, 128.3, 128.03, 128.02, 127.9, 127.3, 126.6, 125.7, 82.0, 74.0, 70.6, 47.8; **IR** (KBr, Cast film, cm^{-1}): 3455 (br), 3062 (m), 2918 (m), 1603 (w), 1494 (m), 1454 (s), 1086 (s), 1063 (m), 1027 (m), 914 (w), 754 (m), 700 (s); **HRMS** (ESI-TOF) *m/z* for C$_{18}$H$_{17}$NNaO$_4$ (M+Na)$^+$: calcd 334.1055; found 334.1048; $[\alpha]_D^{20}$ –50 (*c* 0.71, CHCl$_3$); **HPLC** (Chiralpak IC): 5:95 *i*-PrOH/Hex, 20 °C, 0.5 mL/min, λ = 221 nm, T$_{(1S,3R)}$ = 12.1 min, T$_{(1R,3S)}$ = 17.8 min, er = 1.7:98.3.

4.10 References

(1)   Díaz-de-Villegas, M. D.; Gálvez, J. A.; Badorrey, R.; López-Ram-de-Víu, M. P. *Chem. Eur. J.* **2012**, *18*, 13920–13935.
(2)   Suzuki, T. *Tetrahedron Lett.* **2017**, *58*, 4731–4739.

(3) Meng, S.-S.; Liang, Y.; Cao, K.-S.; Zou, L.; Lin, X.-B.; Yang, H.; Houk, K. N.; Zheng, W.-H. *J. Am. Chem. Soc.* **2014**, *136*, 12249–12252.

(4) Harada, T.; Sekiguchi, K.; Nakamura, T.; Suzuki, J.; Oku, A. *Org. Lett.* **2001**, *3*, 3309–3312.

(5) Chen, Z.; Sun, J. *Angew. Chem. Int. Ed.* **2013**, *52*, 13593–13596.

(6) Ke, Z.; Tan, C. K.; Chen, F.; Yeung, Y.-Y. *J. Am. Chem. Soc.* **2014**, *136*, 5627–5630.

(7) Tay, D. W.; Leung, G. Y.; Yeung, Y. *Angew. Chem. Int. Ed.* **2014**, *53*, 5161–5164.

(8) Zi, W.; Toste, F. D. *Angew. Chem. Int. Ed.* **2015**, *54*, 14447–14451.

(9) Wu, Z.; Wang, J. *ACS Catal.* **2017**, *7*, 7647–7652.

(10) Lewis, C. A.; Sculimbrene, B. R.; Xu, Y.; Miller, S. J. *Org. Lett.* **2005**, *7*, 3021–3023.

(11) Jung, B.; Hong, M. S.; Kang, S. H. *Angew. Chem. Int. Ed.* **2007**, *46*, 2616–2618.

(12) Honjo, T.; Nakao, M.; Sano, S.; Shiro, M.; Yamaguchi, K.; Sei, Y.; Nagao, Y. *Org. Lett.* **2007**, *9*, 509–512.

(13) Hong, M. S.; Kim, T. W.; Jung, B.; Kang, S. H. *Chem. Eur. J.* **2008**, *14*, 3290–3296.

(14) You, Z.; Hoveyda, A. H.; Snapper, M. L. *Angew. Chem. Int. Ed.* **2009**, *48*, 547–550.

(15) Li, B.-S.; Wang, Y.; Proctor, R. S. J.; Jin, Z.; Chi, Y. R. *Chem. Commun.* **2016**, *52*, 8313–8316.

(16) Yamamoto, K.; Ishimaru, S.; Oyama, T.; Tanigawa, S.; Kuriyama, M.; Onomura, O. *Org. Process Res. Dev.* **2019**, *23*, 660–666.

(17) Oriyama, T.; Taguchi, H.; Terakado, D.; Sano, T. *Chem. Lett.* **2002**, *31*, 26–27.

(18) Trost, B. M.; Mino, T. *J. Am. Chem. Soc.* **2003**, *125*, 2410–2411.

(19) Trost, B. M.; Malhotra, S.; Mino, T.; Rajapaksa, N. S. *Chem. Eur. J.* **2008**, *14*, 7648–7657.

(20) Aida, H.; Mori, K.; Yamaguchi, Y.; Mizuta, S.; Moriyama, T.; Yamamoto, I.; Fujimoto, T. *Org. Lett.* **2012**, *14*, 812–815.

(21) Mandai, H.; Ashihara, K.; Mitsudo, K.; Suga, S. *Chem. Lett.* **2018**, *47*, 1360–1363.

(22) Taylor, M. S. *Acc. Chem. Res.* **2015**, *48*, 295–305.

(23) Lee, D.; Williamson, C. L.; Chan, L.; Taylor, M. S. *J. Am. Chem. Soc.* **2012**, *134*, 8260–8267.

(24) Pawliczek, M.; Hashimoto, T.; Maruoka, K. *Chem. Sci.* **2018**, *9*, 1231–1235.

(25) Li, R.-Z.; Tang, H.; Yang, K. R.; Wan, L.-Q.; Zhang, X.; Liu, J.; Fu, Z.; Niu, D. *Angew. Chem. Int. Ed.* **2017**, *56*, 7213–7217.

(26) Lee, D.; Taylor, M. S. *Org. Biomol. Chem.* **2013**, *11*, 5409–5412.

(27) Nakagawa, A.; Nishi, N.; Iijima, K.; Sawa, R.; Takahashi, D.; Toshima, K. *J. Am. Chem. Soc* **2018**, *140*, 3644.

(28) Shimada, N.; Nakamura, Y.; Ochiai, T.; Makino, K. *Org. Lett.* **2019**, *21*, 3789–3794.

(29) Kuwano, S.; Hosaka, Y.; Arai, T. *Org. Biomol. Chem.* **2019**, *17*, 4475–4482.

(30) Kusano, S.; Miyamoto, S.; Matsuoka, A.; Yamada, Y.; Ishikawa, R.; Hayashida, O. *Eur. J. Org. Chem.* **2020**, 1598–1602.

(31) Dewar, M.; Dietz, R. *Tetrahedron Lett.* **1959**, *1*, 21–23.

(32) Greig, L. M.; Kariuki, B. M.; Habershon, S.; Spencer, N.; Johnston, R. L.; Harris, K. D. M.; Philp, D. *New J. Chem.* **2002**, *26*, 701–710.

(33) Greig, L. M.; Slawin, A. M. Z.; Smith, M. H.; Philp, D. *Tetrahedron* **2007**, *63*, 2391–2403.

(34) Zhou, Q. J.; Worm, K.; Dolle, R. E. *J. Org. Chem.* **2004**, *69*, 5147–5149.

(35) Mathew, S. M.; Hartley, C. S. *Macromolecules* **2011**, *44*, 8425–8432.

(36) Sumida, Y.; Harada, R.; Kato-Sumida, T.; Johmoto, K.; Uekusa, H.; Hosoya, T. *Org. Lett.* **2014**, *16*, 6240–6243.

(37) Gao, T.; Jiang, Z.; Chen, B.; Sun, Q.; Orooji, Y.; Huang, L.; Liu, Z. *Dyes Pigm.* **2020**, *173*, 107998.

(38) Stavber, S.; Kralj, P.; Zupan, M. *Synth.* **2002**, 1513–1518.

(39) Velder, J.; Robert, T.; Weidner, I.; Neudörfl, J.; Lex, J.; Schmalz, H. *Adv. Synth. Catal.* **2008**, *350*, 1309–1315.

(40) Yoshida, H.; Okada, K.; Kawashima, S.; Tanino, K.; Ohshita, J. *Chem. Commun.* **2010**, *46*, 1763–1765.

CHAPTER 5

Conclusions

5.1 Conclusions and Future Perspectives

Boronic acid catalysis (BAC) has emerged as a versatile strategy for the direct functionalization of hydroxy and carbonyl-containing compounds, such as alcohols, carboxylic acids, polyols, and ketones, in a mild and selective manner. In the past decade alone, numerous transformations have been adapted successfully to BAC by many research groups worldwide. The astonishing accomplishments of BAC can be attributed to the beneficial physicochemical properties and the diversity of activation mechanisms offered by boronic acids. While great advances have been made in BAC, several challenges and limitations still remain to be addressed. This thesis described efforts toward tackling the existing challenges and limitations to expand the potential of BAC further and to garner valuable insights for the future development of BAC.

In Chapter 2, the concept of BAC was extended successfully to the direct activation of the *N*-hydroxy group of oximes in the Beckmann rearrangement using ortho-carboxyester-substituted arylboronic acid catalysts. Interestingly, instead of the conventional activation mechanism involving direct interaction of a hydroxy-containing substrate to the boron center, mechanistic studies revealed a unique cooperative role of the boronyl group in inducing a transesterification of the oxime substrate and assisting the Beckmann rearrangement. This finding may stimulate new designs of BAC with alternative binding sites to address the long-standing challenges of direct hydroxy group activation of non-π-activated primary and secondary alcohols, which is considered as a "top priority" research target by the ACS Green Chemistry Institute Pharmaceutical Roundtable.[1] By extension, arylboronic acid with ortho-carboxyester or sulfonate groups potentially could be a suitable catalyst for the direct S_N2 reaction and E2 elimination with non-π-activated alcohols (Scheme 5-1). It is envisioned that the activation of such alcohols could be achieved through the similar boron-induced alcohol transesterification or transsulfonylation to generate transient acyl or sulfonate leaving groups.
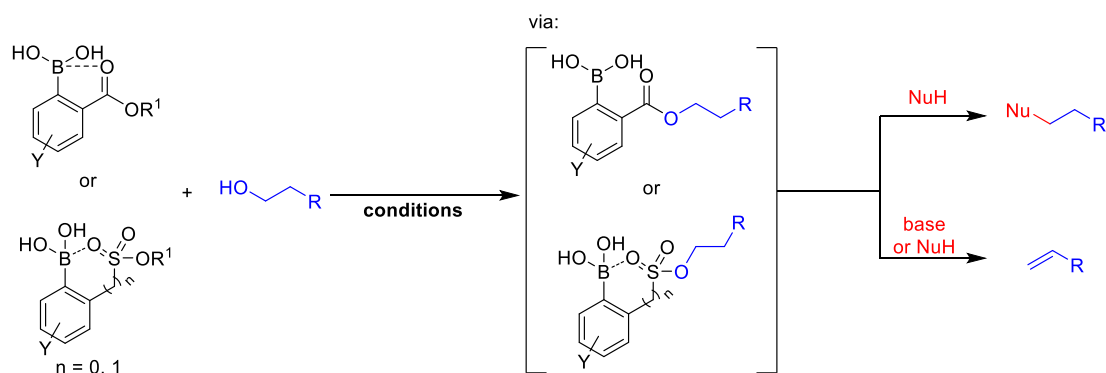
Scheme 5-1 Potential design of boronic acid catalysts for the direct activation of non-π-activated alcohols for S_N2 substitutions or E2 eliminations.

Perfluoropinacol, a highly fluorinated diol, was identified as an effective co-catalyst in enhancing the catalyst's reactivity in the Beckmann rearrangement (Chapter 2). The use of such a diol to improve catalytic activity in BAC was extended successfully to Friedel–Crafts alkylations with electronically deactivated benzylic alcohols, as demonstrated in Chapter 3. Mechanistic investigations revealed that perfluoropinacol condenses with the boronic acid to form a highly Lewis acidic cyclic boronic ester, which leads to the formation of a hydronium boronate species by the interaction of the boronic ester with water or HFIP. While the exact mode of activation still is unclear, it is believed that the ionization process of benzylic alcohols proceeds through a Brønsted acid-dependent mechanism with the hydronium species, which was found to be milder than other conventional Brønsted acid catalyzed methods. It is anticipated that this mild co-catalytic system using electron deficient diols and boronic acids can be extended to current BAC protocols to improve efficiency, as well as improving on existing transformations that require strong Brønsted acids.

While the limitation of poor efficiency with highly deactivated benzylic alcohol substrates in the boronic acid catalyzed Friedel–Crafts alkylation was addressed by using a diol co-catalyst in Chapter 3, the major challenge of direct asymmetric Friedel–Crafts alkylation of unsymmetrical secondary alcohols has yet to be resolved. It is proposed that the alkylations proceed through an S_N1 mechanism via a planar carbocation intermediate, which renders the induction of enantioselectivity of

216

this process highly challenging. In this context, the two-component BAC system sheds light on a probable solution to this challenge. As illustrated in the proposed catalytic cycle in Scheme 3-16 above, the carbocation likely exists as a contact ion pair with a boronate anion (species **D** or **F**). Thus, it is envisioned that the use of a chiral boronic acid or diol in the two-component system potentially could induce facial selectivities of the carbocation via the formation of a chiral contact ion pair (Scheme 5-2). Such a transformation would present a mild and general method to prepare optically enriched diarylmethanes from widely available benzylic alcohols.
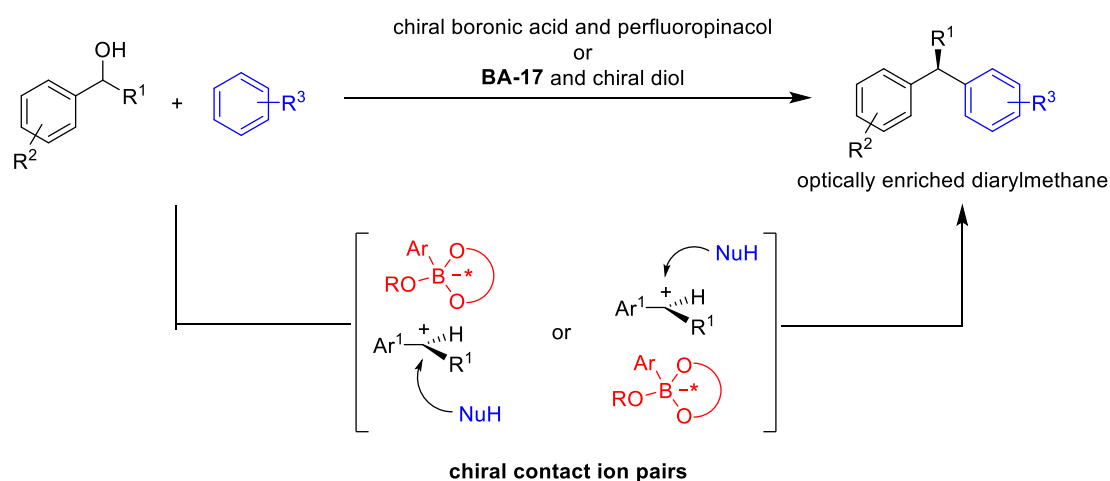
Scheme 5-2 Proposed strategy to achieve asymmetric Friedel–Crafts alkylation of unsymmetrical secondary benzylic alcohols via BAC.

Chapter 4 demonstrated the successful extension of BAC in asymmetric transformations by using a rationally developed chiral boroxarophenanthrene catalyst for the enantioselective desymmetrization of 2-aryl-1,3-propanediols via direct *O*-alkylation under mild conditions. This methodology produces chiral monoalkylated products in high yields and high enantioselectivies (up to 96:4 ee) for a wide range of 2-aryl-1,3-propanediols. It is foreseen that this chiral boroxarophenanthrene catalytic system can be extended to the desymmetrization of other useful prochiral diol substrates, such as meso-1,3-disubstituted-1,3-diols, which resulted in excellent enantioselectivity in a single example (98:2 ee) during the preliminary investigations. Furthermore, the chiral boroxarophenanthrene scaffold can be manipulated further by

installing a larger "steric shield" and "ortho-blocker" to improve the enantioselectivity.

More importantly, it is anticipated that the discovery of this chiral boroxarophenanthrene catalyst would lead to further accomplishments in BAC for other asymmetric transformations. For instance, the applications of this BAC system in enantioselective desymmetrization of 2-substituted-1,3-propanediols can be expanded to other electrophiles, such as phosphorylation, sulfonylation, acylation, and silylation (Scheme 5-3A). Furthermore, dual catalysis or cooperative catalysis also could be explored to generate other useful optically enriched products via other types of transformation. For example, taking inspiration from the groundbreaking work of MacMillan and co-workers on the selective transformation of α-hydroxy C–H bonds of aliphatic alcohols via photoredox-mediated hydrogen atom transfer (HAT) catalysis in the presence of a stoichiometric zinc-based Lewis acid,[2] it is envisioned that the formation of the anionic boronate intermediate with a boroxarophenanthrene catalyst also would increase the hydridic character of the α-hydroxy C–H bonds of 1,3-diols toward hydrogen atom abstraction. Thus, the chiral environment of the catalyst potentially would lead to a stereoselective hydrogen atom abstraction and downstream transformations (Scheme 5-3B). The ability of organoboron compounds to increase the hydridic character of the α-hydroxy C–H bond of cis-1,2-diols in photoredox-mediated (HAT) catalysis was demonstrated by Taylor and co-workers by using diphenylborinic acid catalyst in the stereo- and site selective C–H alkylation of carbohydrates[3] as well as pentafluorophenyl-boronic acid (**BA-16**) as a catalyst in the site selective redox isomerization of furanosides.[4]
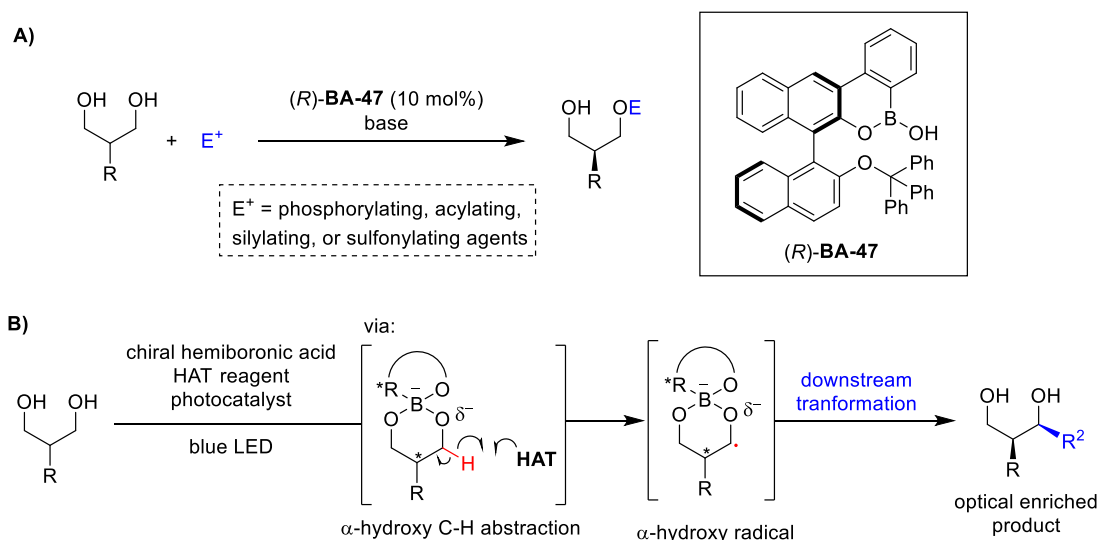
Scheme 5-3 Potential application of chiral boroxarophenanthrene catalyst in A) enantioselective desymmetrization of 2-substituted 1,3-propanediols with other electrophiles; and B) site and stereoselective α-hydroxy functionalization via photoredox-mediated HAT catalysis.

In conclusion, the research described in this thesis only contributed to a small portion of the potential of BAC. While great advances have been achieved in BAC, it is believed that this research area is still in its infancy. With growing interest from the community for mild organocatalytic transformations, further developments of the BAC concept can be anticipated.

5.2 References

(1) Bryan, M. C.; Dunn, P. J.; Entwistle, D.; Gallou, F.; Koenig, S. G.; Hayler, J. D.; Hickey, M. R.; Hughes, S.; Kopach, M. E.; Moine, G.; Richardson, P.; Roschangar, F.; Steven, A.; Weiberth, F. J. *Green Chem.* **2018**, *20*, 5082–5103.
(2)   Twilton, J.; Christensen, M.; DiRocco, D. A.; Ruck, R. T.; Davies, I. W.; MacMillan, D. W. C. *Angew. Chem. Int. Ed.* **2018**, *57*, 5369–5373.
(3) Dimakos, V.; Su, H. Y.; Garrett, G. E.; Taylor, M. S. *J. Am. Chem. Soc.* **2019**, *141*, 5149– 5153.
(4) Dimakos, V.; Gorelik, D.; Su, H. Y.; Garrett, G. E.; Hughes, G.; Shibayama, H.; Taylor, M. S. *Chem. Sci.* **2020**, *11*, 1531–1537.

Bibliography

(1)   Hall, D. G., Ed. *Boronic Acids: Preparation and Applications in Organic Synthesis*, 2nd edn.; Wiley-VCH: Weinheim, 2011.

(2)   Frankland, E.; Duppa, B. F. *Liebigs Ann.* **1860**, *115*, 319–322.

(3)   Michaelis, A.; Becker, P. *Ber. Dtsch. Chem. Ges.* **1880**, *13*, 58–61.

(4)   Miyaura, N.; Yamada, K.; Suzuki, A. *Tetrahedron Lett.* **1979**, *20*, 3437–3440.

(5)   Matteson, D. S.; Collins, B. S. L.; Aggarwal, V. K.; Ciganek, E. The Matteson Reaction. In *Organic Reactions*, **2021**, 427–860.

(6)   Lachance, H.; Hall, D. G. Allylboration of Carbonyl Compounds. In *Organic Reaction,* **2009**, 1–574.

(7)   Pyne, S. G.; Tang, M. The Boronic Acid Mannich Reaction. In *Organic Reactions*, **2014**, 211–498.

(8)   Chen, J.-Q.; Li, J.-H.; Dong, Z.-B. *Adv. Synth. Catal.* **2020**, *362*, 3311–3331.

(9)   Cheng, H.-G.; Chen, H.; Liu, Y.; Zhou, Q. *Asian J. Org. Chem.* **2018**, *7*, 490–508.

(10)   Tian, Y.-M.; Guo, X.-N.; Braunschweig, H.; Radius, U.; Marder, T. B. *Chem. Rev.* **2021**, *121*, 3561–3597.

(11)   Wang, M.; Shi, Z. *Chem. Rev.* **2020**, *120*, 7348–7398.

(12)   Hartwig, J. F. *Chem. Soc. Rev.* **2011**, *40*, 1992–2002.

(13)   Iqbal, S. A.; Pahl, J.; Yuan, K.; Ingleson, M. J. *Chem. Soc. Rev.* **2020**, *49*, 4564–4591.

(14)   Chow, W. K.; Yuen, O. Y.; Choy, P. Y.; So, C. M.; Lau, C. P.; Wong, W. T.; Kwong, F. Y. *RSC Adv.* **2013**, *3*, 12518–12539.

(15)   Plescia, J.; Moitessier, N. *Eur. J. Med. Chem.* **2020**, *195*, 112270.

(16)   António, J. P. M.; Russo, R.; Carvalho, C. P.; Cal, P. M. S. D.; Gois, P. M. P. *Chem. Soc. Rev.* **2019**, *48*, 3513–3536.

(17)   Akgun, B.; Hall, D. G. *Angew. Chem. Int. Ed.* **2018**, *57*, 13028–13044.

(18)   Nishiyabu, R.; Kubo, Y.; D. James, T.; S. Fossey, J. *Chem. Commun.* **2011**, *47*, 1124–1150.

(19)   Brooks, W. L. A.; Sumerlin, B. S. *Chem. Rev.* **2016**, *116*, 1375–1397.

(20)   Kubo, Y.; Nishiyabu, R.; D. James, T. *Chem. Commun.* **2015**, *51*, 2005–2020.

(21)   Wang, R.; Bian, Z.; Zhan, D.; Wu, Z.; Yao, Q.; Zhang, G. *Dyes and Pigments* **2021**, *185*, 108885.

(22)   Fang, G.; Wang, H.; Bian, Z.; Sun, J.; Liu, A.; Fang, H.; Liu, B.; Yao, Q.; Wu, Z. *RSC Adv.* **2018**, *8*, 29400–29427.

(23)   Espina-Benitez, M. B.; Randon, J.; Demesmay, C.; Dugas, V. *Sep. Purif. Rev.* **2018**, *47*, 214–228.

(24)   Zheng, H.; Hall, D. G. *Aldrichimica Acta* **2014**, *47*, 41–51.

(25)   Hall, D. G. *Chem. Soc. Rev.* **2019**, *48*, 3475–3496.

(26)   Martínez-Aguirre, M. A.; Yatsimirsky, A. K. *J. Org. Chem.* **2015**, *80*, 4985–4993.

(27)   Letsinger, R. L.; Dandegaonker, S.; Vullo, W. J.; Morrison, J. D. *J. Am. Chem. Soc.* **1963**, *85*, 2223–2227.

(28)   Rao, G.; Philipp, M. *J. Org. Chem.* **1991**, *56*, 1505–1512.

(29)   Ishihara, K.; Ohara, S.; Yamamoto, H. *J. Org. Chem.* **1996**, *61*, 4196–4197.

(30)   Arnold, K.; Batsanov, A. S.; Davies, B.; Whiting, A. *Green Chem.* **2008**, *10*, 124–134.

(31) Al-Zoubi, R. M.; Marion, O.; Hall, D. G. *Angew. Chem. Int. Ed.* **2008**, *47*, 2876–2879.

(32) Gernigon, N.; Al-Zoubi, R. M.; Hall, D. G. *J. Org. Chem.* **2012**, *77*, 8386–8400.

(33) Mohy El Dine, T.; Erb, W.; Berhault, Y.; Rouden, J.; Blanchet, J. *J. Org. Chem.* **2015**, *80*, 4532–4544.

(34) Ishihara, K.; Lu, Y. *Chem. Sci.* **2016**, *7*, 1276–1280.

(35) Wang, K.; Lu, Y.; Ishihara, K. *Chem. Commun.* **2018**, *54*, 5410–5413.

(36) Noda, H.; Furutachi, M.; Asada, Y.; Shibasaki, M.; Kumagai, N. *Nat. Chem.* **2017**, *9*, 571–577.

(37) Arkhipenko, S.; Sabatini, M. T.; Batsanov, A. S.; Karaluka, V.; Sheppard, T. D.; Rzepa, H. S.; Whiting, A. *Chem. Sci.* **2018**, *9*, 1058–1072.

(38) Maki, T.; Ishihara, K.; Yamamoto, H. *Org. Lett.* **2005**, *7*, 5047–5050.

(39) Sakakura, A.; Ohkubo, T.; Yamashita, R.; Akakura, M.; Ishihara, K. *Org. Lett.* **2011**, *13*, 892–895.

(40) Zheng, H.; Hall, D. G. *Tetrahedron Lett.* **2010**, *51*, 3561–3564.

(41) Zheng, H.; McDonald, R.; Hall, D. G. *Chem. Eur. J.* **2010**, *16*, 5454–5460.

(42) Azuma, T.; Murata, A.; Kobayashi, Y.; Inokuma, T.; Takemoto, Y. *Org. Lett.* **2014**, *16*, 4256–4259.

(43) Hayama, N.; Azuma, T.; Kobayashi, Y.; Takemoto, Y. *Chem. Pharm. Bull.* **2016**, *64*, 704–717.

(44) McCubbin, J. A.; Hosseini, H.; Krokhin, O. V. *J. Org. Chem.* **2010**, *75*, 959–962.

(45) Zheng, H.; Lejkowski, M.; Hall, D. G. *Chem. Sci.* **2011**, *2*, 1305–1310.

(46) Zheng, H.; Ghanbari, S.; Nakamura, S.; Hall, D. G. *Angew. Chem. Int. Ed.* **2012**, *51*, 6187–6190.

(47) Ricardo, C. L.; Mo, X.; McCubbin, J. A.; Hall, D. G. *Chem. Eur. J.* **2015**, *21*, 4218–4223.

(48) Mo, X.; Yakiwchuk, J.; Dansereau, J.; McCubbin, J. A.; Hall, D. G. *J. Am. Chem. Soc.* **2015**, *137*, 9694–9703.

(49) Mo, X.; Hall, D. G. *J. Am. Chem. Soc.* **2016**, *138*, 10762–10765.

(50) Wolf, E.; Richmond, E.; Moran, J. *Chem. Sci.* **2015**, *6*, 2501–2505.

(51) Verdelet, T.; Ward, R. M.; Hall, D. G. *Eur. J. Org. Chem.* **2017**, 5729–5738.

(52) Estopiñá-Durán, S.; Donnelly, L. J.; Mclean, E. B.; Hockin, B. M.; Slawin, A. M.; Taylor, J. *Chem. Eur. J.* **2019**, *25*, 3950–3956.

(53) Zheng, H.; Lejkowski, M.; Hall, D. G. *Tetrahedron Lett.* **2013**, *54*, 91–94.

(54) Tang, W.-B.; Cao, K.-S.; Meng, S.-S.; Zheng, W.-H. *Synthesis* **2017**, *49*, 3670–3675.

(55) Cao, K.-S.; Bian, H.-X.; Zheng, W.-H. *Org. Biomol. Chem.* **2015**, *13*, 6449–6452.

(56) Debache, A.; Boumoud, B.; Amimour, M.; Belfaitah, A.; Rhouati, S.; Carboni, B. *Tetrahedron Lett.* **2006**, *47*, 5697–5699.

(57) Aelvoet, K.; Batsanov, A. S.; Blatch, A. J.; Grosjean, C.; Patrick, L. G.; Smethurst, C. A.; Whiting, A. *Angew. Chem. Int. Ed.* **2008**, *47*, 768–770.

(58) Georgiou, I.; Whiting, A. *Org. Biomol. Chem.* **2012**, *10*, 2422–2430.

(59) Li, M.; Yang, T.; Dixon, D. J. *Chem. Commun.* **2010**, *46*, 2191–2193.

(60) Lee, D.; Taylor, M. S. *Org. Biomol. Chem.* **2013**, *11*, 5409–5412.

(61) Tanaka, M.; Nakagawa, A.; Nishi, N.; Iijima, K.; Sawa, R.; Takahashi, D.; Toshima, K. *J. Am. Chem. Soc.* **2018**, *140*, 3644–3651.

(62) William, J. M.; Kuriyama, M.; Onomura, O. *Adv. Synth. Catal.* **2014**, *356*, 934–940.

(63)   Hashimoto, T.; Galvez, A. O.; Maruoka, K. *J. Am. Chem. Soc.* **2015**, *137*, 16016–16019.

(64)   Liu, J.; Yao, H.; Wang, C. *ACS Catal.* **2018**, *8*, 9376–9381.

(65)   Yao, H.; Liu, J.; Wang, C. *Org. Biomol. Chem.* **2019**, *17*, 1901–1905.

(66)   Tatina, M. B.; Moussa, Z.; Xia, M.; Judeh, Z. M. A. *Chem. Commun.* **2019**, *55*, 12204–12207.

(67)   Estopina-Duran, S.; Mclean, E. B.; Donnelly, L. J.; Hockin, B. M.; Taylor, J. E. *Org. Lett.* **2020**, *22*, 7547–7551.

(68)   Twilton, J.; Christensen, M.; DiRocco, D. A.; Ruck, R. T.; Davies, I. W.; MacMillan, D. W. C. *Angew. Chem. Int. Ed.* **2018**, *57*, 5369–5373.

(69)   Dimakos, V.; Su, H. Y.; Garrett, G. E.; Taylor, M. S. *J. Am. Chem. Soc.* **2019**, *141*, 5149–5153.

(70)   Reddy, R. J.; Waheed, M.; Krishna, G. R. *Org. Biomol. Chem.* **2020**, *18*, 3243–3248.

(71)   Shimada, N.; Hirata, M.; Koshizuka, M.; Ohse, N.; Kaito, R.; Makino, K. *Org. Lett.* **2019**, *21*, 4303–4308.

(72)   Koshizuka, M.; Makino, K.; Shimada, N. *Org. Lett.* **2020**, *22*, 8658–8664.

(73)   Fatemi, S.; Gernigon, N.; Hall, D. G. *Green Chem.* **2015**, *17*, 4016–4028.

(74)   Shimada, N.; Ohse, N.; Takahashi, N.; Urata, S.; Koshizuka, M.; Makino, K. *Synlett* **2021**, *32*, 1024–1028.

(75)   Michigami, K.; Sakaguchi, T.; Takemoto, Y. *ACS Catal.* **2020**, *10*, 683–688.

(76)   Horibe, T.; Hazeyama, T.; Nakata, Y.; Takeda, K.; Ishihara, K. *Angew. Chem. Int. Ed.* **2020**, *59*, 17256–17260.

(77)   Shimada, N.; Nakamura, Y.; Ochiai, T.; Makino, K. *Org. Lett.* **2019**, *21*, 3789–3794.

(78)   Shimada, N.; Sugimoto, T.; Noguchi, M.; Ohira, C.; Kuwashima, Y.; Takahashi, N.; Sato, N.; Makino, K. *J. Org. Chem.* **2021**, *86*, 5973–5982.

(79)   Nakamura, Y.; Ochiai, T.; Makino, K.; Shimada, N. *Chem. Pharm. Bull.* **2021**, *69*, 281–285.

(80)   Kuwano, S.; Hosaka, Y.; Arai, T. *Org. Biomol. Chem.* **2019**, *17*, 4475–4482.

(81)   Kusano, S.; Miyamoto, S.; Matsuoka, A.; Yamada, Y.; Ishikawa, R.; Hayashida, O. *Eur. J. Org. Chem.* **2020**, 1598–1602.

(82)   Tanaka, M.; Sato, K.; Yoshida, R.; Nishi, N.; Oyamada, R.; Inaba, K.; Takahashi, D.; Toshima, K. *Nat. Commun.* **2020**, *11*, 2431.

(83)   Siitonen, J. H.; Kattamuri, P. V.; Yousufuddin, M.; Kürti, L. *Org. Lett.* **2020**, *22*, 2486–2489.

(84)   Adhikari, P.; Bhattacharyya, D.; Nandi, S.; Kancharla, P. K.; Das, A. *Org. Lett.* **2021**, *23*, 2437–2442.

(85)   Diemoz, K. M.; Franz, A. K. *J. Org. Chem.* **2019**, *84*, 1126–1138.

(86)   Dhayalan, V.; Gadekar, S. C.; Alassad, Z.; Milo, A. *Nat. Chem.* **2019**, *11*, 543–551.

(87)   Zhang, S.; Lebœuf, D.; Moran, J. *Chem. Eur. J.* **2020**, *26*, 9883–9888.

(88)   Boyes, R. N.; Scott, D. B.; Jebson, P. J.; Godman, M. J.; Julian, D. G. *Clin. Pharmacol. Ther.* **1971**, *12*, 105–116.

(89)   O'Connor, S. E.; Brown, R. A. *Vasc. Pharmacol.* **1982**, *13*, 185–193.

(90)   Balfour, J. A.; Goa, K. L. *Drugs* **1991**, *42*, 511–539.

(91)   Ritz, J.; Fuchs, H.; Kieczka, H.; Moran, W. C. Caprolactam. In *Ullmann's Encyclopedia of Industrial Chemistry*, **2011**.

(92)   Gabara, V. High-Performance Fibers. In *Ullmann's Encyclopedia of Industrial Chemistry*, **2016**, 1–22.

(93)   Santos, A. S.; Silva, A. M. S.; Marques, M. M. B. *Eur. J. Org. Chem.* **2020**, 2501–2516.

(94)   Beckmann, E. *Ber. Dtsch. Chem. Ges.* **1886**, *19*, 988–993.

(95)   Aguilar, D. a; Fritch, J. R.; Fruchey, O. S.; Hilton, C. B.; Horlenko, T.; Seeliger, W. J.; Snyder, P. S. Production of Acetaminophen. US5155273A, October 13, 1992.

(96)   Yamabe, S.; Tsuchida, N.; Yamazaki, S. *J. Org. Chem.* **2005**, *70*, 10638–10644.

(97)   Gawley, R. E. The Beckmann Reactions: Rearrangements, Elimination–Additions, Fragmentations, and Rearrangement–Cyclizations. In *Organic Reactions*, **2004**, 1–420.

(98)   Kaur, K.; Srivastava, S. *New J. Chem.* **2020**, *44*, 18530–18572.

(99)   Furuya, Y.; Ishihara, K.; Yamamoto, H. *J. Am. Chem. Soc.* **2005**, *127*, 11240–11241.

(100)   Zhu, M.; Cha, C.; Deng, W.-P.; Shi, X.-X. *Tetrahedron Lett.* **2006**, *47*, 4861–4863.

(101)   Pi, H.-J.; Dong, J.-D.; An, N.; Du, W.; Deng, W.-P. *Tetrahedron* **2009**, *65*, 7790–7793.

(102)   Hashimoto, M.; Obora, Y.; Sakaguchi, S.; Ishii, Y. *J. Org. Chem.* **2008**, *73*, 2894–2897.

(103)   Vanos, C. M.; Lambert, T. H. *Chem. Sci.* **2010**, *1*, 705–708.

(104)   Augustine, J. K.; Kumar, R.; Bombrun, A.; Mandal, A. B. *Tetrahedron Lett.* **2011**, *52*, 1074–1077.

(105)   Gao, Y.; Liu, J.; Li, Z.; Guo, T.; Xu, S.; Zhu, H.; Wei, F.; Chen, S.; Gebru, H.; Guo, K. *J. Org. Chem.* **2018**, *83*, 2040–2049.

(106)   Chapman, A. W. *J. Chem. Soc.* **1935**, 1223–1225.

(107)   An, N.; Tian, B.-X.; Pi, H.-J.; Eriksson, L. A.; Deng, W.-P. *J. Org. Chem.* **2013**, *78*, 4297–4302.

(108)   Tian, B.-X.; An, N.; Deng, W.-P.; Eriksson, L. A. *J. Org. Chem.* **2013**, *78*, 6782–6785.

(109)   Chandrasekhar, S.; Gopalaiah, K. *Tetrahedron Lett.* **2002**, *43*, 2455–2457.

(110)   Colomer, I.; Chamberlain, A. E. R.; Haughey, M. B.; Donohoe, T. J. *Nat Rev Chem* **2017**, 0088.

(111)   Pereira, M.; Santos, P. *The Chemistry of Hydroxylamines, Oximes, and Hydroxamic Acids* **2009**, 343–498.

(112)   Pozhydaiev, V.; Power, M.; Gandon, V.; Moran, J.; Lebœuf, D. *Chem. Commun.* **2020**, *56*, 11548–11564.

(113)   Kuhara *Mem. Coll. Sci. Eng. Kyoto Imp. Univ.* **1906**, *1*, 254.

(114)   Blatt, A. H. *Chem. Rev.* **1933**, *12*, 215–260.

(115)   Yuen, A. K. L.; Hutton, C. A. *Tetrahedron Lett.* **2005**, *46*, 7899–7903.

(116)   Pusterla, I.; Bode, J. W. *Angew. Chem. Int. Ed.* **2012**, *51*, 513–516.

(117)   Ang, H. T.; Rygus, J. P. G.; Hall, D. G. *Org. Biomol. Chem.* **2019**, *17*, 6007–6014.

(118)   Wang, H.; Xu, J.; Yang, Q.; Zhang, H.; Zhao, S. Method for Preparing Tert-Butoxycarbonyl Phenylboronic Acid. CN105017301A, November 4, 2015.

(119)   Fattahi, N.; Ayubi, M.; Ramazani, A. *Tetrahedron* **2018**, *74*, 4351–4356.

(120)   Dhaon, M. K.; Olsen, R. K.; Ramasamy, K. *J. Org. Chem.* **1982**, *47*, 1962–1965.

(121)   Neises, B.; Steglich, W. *Angew. Chem. Int. Ed.* **1978**, *17*, 522–524.

(122)   Fitzjarrald, V. P.; Pongdee, R. *Tetrahedron Lett.* **2007**, *48*, 3553–3557.

(123) Molander, G. A.; Trice, S. L. J.; Kennedy, S. M.; Dreher, S. D.; Tudge, M. T. *J. Am. Chem. Soc.* **2012**, *134*, 11667–11673.

(124) Wang, X.; Sun, X.; Zhang, L.; Xu, Y.; Krishnamurthy, D.; Senanayake, C. H. *Org. Lett.* **2006**, *8*, 305–307.

(125) Wang, Z.; Tang, J.; Salomon, C. E.; Dreis, C. D.; Vince, R. *Bioorg. Med. Chem.* **2010**, *18*, 4202–4211.

(126) Lafontaine, J. A.; Day, R. F.; Dibrino, J.; Hadcock, J. R.; Hargrove, D. M.; Linhares, M.; Martin, K. A.; Maurer, T. S.; Nardone, N. A.; Tess, D. A. *Bioorg. Med. Chem. Lett.* **2007**, *17*, 5245–5250.

(127) Bair, K.; Baumeister, T.; Buckmelter, A.; Clodfelter, K.; Dragovich, P.; Gosselin, F.; Han, B.; Lin, J.; Reynolds, D. J.; Roth, B.; Smith, C.; Wang, Z.; Yuen, P.-W.; Zheng, X. Novel Compounds and Compositions for the Inhibition of Nampt, March 8, 2012.

(128) Beyer, T. A.; Chambers, R. J.; Lam, K.; Li, M.; Morrell, A. I.; Thompson, D. D. Pyrido[2,3-D]Pyrimidine-2,4-Diamines as Pde 2 Inhibitors. WO2005061497 (A1), July 7, 2005.

(129) Liu, Z.; Larock, R. C. *Org. Lett.* **2004**, *6*, 99–102.

(130) Mondal, S.; Panda, G. *RSC Adv* **2014**, *4*, 28317–28358.

(131) Gennari, L.; Merlotti, D.; Martini, G.; Nuti, R. *Expert Opin. Investig. Drugs* **2006**, *15*, 1091–1103.

(132) Rovner, E. S. *Expert Opin. Pharmacother.* **2005**, *6*, 653–666.

(133) Finder, R. M.; Brogden, R. N.; Sawyer, P. R.; Speight, T. M.; Spencer, R.; Avery, G. S. *Drugs* **1976**, *12*, 1–40.

(134) Tsutsui, C.; Yamada, Y.; Ando, M.; Toyama, D.; Wu, J.; Wang, L.; Taketani, S.; Kataoka, T. *Bioorg. Med. Chem. Lett.* **2009**, *19*, 4084–4087.

(135) Nair, V.; Thomas, S.; Mathew, S. C.; Abhilash, K. G. *Tetrahedron* **2006**, *62*, 6731–6747.

(136) Nambo, M.; Crudden, C. M. *ACS Catal.* **2015**, *5*, 4734–4742.

(137) Olah, G. A.; Kobayashi, S.; Tashiro, M. *J. Am. Chem. Soc.* **1972**, *94*, 7448–7461.

(138) Friedel, C. R.; Crafts, J. M. *Compt Rend* **1877**, *84*, 1450–1454.

(139) Tsuchimoto, T.; Tobita, K.; Hiyama, T.; Fukuzawa, S. *Synlett* **1996**, *1996*, 557–559.

(140) Sarca, V. D.; Laali, K. K. *Green Chem.* **2006**, *8*, 615–620.

(141) Noji, M.; Ohno, T.; Fuji, K.; Futaba, N.; Tajima, H.; Ishii, K. *J. Org. Chem.* **2003**, *68*, 9340–9347.

(142) Bonrath, W.; Dittel, C.; Giraudi, L.; Netscher, T.; Pabst, T. *Catal. Today* **2007**, *121*, 65–70.

(143) Iovel, I.; Mertins, K.; Kischel, J.; Zapf, A.; Beller, M. *Angew. Chem. Int. Ed.* **2005**, *44*, 3913–3917.

(144) Mertins, K.; Iovel, I.; Kischel, J.; Zapf, A.; Beller, M. *Angew. Chem. Int. Ed.* **2005**, *44*, 238–242.

(145) Mertins, K.; Iovel, I.; Kischel, J.; Zapf, A.; Beller, M. *Adv. Synth. Catal.* **2006**, *348*, 691–695.

(146) Choudhury, J.; Podder, S.; Roy, S. *J. Am. Chem. Soc.* **2005**, *127*, 6162–6163.

(147) Yadav, J. S.; Bhunia, D. C.; Vamshi Krishna, K.; Srihari, P. *Tetrahedron Lett.* **2007**, *48*, 8306–8310.

(148) Qin, Q.; Xie, Y.; Floreancig, P. E. *Chem. Sci.* **2018**, *9*, 8528–8534.

(149) Rueping, M.; Nachtsheim, B. J.; Ieawsuwan, W. *Adv. Synth. Catal.* **2006**, *348*, 1033–1037.

(150) Yasuda, M.; Somyo, T.; Baba, A. *Angew. Chem. Int. Ed.* **2006**, *45*, 793–796.

(151) Sun, H.-B.; Li, B.; Chen, S.; Li, J.; Hua, R. *Tetrahedron* **2007**, *63*, 10185–10188.

(152) Niggemann, M.; Meel, M. J. *Angew. Chem. Int. Ed.* **2010**, *49*, 3684–3687.

(153) Sun, G.; Wang, Z. *Tetrahedron Lett.* **2008**, *49*, 4929–4932.

(154) Sanz, R.; Martínez, A.; Miguel, D.; Álvarez-Gutiérrez, J. M.; Rodríguez, F. *Adv. Synth. Catal.* **2006**, *348*, 1841–1845.

(155) Le Bras, J.; Muzart, J. *Tetrahedron* **2007**, *63*, 7942–7948.

(156) Vuković, V. D.; Richmond, E.; Wolf, E.; Moran, J. *Angew. Chem. Int. Ed.* **2017**, *56*, 3085–3089.

(157) Motokura, K.; Nakagiri, N.; Mizugaki, T.; Ebitani, K.; Kaneda, K. *J. Org. Chem.* **2007**, *72*, 6006–6015.

(158) Desroches, J.; Champagne, P. A.; Benhassine, Y.; Paquin, J.-F. *Org. Biomol. Chem.* **2015**, *13*, 2243–2246.

(159) Mo, X.; Morgan, T. D. R.; Ang, H. T.; Hall, D. G. *J. Am. Chem. Soc.* **2018**, *140*, 5264–5271.

(160) Gillis, E. P.; Eastman, K. J.; Hill, M. D.; Donnelly, D. J.; Meanwell, N. A. *J. Med. Chem.* **2015**, *58*, 8315–8359.

(161) Purser, S.; Moore, P. R.; Swallow, S.; Gouverneur, V. *Chem. Soc. Rev.* **2008**, *37*, 320–330.

(162) Ojima, I. *Fluorine in Medicinal Chemistry and Chemical Biology*; John Wiley & Sons, **2009**.

(163) Moore, A. N.; Wayner, D. *Can. J. Chem.* **1999**, *77*, 681–686.

(164) Brown, H. C.; Kanner, B. *J. Am. Chem. Soc.* **1966**, *88*, 986–992.

(165) Ishihara, K.; Nakamura, S.; Kaneeda, M.; Yamamoto, H. *J. Am. Chem. Soc.* **1996**, *118*, 12854–12855.

(166) Ishihara, K.; Kaneeda, M.; Yamamoto, H. *J. Am. Chem. Soc.* **1994**, *116*, 11179–11180.

(167) Jiang, Z.-Y.; Wu, J.-R.; Li, L.; Chen, X.-H.; Lai, G.-Q.; Jiang, J.-X.; Lu, Y.; Xu, L.-W. *Cent. Eur. J. Chem.* **2010**, *8*, 669–673.

(168) Li, Y.; Xiong, Y.; Li, X.; Ling, X.; Huang, R.; Zhang, X.; Yang, J. *Green Chem.* **2014**, *16*, 2976–2981.

(169) Vuković, V. D.; Richmond, E.; Wolf, E.; Moran, J. *Angew. Chem. Int. Ed.* **2017**, *56*, 3085–3089.

(170) Jin, T.; Himuro, M.; Yamamoto, Y. *Angew. Chem. Int. Ed.* **2009**, *48*, 5893–5896.

(171) Gonzalez-Rodriguez, C.; Escalante, L.; Varela, J. A.; Castedo, L.; Saa, C. *Org. Lett.* **2009**, *11*, 1531–1533.

(172) Sato, Y.; Aoyama, T.; Takido, T.; Kodomari, M. *Tetrahedron* **2012**, *68*, 7077–7081.

(173) Kuznetsov, A.; Makarov, A.; Rubtsov, A. E.; Butin, A. V.; Gevorgyan, V. *J. Org. Chem.* **2013**, *78*, 12144–12153.

(174) Patil, D. V.; Kim, S. W.; Nguyen, Q. H.; Kim, H.; Wang, S.; Hoang, T.; Shin, S. *Angew. Chem. Int. Ed.* **2017**, *56*, 3670–3674.

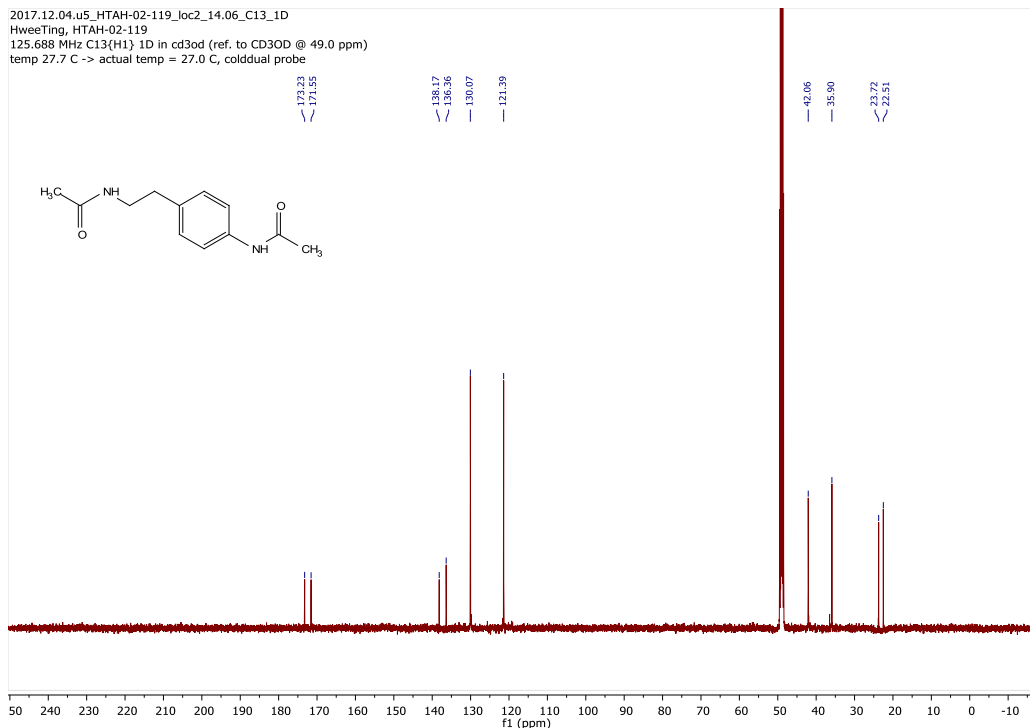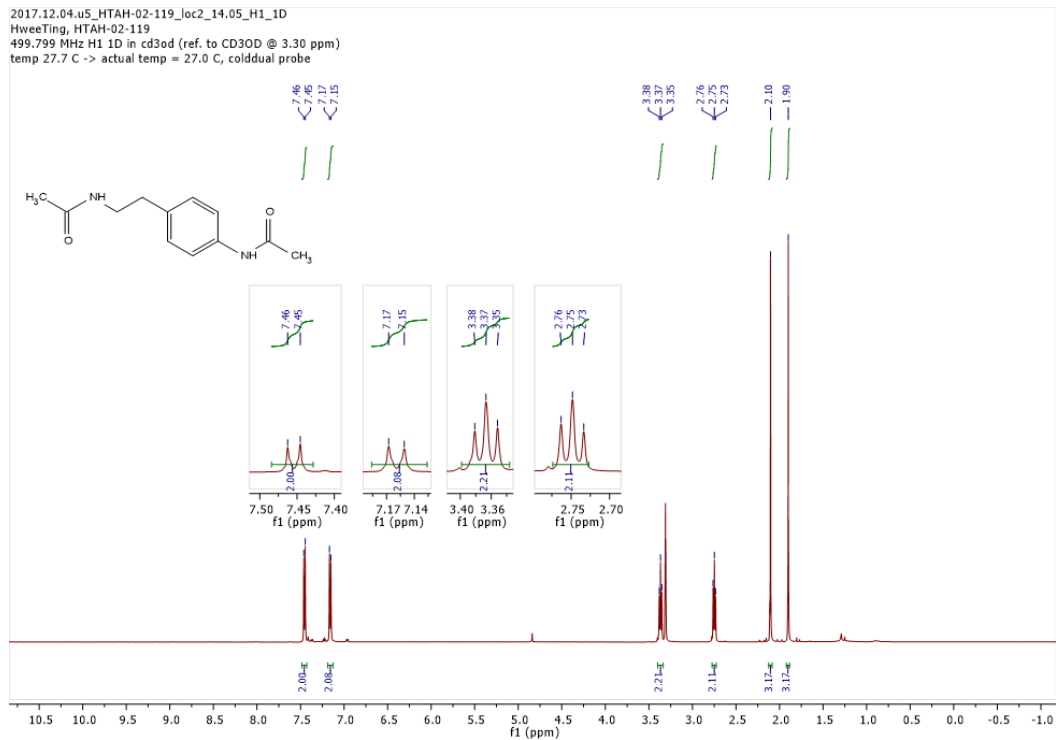(175) Soni, R.; Hall, T. H.; Mitchell, B. P.; Owen, M. R.; Wills, M. *J. Org. Chem.* **2015**, *80*, 6784–6793.

(176)   Jeyakumar, K.; Chakravarthy, R. D.; Chand, D. K. *Catal. Commun.* **2009**, *10*, 1948–1951.

(177)   Saito, T.; Nishimoto, Y.; Yasuda, M.; Baba, A. *J. Org. Chem.* **2006**, *71*, 8516–8522.

(178)   Munoz, S. B.; Ni, C.; Zhang, Z.; Wang, F.; Shao, N.; Mathew, T.; Olah, G. A.; Prakash, G. S. *Eur. J. Org. Chem.* **2017**, 2322–2326.

(179)   Díaz-de-Villegas, M. D.; Gálvez, J. A.; Badorrey, R.; López-Ram-de-Víu, M. P. *Chem. Eur. J.* **2012**, *18*, 13920–13935.

(180)   Suzuki, T. *Tetrahedron Lett.* **2017**, *58*, 4731–4739.

(181)   Meng, S.-S.; Liang, Y.; Cao, K.-S.; Zou, L.; Lin, X.-B.; Yang, H.; Houk, K. N.; Zheng, W.-H. *J. Am. Chem. Soc.* **2014**, *136*, 12249–12252.

(182)   Harada, T.; Sekiguchi, K.; Nakamura, T.; Suzuki, J.; Oku, A. *Org. Lett.* **2001**, *3*, 3309–3312.

(183)   Chen, Z.; Sun, J. *Angew. Chem. Int. Ed.* **2013**, *52*, 13593–13596.

(184)   Ke, Z.; Tan, C. K.; Chen, F.; Yeung, Y.-Y. *J. Am. Chem. Soc.* **2014**, *136*, 5627–5630.

(185)   Tay, D. W.; Leung, G. Y.; Yeung, Y. *Angew. Chem. Int. Ed.* **2014**, *53*, 5161–5164.

(186)   Zi, W.; Toste, F. D. *Angew. Chem. Int. Ed.* **2015**, *54*, 14447–14451.

(187)   Wu, Z.; Wang, J. *ACS Catal.* **2017**, *7*, 7647–7652.

(188)   Lewis, C. A.; Sculimbrene, B. R.; Xu, Y.; Miller, S. J. *Org. Lett.* **2005**, *7*, 3021–3023.

(189)   Jung, B.; Hong, M. S.; Kang, S. H. *Angew. Chem. Int. Ed.* **2007**, *46*, 2616–2618.

(190)   Honjo, T.; Nakao, M.; Sano, S.; Shiro, M.; Yamaguchi, K.; Sei, Y.; Nagao, Y. *Org. Lett.* **2007**, *9*, 509–512.

(191)   Hong, M. S.; Kim, T. W.; Jung, B.; Kang, S. H. *Chem. Eur. J.* **2008**, *14*, 3290–3296.

(192)   You, Z.; Hoveyda, A. H.; Snapper, M. L. *Angew. Chem. Int. Ed.* **2009**, *48*, 547–550.

(193)   Li, B.-S.; Wang, Y.; Proctor, R. S. J.; Jin, Z.; Chi, Y. R. *Chem. Commun.* **2016**, *52*, 8313–8316.

(194)   Yamamoto, K.; Ishimaru, S.; Oyama, T.; Tanigawa, S.; Kuriyama, M.; Onomura, O. *Org. Process Res. Dev.* **2019**, *23*, 660–666.

(195)   Oriyama, T.; Taguchi, H.; Terakado, D.; Sano, T. *Chem. Lett.* **2002**, *31*, 26–27.

(196)   Trost, B. M.; Mino, T. *J. Am. Chem. Soc.* **2003**, *125*, 2410–2411.

(197)   Trost, B. M.; Malhotra, S.; Mino, T.; Rajapaksa, N. S. *Chem. Eur. J.* **2008**, *14*, 7648–7657.

(198)   Aida, H.; Mori, K.; Yamaguchi, Y.; Mizuta, S.; Moriyama, T.; Yamamoto, I.; Fujimoto, T. *Org. Lett.* **2012**, *14*, 812–815.

(199)   Mandai, H.; Ashihara, K.; Mitsudo, K.; Suga, S. *Chem. Lett.* **2018**, *47*, 1360–1363.

(200)   Taylor, M. S. *Acc. Chem. Res.* **2015**, *48*, 295–305.

(201)   Lee, D.; Williamson, C. L.; Chan, L.; Taylor, M. S. *J. Am. Chem. Soc.* **2012**, *134*, 8260–8267.

(202)   Pawliczek, M.; Hashimoto, T.; Maruoka, K. *Chem. Sci.* **2018**, *9*, 1231–1235.

(203)   Li, R.-Z.; Tang, H.; Yang, K. R.; Wan, L.-Q.; Zhang, X.; Liu, J.; Fu, Z.; Niu, D. *Angew. Chem. Int. Ed.* **2017**, *56*, 7213–7217.

(204)   Nakagawa, A.; Nishi, N.; Iijima, K.; Sawa, R.; Takahashi, D.; Toshima, K. *J. Am. Chem. Soc* **2018**, *140*, 3644.

(205)   Dewar, M.; Dietz, R. *Tetrahedron Lett.* **1959**, *1*, 21–23.

(206)   Greig, L. M.; Kariuki, B. M.; Habershon, S.; Spencer, N.; Johnston, R. L.; Harris, K. D. M.; Philp, D. *New J. Chem.* **2002**, *26*, 701–710.

(207) Greig, L. M.; Slawin, A. M. Z.; Smith, M. H.; Philp, D. *Tetrahedron* **2007**, *63*, 2391–2403.

(208) Zhou, Q. J.; Worm, K.; Dolle, R. E. *J. Org. Chem.* **2004**, *69*, 5147–5149.

(209) Mathew, S. M.; Hartley, C. S. *Macromolecules* **2011**, *44*, 8425–8432.

(210) Sumida, Y.; Harada, R.; Kato-Sumida, T.; Johmoto, K.; Uekusa, H.; Hosoya, T. *Org. Lett.* **2014**, *16*, 6240–6243.

(211) Gao, T.; Jiang, Z.; Chen, B.; Sun, Q.; Orooji, Y.; Huang, L.; Liu, Z. *Dyes Pigm.* **2020**, *173*, 107998.

(212) Stavber, S.; Kralj, P.; Zupan, M. *Synth.* **2002**, *2002*, 1513–1518.

(213) Velder, J.; Robert, T.; Weidner, I.; Neudörfl, J.; Lex, J.; Schmalz, H. *Adv. Synth. Catal.* **2008**, *350*, 1309–1315.

(214) Yoshida, H.; Okada, K.; Kawashima, S.; Tanino, K.; Ohshita, J. *Chem. Commun.* **2010**, *46*, 1763–1765.

(215) Bryan, M. C.; Dunn, P. J.; Entwistle, D.; Gallou, F.; Koenig, S. G.; Hayler, J. D.; Hickey, M. R.; Hughes, S.; Kopach, M. E.; Moine, G.; Richardson, P.; Roschangar, F.; Steven, A.; Weiberth, F. J. *Green Chem.* **2018**, *20*, 5082–5103.

Appendices

Appendix 1: Selected Copies of NMR Spectra

^{1}H, ^{13}C and ^{19}F NMR Spectra of Compound 2-10b in CD$_3$OD:

¹H, ¹³C and ¹⁹F NMR Spectra of Compound 3-3i in CDCl₃:

2019.04.24.u5_HTAH-02-66_loc3_14.15_H1_1D
HweeTing, HTAH-02-66
499.787 MHz H1 1D in cdcl3 (ref. to CDCl3 @ 7.26 ppm)
temp 27.7 C -> actual temp = 27.0 C, colddual probe

2019.04.24.u5_HTAH-02-66_loc3_14.16_C13_1D
HweeTing, HTAH-02-66
125.685 MHz C13{H1} 1D in cdcl3 (ref. to CDCl3 @ 77.06 ppm)
temp 27.7 C -> actual temp = 27.0 C, colddual probe

468.652 MHz F19 1D in cdcl3
temp 26.9 C -> actual temp = 27.0 C, autoxdb probe

¹H, ¹¹B, and ¹³C NMR Spectra of Compound 4-9 in CD₃COCD₃ + D₂O drop:

2021.01.23.mr4_HTAH-07-37_H1_PRESAT
399.980 MHz H1 1D in acetone (ref. to acetone @ 2.04 ppm)
temp 25.9 C -> actual temp = 27.0 C, onenmr probe

2021.01.23.mr4_HTAH-07-37_B11_1D
128.329 MHz B11{H1} 1D in acetone
temp 25.9 C -> actual temp = 27.0 C, onenmr
probe

— 27.76

150 140 130 120 110 100 90 80 70 60 50 40 30 20 10 0 -10 -20 -30 -40 -50 -60 -70 -80 -90 -100 -110 -120 -130 -140 -15

2021.01.23.i4_HTAH-07-37_loc17_15.19_C13_1D
100.540 MHz C13{H1} 1D in acetone (ref. to acetone @ 29.8 ppm)
temp 26.5 C -> actual temp = 27.0 C, autoxdb probe

153.42
148.73
146.59
142.48
142.23
134.97
134.10
131.64
130.35
129.69
129.24
129.16
128.49
126.82
126.60
125.48
125.15
124.86
124.64
124.39
123.21
121.02
120.03
119.00
116.08

30.06 acetone
29.87 acetone
29.68 acetone
29.48 acetone
29.29 acetone
29.10 acetone
28.91 acetone
22.77
21.58

134.97
134.10
131.64
130.35
129.69
129.24
129.16
128.49
126.82
126.60
125.48
125.15
124.86
124.64
124.39
123.21
121.02
119.00
116.08

136 134 132 130 128 126 124 122 120 118 116

150 240 230 220 210 200 190 180 170 160 150 140 130 120 110 100 90 80 70 60 50 40 30 20 10 0 -10

231

^{1}H, ^{11}B, and ^{13}C NMR Spectra of Compound BA-49 in CD$_3$COCD$_3$ + D$_2$O drop:

HweeTing, HTAH-06-188
499.789 MHz H1 1D in acetone (ref. to acetone @ 2.04 ppm)
temp 27.7 C -> actual temp = 27.0 C, colddual probe

HTAH-06-188
128.329 MHz B11{H1} 1D in acetone
temp 25.9 C -> actual temp = 27.0 C, onenmr probe

HweeTing, HTAH-06-188
125.686 MHz C13{H1} 1D in acetone (ref. to acetone @ 29.8 ppm)
temp 27.7 C -> actual temp = 27.0 C, colddual probe
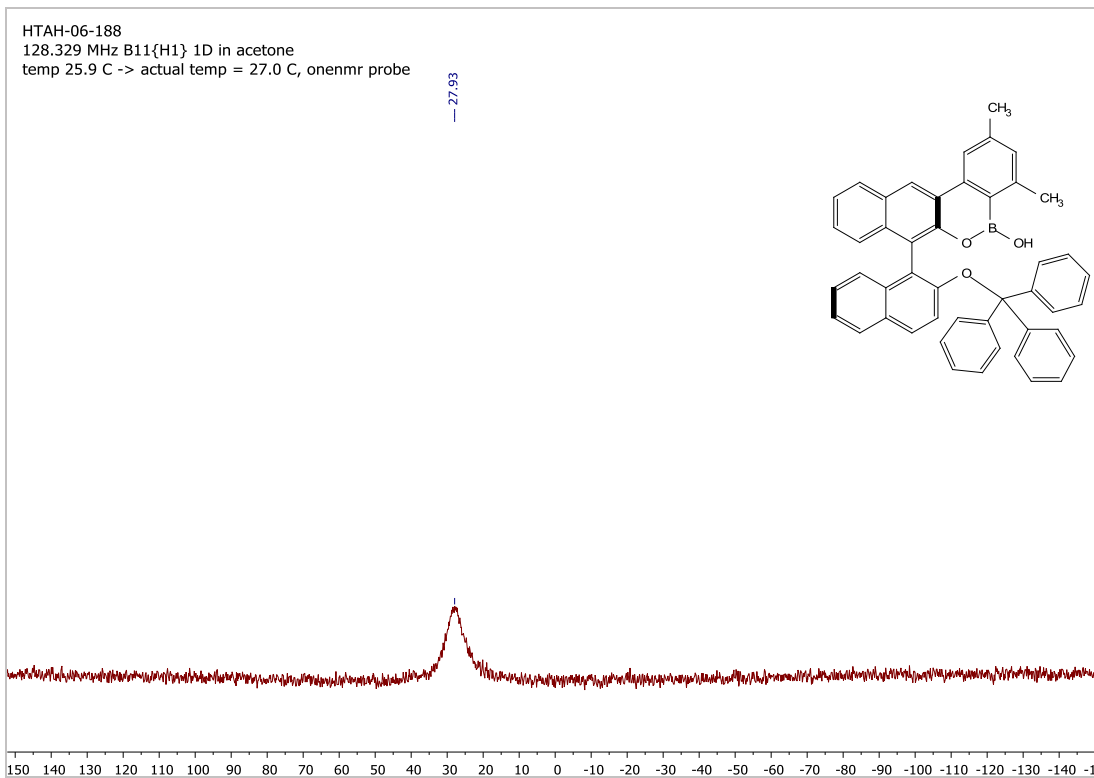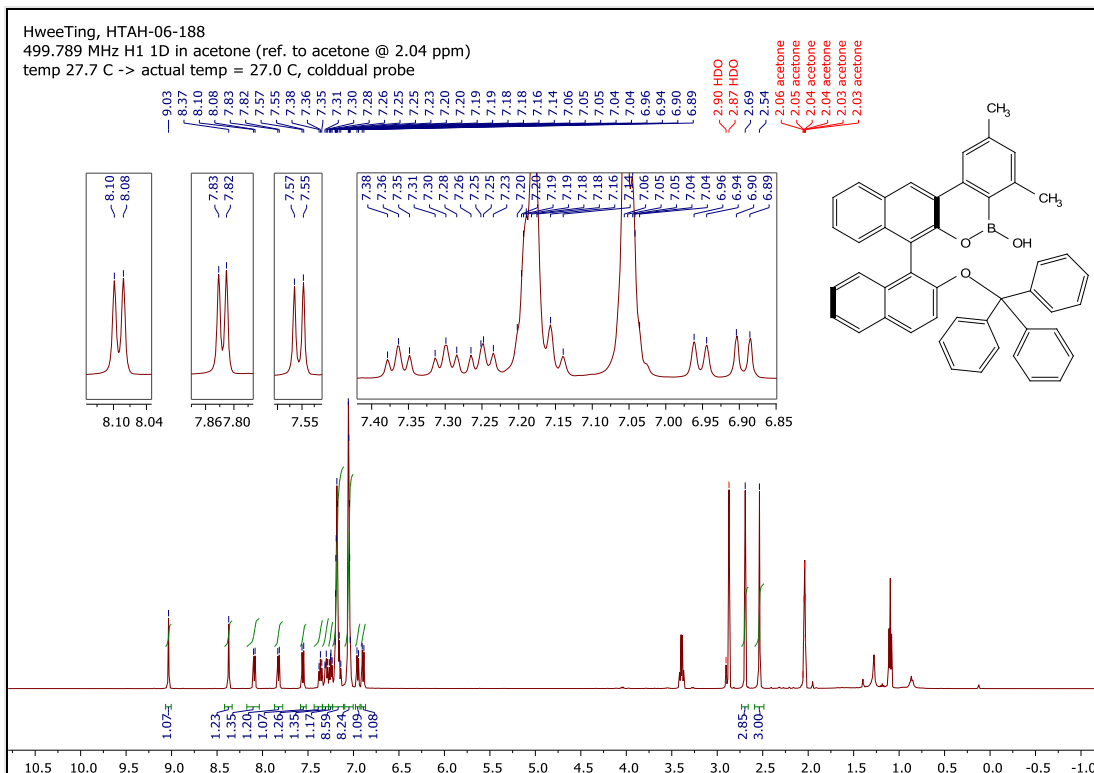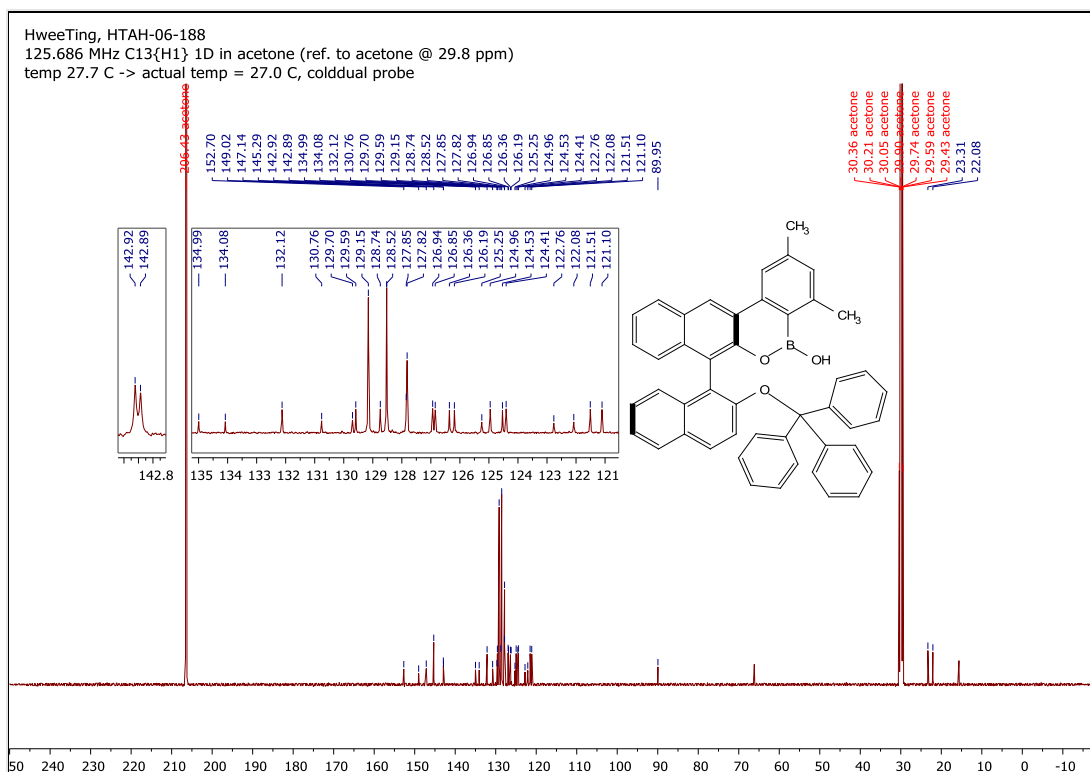
^{1}H and ^{11}B NMR Spectra of Compound 4-5 in CD$_3$CN:

HTAH-05-67
399.980 MHz H1 1D in cd3cn
temp 25.9 C -> actual temp = 27.0 C, onenmr probe

— 2.42

150 140 130 120 110 100 90 80 70 60 50 40 30 20 10 0 -10 -20 -30 -40 -50 -60 -70 -80 -90 -100 -110 -120 -130 -140 -15
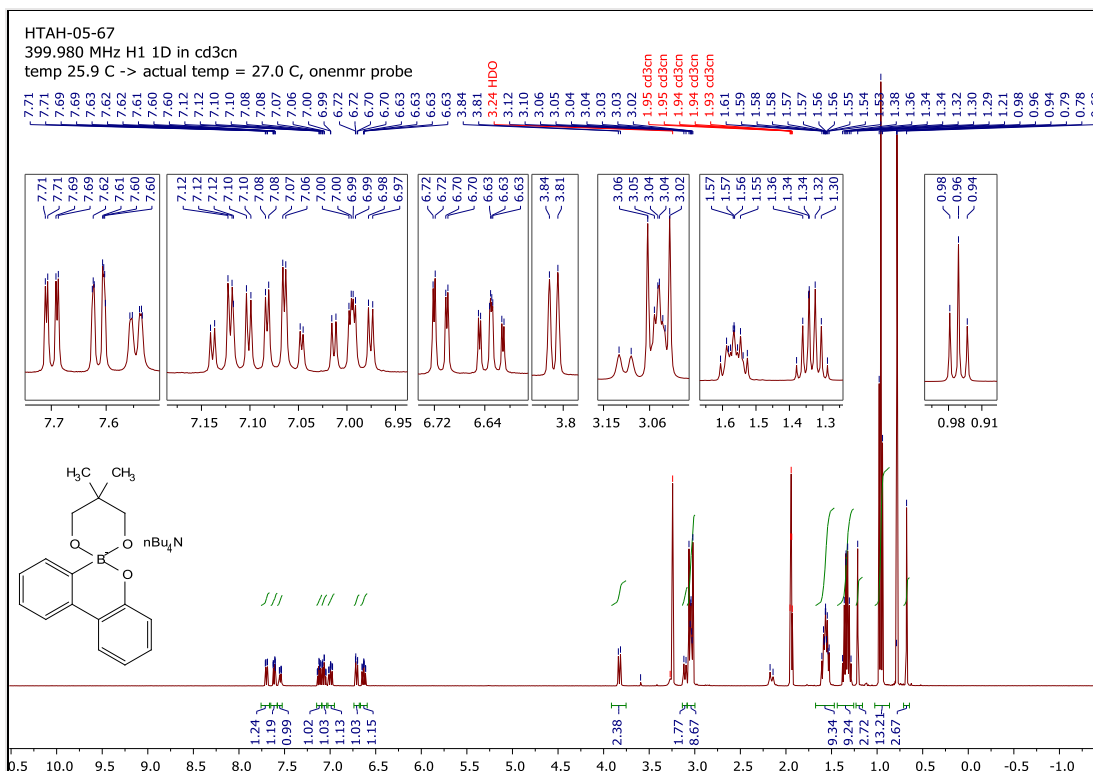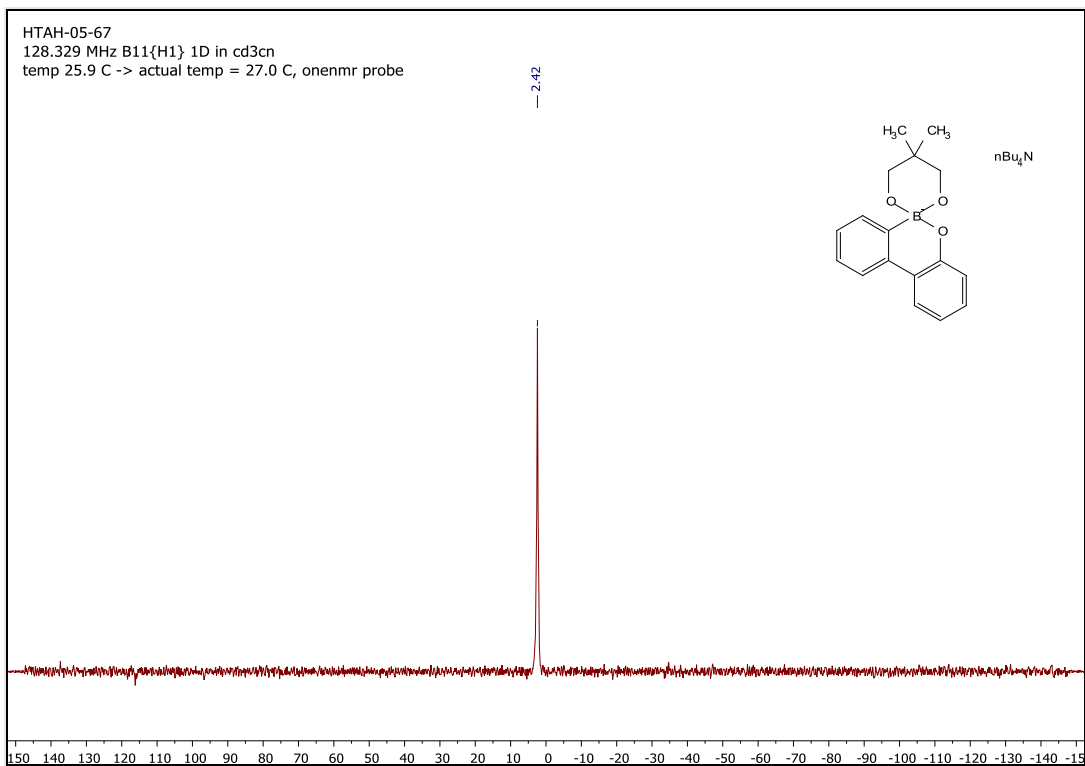
^{1}H and ^{13}C NMR Spectra of Compound 4-4u in CDCl$_3$:

7.27 cdcl3

8.19 8.19 8.18 8.17 8.16 8.16 7.45 7.45 7.44 7.43 7.42 7.42 7.38 7.38 7.37 7.36 7.36 7.35 7.34 7.34 7.34 7.33 7.33 7.32 7.32 7.31 7.30 7.29 7.28 7.28 7.28 4.55 4.03 4.02 4.01 4.00 3.99 3.98 3.96 3.94 3.93 3.92 3.90 3.85 3.83 3.83 3.82 3.81 3.80 3.78 3.31 3.29 3.28 3.26 3.25 2.15 2.14 2.12

8.19 8.18 8.17 8.16

7.45 7.42 7.36 7.35 7.34 7.34 7.30 7.29 7.28

4.01 4.00 3.99 3.98 3.94 3.93 3.92 3.83 3.82 3.81 3.81

3.31 3.29 3.28 3.26 3.25

2.15 2.14 2.12

8.22 8.16   7.4   7.3   4.0   3.9   3.8   3.29 3.22   2.16 2.07

OH
O

NO$_2$

1.84   5.13   1.82   1.16   1.08   1.97   1.13   0.97

10.5 10.0 9.5 9.0 8.5 8.0 7.5 7.0 6.5 6.0 5.5 5.0 4.5 4.0 3.5 3.0 2.5 2.0 1.5 1.0 0.5 0.0 -0.5 -1.0

234

HweeTing, HTAH-06-166
100.539 MHz C13{H1} 1D in cdcl3 (ref. to CDCl3 @ 77.06 ppm)
temp 26.5 C -> actual temp = 27.0 C, autoxdb probe

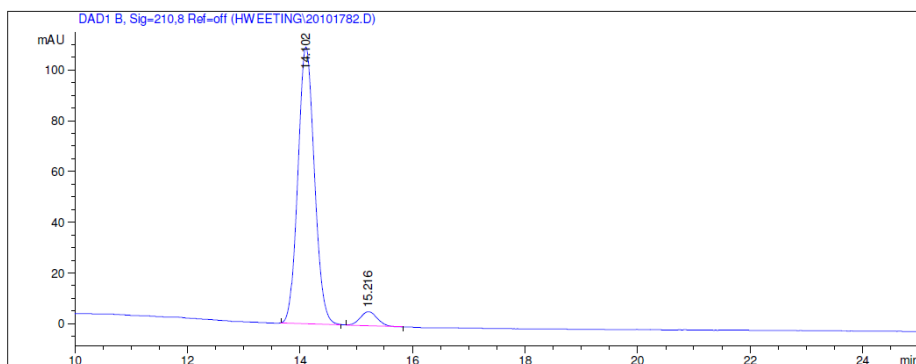# Appendix 2: Selected Chromatograms of Enantiomeric Excess Measurement

Chiral HPLC Data for Racemic and Optically Enriched (*S*)- and (*R*)-4-4a:
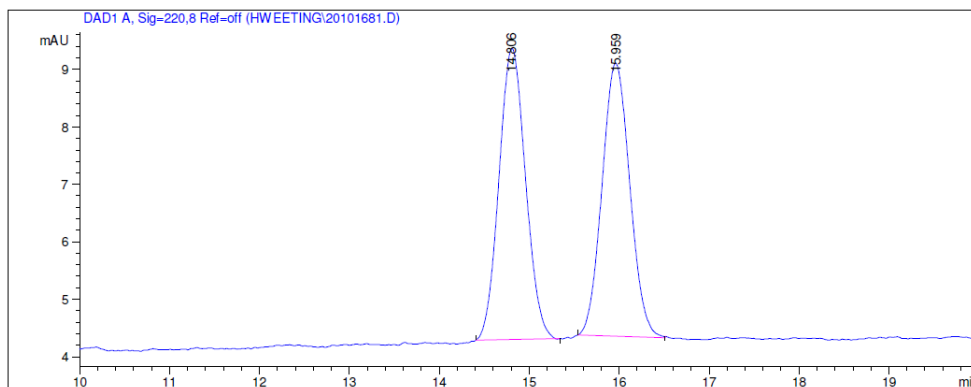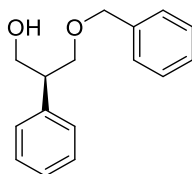
Signal 1: DAD1 A, Sig=220,8 Ref=off

```
Peak RetTime Type  Width      Area       Height     Area
  #   [min]        [min]    [mAU*s]       [mAU]       %
----|-------|----|-------|----------|----------|--------|
  1  14.806 BP   0.3115  104.23595    5.07714  50.5334
  2  15.959 BB   0.3281  102.03530    4.75975  49.4666

Totals :                 206.27126    9.83689
```


Signal 1: DAD1 B, Sig=210,8 Ref=off

```
Peak RetTime Type  Width      Area       Height     Area
  #   [min]        [min]    [mAU*s]       [mAU]       %
----|-------|----|-------|----------|----------|--------|
  1  14.102 BB   0.3171 2237.39966  109.17632  94.9389
  2  15.216 BB   0.3169  119.27364    5.59181   5.0611

Totals :                2356.67330  114.76812
```
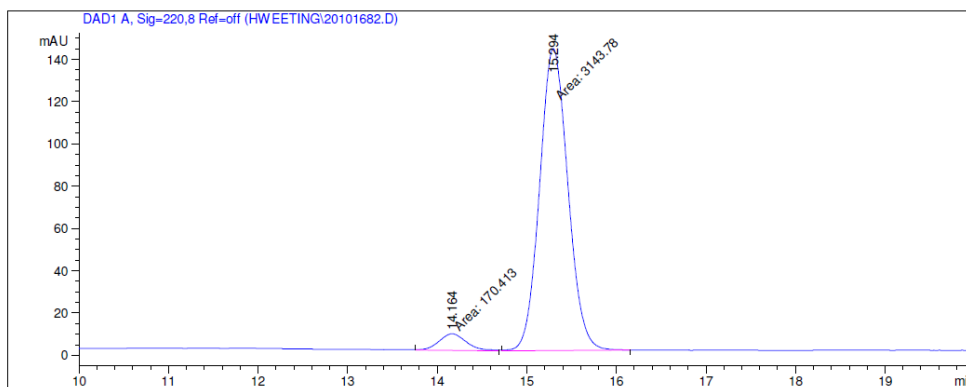

Signal 1: DAD1 A, Sig=220,8 Ref=off

```
Peak RetTime Type  Width      Area       Height     Area
  #   [min]        [min]    [mAU*s]       [mAU]       %
----|-------|----|-------|----------|----------|--------|
  1  14.164 MM   0.3588  170.41336    7.91666   5.1419
  2  15.294 MM   0.3668 3143.78003  142.83772  94.8581

Totals :                3314.19339  150.75438
```

236

Chiral HPLC Data for Racemic and Optically Enriched 4-4b:
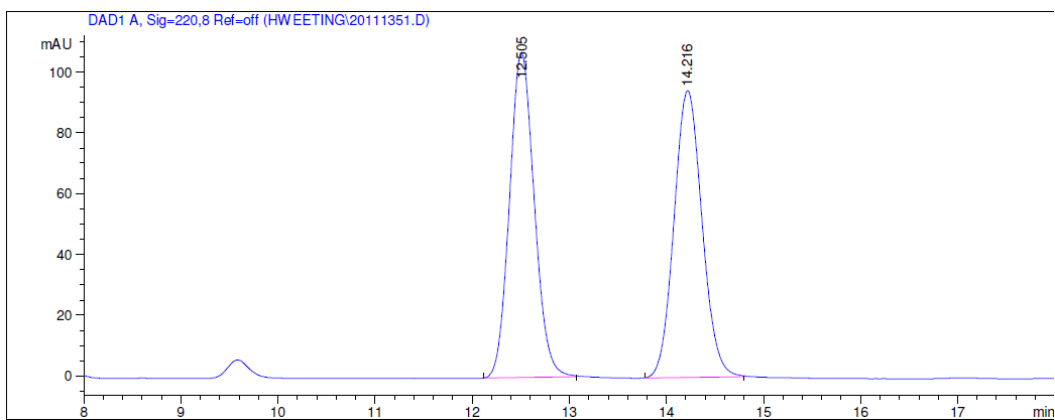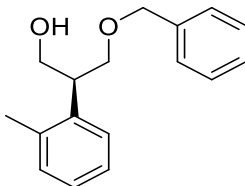
Signal 1: DAD1 A, Sig=220,8 Ref=off

```
Peak RetTime Type  Width     Area       Height     Area
  #   [min]        [min]    [mAU*s]      [mAU]       %
----|-------|----|-------|----------|----------|--------|
  1  12.505 BB    0.2748 1895.69617  106.96880  50.0071
  2  14.216 BB    0.3123 1895.16016   94.36245  49.9929

Totals :                 3790.85632  201.33125
```


Signal 1: DAD1 A, Sig=220,8 Ref=off

```
Peak RetTime Type  Width     Area       Height     Area
  #   [min]        [min]    [mAU*s]      [mAU]       %
----|-------|----|-------|----------|----------|--------|
  1  11.946 MM    0.2991 3385.37573  188.62729  96.0346
  2  13.623 MM    0.3360  139.78545    6.93337   3.9654

Totals :                 3525.16118  195.56066
```
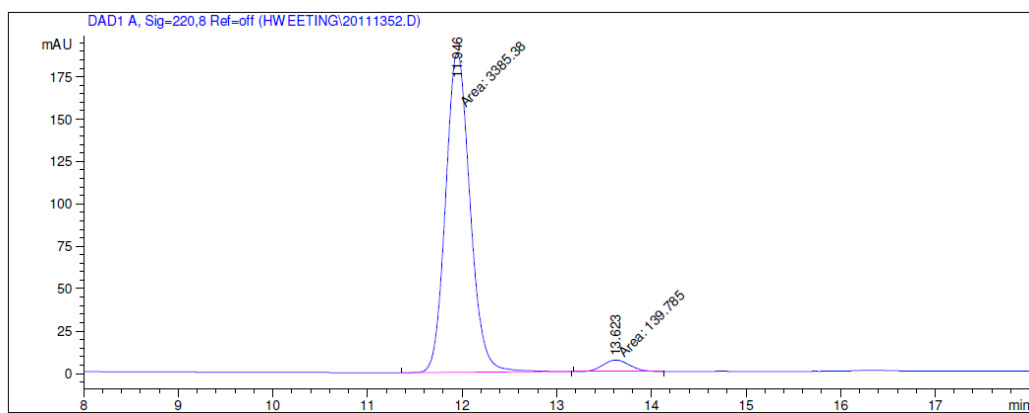
Chiral HPLC Data for Racemic and Optically Enriched 4-4m:
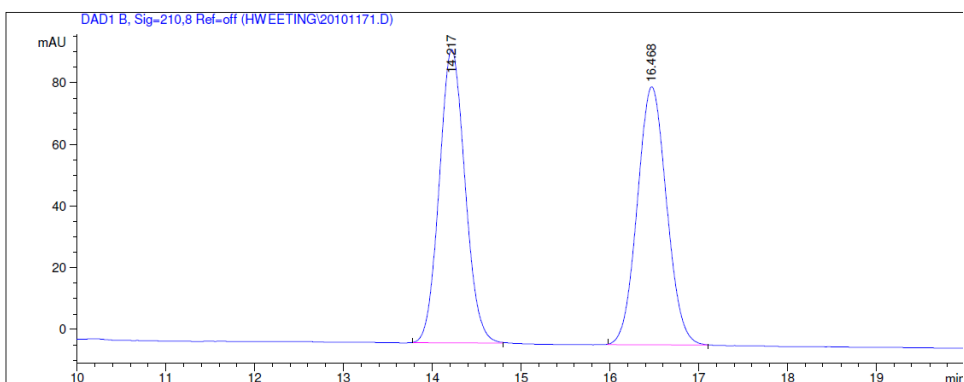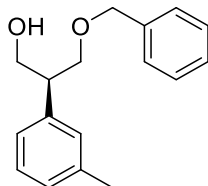
Signal 1: DAD1 B, Sig=210,8 Ref=off

Peak #	RetTime [min]	Type	Width [min]	Area [mAU*s]	Height [mAU]	Area %
1	14.217	BB	0.3113	1920.31836	95.19438	49.9930
2	16.468	BB	0.3596	1920.85669	83.74030	50.0070

Totals :   3841.17505   178.93468
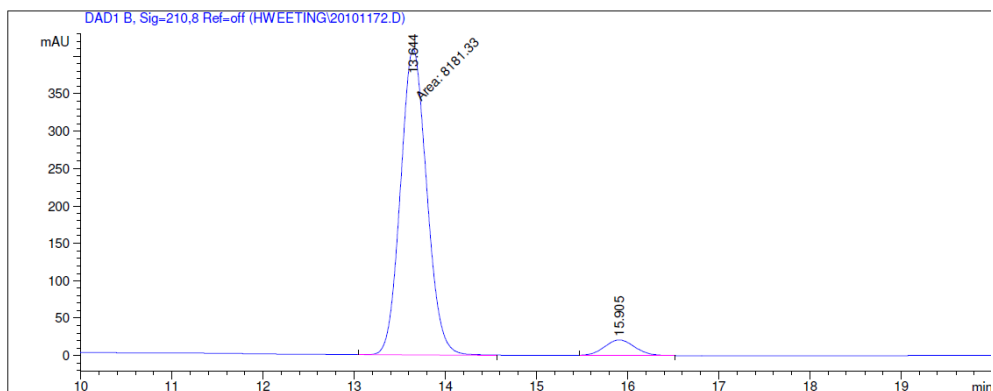

Signal 1: DAD1 B, Sig=210,8 Ref=off

Peak #	RetTime [min]	Type	Width [min]	Area [mAU*s]	Height [mAU]	Area %
1	13.644	MM	0.3333	8181.33398	409.10516	94.4848
2	15.905	BB	0.3545	477.55441	20.75185	5.5152

Totals :   8658.88840   429.85701

Chiral HPLC Data for Racemic and Optically Enriched 4-4n:
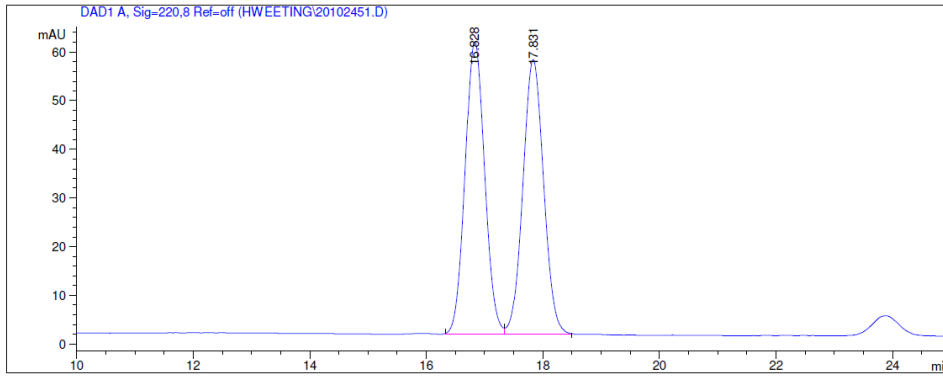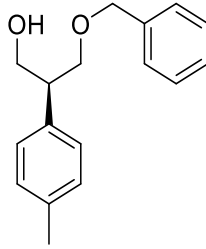
Signal 1: DAD1 A, Sig=220,8 Ref=off

```
Peak RetTime Type  Width      Area       Height      Area
 #   [min]         [min]    [mAU*s]      [mAU]        %
----|-------|----|-------|----------|----------|--------|
  1  16.828 BV   0.3641 1401.32654   60.08754  50.0021
  2  17.831 VB   0.3879 1401.20874   56.39415  49.9979

Totals :                2802.53528  116.48169
```


Signal 1: DAD1 A, Sig=220,8 Ref=off

```
Peak RetTime Type  Width      Area       Height      Area
 #   [min]         [min]    [mAU*s]      [mAU]        %
----|-------|----|-------|----------|----------|--------|
  1  16.176 MF   0.3911 3285.87427  140.01212  95.3636
  2  17.191 FM   0.4261  159.75279    6.24870   4.6364

Totals :                3445.62706  146.26082
```
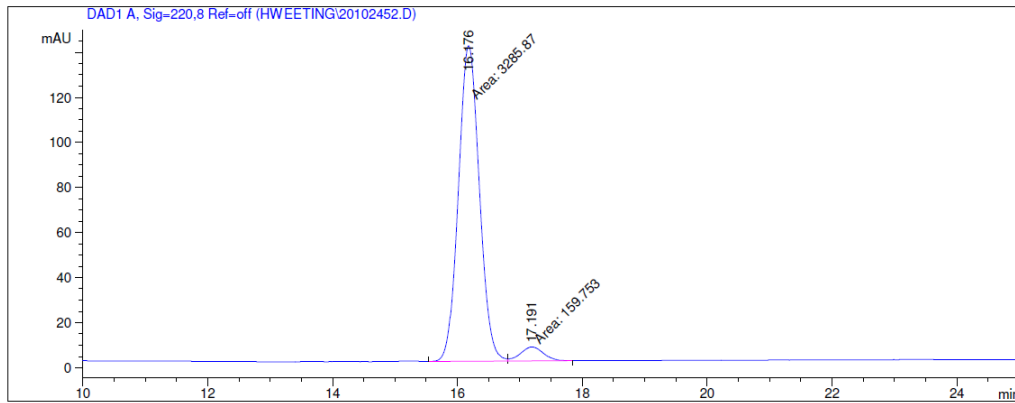
239

Chiral HPLC Data for Racemic and Optically Enriched 4-11:
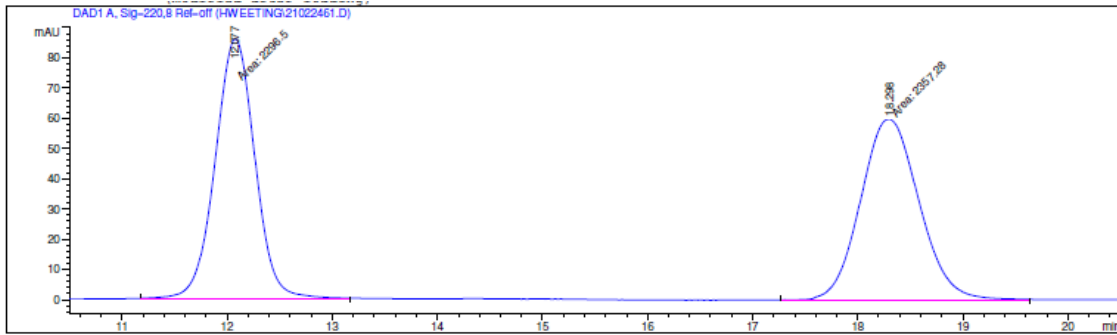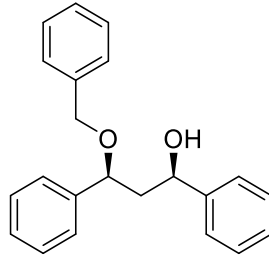
Signal 1: DAD1 A, Sig=220,8 Ref=off

```
Peak RetTime Type  Width     Area       Height     Area
 #   [min]         [min]   [mAU*s]      [mAU]        %
----|-------|----|-------|----------|-----------|--------|
  1  12.077 MM   0.4448  2296.50415  86.05598  49.3470
  2  18.298 MM   0.6546  2357.27808  60.01848  50.6530

Totals :                 4653.78223 146.07446
```


Signal 1: DAD1 A, Sig=220,8 Ref=off
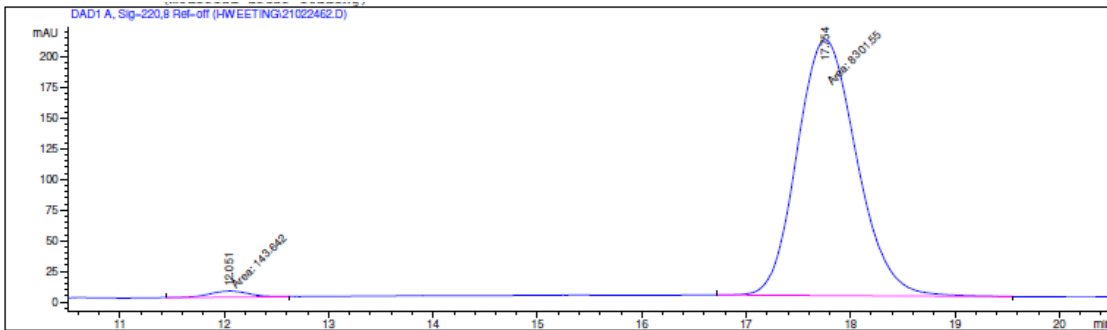
```
Peak RetTime Type  Width     Area       Height     Area
 #   [min]         [min]   [mAU*s]      [mAU]        %
----|-------|----|-------|----------|-----------|--------|
  1  12.051 MM   0.4588   143.64214   5.21851   1.7009
  2  17.754 MM   0.6634  8301.54590 208.57378  98.2991

Totals :                 8445.18803 213.79228
```

Appendix 3: X-Ray Crystallography Reports

Structure Report of Compound 4-5:

CCDC 2051073 (compound **4-5**) contains the supplementary crystallographic data for this thesis. These data can be obtained free of charge from The Cambridge Crystallographic Data Center.

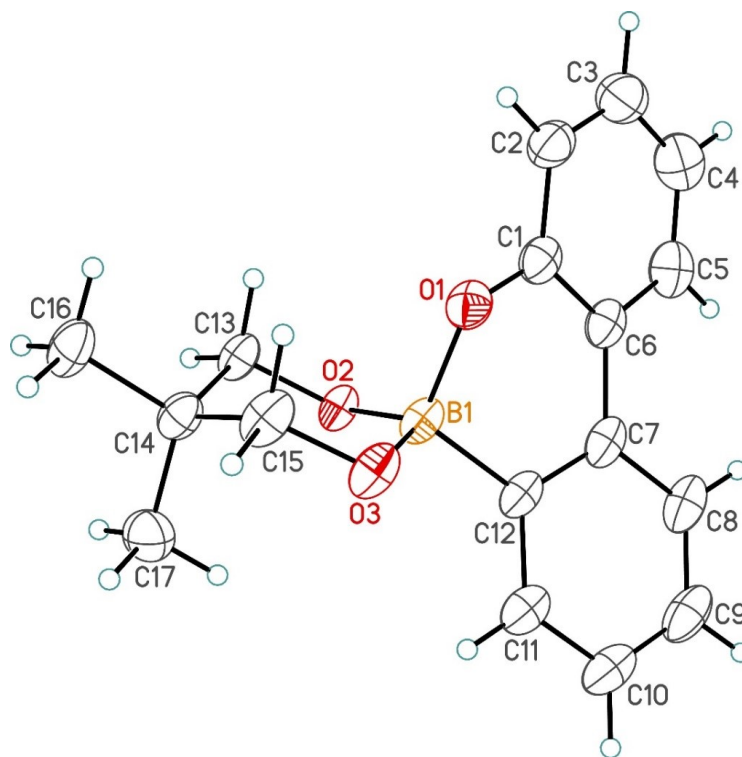**XCL Code:**   DGH1919   **Date:**   15 November 2019

Compound: tetrabutylammonium   5',5'-dimethylspiro[dibenzo[1,2]oxaborinine-6,2'-[1,3,2]dioxaborinan]-6-uide

Formula: $C_{33}H_{54}BNO_3$

**Supervisor:**   D. G. Hall   **Crystallographer:**   M. J. Ferguson

Perspective   view   of   the   5',5'-dimethylspiro[dibenzo[1,2]oxaborinine-6,2'-[1,3,2]dioxaborinan]-6-uide ion showing the atom labelling scheme. Non-hydrogen atoms are represented by Gaussian ellipsoids at the 30% probability level. Hydrogen atoms are shown with arbitrarily small thermal parameters.

View of the tetrabutylammonium 5',5'-dimethylspiro[dibenzo[1,2]oxaborinine-6,2'-[1,3,2]dioxaborinan]-6-uide salt. Hydrogen atoms are not shown.
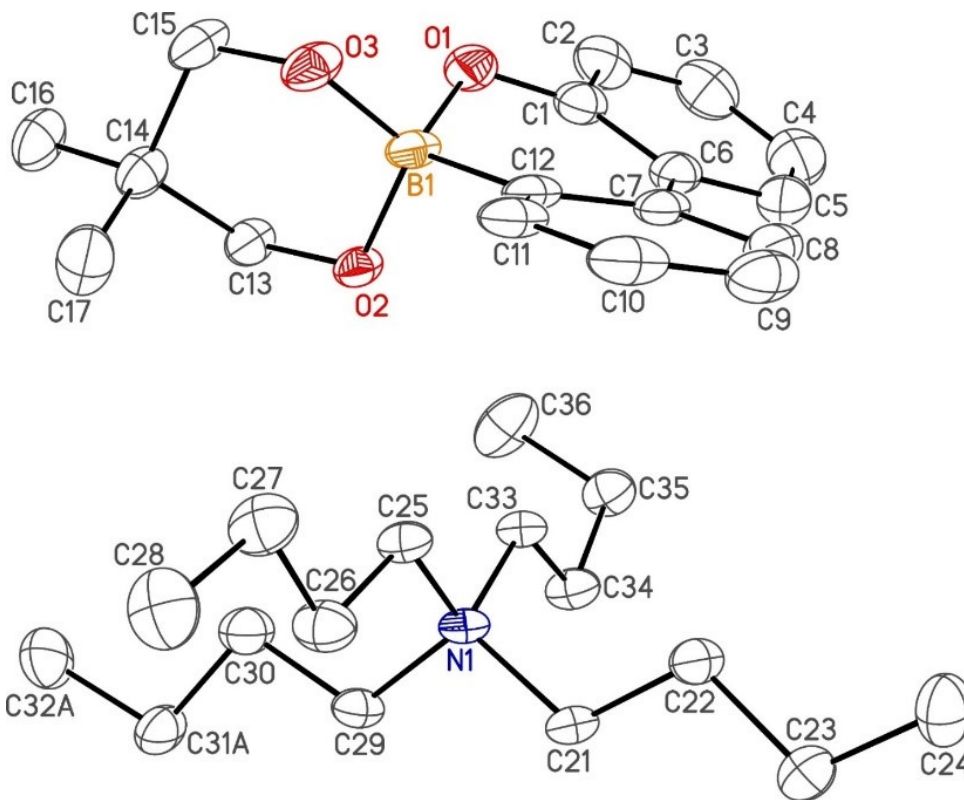
Crystallographic Experimental Details:

A. Crystal Data

formula	$C_{33}H_{54}BNO_3$
formula weight	523.58
crystal dimensions (mm)	$0.35 \times 0.09 \times 0.06$
crystal system	monoclinic
space group	*Cc* (No. 9)
unit cell parameters*a*	
a (Å)	22.3266(5)
b (Å)	9.6352(2)
c (Å)	17.1687(3)
β (deg)	117.8694(12)
V (Å^3)	3264.98(12)
Z	4
ρ_{calcd} (g cm^{-3})	1.065
μ (mm^{-1})	0.506

B. Data Collection and Refinement Conditions

diffractometer	Bruker D8/APEX II CCD[b]
radiation (λ [Å])	Cu Kα (1.54178) (microfocus source)
temperature (°C)	–80
scan type	ω and ϕ scans (1.0°) (5-5-10 s exposures)[c]
data collection 2θ limit (deg)	140.36
total data collected	9378 (-27 $\leq$ h $\leq$ 26, -11 $\leq$ k $\leq$ 11, -20 $\leq$ l $\leq$ 20)
independent reflections	5661 (R_{int} = 0.0210)
number of observed reflections (*NO*)	5061 [$F_o^2 \geq 2\sigma\,(F_o^2)$]
structure solution method	intrinsic phasing (*SHELXT-2014*[d])
refinement method	full-matrix least-squares on F^2 (*SHELXL–2017*[e])
absorption correction method	Gaussian integration (face-indexed)
range of transmission factors	1.0000–0.8258
data/restraints/parameters	5661 / 8[f] / 358
extinction coefficient (x)[g]	0.00051(9)
Flack absolute structure parameter[h]	0.1(2)
goodness-of-fit (*S*)[i] [all data]	1.054
final *R* indices[j]	
R_1 [$F_o^2 \geq 2\sigma\,(F_o^2)$]	0.0368
wR_2 [all data]	0.0995
largest difference peak and hole	0.158 and –0.126 e Å^{-3}

[a]Obtained from least-squares refinement of 6425 reflections with 8.96° < 2θ < 139.62°.
[b]Programs for diffractometer operation, data collection, data reduction and absorption correction were those supplied by Bruker.
[c]Data were collected with the detector set at three different positions. Low-angle (detector 2θ = –33º) data frames were collected using a scan time of 5 s, medium-angle (detector 2θ = 75º) frames using a scan time of 5 s, and high-angle (detector 2θ = 117º) frames using a scan time of 10 s.
[d]Sheldrick, G. M. *Acta Crystallogr.* **2015**, *A71*, 3–8. (*SHELXT-2014*)
[e]Sheldrick, G. M. *Acta Crystallogr.* **2015**, *C71*, 3–8. (*SHELXL-2017*)
[f]The C–C distances within the disordered fragment of one of the butyl groups were restrained to be approximately the same by use of the *SHELXL* **SADI** instruction.
[g]$F_c^* = kF_c[1 + x\{0.001F_c^2\lambda^3/\sin(2\theta)\}]^{-1/4}$, where k is the overall scale factor.
[h]Flack, H. D. *Acta Crystallogr.* **1983**, *A39*, 876–881; Flack, H. D.; Bernardinelli, G. *Acta Crystallogr.* **1999**, *A55*, 908–915; Flack, H. D.; Bernardinelli, G. *J. Appl. Cryst.* **2000**, *33*, 1143–1148. The Flack parameter will refine to a value near zero if the structure is in the correct configuration and will refine to a value near one for the inverted configuration. The value observed herein is indicative of racemic twinning and was accommodated during the refinement (using the *SHELXL-2014* TWIN instruction [see reference e]).

Structure Report of Compound 4-6:

CCDC 2063743 (compound **4-6**) contains the supplementary crystallographic data for this thesis. These data can be obtained free of charge from The Cambridge Crystallographic Data Center.

|			
XCL Code:	DGH2110	**Date:**	18 February 2021
Compound:	(2*R*)-3-(benzyloxy)-2-phenylpropyl 3,5-dinitrobenzoate		
Formula:	$C_{23}H_{20}N_2O_7$		
Supervisor:	D. G. Hall	**Crystallographer:**	M. J. Ferguson

Perspective view one of two crystallographically independent (2*R*)-3-(benzyloxy)-2-phenylpropyl 3,5-dinitrobenzoate molecules (*molecule A*) showing the atom labelling scheme. Non-hydrogen atoms are represented by Gaussian ellipsoids at the 30% probability level. Hydrogen atoms are shown with arbitrarily small thermal parameters.
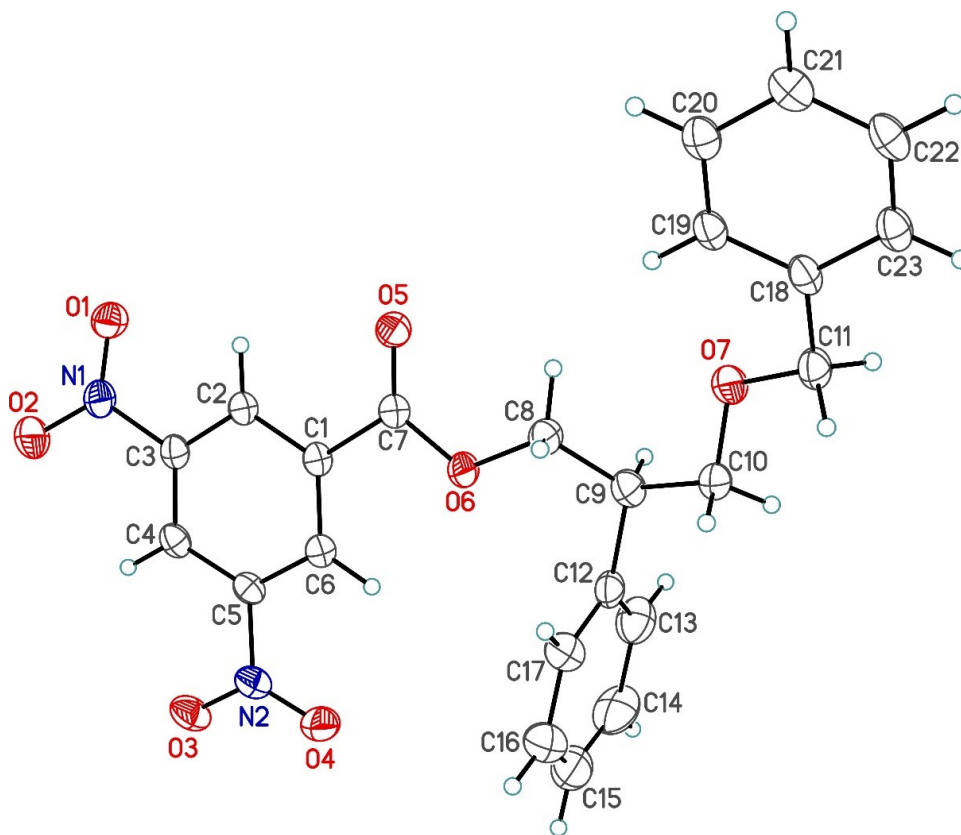
Same approximate view of the second crystallographically-independent molecule (*molecule B*).
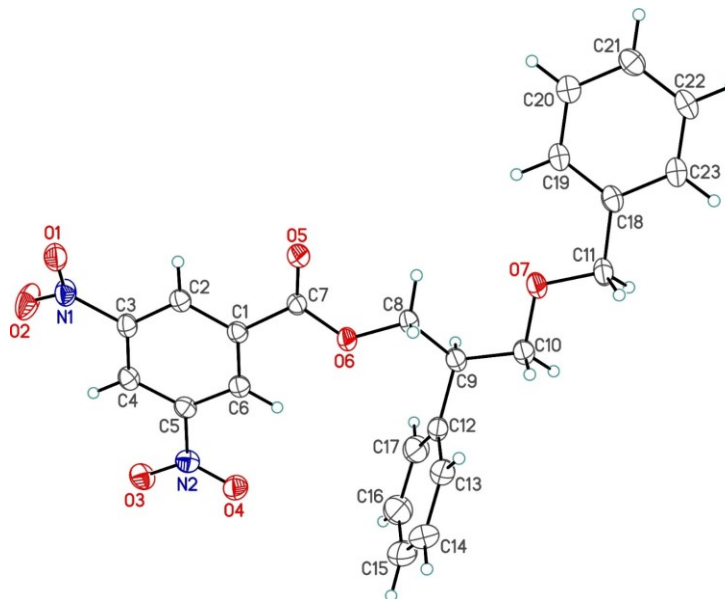
View showing the pseudo-inversion symmetry between the two independent molecules (the symmetry is broken by the chiral centers at carbon atoms C9).
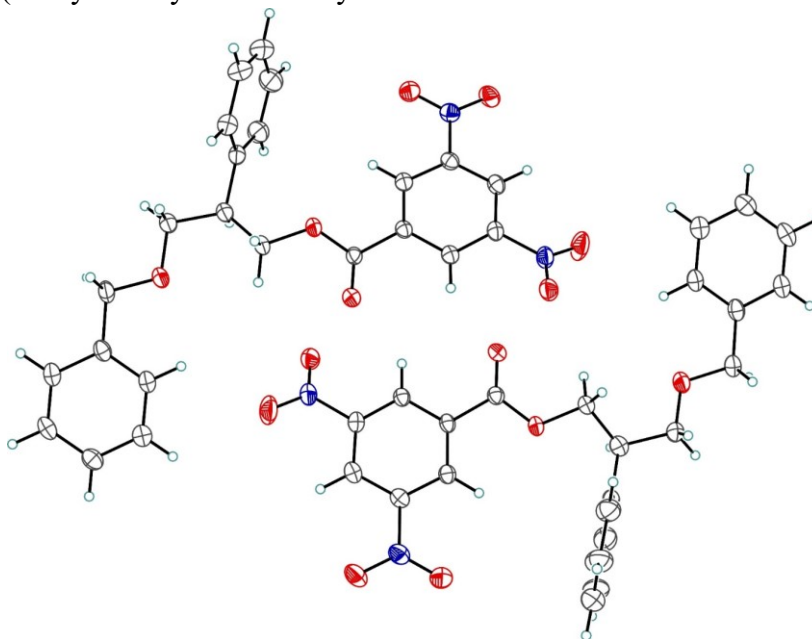
Crystallographic Experimental Details:

A. Crystal Data

formula	$C_{23}H_{20}N_2O_7$
formula weight	436.41

crystal dimensions (mm)	$0.30 \times 0.10 \times 0.03$
crystal system	monoclinic
space group	$P2_1$ (No. 4)
unit cell parameters[a]	
$\quad a$ (Å)	17.7181(7)
$\quad b$ (Å)	6.8759(3)
$\quad c$ (Å)	17.9417(6)
$\quad \beta$ (deg)	106.090(2)
$\quad V$ (Å^3)	2100.18(14)
$\quad Z$	4
r_{calcd} (g cm^{-3})	1.380
μ (mm^{-1})	0.868

B. Data Collection and Refinement Conditions

diffractometer	Bruker D8/APEX II CCD[b]
radiation (λ [Å])	Cu Kα (1.54178) (microfocus source)
temperature (°C)	-100
scan type	ω and ϕ scans (1.0°) (5 s exposures)
data collection 2θ limit (deg)	141.27
total data collected	77033 ($-21 \leq h \leq 21$, $-8 \leq k \leq 8$, $-21 \leq l \leq 21$)
independent reflections	7768 ($R_{int} = 0.0854$)
number of observed reflections (*NO*)	6429 [$F_o^2 \geq 2\sigma (F_o^2)$]
structure solution method	intrinsic phasing (*SHELXT-2014[c]*)
refinement method	full-matrix least-squares on F^2 (*SHELXL–2018[d]*)
absorption correction method	Gaussian integration (face-indexed)
range of transmission factors	1.0000–0.7596
data/restraints/parameters	7768 / 0 / 577
Flack absolute structure parameter[e]	0.07(13)
goodness-of-fit (*S*)[f] [all data]	1.059
final *R* indices[g]	
$\quad R_1$ [$F_o^2 \geq 2\sigma (F_o^2)$]	0.0415
$\quad wR_2$ [all data]	0.1171
largest difference peak and hole	0.205 and -0.252 e Å^{-3}

[a]Obtained from least-squares refinement of 8276 reflections with 5.20° < 2θ < 140.32°.

[b]Programs for diffractometer operation, data collection, data reduction and absorption correction were those supplied by Bruker.

[c]Sheldrick, G. M. *Acta Crystallogr.* **2015**, *A71*, 3–8. (*SHELXT-2014*)

[d]Sheldrick, G. M. *Acta Crystallogr.* **2015**, *C71*, 3–8. (*SHELXL-2018/3*)

[e]Flack, H. D. *Acta Crystallogr.* **1983**, *A39*, 876–881; Flack, H. D.; Bernardinelli, G. *Acta Crystallogr.* **1999**, *A55*, 908–915; Flack, H. D.; Bernardinelli, G. *J. Appl. Cryst.* **2000**, *33*, 1143–1148. The Flack parameter will refine to a value near zero if the structure is in the correct configuration and will refine to a value near one for the inverted configuration.